Mucoadhesive microcontainers for oral drug delivery

Mosgaard, Mette Dalskov

Publication date:
2021

Document Version
Publisher's PDF, also known as Version of record

Mucoadhesive microcontainers for oral drug delivery

Mette Dalskov Mosgaard

PhD thesis

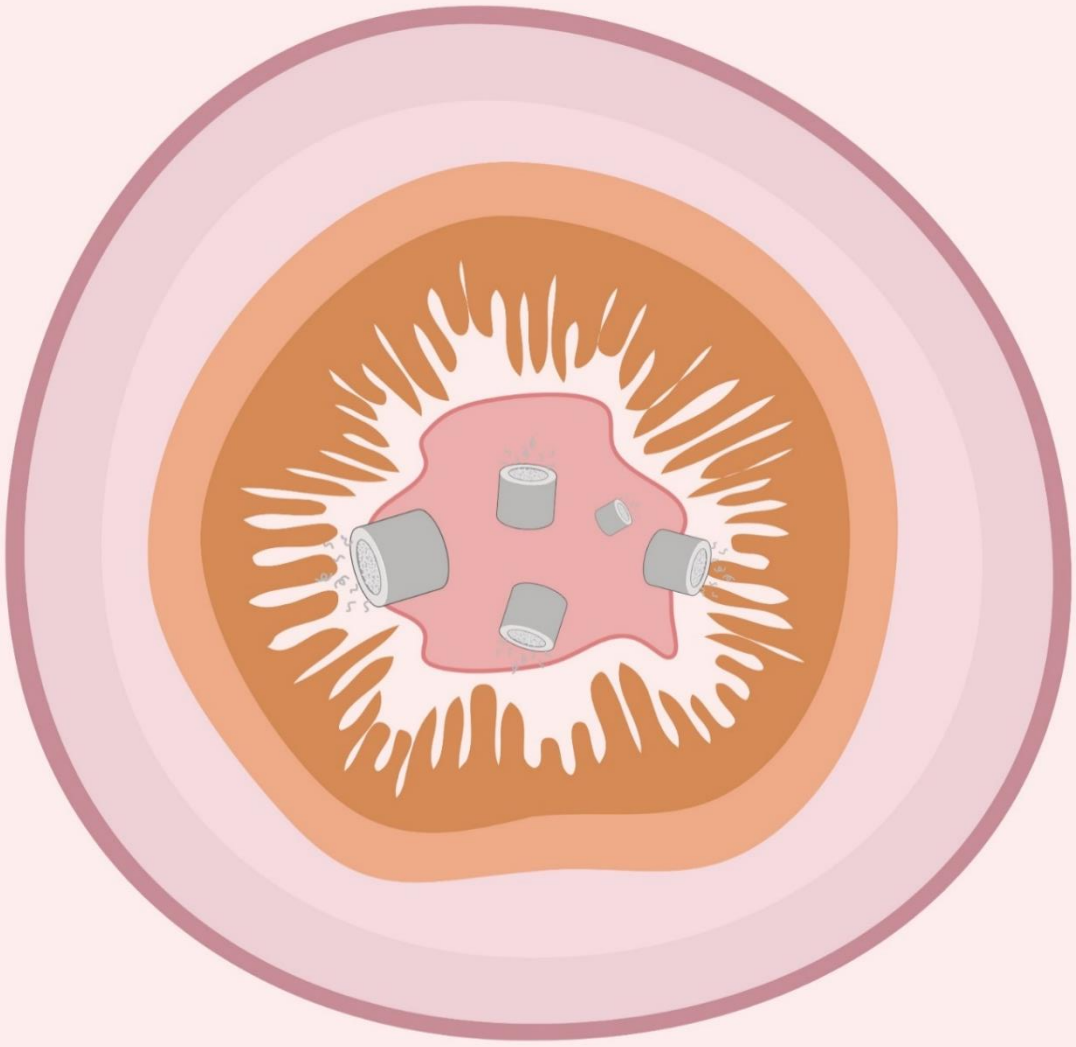

May 2021

Department of Health Technology, Technical University of Denmark (DTU)

Supervisor: Anja Boisen

Co-supervisors: Anette Müllertz and Line Hagner Nielsen

Preface

This thesis is submitted as a partial obligation for obtaining a PhD degree from the Technical University of Denmark (DTU). The research was carried out at the Department of Health Technology from the 15th of September 2016 to the 6th of May 2021, in the center for Intelligent Drug delivery and sensing Using microcontainers and Nanomechanics (IDUN). The work is part of the IDUN project. Funded by the Danish National Research Foundation (grant no. DNRF122) and by the Villum Fonden (grant no. 9301). This PhD project main supervisor is Professor Anja Boisen, Dr. Alina Joukainen Andersen has been a co-supervisor from September 2016 until May 2018, Associate Professor Line Hagner Nielsen replaced Alina as co-supervisor from May 2018 until May 2021. All are associated with the Department of Health Technology at the Technical University of Denmark. Professor Anette Müllertz has contributed as co-supervisor throughout the entire PhD and she is affiliate with the Department of Pharmacy at the University of Copenhagen.

Mette Dalskov Mosgaard

Department of Health Technology, Technical University of Denmark

Kongens Lyngby, May 2021

Danmarks Grundforskningsfond Danish National Research Foundation
IDUN
VILLUM FONDEN

Acknowledgements

First, I would like to acknowledge my main supervisor, Prof. Anja Boisen, who has made this PhD possible. Anja has been an exceptional guide through the years and has always been available, motivating and supportive. A big thank you to my co-supervisor, Prof. Anette Müllertz, for her guidance over the years and for always supporting me. Associate Prof. Line Hagner Nielsen has played a major role throughout my PhD project. I would like to express my deepest gratitude to you for always being there for me. Line has not only provided guidance, encouragement and inspiration scientifically, but also personally.

I would like to thank my students Abi and Mia, whose work was crucial for this PhD project. It was a pleasure to follow your progress and to be your supervisor. The teaching process has meant a lot to me and it also contributed greatly to the project. A major thank you to everyone in the IDUN group and the Nanoprobes group, it has truly been a pleasure to work with you and it has meant so much, both scientifically and personally. You have provided support, great company and most importantly, lots of fun. There are so many different backgrounds in the group and I have learnt something from all of you. Special thanks to my colleagues and friends Stine, Juliane, Chiara, Morten, Rolf, Philip, Marlitt, Varadarajan, Sophie and Zarmeena for all our talks on scientific and less scientific topics. Marlitt, thank you for being an amazing office mate and for our friendship. Thanks to Juliane, Stine, Rolf and Philip for proofreading this thesis, for that I am truly grateful. Thanks to Lasse for all our talks and for initiating new exciting project where both of our worlds meet. I have truly learned a lot from you. I would also like to acknowledge our brilliant lab technicians and administrative staff for always being helpful and for making this a great work place: Lotte, Christina, Lars, Tine, Louise and Dorthe. Big thanks to Julie and Sanne for helping me with practicalities and for being amazing colleagues.

Finally, I would like to thank my friends and family for all their never ending support, understanding, encouragement and love during this PhD project. A big thanks to my parents, brother, Ilaria and in-laws for all your support throughout the frustrations and successes. A special thanks to Ilaria for proofreading the thesis. To my amazing husband Søren Schnoor Hansen, I could not have done this PhD without you and your endless support. Thank you for all your love and for putting up with me during tough times. Lastly, Thanks to my two amazing girls you make my life special.

Abstract

Oral administration is the preferred administration route by patients and is often associated with high patient compliance. The oral route is a challenging administration route as the gastrointestinal tracts physiological properties often hampers drug absorption. Microcontainers as a drug delivery system have been introduced to improve oral absorption of drugs. Microcontainers are cylindrical micrometer-sized reservoirs, facilitating unidirectional drug release. The unidirectional drug release of the microcontainers is believed to enhance absorption, as the drug can be delivered directly into the mucosa. It has been shown that microcontainers embed themselves into mucus in the small intestine, which might explain the enhanced oral bioavailability of drugs. The characteristics of the unidirectional release and the microcontainers behavior in mucus require investigated, in order to clarify their effect on drug absorption.

In this work, we explore the microcontainers behavior in the small intestine in relation to mucoadhesion and their orientation of unidirectional drug release. Different mucoadhesion strategies have been investigated in this PhD project, including microcontainers with different functionalized polymers, surface topography and morphology. The strategies have been evaluated in relation to mucoadhesion, impact on unidirectional drug release and how the drug release profile is affected. In order to determine the impact of different strategies on mucoadhesion a new *ex vivo* perfusion setup was developed, to enable evaluation of the microcontainers behavior in the small intestine. A texture analyzer was used to determine the adhesion forces of different topographies. From repeating measurements it was observed that the force measurements were strongly affected by disturbing factors such as tissue variations and the time interval between measurements. A statistical design was then developed in order to correct for the disturbing factors and enable a reproducible and reliable evaluation of the topographies adhesion force to mucosa. Microcontainers are fabricated in epoxy-based SU-8 and therefore not suitable for oral intake. For this reason, fabricating microcontainers in biocompatible and biodegradable polymers has been crucial to demonstrate the versatility of microcontainers. In this PhD, I investigated the impact of using different polymeric materials for microcontainers, in relation to their behavior in the small intestine, including mucoadhesion, orientation and degradation.

This thesis presents novel experimental models and validation strategies to improve investigation of mucoadhesive microcontainers. This approach led to a number of interesting

conclusion. First and foremost, this work attests to microcontainers strong ability to adhere to mucosa, with only minor improvements observed when varying the size, shape and material of the microcontainer. Interestingly, applying mucoadhesive polymers onto the microcontainers cavity shows great potential for improved adhesion to mucosa *ex vivo*. Additionally, we were able to conclude that biodegradable and biocompatible microcontainers fabricated in poly(lactic-co-glycolic acid) (PLGA) and poly-ε-caprolactone (PCL) show similar adhesion to the mucosal lining as the SU-8 fabricated microcontainers. While the results indicated a slightly stronger ability to adhere for SU-8 microcontainers compared to the biodegradable and biocompatible microcontainers, this was not supported statistically.

The overall conclusion is that, microcontainers show strong adhesion to mucosa and modifying the microcontainers in terms of functionalized polymeric coatings and varying morphology appears to only show minor improvements of the abilities to adhere to the mucosal surface in the small intestine.

Resumé

Oral levering er den mest fortrukne administrationsvej for patienter og medfører ofte god compliant behandling. Den orale administrationsvej er udfordret af mave-tarm kanalens fysiologiske egenskaber som ofte svækker absorptionen af lægemiddelstoffer. For at forbedre oral absorption af lægemiddelstoffer er mikrocontainere blevet introduceret som lægemiddelstof leveringssystem. Mikrocontainere er cylinder formede mikrometer store reservoirers der har en åbning til frigivelse af lægemiddelstoffer. Den ensrettede frigivelse af lægemiddelstoffer fra mikrocontainere menes at fremme absorptionen da stofferne kan leveres direkte ind i slimlaget af mucus som dækker tarmoverfladen i tyndtarmen. Studier har vist at mikrocontainerne kan sætte sig fast i mucus laget i tyndtarmen hvilket kan forklare en bedre oral biotilgængelighed af lægemiddelstoffer. Den ensrettede frigivelse og mikrocontainernes opførsel i mucus laget skal dog undersøges yderligere for at kunne afgøre dets effekt på absorptionen af lægemiddelstoffer.

Dette arbejde har fokuseret på at undersøge mikrocontainernes opførsel i tyndtarmen i forhold til deres adhæsion til mucosa samt deres orientering af den ensrettede frigivelse af lægmiddelstoffer. Igennem dette PhD projekt er forskellige mucoadhæsions strategier blevet undersøgt. Dette har inkluderet mikrocontainer med forskellige funktionelle polymer overfladestrukturer og morfologier. Disse strategier er blevet evalueret i forhold til mucoadhæsion samt deres indvirkning på den ensrettede frigivelse af lægemiddelstof og hvordan det påvirker frigivelsen. For at kunne bestemme disse adhæsions strategiers indvirkning på mucoadhæsionen er en ny *ex vivo* perfusions model udviklet for at evaluere mikrocontainernes opførsel i tyndtarmen. En texture analyzer er blevet benyttet til at bestemme adhæsions kraften af forskellige overfladestrukturer. Under gentagne målinger blev det observeret at adhæsions kræfterne blev påvirket af forstyrrende faktorer så som vævs variation og tids intervallet mellem målingerne. Derfor blev der udviklet et statistisk design for at kunne korrigere for forstyrrende faktorer og muliggøre reproducerbar og troværdige målinger af overfladestruktures adhæsions kræft til mucosa. Mikrocontainerne er fremstillet i SU-8 som er en epoxy-baseret polymer, hvilket gør at de ikke er godkendt til oral indtagelse. Af denne grund har der været stor interesse i at kunne fremstille mikrocontainere i bionedbrydelig og biosammenlignelige polymer for at kunne vise alsidigheden af mikrocontainer. I dette PhD projekt er mikrocontainere fremstillet i forskellige polymere blevet undersøgt i forhold til deres opførsel i tyndtarmen. Dette indbefatter mucoadhæsion, orientering samt nedbrydning.

Denne afhandling præsenter nye eksperimentelle modeller og validerings strategier til at forbedre undersøgelsen af mucoadhæsive mikrocontainer. Denne fremgangsmåde førte til flere interessante konklusioner. Først og fremmest fremhæver denne afhandling at mikrocontainerne har en stærk evne til at adhærer til mucosa og ændring af mikrocontainernes form, størrelse og materiale viser kun en lille forbedring i adhæsionen af mikrocontainere. Mucoadhæsive polymere tilføjet mikrocontainernes åbning viste potentiale i at forbedre mikrocontainernes adhæsion til mucosa *ex vivo*. Endvidere viser bionedbrydelige og biokompatible mikrocontainere fremstillet i poly(lactic-co-glycolic acid) (PLGA) og poly-ε-caprolactone (PCL) lignende adhæsion til mucosa som SU-8 fremstillede mikrocontainer. Resultaterne kunne indikere at SU-8 mikrocontainerne havde en smugle stærkere adhæsion end de bionedbrydelige og biokompatible mikrocontainer men det var dog ikke eftervist statistisk.

Den samlede konklusion er at mikrocontainere viser stærke adhæsions evner til mucosa og det at modificer mikrocontainerne i forhold til at påføre funktionelle polymer og variere deres morfologier viste, at det kun i mindre grad forbedrede adhæsionen til den mucosale overflade i tyndtarmen.

Table of contents

List of abbreviations

3D	Three dimensional
AFM	Atomic force microscopy
API	Active pharmaceutical ingredient
BCS	Biopharmaceutics classification system
C10	Sodium decanoate
DNA	Deoxyribonucleic acid
FaSSIF	Fasted state simulated intestinal fluid
Fc	Fluorocarbon
FDA	Food and drug administration
GI	Gastrointestinal
PCL	Poly-ε-caprolactone
PEG	Polyethylene glycol
PDMS	Polydimethylsiloxane
PLGA	Poly (lactic-co-glycolic acid)
PLLA	Poly (L-lactic acid)
PRINT	Particle replication in nonwetting templates
PTFE	polytetrafluoroethylene
PVA	Polyvinyl alcohol
SEAL	Stamped assembly of polymer layers
SEM	Scanning electron microscopy
T_g	Glass transition temperature
Ti/Au	Titanium/gold
UV	Ultraviolet

List of publications and other contributions

This PhD project has led to six papers and three scientific conference contributions. Throughout the PhD thesis, the following papers will be included and referred to as **Paper I**, **paper II**, **Paper III** and **paper IV**. **Paper V** has not been included in this PhD thesis as the work is confidential and **Paper VI** was excluded due to the story line of the PhD thesis.

Publications

Paper I	*Ex vivo intestinal perfusion model for investigating mucoadhesion of microcontainers* M. D. Mosgaard, S. Strindberg, Z. Abid, R. S. Petersen, L. Thamdrup, S. S. Keller, A. Müllertz, L. H. Nielsen, A. Boisen. International Journal of Pharmaceutics. 2019, 570, 118658.
Paper II	*General experimental design for testing adhesion to mucosal tissue* M. D. Mosgaard, A. J. Andersen, E. Ingallinera, M. Viehrig, L. H. Nielsen, T. S. Alstrøm and A. Boisen In preparation.
Paper III	*Optimization of mucoadhesive coatings on microcontainers for oral drug delivery* M. D. Mosgaard, M. C. Johannesen, A. Müllertz, A. Boisen and L. H. Nielsen In preparation.
Paper IV	*Investigation of mucoadhesion and degradation of PCL and PLGA microcontainers for oral drug delivery* Z. Abid, M. D. Mosgaard, G. Manfroni, R. S. Petersen, L. H. Nielsen, A. Müllertz, A. Boisen and S. S. Keller. Polymers 2019, 11,1828.
Paper V	*Biodegradable microdevices for oral delivery of salmon calcitonin* M. D. Mosgaard, L. H. E. Thamdrup, R. B. Kjeldsen, L. H. Nielsen and A. Boisen. This manuscript is in a non-disclosure agreement and therefore not included in this PhD thesis
Paper VI	*Management of oral biofilms by nisin delivery in adhesive microdevices* S.E. Birk, M.D. Mosgaard, R.B. Kjeldsen, A. Boisen, R.L. Meyer, L.H. Nielsen. 2021. (Research note, submitted to European Journal of Pharmaceutics and Biopharmaceutics).

Other contributions

Oral talk	*Ex vivo intestinal perfusion model to determine mucoadhesion of microcontainers* M. D. Mosgaard, L. Vaut, S. Strindberg, Z. Abid, A. J. Andersen, R. S. Petersen, S. S. Keller, A. Müllertz, L. H. Nielsen, A. Boisen. NordicPOP, Oslo, Jan 2019.

Poster I *Development of an ex vivo intestinal perfusion model to determine mucoadhesion of microcontainers*
M. D. Mosgaard, L. Vaut, S. Strindberg, Z. Abid, A. J. Andersen, R. S. Petersen, S. S. Keller, A. Müllertz, L. H. Nielsen, A. Boisen.
Controlled Release Society Annual Meeting and Exposition, Valencia, July 2019

Poster II *Fabrication and ex vivo retention study of biodegradable microcontainers for oral drug delivery*
Z. Abid, M. D. Mosgaard, G. Manfroni, R. S. Petersen, L. H. Nielsen, A. Müllertz, A. Boisen, S. S. Keller. Micro & Nano Engineering, Rhodes, Sep. 2019.

1. Introduction

Oral administration is the most preferred route of drug delivery, as it is more convenient for the patients than using the intravenous administration route. As a consequence, choosing the oral route results in high patient compliance, which is crucial for achieving optimal treatments (1). From an economic perspective, production of e.g. solid dosage forms for oral intake is less costly, resulting in lower expenses for the patients, which can have a major impact on the choice of treatments as well as on compliance (2,3).

The pharmaceutical field is facing a growing challenge in delivery of new active ingredients orally. Around 40% of approved drugs are classified as poorly soluble (based on the biopharmaceutical classification system (BCS)) and around 90% of drugs in the pipeline show poor solubility (4,5). In addition, a high number of these drugs demonstrates poor permeability as well, which also compromises the effect of the drugs (6). An increased interest in oral delivery of peptides and proteins also calls for new drug delivery systems that can improve oral bioavailability.

The challenge in delivering drugs orally is not only related to the properties of the drugs but also by the characteristics of the gastrointestinal (GI) tract. The small intestine is an excellent absorption site for many drugs but some drugs are recognized by the GI tract as harmful molecules and are not easily permitted access (7,8). The existing challenges provide evidence for the need of new oral drug delivery systems that can improve oral delivery (9).

Microcontainers as drug delivery devices can facilitate protection against the harsh acidic environment and enzymatic degradation in the stomach. Microcontainers are cylindrically shaped devices with one cavity allowing unidirectional drug release. Controlling the unidirectional release into the mucus layer located on the epithelium wall, enables direct delivery close to the absorption site. The microcontainers have to adhere to the mucosal surface, which is believed to increase retention time at the target site. This would allow protected delivery of peptides to the intestinal wall as well as allow poorly soluble drugs to be released slowly as the retention time is increased (10,11). Optimizing and controlling the adhesion of the microcontainers to the mucosal surface in the small intestine is an important aspect when facing delivery of challenging drugs such as peptides (12).

1.1. Aim and hypothesis

In this thesis, it is hypothesized that by applying surface modifications on drug delivery devices, such as microcontainers, the adhesion and delivery of the drug into the small intestinal mucus layer will be enhanced, thus improving drug bioavailability.

The overall aim of this work is to develop, characterize and evaluate the ability of microcontainers to adhere to the mucosal surface in the small intestine. The project has been divided into five parts with the following aims:

I) Develop models to evaluate the mucoadhesive strength of the microcontainers as well as their orientation in order to emphasize the unidirectional drug release into the mucus layer.

II) Design and evaluate novel microcontainers in various shapes and sizes for improved mucoadhesion.

III) Estimate the mucoadhesive abilities of microstructures to determine the impact of a structured surface on microcontainers to enhance mucoadhesion.

IV) Evaluate mucoadhesion of microcontainers after modifying the surface chemistry with mucoadhesive and/or mucopenetrating polymers.

V) Design, fabricate and assess biocompatible and biodegradable microcontainers in regard to mucoadhesion.

1.2. Outline of the thesis

In this PhD project, the behavior of the microcontainers in the small intestine will be explored and strategies to improve their abilities to adhere to the intestinal wall will be investigated. The main results are presented through four original research papers (**Paper I-IV**) and an overview of the PhD project is illustrated in **Figure 1.** Two additional papers (**Paper V-VI**) have been produced during this PhD project. These are not included in the PhD thesis as the work is either confidential (**Paper V**) or not within the story line of the thesis (**Paper VI**), and will therefore, not be mentioned further. **Paper V** compiles the PhD project with an *in vivo* study.

The following background section includes an introduction to oral drug delivery and provides an insight into the mucus layer and its main purpose in the GI tract. The concept of mucoadhesion is introduced as well as the different possibilities of improving adhesion of microcontainers. A short summary of microdevices as drug delivery systems, covering both

mucoadhesion and development of biodegradable and biocompatible microdevices, completes the section.

In **paper I**, mucoadhesion of microcontainers with different shapes, sizes and fabrication materials were evaluated on a newly developed *ex vivo* perfusion model. In **Paper II**, tensile adhesion force measurements of microstructures were performed, which led to the development of a statistical design to perform reliable adhesion measurements. In **Paper III**, microcontainers were functionalized with various polymeric coatings to enhance mucoadhesion. Additionally, different polymeric coating thicknesses were also investigated and compared in this paper. In **Paper IV,** we explored biodegradable and biocompatible microcontainers and their ability to adhere to mucosa as well as their degradation.

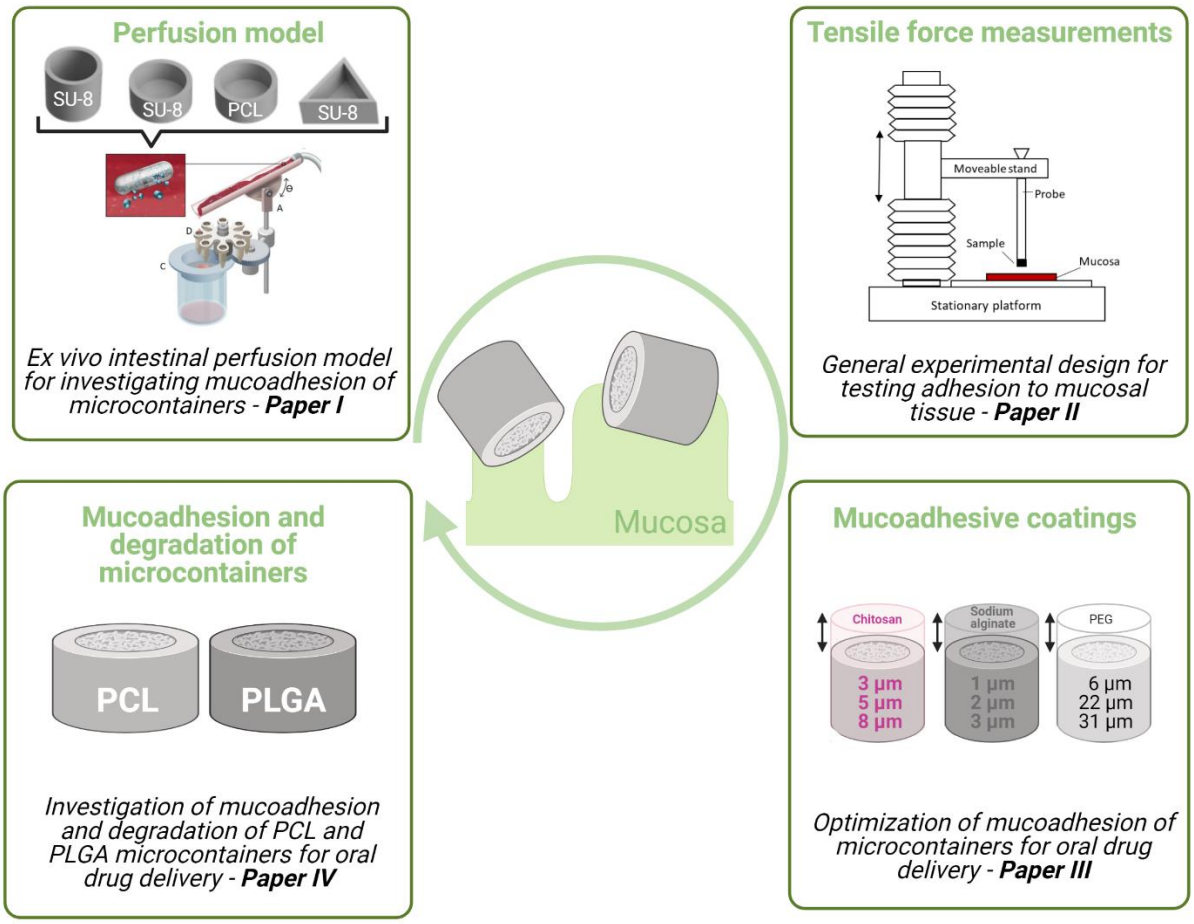

Figure 1: Schematic overview of the outline of this PhD thesis. The main goal of this thesis is to explore the behavior of the microcontainers in the small intestine and strategies to improve their abilities to adhere to the mucosal surface. Experiments have been conducted to investigate this, which resulted in four papers. Development of a new *ex vivo* perfusion model to explore mucoadhesion of microcontainers with different morphology was presented in Paper I. In Paper II, a texture analyzer was used to measure tensile forces of different surface topographies. In Paper III, different mucoadhesive polymeric coatings were explored to estimate their impact on the behavior of the microcontainers at the mucosal lining. Lastly, in Paper IV, we explored fabrication of microcontainers in biocompatible and biodegradable materials and how that affected their behavior at the mucosal surface. All the schematic figures in this PhD thesis has been created with BioRender.com.

2. Background

2.1. Oral drug delivery

Oral administration is the most preferred route for drug administration mainly due to high patient compliance (13). The oral route is convenient for patients as it does not require specially trained professionals for dosing, and this reduces the cost and time needed for patients as well as for the healthcare professionals (14). Reduced cost of oral dosage forms is also due to the manufacturing process since no sterile production is needed and therefore, it is cheaper than e.g. injectables (1). Stability of oral formulations is another advantage since they often requires less complicated storage and transportation conditions compared to many intravenous formulations where cold temperatures during storage are required (15,16).

The gastrointestinal (GI) tracts mucosal surface in human adults is a very good absorption site due to its large surface area, which is approximately 30-40 m^2 where the large intestine refers to approximately 2 m^2 (17). Nevertheless, the GI tract presents some physiological challenges limiting oral delivery of some drugs as e.g. protein and peptides. The main purpose of the GI tract is to digest and absorb food and other nutrition sources, which therefore, makes it an optimal site for drug absorption (18). Another physiological role of the GI tract is to prevent harmful or unknown compounds from entering the body. Oral delivery of drugs has to overcome the defenses of the body against unknown molecules (19). The first obstacle is the hostile environment in the stomach where the acidic pH and digestive enzymes challenge many drugs. When reaching the small intestine more digestive enzymes are present and the place of absorption is well protected by a complex mucus layer covering a tight epithelium layer (13,18,20). When developing oral drug formulations, the physiological properties of the GI tract needs to be taken into account for optimal drug absorption. Among numerous parameters, pH and transition time are two important factors when administering drug orally and both properties play a central role in the work of this PhD thesis. The pH and transition time down the GI tract of a micrometer sized drug delivery system is shown in **Figure 2**.

All the challenges presented by the GI tract are crucial for the functionality of the body and can, therefore, not be removed or damaged. Many have tried to circumvent these challenges and use them to our advantage. The mucus layer inhibits the diffusion of drugs and may hamper their path to the epithelium lining. Thereby, the mucus layer retains the drug delivery system in the small intestine, which has proven to be beneficial for drug absorption if the molecule can reach the epithelium lining (21).

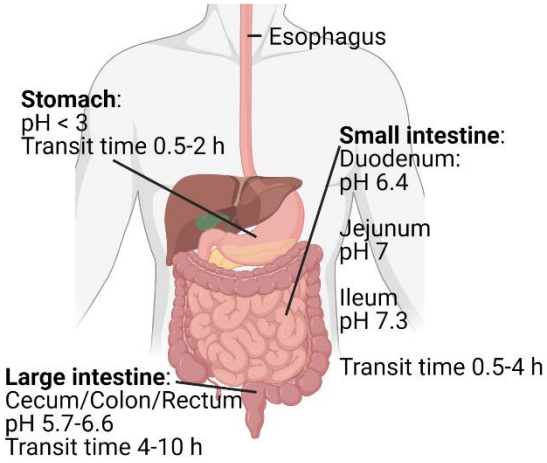

Figure 2: Drawing illustrating the anatomy of the human gastrointestinal (GI) tract. The main areas in the GI tract are shown esophagus, stomach, small intestine (duodenum, jejunum and ileum) and large intestine (cecum, colon and rectum). Their respective pH values are indicated (22,23) as well as the transit time of microcontainers through the GI tract (24).

2.2. Mucoadhesion

The advantages of developing mucoadhesive drug delivery systems have been 1) prolonged residence time at the site of absorption, 2) intensifying the contact to the underlying epithelium layer, which has shown to increase drug absorption. In general, numerus studies have shown an increased absorption when improving the ability of drug delivery systems to adhere to the mucosal surface (25,26).

2.2.1. Mucus

All mucosal surfaces in the body are covered with a viscoelastic mucus layer. One of the first physical barrier foreign molecules and bacteria encounter is mucus and to be absorbed and reach the circulatory system, they must diffuse through it (27). However, specific molecules such as gases and water are allowed to diffuse through the mucus layer to conserve the water balance that keeps the underlying epithelium hydrated (28). This highly hydrated mucus layer also works as a lubricator enabling smooth passage of food (29). Mucus consists of water (95-99% by weight), glycoproteins called mucins (1-5%) and smaller amounts of electrolytes, proteins, enzymes, lipids, DNA, carbohydrates, inorganic salts and mucopolysaccharides in a heterogeneous mixture (29–31). Mucus, in the small intestine, is secreted by goblet cells located in the lining of the intestinal epithelium and is constantly secreted with a turnover time estimated to be between 47-270 min (32,33). The thickness of the mucus layer highly depends on the region in the GI tract and the thicknesses varies depending on diet. The mucus thickness in the small intestine of a rat has been determine to the following; duodenum 170±38 µm, jejunum 123±4 µm and ilium 480±47 µm (34). Determining the mucus layer thickness in the

small intestine of humans is more complicated but studies have estimated the mucus layer to be approximately 10 µm in ileum (35).

As mentioned earlier, the key component in mucus is mucin, which consists of an O-glycosylated polypeptide backbone, which is rich in serine, threonine and proline. Mucins are macromolecules with a molecular mass of 0.5-20 MDa where 10-30% of the weight consists of the peptide core and 70-80% consist of o-glycosylated oligosaccharide (29,36,37). The oligosaccharide chains can contain approximately 1-20 monosaccharides residuals and many of them contains negatively charged sulphate or carboxyl (sialic acid) end groups (38–40). Therefore, the mucin network is negatively charged in the small intestine at pH 6.4 (27). The polypeptide core is connected to cysteine rich regions with no glycosylation (**Figure 3**). This allows monomers of mucin to link together by disulfide bridges resulting in a folded structure (41). Mucin are encoded by the MUC gene family and there is a variety of them. These genes are divided into two sub-families; the genes encoded for secretory gel-forming mucins and the genes encoded for membrane bound mucins (42). The membrane bound mucins contain a hydrophobic domain that anchors to the epithelium lining. In addition, the membrane bound mucins are more hydrophilic as they lack intermolecular disulfide bridges (43). The interaction between epithelium cells and mucins are believed to involve entanglement and adhesion with the cell surface, which forms glycocalyx (44). Mucus is divided into two layers; a firmly adherent layer connected with the glycocalyx and an overlying loosely adherent layer. However, there are some discrepancy to whether the mucus layer in the small intestine consists of one or two layers (45).

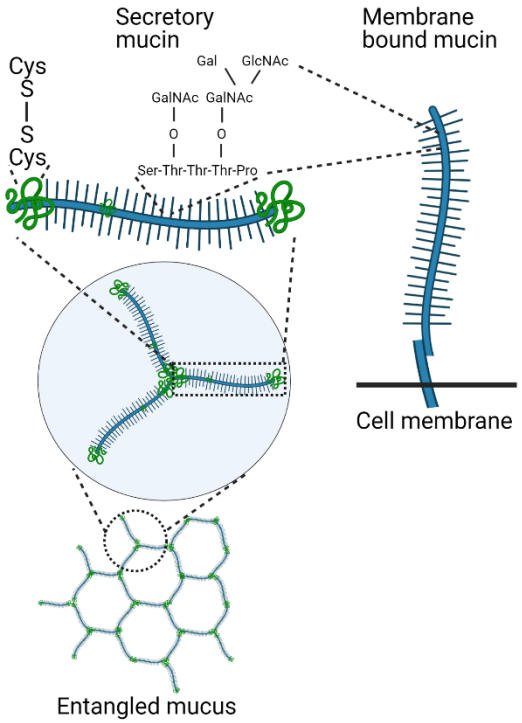

Figure 3: Simple representation of an entangled network of mucin chains covering the intestinal epithelium lining. A zoom-in of three connected mucin monomers attached through disulfide bonds. A final zoom-in on a single secretory mucin monomer is also represented. The anchored membrane bound mucin chain is also illustrated. Inspired by (46).

Mucus is a complex network of entangled macromolecules that act as a trap for foreign molecules such as active pharmaceutical ingredients (API) (47). This network is affected by environmental factors such as ionic strength, water content and pH (48,49). These parameters can affect the mesh size of the network, which is approximately 200-300 nm and challenge the diffusion of molecules through the mucus layer to a greater or lesser extent (50). Another obstacle for molecules or particles is the ability of the mucus layer to form numerous intra- and intermolecular interactions (**Figure 4)**. The disulphide groups in the mucin structure promote aggregation of mucin monomers as they form covalent bonds (51). Foreign molecules with disulphide groups can also interact with these groups, thereby, hampering their diffusion through the mucus layer (52). The glycosylated residues in mucin contain negatively charged groups at intestinal pH. Positively charged particles can form electrostatic interactions with negatively charged mucin (53–55). A large extent of hydrophilic oligosaccharide chains in mucin can make hydrogen bonds that bind to other hydrophilic domains (53,56), and Van Der Waal's forces can attract two complementary saccharide moieties causing them to attach to each other (53). When many mucin monomers interact, a large physical entanglement of chains occurs, which will facilitate a tight complex network compromising passage of foreign

molecules (56). The cysteine rich regions in mucins are hydrophobic domains where hydrophobic interactions can occur between e.g. lipophilic drugs (55,56).

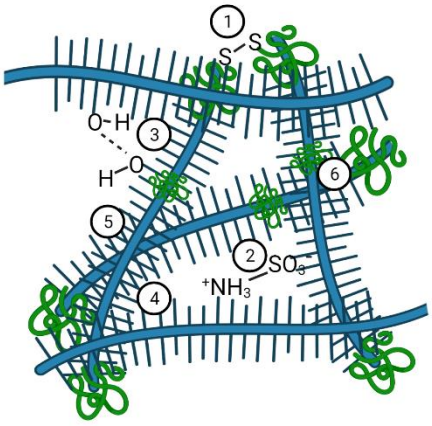

Figure 4: Illustration of intra – and intermolecular interactions in mucus with **1)** covalent bonds, **2)** electrostatic interactions, **3)** hydrogen bonds, **4)** Van der Waal's forces, **5)** intermingling and **6)** hydrophobic interactions.

2.2.2 Adhesion

The ability of materials to adhere to the mucosal surface, also called mucoadhesion, has been a well-known phenomenon since 1962 (57). Mucoadhesion is defined as the adhesion between any surface and a mucosal lining. Mucoadhesion consists of a *contact stage* and a *consolidation stage*. In the *contact stage*, contact is reached between a surface and the mucosal membrane where the surface is wetted, which may lead to swelling. Adhesive interactions are made in the *consolidation stage*, where the surface will interpenetrate mucus promoting entanglement into the mucus mesh where chemical interactions may occur (58). Adhesion is a complex process and many theories exist allowing us to explain and understand the mechanisms involved.

The **wettability theory** is mainly applicable to low viscosity mucoadhesive systems or liquids and their ability to spread over a biological surface such as mucus. This theory suggests that the adhesive component penetrates mucus irregularly, hardening and anchoring themselves to mucosa (21,59).

The **electronic adhesion theory** suggests that an electron transfer occurs between mucus and the adhesive surface, which results in the formation of a double layer of electrical charge at the interface. The adhesive effect is believed to occur due to attraction forces across the double layer (59,60).

The **fracture theory** describes adhesion as the force needed to detach two surfaces after adhesion. At the interface, detachment of the adhesive bonds will occur, normally at the weakest component (59,61).

The **absorption theory** defines adhesive attachment on the basis of chemical interactions, such as hydrogen bonding and Van Der Waals forces (62). These forces are believed to be main contributors to the adhesive interactions. A subsection to this theory assumes that strong covalent bonds result in adhesion at the interface (59).

The **diffusion theory** explains that adhesion occurs due to entanglement of mucus and adhesive polymer chains. This is driven by concentration gradients, which are affected by molecular chain length and their mobility. The diffusion coefficient and contact time controls the depth of interpenetration of the chains (59,61).

The **mechanical theory** suggests that adhesion occurs between liquid adhesives and irregularities on rough surfaces. However, other factors such as increased surface area of rough surfaces and enhanced viscoelastic and plastic properties are believed to be more central in the adhesion process than a mechanical effect (59,63).

The complex nature of mucoadhesion makes it unlikely that only one of these theories can describe the adhesion.

2.3. Microdevices for oral drug delivery

The pharmaceutical field faces a major challenge in delivering orally poorly water-soluble drugs as well as poorly permeable drugs (4). This means that a large fraction of developed drugs will be wasted due to poor dissolution and poor absorption if we, as a scientific field, cannot succeed in delivering these problematic drugs orally in a correct manner. Furthermore, this challenge is not just limited to small molecules but the pharmaceutical field also faces the challenge of delivering biologics orally. The use of large molecules as biologics has increased worldwide and they include a large percentage of candidates in pre-clinical discovery (1). Many oral drug delivery systems, such as nanoparticles and lipid based drug delivery systems, have been developed over the years trying to circumvent poor oral absorption of both small and large molecules (64–66).

Microfabricated devices as drug delivery vehicles have gained increased interest in the pharmaceutical research field, especially in regards to oral drug delivery of challenging molecules like peptides and proteins (12,65,67). Microdevices are drug reservoirs, fabricated

in numerous different shapes and dimensions, with one open side to allow unidirectional drug release (**Figure 5A**) (68–70). In **Figure 5B-E** is shown examples of microfabricated devices in different shapes, dimensions and materials, which demonstrates the versatility of microfabricated devices. Microdevices have shown to be able to protect the drug inside the cavity by sealing off the opening with an enteric coating. This allows protection against the acidic environment in the stomach and enables release when it reaches the small intestine (71). Microdevices have shown to increase drug absorption of poorly water-soluble and poorly permeable drugs, explained by their ability to release the drug unidirectional into the mucus layer (11,72). Controlling the unidirectional drug release into the mucosal surface may enable a high drug concentration at the intestinal wall, which reduces drug release into the lumen. In this way, waste of drug in the GI tract might be limited as the drug can be released directly at the absorption site (**Figure 5A**). This is an important aspect as microdevices might reduce toxic effects from the fraction of non-absorbed drug located in the lumen (73).

Integration of structural cues or chemical surface modifications on the cavity of the microdevices have shown to promote drug release directly into the mucus layer, resulting in an increased drug absorption (74,75). These modifications have also shown to improve adhesion of the microdevices to the mucosal lining facilitating an increased retention time, which enable high drug absorption.

An additional advantage of microdevices are the fabrication techniques that ensure low variations of the size of the devices allowing for more equal drug loading (68,76). Furthermore, various fabrication methods and materials enable possibilities for fabricating microdevices with varying sizes and shapes (72,77,78). This supports the versatility of the microdevices and allows for creative approaches for improving drug absorption. The fabrication techniques are often limited in relation to upscaling the fabrication for microdevices. This is especially the case for the more advanced microdevices such as micromotors, self-folding microstructures and star-shaped long-acting dosage forms (81–83). Numerous types of microdevices have been developed and creative engineering has resulted in some impressive microdevices as shown in **Figure 5B-E** (82).

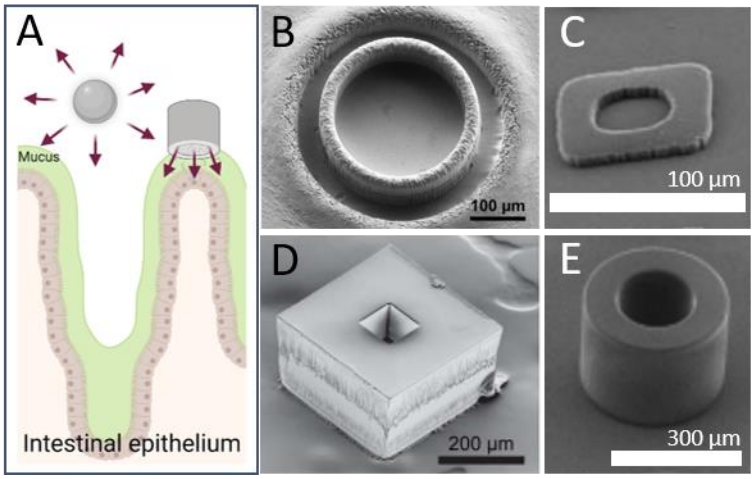

Figure 5: **A)** Illustration of drug release from a microparticulate system (left) and microcontainer (right). **B)** SEM image of microwells fabricated in poly(L-lactic acid) (PLLA) by hot embossing (71). **C)** SEM image of self-folding hydrogel microparticles fabricated in poly(ethylene glycol methacrylate) (PEGMA) and poly(ethylene glycol di- methacrylate) (PEGDMA) (83). **D)** SEM image of microsquared devices fabricated in poly (lactic-co-glycolic acid) (PLGA) with the newly developed 'stamped assembly of polymer layers' (SEAL) technique (84). **E)** SEM image of microcontainer fabricated in SU-8 by photolithography. Reprinted/adapted with permission from Springer Nature, John Wiley and Sons, American Association for the Advancement of Science, American Chemical Society.

2.3.1 SU-8 microcontainers

Microcontainers are one type of microdevices, which possess many of the advantages stated in previous section. Microcontainers are fairly simple to fabricate, they can be functionalized and they have a high drug loading capacity (6,85). Microcontainers are micrometer-sized hollow cylindrical reservoirs with an inner cavity for drug storage (**Figure 5E**). They can be fabricated in SU-8 using two-step photolithography as originally described by Tao *et al.* and further modified by Nielsen *et al.* (76,86).

Fabrication of SU-8 microcontainers

Photolithography enables fabrication of micrometer-sized devices with spatial precision and enables fabrication of asymmetrical devices (87). Photolithography, used for fabricating SU-8 microcontainers, is a relatively simple fabrication process. SU-8 is a negative epoxy-based photoresist that is chemically stable and exhibits high mechanical strength. **Figure 6A** illustrates the two fabrication steps that define the bottom and walls of the microcontainers. This is done by UV exposure of uncrosslinked SU-8, where a UV mask is used for defining the microcontainer shape. The microcontainers are fabricated on a silicon wafer (**Figure 6B**) and to allow dry release of the microcontainers, the wafer is either coated with fluorocarbon (Fc) or titanium/gold (Ti/Au) (78,88). The Ti/Au release layer ensures adequate adhesion to the wafer during drug loading and allow harvesting of microcontainers without damaging them.

The same is seen for Fc coated wafers, however, the microcontainers show weaker adherence to the Fc layer. This challenges the drug loading process as the microcontainers can easily detached themselves from the wafer (78,88).

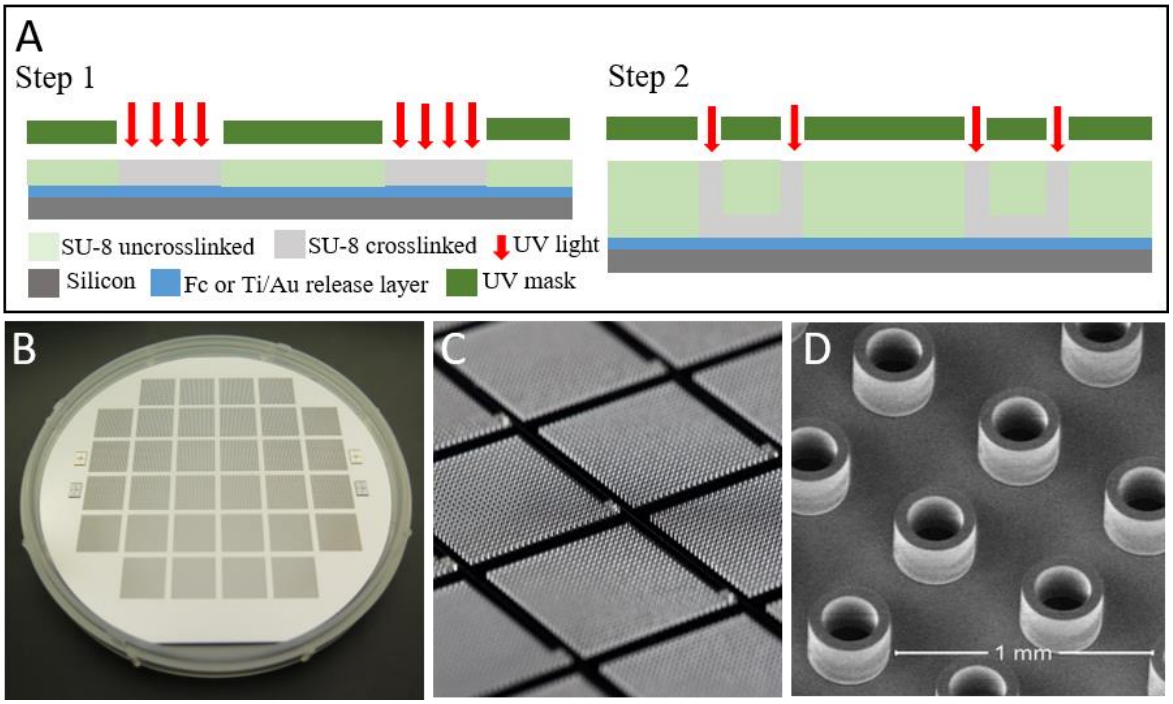

Figure 6: Overview of **A)** fabrication steps of microcontainers. Step 1) shows fabrication of the microcontainers bottom, which is fabricated on top of a silicon wafer using UV photolithography. Step 2) shows fabrication of the walls of the microcontianers. A release layer of fluorocarbon (Fc) or titanium/gold (Ti/Au) can be applied to allow individual removal of the microcontainers. **B)** Image of a wafer holding 32 squares/chips where each chip contains 625 individual microcontainers. **C)** Zoom-in of a chip. **D)** Zoom-in of a microcontainer.

SU-8 microcontainers can be fabricated in many different sizes and shapes such as cylindrical, squared, triangular, more planar or with symmetrical height and width (77,78). Furthermore, the microcontainers have evolved during the years to ease their usability and their quality, which has resulted in the creation of thin-walled microcontainers. The once mostly studied has an inner height of 210-270 µm and inner diameter of 73-413 µm (10,76,78,89). To enable increased drug loading, the microcontainers were modified to have 230 µm in inner diameter and 220 µm in inner height (78). In this PhD, microcontainers with varying dimensions have been used as this project was carried out during the evolvement of the microcontainers.

SU-8 is biocompatible and has been reported to be suitable as implant material (90), but it is not biodegradable, which is a major drawback when being administered to humans. This is of great importance both for physiological effect on the body after long-term use but also in regard to an environmental aspect. SU-8 has shown to be a great material to test the ability of microcontainers as an oral drug delivery system. However, the material used for fabrication

has to be approved for oral intake to be an actual success. Therefore, microcontainers need to be fabricated in a material that is both biocompatible and biodegradable without complicating the fabrication process and compromising the ability for upscaling the fabrication process.

2.3.2 Biodegradable and biocompatible microdevices

Biodegradable polymers are defined by polymers that in bioactive environments degrade over time. Enzymatic degradation arises in the presence of microorganisms such as fungi, bacteria and algae, where the polymer chains are broken down. Cleavage of the polymer chains can also occur by non-enzymatic processes like chemical hydrolysis (91). After disposal, biodegradable polymers will degrade and will not interfere with the ecosystem, whereas non-degradable polymers will persist for many years after disposal. Administration of non-degradable polymers into our body in regard to drug delivery is not an option. Another important aspect for microdevices is that they have to be biocompatible. As a general term, biocompatibility of a material is when a living body accepts its presence (91). There is a huge interest in fabricating microdevices in biocompatible and biodegradable polymers like poly-L-lactic acid (PLLA), poly-ε-caprolactone (PCL) and poly(lactic-co-glycolic acid) (PLGA) as they are approved by the US Food and Drug Administration (FDA) for applications in oral drug delivery (92,93). Change in polymeric materials often compromises the fabrication process of microdevices as well as size dimensions because the physiochemical properties of the polymers often determine both factors.

Fabrication techniques of biodegradable microdevices

In the last years, there has been an increased interest in fabricating microdevices in biocompatible and biodegradable polymers. This has resulted in many different fabrication techniques providing microdevices in different sizes, shapes and materials (84,94,95). Fabrication of microdevices in biodegradable materials are highly controlled by the polymer and the desired structure or shape of the microdevices. DeSimone *et al.* have developed the PRINT (Particle Replication in Non- Wetting Templates) technique for fabrication of micro-scale and sub-micro-scale structures in a mold using a polymer stamp. This technique has succeeded in fabricating particles with precise size control from 50 nm to > 100 μm, featuring different shapes, different polymers (biodegradable polymers) and included surface chemistry (94,96,97). Although, future applications of these particles for oral delivery are possible, studies so far have mainly been focusing on more fundamental aspects related to microfabrication and intravenous drug delivery. Their behavior in relation to oral drug delivery

needs to be further investigated to establish their usability as oral delivery vehicles. McHugh *et al*. have introduced the StampEd Assembly of polymer Layers (SEAL) fabrication technique to create microdevices in complex geometrical forms in biodegradable polymers including PLGA and PCL. This process combines soft lithography and an aligned sintering process to produce ≤400 μm sized polymeric structures (84). This process has been used to fabricate microdevices for injection purposes for delivery of a controlled pulsatile antigen.

Previous studies have demonstrated fabrication of PLGA and gelatin microwells by first defining the microstructures in SU-8 using photolithography and then replicated in polydimethylsiloxane (PDMS), which serves as a mold for PLGA or gelatin (98). Fabrication of microwells in both PLLA and PCL by the use of hot embossing has been shown in the literature. Microwells are small devices consisting of a walled reservoir for drug loading extending from a flat base. Hot embossing is a technique where heat and pressure are applied on a 3D stamp into a polymer film (99). This results in a film sheet with microwells. One major drawback with this method is that all the microwells are connected on the sheet. Obtaining individual microwells is possible, however, this would require additional processing steps such as reactive ion etching or by punching them out by applying higher pressure.

Fabrication of microcontainers in biodegradable polymers has been established in previous studies (92,95,100,101). They have shown promising techniques for fabrication of microcontainers in PLLA, PCL and PLGA. Petersen and coworkers addressed the issue of fabricating individual microcontainers in biodegradable materials by using mechanical punching and hot punching (92,95). The latter method is a modification of the hot embossing technique. Abid *et al.* were able to fabricate microcontainers in both PCL and PLGA by a novel fabrication technique based on compression molded polymer films and hot punching (**Figure 7**) (102). This process avoids the need for solvents or expensive batch processes and allows patterning of PCL and PLGA microcontainers that are thermally bound to the underlying poly(vinylalcohol) (PVA) substrate (release layer) in a single process. The PVA substrate is water-soluble allowing for release of individual microcontainers. The fabrication process might be implemented in a continuous manufacturing processes in a roll-to-roll configuration, which potentially is applicable for other polymers. The PCL microcontainers are 304 ± 3 μm in diameter and the reservoirs depth is 64.1 ± 1.0 μm with a volume of approximately 2.7 nL per microcontainer. The PLGA microcontainers are 275 ± 0.5 μm in outer diameter and the reservoir depth is 56 ± 1 μm, which resulted in a volume of 1.8 nL (77,102). Some of the advantages for using hot punching are that it is a simple and relatively cheap technique and it

is a scalable process suitable for high structural replication of individual polymeric microcontainers. In this PhD project, both PCL and PLGA microcontainers were used.

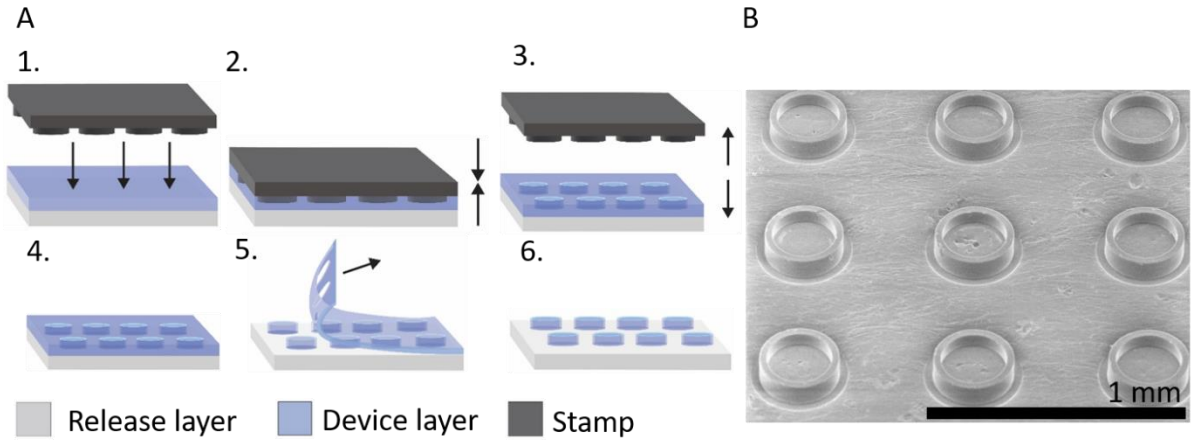

Figure 7: **A)** Schematic overview of a fabrication process for creating microcontainers in biopolymers. **1)** Here, a poly(vinylalcohol) (PVA) substrate (release layer) is assembled with a compression molded poly-ε-caprolactone (PCL) film (device layer). **2)** Hot punching is executed by applying heat and pressure with a nickel (Ni) stamp (stamp). **3)** The Ni stamp is demolded, **4)** resulting in PCL microcontainers separated from the surrounding film. **5)** The surrounding PCL film is peeled off and **6)** individual microcontainers are shown on the PVA substrate. **B)** SEM image of PCL microcontainer array after removal of the surrounding PCL film. Adapted from (102) with permission.

2.3.3 Drug loading and drug sealing in microcontainers

Several drug loading procedures have been developed for microcontainers and similar microdevices. This includes supercritical CO_2 impregnation (103–105), inject printing (74,106,107), photolithography (72,108,109) and spin coating of drug-polymer mixtures that are hot punched into the microcontainers (110). In addition, more manual techniques also exist such as manual powder filling with spatula or brush (76,85), powder embossing (111) or centrifugal compaction (112). Abid *et al.* showed that by combining a shadow mask with the latter methods, it was possible to prevent drug powder from accessing the gaps between the microcontainers, which allowed efficient loading of only the cavities (**Figure 8A**) (111). This is a fast procedure where only minor equipment is needed. The optimal choice of drug loading procedure highly depends on the physiochemical properties of the chosen drug and whether the drug needs to be co-delivered together with a polymer or if the drug is very costly. Each drug loading requires homogeneous filling that is reproducible and where the drug waste is limited. The average drug loading capacity highly depends on the drugs physiochemical properties such as stickiness, particle size and particle size distribution but also the cavity size of the microcontainers. Mazzoni *et al.* were able to load 3.1 ± 0.6 µg/microcontainer of a powder mixture consisting of lysozyme and the permeation enhancer C10 (7:3) and Birk *et al.* loaded 4.39 ± 0.77 µg of ciprofloxacin hydrochloride into each microcontainer (67,113). Both

studies applied the manual loading technique with a brush and a shadow mask. In this PhD project, a combination of manual powder filling with a brush and powder embossing has been used together with a shadow mask.

The mentioned fabrication techniques of biodegradable microdevices often lack or need optimization in relation to drug loading, sealing and release of individual microdevices (84,99). Abid *et al.* have focused on these aspects when designing the fabrication technique of PCL and PLGA microcontainers. The microcontainers are punched in PCL or PLGA leaving a removable film of non-usable PCL or PLGA. This film is used as shadow mask for the drug loading process to avoid drug deposition in between the microcontainers (**Figure 8B-C**). For drug loading the microcontainers, drug is placed in a holder and pressure is applied on the microcontainers, afterwards is the surrounding film of PCL removed.

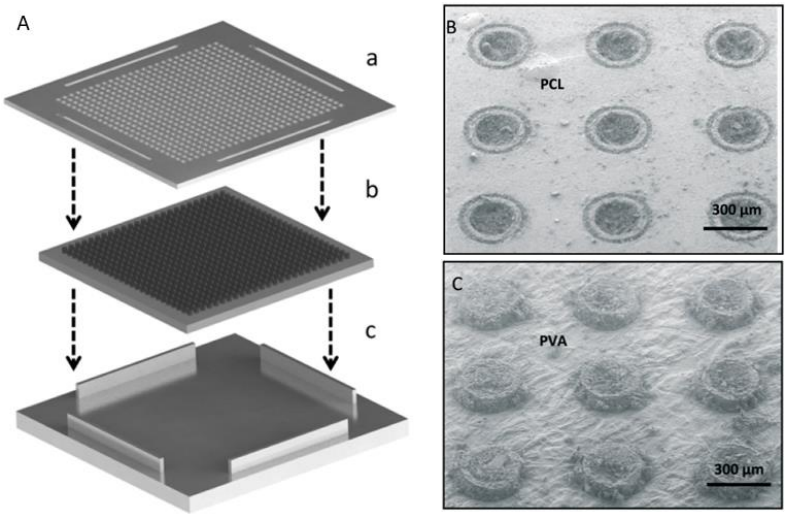

Figure 8: Schematic overview of the drug loading process of microcontainers. **A)** Illustrates a shadow mask used drug loading of SU-8 microcontainers, a) is the shadow mask, b) chip with microcontainers and c) holder for the chip (111). **B)** SEM image of poly-ε-caprolactone (PCL) microcontainer array after drug loading and before removal of the surrounding PCL film, **C)** SEM image of PCL microcontainers after drug loading and removal of the surrounding PCL film (102). Reprinted/adapted with permission from Elsevier and Royal Society of Chemistry.

Sealing the drug by applying a functionalized lid can provide protection from the harsh acidic environment in the stomach and can provide release in the small intestine where most drugs are absorbed (71). Studies have shown that an applying enteric coated lid onto the microcontainers can provide efficient protection of the loaded drug until the small intestine is reached (11,71). Various techniques for depositing polymeric films onto microdevices exist. Ultrasonic spray coating has shown to be very efficient in coating surfaces such as the microcontainers. High frequency sound vibrations forms a fine mist of polymeric solution that is deposited and coalescenced onto a substrate. This allow film coating of planar as well as non-planar surfaces with controllable coating thicknesses and high reproducibility (114).

Sealing the drug into the PCL and PLGA microcontainers were obtained by spray coating the cavity of the microcontainers with the enteric coating. Individual microcontainers were harvested by dissolving the PVA substrate (101,102). However, the film layer of enteric coating caused clusters of microcontainers but separation by manual force was possible. The enteric coating film is brittle and easy to break without support from the microcontainers.

2.4 Strategies to improve mucoadhesion of microdevices

Many research groups have focused on improving the adhesion of microdevices to the mucosal surface in order to prolong the residence time and, thereby, achieving improved drug absorption. Several strategies have been developed to improve mucoadhesion of microdevices such as: Polymeric functionalization, morphology of the microdevices and surface topography. All three methods have, in this PhD project, been used to improve mucoadhesion of microcontainers.

2.4.1 Polymeric functionalization of microdevices

Different mucoadhesive or mucopenetrating polymers can be deposited onto microdevices to enable stronger adhesion to the mucus layer. Various techniques exist, among these are ultrasonic spray coating, as previously mentioned in section 2.3.3, which has shown great results in coating three-dimensional structures such as the microcontainers with various polymers (115,116). This technique is very versatile and has a fast and reproducible outcome of uniform film coatings that can cover most surfaces. However, this highly depends on the polymer in focus.

Numerous polymers have shown great potential in adhering to mucosal surfaces. Each polymer promotes various interaction possibilities to mucus, which also determines their adhesion strength (117). One of the most promoted strategies is to use cationic polymers as they can form electrostatic interactions with the anionic mucin chains (118–120). Chitosan is the most studied cationic polymer mainly due to its adhesion ability, low toxicity, biocompatibility and moreover that it is biodegradable (121). Chitosan is a natural polysaccharide consisting of N-acetyl-D-glucoamines and D-glucosamine that are linked together via 1-4-β-glycosidic bonds (**Figure 9A**). It is obtained from partly deacetylation of chitin in basic environment by removing the acetate groups from chitin (122–124). Chitin is the second most abundant polysaccharide found in nature and is produced in crustacean shells (125). Chitosan is commercially available in different degrees of deacetylation and different molecular weights, which both contribute to its viscosity and solubility (122,124). Another key characteristic of

chitosan is that it swells in pH values above 6.2 and this gelation has been shown to control the drug release through chitosan (126). Chitosan can interact with mucin in different ways. First, physical entanglement into the mucus mesh is possible due to the long chain structure of chitosan. Secondly, chitosan contains –OH and $–NH_2$ groups, which promote both hydrogen and electrostatic bonding with mucin. Furthermore, hydrophobic interactions have also been shown to play a role in the mucoadhesion of chitosan (120).

Poly (ethylene glycol) (PEG) is a hydrophilic neutral polymer, which chemical structure allows very few options for interacting with mucin or any other molecule (**Figure 9B**). For this reason, PEG has been introduced as a mucopenetrating polymer (127,128). However, studies have shown that PEG also promotes adhesion to the mucosal lining. The interaction of PEG with mucus is highly affected by its molecular weight (35). Wang *et al.* have shown an improved penetration of polystyrene nanoparticles when coated with low molecular PEG weight (2 kDa) and an increased mucoadhesion when coated with high molecular weight PEG (10 kDa) (129). Mucoadhesion of high molecular weight PEG is believed to be related to penetration of the long PEG chains into the mucus mesh where hydrogen bonding or chain entanglement can occur (130,131).

Sodium alginate is an anionic linear polysaccharide derived from brown algae. Alginate contains varying amounts of 1.4-linked-β-D-mannuronic and α-L-guluronic acid (**Figure 9C**). These residues can vary in sequence and composition and can be arranged in different patterns of blocks along the chain, which will affect the molecular weight (132). Alginate is commercially available in different molecular weights and is often used as sodium alginate. This polymer is widely used due to its low-toxicity, biocompatibility and biodegradable properties together with low cost and its abilities to form a gel (133). Furthermore, alginate has shown strong mucoadhesion in its solid state mainly through hydrogen bonding, hydration and gelation (134). Alginate also possesses viscous slippery gel-like properties when in solution promoting adhesion (135). Previously, sodium alginate has shown a potential improvement in the relative bioavailability after oral dosing of sodium alginate microspheres loaded with insulin (136).

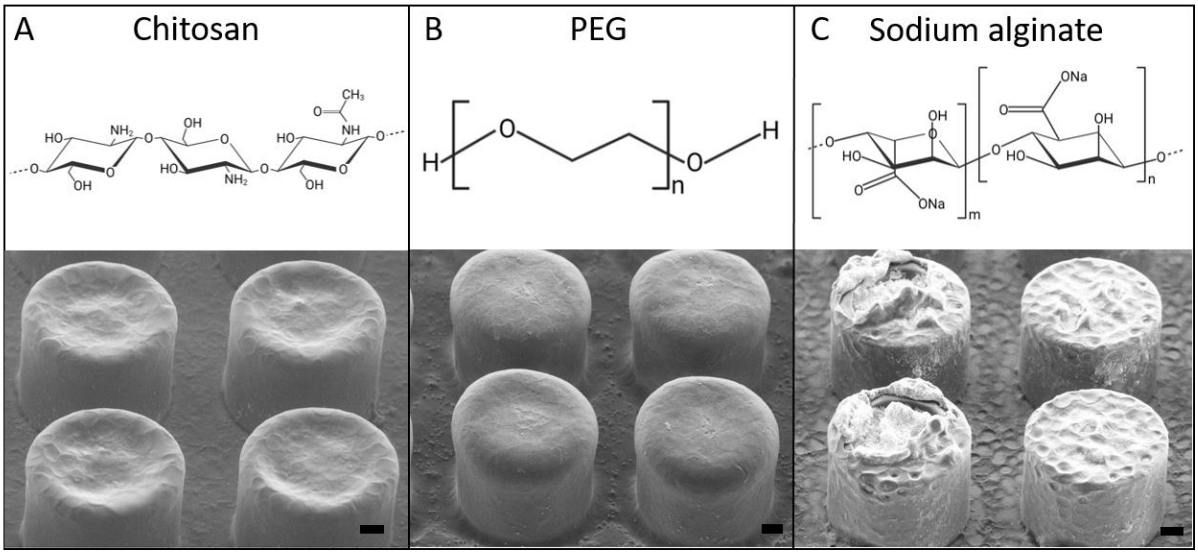

Figure 9: Presentation of chemical structures of the polymers applied in this PhD thesis together with a SEM images of the polymers coating layer. **A)** Chitosan consists of a linear polysaccharide chain composed of random distribution of D-glucosamine (deacetylated part) and N-acetyl-D-glucosamine subunits. Chitosan-coated microcontainers with an average thickness of 7.82±0.48 µm is shown. **B)** Poly(ethylene glycol) (PEG) is a hydroxyl polyether chain and is coated on microcontainers with a thickness of 30.57±3.45 µm. **C)** Sodium alginate consists of linear polysaccharide chain composed of varying amounts of 1.4-linked-β-D-mannuronic and α-L-guluronic acid. Sodium alginate-coated microcontainers are shown with a sodium alginate thickness of 1.97±0.12 µm. They are all examples of coatings applied on microcontainers in this PhD project. The coating thicknesses are reproduced from Paper II. All scale bars represent 50 µm.

Numerous polymers are classified as being mucoadhesive, but in general all materials that have the possibility of forming hydrogen bonding, hydrophobic interactions or any other type of interactions with the mucus layer can adhere to mucus. All microdevices fabricated in polymeric materials might show some degree of adhesion. Utilizing fabrication techniques for a broad variety of polymers can promote the possibility of fabricating mucoadhesive microdevices without further processing steps.

2.4.2 Morphology of microdevices

Morphology based approaches for promoting adhesion of microdevices have been utilized by many, consequently resulting in a variety of different shapes and sizes. Both parameters are believed to affect microdevices behavior and performance in *in vivo* settings, mainly explained by the contact area to mucosa and by their movement when exposed to a flow in the GI tract (72,137,138). Size differences of polymeric carriers have shown to influences the flow properties, clearance and degradation in the mucus layer located in the small intestine (139,140). The shape of the microdevices are believed to play a part in their ability to adhere to the mucosal surface. Many different shapes have been developed over the years such as cylindrical, planar, squared and triangular (74,78,85). Chirra *et al.* introduced a flat or planar device shape with the dimensions of 200 µm in diameter and a thickness of 7.5 µm

(74,109,141). This planar geometry showed promising abilities of adhering *in vivo* in mice GI tract explained by 1) an increased contact area available for interaction with the epithelium in the GI tract and 2) decreasing the force applied on the microdevices from the fluid flow in the GI tract. These planar microdevices reported better adhesion to the proximal and medial intestine compared to microspheres with the same surface area. In the colon, microspheres were retained approximately two times more than the microdevices (**Figure 10A**) (72).

In contrast to the planar microdevice has high (approximately 300 µm) cylindrical microcontainers shown an increase oral bioavailability of ketoprofen and furosemide, which was explained by their ability to adhere into the mucosal surface (**Figure 10B**) (11,85). The high microcontainers have a larger surface for adhesion compared to the more planar microdevices and both showed great potential in adhering to mucosa. High microcontainers are also heavier than the more planar microdevices and thus, they can promote deep embedment into mucus. Christfort *et al.* developed cylindrical, cubic and triangular shaped microcontainers with the same surface area and compared their ability to adhere in the colonic mucus layer. They saw that the number of corners, edges and surfaces strongly influence retention of microcontainers to the mucus layer (**Figure 10C-E**) (78).

More advanced shapes have also been developed to improve mucoadhesion, examples are multiclawed devices with sharp microtips to latch onto the mucosal tissue (82). They have been designed with thermal-sensitive grippers, called microtips, which attach themselves into the GI mucosa allowing extended drug release. This device showed excellent retention to the colonic mucus layer as well as increase rectal bioavailability of ketorolac (**Figure 10F**).

This clearly demonstrates how both size and shape of microdevices play a great part in improving their ability to adhere to mucus.

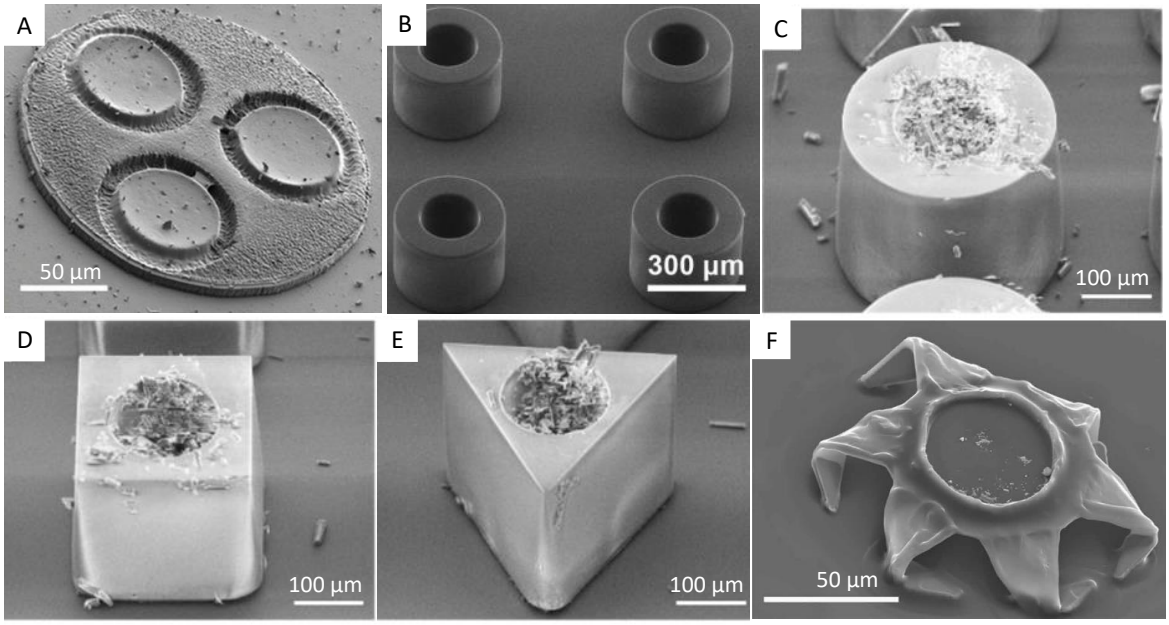

Figure 10: Overveiw of microdevices with different morphologies. **A)** SU-8 fabricated patches loaded with mulitiple different drugs into the three reservoirs (72,142). **B)** Originally high SU-8 microcontainers (89). **C)** SU-8 cylindrical microcontainer with the same surface area as **D)** SU-8 squred mircrocontainer and **E)** triangular SU-8 microcontainer (78). **F)** Thermal-sensitive grippers for rectal administration that can grap onto the colonic mucosa to increase retention time (81). Reprinted/adapted with permission from John Wiley and Sons, American Chemical Society, Multidisciplinary Digital Publishing Institute, American Association for the Advancement of Science.

2.4.3 Surface topography of microdevices

Topography-mediated adhesion represents an alternative approach for promoting mucoadhesion. Micro- and nanofeatures at the interfacial surface has shown increased adhesion to mucosa mainly explained by the increased surface area. This field has been greatly inspired by the ability of insects and lizards to adhere to surfaces by the help of hundred thousand micro-sized hairs (143). Structuring of surfaces will result in an increased surface area but also an increased roughness of the surface. Both are believed to improve the adhesion to mucosa as well as prolonging the retention time (144). The concept of planar microdevices mentioned previously was further developed with inclusion of nanostraw structures on the surface of the devices. The authors observed an enhanced bioadhesion, when compared to similar microdevices without nanostraws, in a Caco-2 cell flow system (**Figure 11A-B**) (75). Fox *et al.* believe that the increased adhesion is due to penetration of the nanostraws into the mucus layer, which prevents detachment of the devices due to increased interfacial surface area and hampered lateral movement of the device (75). This has also been demonstrated by Fischer *et al.* that silicon nanowires on glass microbeads increased adhesion to epithelium both *in vitro* and *in vivo*. Under *in vitro* mucus flow, they saw that microbeads with longer nanowires showed better resistance at higher shear forces than shorter nanowires or lectin coated nanowires. Lectin is a carbohydrate-binding protein, which can bind to a multitude of lectin

binding sites along the GI tract (145). When comparing microbeads with nanowires to a control without nanowires, they saw a 100-fold increase in the force needed for dislodgement. Under *in vivo* conditions, nanowire microbeads increased residence time in the GI tract by 10-folds when compared to control without nanowires (**Figure 11C**) (146,147). Vaut *et al.* tested mucoadhesion of 3D printed devices with different anchor-like surface structures and they saw, up to two-fold increase in adhesiveness to the mucosal surface when compared to a control without the presence of the surface structures (**Figure 11D-G**) (148). Nano- and micro-surface structures clearly show an improvement in surface adhesion, thereby, making it a promising strategy for enhancing mucoadhesion of microdevices. However, this strategy is limited by the fabrication method and the resolution of the desired structures on the device.

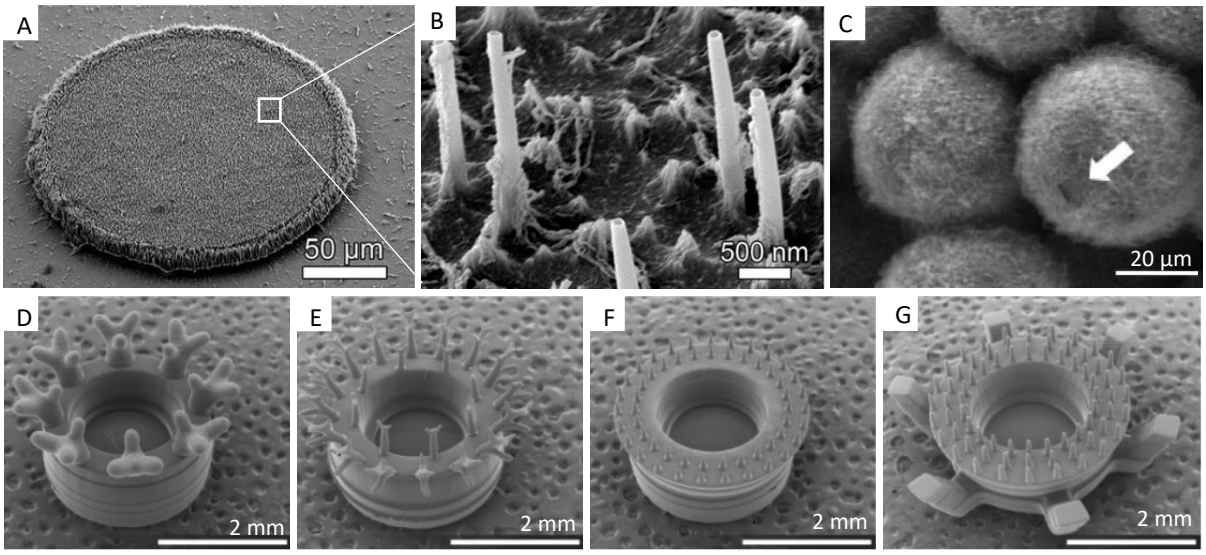

Figure 11: Illustration of microdevices with different topography. **A)** Sealed microdevice with nanostraw membranes and **B)** is a zoom-in of the nanostraw membrane, illustrating the nanostraws (75). **C)** Nanowire-coated microspheres and the arrow indicates an area with a reduced amount of nanowires (147). **D-G)** Demonstrates microcontainers fabricated with altering surface topography. D) Surface topography with large branching edge anchors **E)** Small branching edge anchors applied on the container surface F) overhang and straight anchor spikes on the surface **G)** Bioinspired surface design with phage-style and straight anchor spikes (148). Reprinted/adapted with permission from American Chemical Society.

2.5 Methods to study mucoadhesion

Mucoadhesion was defined back in the 1960's and ever since, researches have invented new ways for analyzing mucoadhesion. Mucus is a complex network of mucin monomers and is very easily affected by its surroundings. This highly compromises the reproducibility of adhesion tests. Several methods have been developed to evaluate mucoadhesion, each contributing to both limitations but also valuable insight into the nature of mucoadhesion. In this paragraph, a few methods will be elaborated as they have played a part in this PhD thesis.

2.5.1 Flow through method

The flow through method was first described by Rao and Buri in 1989 for testing bioadhesion of microparticles (149). This method has often been used to estimate mucoadhesion of different pharmaceutical dosage forms administered in regions where the mucosal surface is highly exposed to a continuous flow, such as the GI tract. Over the years, this method has been modified and new features have been added for optimization (150,151). The principle of the flow through method is illustrated in **Figure 12**. The typical principle is that a mucosal surface is placed on a slide/ holder that allows the tissue to be fixated in a desired angle. A chosen dosage form, such as a microdevice, is then placed on the tissue and allowed to interact with the surface of the tissue. A flow of simulated body fluid is then initiated and maintained. The dosage forms retention to the mucosal surface gives an idea of its ability to adhere to mucosa (149,152). This method has especially been used to evaluate mucoadhesion of microdevices as their adhesion is challenging to determine by other methods such as rheology and tensile forces (67). Microdevices are made in solid polymers and these can potentially damage the very sensitive equipment surface and interfere with the measurements. This removes the possibility of measuring adhesion by the use of the commercially available rheometer.

Devices in the micrometer size range makes it difficult to measure tensile forces. The devices are too small for allowing tensile force measurements with the commercially available texture analyzer due to force limitations of the instrument. Measuring tensile forces with atomic force microscope is also compromised by the size of the microdevices as they are too big (153). The flow through method has shown promising results in determining mucoadhesion of both microparticles, dual-sided devices and microcontainers (115,150,151).

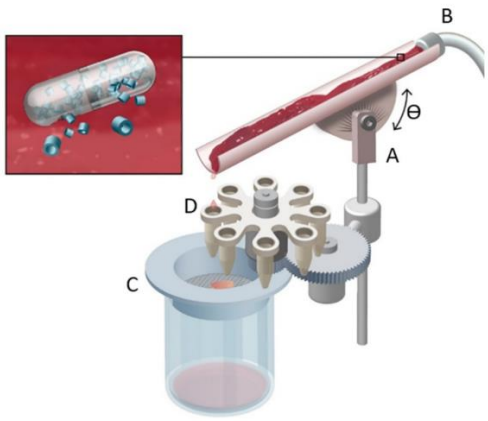

Figure 12: Schematic overview of the flow through principle, which consists of a tissue piece placed in an angle on a angle holder (**A**). The tested microcontainers are placed on the tissue and a continous flow is initiated (**B**). Underneath is placed a filter (**C**) where fluid and microcontainers are collected. An automated sample collector is shown underneach the tissue (**D**). Reprinted/adapted with permission from (77).

2.5.2 Texture analyzer

The texture analyzer is a commercially available instrument often used for measuring tensile forces required to detach a polymer sample from a piece of tissue. The instrument consists of a vertically movable stand that is attached on a stationary platform (**Figure 13**). The desired sample is attached to a probe mounted on a movable stand. A piece of animal tissue or hydrogel (whatever is desired to test adhesion to) is attached to the stationary platform. The movable stand is then slowly lowered downwards to the stationary stand where the tissue is placed. After reaching a given resistance between the sample and mucosa is the downward movement ended. Attachment is then held between the two surfaces and after a fixed time the sample is lifted from the tissue. The force needed to detach them is called detachment force and gives a relative adhesion value between the two surfaces.

Despite the simplicity of the instrument, many considerations are needed before conducting tensile force measurements as many factors can affect the outcome. Individual settings such as contact time and contact force are required for each sample to achieve optimal measurements (154,155). This compromises the possibility of comparing samples which, therefore, is rarely seen in the literature. Thus, all samples are conducted with the same settings to enable comparison (156). Comparing mucoadhesive results from the literature is not possible as test parameters and test environments are different (154,155). In general, force measurements can easily be affected by outer additives such as tissue variations, pH, ionic strength, temperature and hydration or dehydration of the tissue (155). Some of the factors are controllable, however, tissue variation and tissue conditions during the measurements are difficult to control and measure. The use of animal tissue for testing mucoadhesion contributes to large standard deviations of the measurements, which often results in no statistical evidence in the comparison of adhesion forces (157). Tissue variations are a huge disturbing factor of tensile force measurements and precautions are highly recommended when interpreting tensile force measurements (155).

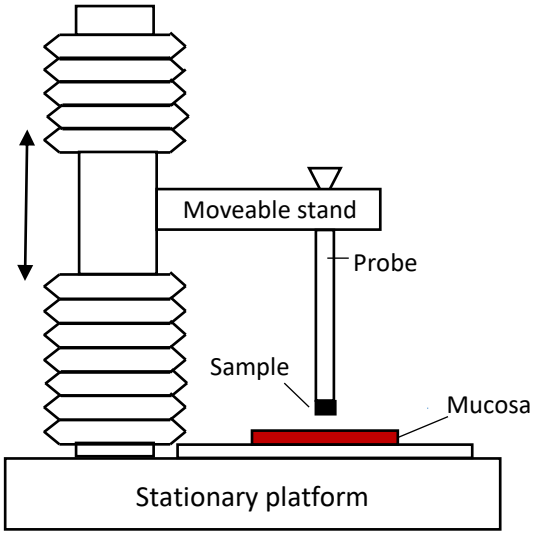

Figure 13: Schematic illustration of the texture analyzer for measuring tensile adhesion forces between mucosa and sample surfaces.

2.5.3 Reproducible data and experimental design

Evaluation of mucoadhesion often requires the use of a mucosal surface obtained from animals, which often contributes to large variation in data and compromises statistical evidence in the results. This is commonly known, especially in the pharmaceutical research field where animals often are used in pre-test of drug delivery systems. Many groups have developed artificial mucus simulating native mucus to prevent the need of animal tissue both from an ethical point of view but also to obtain more reproducible data that can be compared across the research field (158). This has resulted in some simple single component dispersions of mucin or hyaluronic acid (159). More complex mixtures have also been developed by mixing mucin, diethylene triamine penta-acetic acid, egg yolk and DNA (160). Boegh *et al.* demonstrated a potential *in vivo*-like biocompatible mucus, based on relevant constituents, similar barrier properties as mucus and similar rheological properties to porcine intestinal mucus (158). However, using artificially-made physiological mucus can also give a poor *in vivo*/*in vitro* correlation, as biological variation always will be a part of *in vivo* experiments. *In vitro* pre-evaluation before *ex vivo* and *in vivo* studies is, however, a useful tool and can provide indications to the behavior of a given drug delivery system.

Another strategy for improving reproducibility when evaluating mucoadhesion is by using the correct statistical design. Poor experimental design is a mutual problem across all scientific fields and awareness to poor reproducibility in research has gained much attention in the research world. Many researchers believe that poor reproducibility can be improved by “more robust experimental design”, “better mentorship” and “better statistics” (161). In general,

laboratory scientists have insufficient exercise in statistical methods and study design (162). Therefore suggest Ioannidis and coworkers that a statistician and/or methodologist should be involved in all stages of a research project (162). Good experimental designs and stronger understanding of statistical methods are needed to improve the reproducibility and validity of data.

3 Results and Discussion

The following section has been divided according to the papers presented in this PhD thesis (**Paper I-IV**). Each subsection represents the overall purpose, as well as a part describing and discussing selected results of the paper alongside the methods, further observations, and challenges associated to each part of the work. Furthermore, the connection and relations between the papers will be elaborated.

3.1 *Ex vivo* intestinal perfusion model for investigation of mucoadhesion of microcontainers

This subsection presents results obtained in **Paper I** "*Ex vivo* intestinal perfusion model for investigation of mucoadhesion of microcontainers" (full paper, see Appendix I).

Purpose

The aim of this study was to develop and evaluate an *ex vivo* perfusion model and to test the mucoadhesion of microcontainers with different morphology as well as their orientation at the mucosal surface.

Outcomes

This study was conducted to establish the foundation of this PhD project. The overall adhesion of microcontainers had to be established to emphasize the need of improvement in regard to mucoadhesion and how they oriented themselves at the mucosal lining.

Perfusion model

To understand the behavior of the microcontainers *in vivo*, a new model had to be established. The established perfusion model was highly inspired by the flow through model developed by Rao and Buri (149). The main difference in the two setups is that the new perfusion model keeps the intestinal tissue intact (piece of untreated small intestine from a pig) to maintain a closed system resembling the *in vivo* conditions (**Figure 14**). Maintaining a closed system minimizes disturbing factors such as fast dehydration, which affects the viscosity and adhesiveness of the mucus layer (48,49).

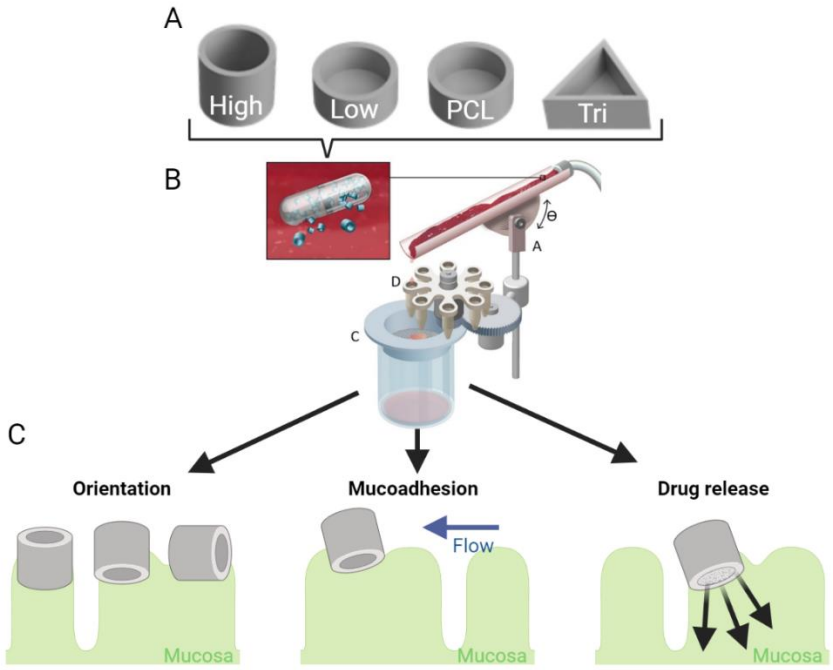

Figure 14: Schematic overveiw of Paper I, illustrating **A)** the tested microcontainers with different morphology and fabrication materials. **B)** the experimental perfusion model and **C)** illustrates the main outcome of the experiemental tests, which includs orientation, mucoadhesion and drug release.

Morphology of microcontainers

To evaluate the newly developed *ex vivo* model, microcontainers in different heights, sizes and materials were tested in relation to their mucoadhesion and their orientation on the mucosal surface after exposure to a continuous flow (**Figure 14**). Microcontainers have shown to engulf themselves into mucus after both *in situ* and *in vivo* studies. This indicated that microcontainers (called high microcontainers in this study) without any modifications showed promising adhesion to mucosa (11,85). Fabricating microcontainers in the biodegradable and biocompatible polymer, PCL was carried out by Abid *et al.* (100). Comparing the ability of mucoadhesion of SU-8 and PCL microcontainers were very interesting to establish the effect of the fabrication materials on adhesion. To enable a better comparison, low microcontainers were fabricated in SU-8 to resemble the height of the PCL microcontainers. Comparing low (108 ± 11 µm) and high (257 ± 4 µm) SU-8 microcontainers were also interesting because, as Chirra *et al.* have stated, planar microdevices (height of 7.5 µm) result in an enhanced retention time in mucus as the planar surface experience low shear stress and can remain longer in the intestine (72,74). The triangular microcontainers were developed to investigate the impact of edges on mucoadhesion of SU-8 microcontainers and whether they were more prone to adhere and be engulfed by mucus (59).

Drug loading and drug release

In this setup, it was necessary to select a model drug that possessed fast release, was easy to load into microcontainers and was easy to detect. Paracetamol was chosen due to its low toxicity, high water-solubility and ease of access (163). A fast release was required to be able to detect the drug concentration through the perfusion study, only running for 30 min.

Mucoadhesion of microcontainers

The mucoadhesion of microcontainers with different heights, shapes and materials was estimated based on their observed position on the intestinal tissue after exposure to a continuous flow. The movement of the microcontainers gave an estimate of the adhesion of microcontainers to mucosa. Meaning, the longer the microcontainers moved in the intestine the less they adhered. High microcontainers were compared with low microcontainers, both fabricated in SU-8, and they showed similar behavior. The majority was adhering in the start section of the tissue rather than in other sections (77.6 ± 25.1 % and 80.8 ± 12.9 %, respectively) (**Figure 15**). Triangular and low microcontainers (also fabricated in SU-8) were also highly dominating in the start section of the tissue compared to the other sections (67.1 ± 13.8 % and 80.8 ± 12.9 %, respectively). Significantly more of the triangular microcontainers were present in the middle part than observed for the low microcontainers. This could indicate that the sharp edges were able to adhere to mucosa after disruption from the mucosal surface, which was not observed for the low microcontainers. PCL microcontainers were compared to SU-8 microcontainers with the same height, and here, the SU-8 microcontainers appeared to be more adhesive than PCL microcontainers. Further optimization of the PCL microcontainers might be needed to facilitate drug release directly into the mucus layer. This could be obtained by applying mucoadhesive coatings on the cavity ensuring adhesion between the cavity and mucosa. This led to the development of **Paper IV**, where adhesion and degradation of PCL microcontainers were investigated. The adhesion between the varying shapes and mucus is believed to be controlled by the different contact surfaces between the microcontainers and mucosa. The high microcontainers had a larger contact surface than the low microcontainers if both were lying sideways and would, therefore, be expected to adhere more to the mucus layer (75).

All four types of microcontainers showed good adhesion properties as the majority of the microcontainers were found in the beginning of the tissue. This emphasizes the observations

done by Mazzoni *et al.* and Nielsen *et al.* where the microcontainers show promising adhesion to mucosa after *in vivo* and *in situ* studies (10,11).

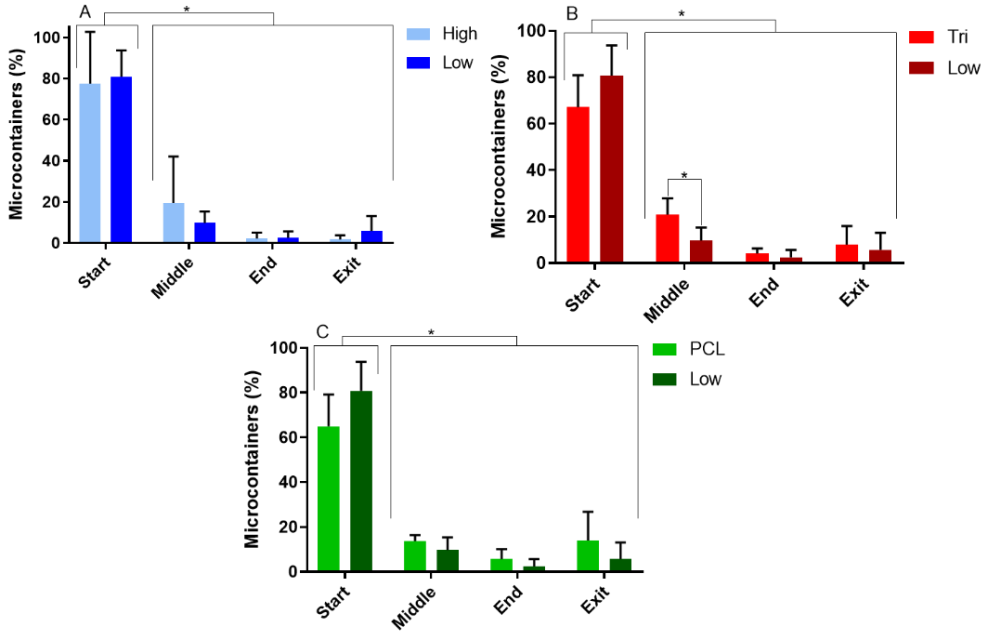

Figure 15: Percentage of microcontainers placed in the start, middle, end and exit on a piece of small intestine from a pig after *ex vivo* perfusion studies. Graphs showing **A)** comparison of microcontainers with varying heights of high microcontainers (257 ± 4 µm) and low microcontainers (108 ± 11 µm), **B)** comparison of triangular (tri) and cylindrical (low) shaped microcontainers and they processed similar heights and **C)** comparison of microcontainers fabricated in different materials of poly-ε-caprolactone (PCL) and SU-8, but with similar heights. Data represents mean ± SD with n=4.* indicates significant difference.

Orientation of microcontainers

Controlling the unidirectional drug release from the microcontainers directly into the mucus layer is believed to play a major part in achieving increased oral absorption. The orientation of microcontainers at the mucosal surface was investigated (**Figure 16)**. The microcontainers were categorized into the following orientations: sideways, up/down (up: cavity pointing away from mucus or down: cavity pointing into mucus) and deeply covered in mucus. The high microcontainers were mainly lying sideways, whereas the low microcontainers were mostly lying up or down in mucus. Both the triangular and low microcontainers were mainly lying up or down in mucus and showed similar orientation in general. Significantly more of the PCL microcontainers were lying up or down compared to the SU-8 microcontainers. The orientation of the microcontainers was strongly controlled by the height of the microcontainers. The data indicated that high microcontainers were mainly half embedded into the mucus, which means that the drug was released very close to the epithelial lining, whereas the low microcontainers were either positioned with the cavity away from mucosa or directly into mucosa.

The orientation of the microcontainers matters in regard to drug absorption, however, the drug release profile affects this process. Most drugs diffuse out of the microcontainers due to a concentration gradient, and if this process occurs fast, the drug will probably not be able to be as up-concentrated as if the drug release was slower. Simply explained, the microcontainers will not be able to attach themselves before drug release. Paracetamol has shown to be released from microcontainers within 2 h, however, the estimation of the time needed for the microcontainers to be established in the mucosal surface *in vivo* still needs to be clarified (164).

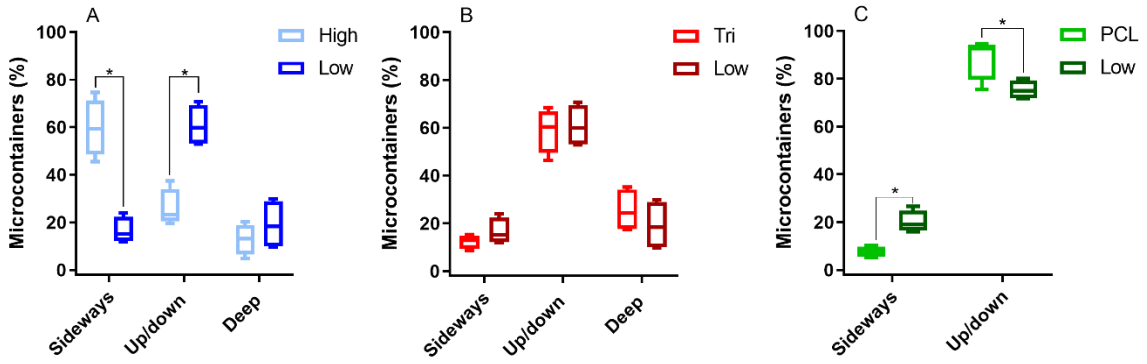

Figure 16: Percentage of microcontainers oriented sideways, up/down or deep in the surface of the small intestine of a pig after *ex vivo* perfusion studies. Diagrams showing **A)** orientation of high (257 ± 4 µm) and low (108 ± 11 µm) microcontainers, **B)** orientation of triangular (tri) and cylindrical microcontainers (low) and **C)** orientation of poly-ε-caprolactone (PCL) and SU-8 (low) microcontainers. Data is represented as mean ± SD with n=4. * indicates significant difference.

Further development of the newly designed perfusion setup could strengthen the model and may better resemble *in vivo* conditions. Applying peristaltic movement to the model (not just a peristaltic pump) could potentially give the ideal setup for testing mucoadhesive microdevices behavior *ex vivo*. In addition, simulating food passage could be used to challenge the ability of the microcontainers to adhere to mucosa, and testing the adhesion of the microcontainers during extreme conditions, such as a high perfusion flow, increased vertical tissue angle, could also potentially indicate the adhesion forces between the microcontainers and mucosa.

Drug permeation

An *in vitro* cell model of Caco-2 cells with an applied mucus layer was investigated, in relation to the perfusion setup, to be able to estimate the impact of adhesion of the microcontainers and the orientation on drug permeation. This work was not included in **Paper I** and therefore unpublished as more studies were needed. Permeation through a realistic mucus layer could elucidate the impact, the unidirectional release has on drug permeation *in vitro*. A mucus-secreting Caco-2/HT29-MTX-E12 co-culture monolayer is available but several studies have experienced a secretion of a non-coherent mucus layer which, thereby, indicates poor barrier

properties of the mucus layer (165). Jørgensen *et al.* compared permeation of insulin across both a Caco-2 cell monolayer and a Caco-2/HT29-MTX-E12 monolayer when dosed in microcontainers. No significant difference was observed in insulin transport across the two cell cultures (112). This could indicate that insulin transport was not hampered by the mucus layer present on the Caco-2/HT29-MTX-E12 co-culture. There could be several reasons for this outcome and one of them could be a poorly covering mucus layer. In this respect, a Caco-2 cell culture combined with a mucus layer could be used for evaluating permeation across mucus. A study was conducted to observe if different sources of mucus could be applied onto Caco-2 cells. Two different mucus sources were investigated, porcine small intestinal mucus was used in its native start and as purified mucus as described by Fabiano *et al.* (166). Caco-2 cells incubated with HBSS buffer or the two mucus sources were stained with alcian blue, which showed that both mucus sources were attaching to the cell surface. Further studies were needed to evaluate the attachment between mucins and the cell surface. Cell viability tests were conducted to evaluate if the Caco-2 cells were compatible with the mucus sources. However, the mucus sources interfered with the measurements, which made the viability test less reliable. A permeation study was conducted to determine permeation of amorphous sodium salt of furosemide (ASSF) through Caco-2 cells applied the two mucus sources. High permeation was seen for Caco-2 cells applied mucus, which could be explained by a damage cell layer. Unfortunately, we were not able to make Caco-2 cells compatible with the applied mucus sources and further studies are needed to make them more compatible.

3.2 General experimental design for testing adhesion to mucosal tissue

The following subsection presents results based on **Paper II** "General experimental design for testing adhesion to mucosal tissue" (full paper, see Appendix II).

Purpose

The aim of this study was to provide statistical guidelines for designing, analyzing and evaluating *ex vivo* experiments to obtain reproducible results with smaller standard deviations. To validate the statistical design, tensile force measurements of different topographies were tested and compared as a case study to emphasize the effect, these statistical guidelines have on the results (**Figure 17**).

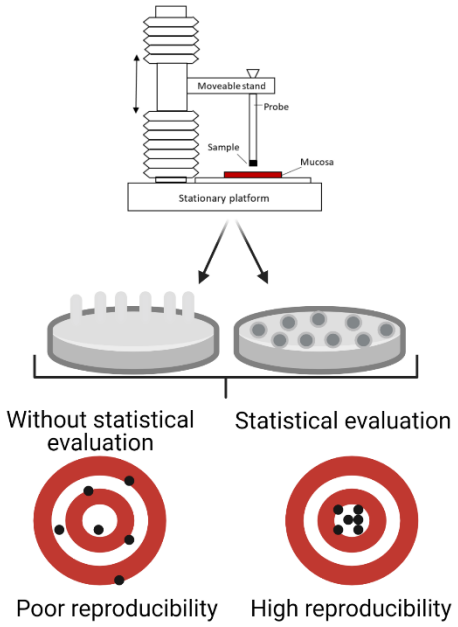

Figure 17: Shcematic overveiw of Paper II illustrating a texture anlyzer, the surface topographies tested and that the tensile force measurements were evaluated with and without statistical evaluation. The aim were to improve the reproduciblity of tensile force measurements on tissue.

Outcomes

PDMS microstructures

The texture analyzer has been highly used in the pharmaceutical industry to determine mucoadhesive forces (167). To elucidate the adhesive properties of different surface topographies, we tested surfaces with micropillars and surfaces with microcavities (**Figure 18**). Increasing the surface area has shown to promote and enhance adhesion to mucosa (168). This is in accordance with the mechanical theory of mucoadhesion (introduced in the section 2.2.2),

as the pillars and cavities introduce a rough surface. Clarifying the effect of surface topography on mucoadhesion was desired before initiating challenging fabrication processes to obtain microcontainers with surface structures. The following microstructures were investigated in this study: T1 microcavities, T2 micropillars, T3 microcavities and T4 micropillars (**Figure 18**). The micropillars in T2 were longer than T4 (60 µm and 15 µm, respectively) and they have a tendency to bend, which makes the surface more smooth and less pillar-like. T4 facilitated pillar-like structures that were more closely placed than for T2. The largest difference between the microcavity surfaces was the cavity width, which were twice as large for T3 compared to T1.

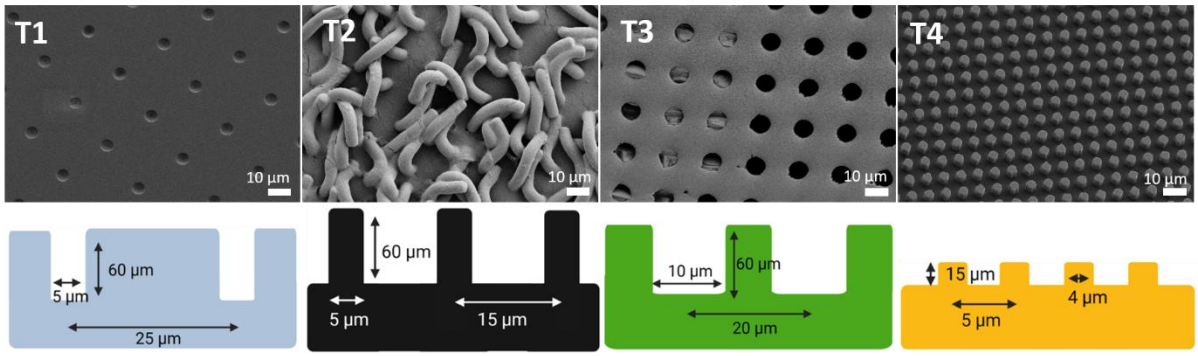

Figure 18: Schematic overview of the four microstructures investigated. **T1** PDMS surfaces processes microcavities, **T2** PDMS microstructures has long micropillars, **T3** PDMS also has microcavities and **T4** PDMS surfaces show short micropillars. Scale bars represents 10 µm.

After initiating tensile force measurements, it became evident that large test variations were affecting the results and that it was difficult to obtain reliable results. This led to **Paper II**, as it was realized that a suitable evaluation was needed to eliminate disturbing factors and make the results more reproducible.

To determine the disturbing factors, a PDMS microstructured surface T1 was measured ten times with the same parameters on the same piece of tissue in 4 replicates (**Figure 19**). These measurements showed linear fits but all four fits were very different from one another and the measurements were either decreasing or increasing over time. Both these observations made it clear that tissue variations and time of the measurements affected the measured tensile forces. Eliminating such factors could potentially improve the measurements and give a more realistic evaluation of the effect of the topographies on tensile forces.

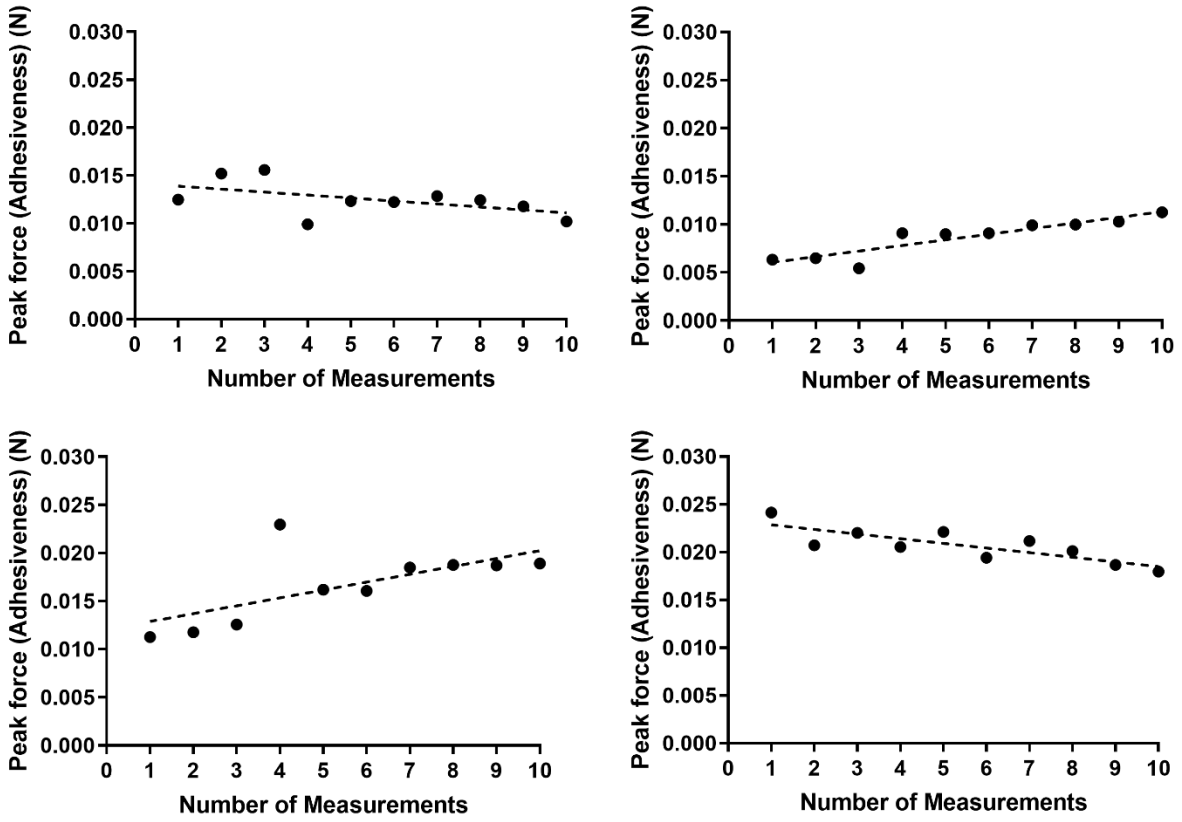

Figure 19: The four graphs shows repeating peak force measurements of PDMS microstructure T1 to four different porcine intestinal tissues (each piece represents each graph). n = 10.

Tissue variations

One way to correct for tissue variations in the tensile force measurements was to conduct baseline measurements of the tissue before and after each measurement. A flat PDMS sample was used as baseline sample. The flat measurements before and after each actual sample gave an indication of the adhesiveness of the tissue (**Figure 20**). As stated previously, tissue variations is a well-known phenomenon and even site to site variations on the same tissue piece occurs.

Time variations

The time aspect was also shown to affect the measurements, as indicated in **Figure 19**. Over time, the tissue will be affected by either hydration or dehydration depending on how water rich the surrounding environment was. Furthermore, ionic strength and pH can influence the mucus layer. To eliminate the variations due to passing time, the samples corresponding to different topographies were measured in a random order, to make sure that time affected the measured topographies equally. **Figure 20** shows all the measurements of both flat baseline samples and the four different topographies.

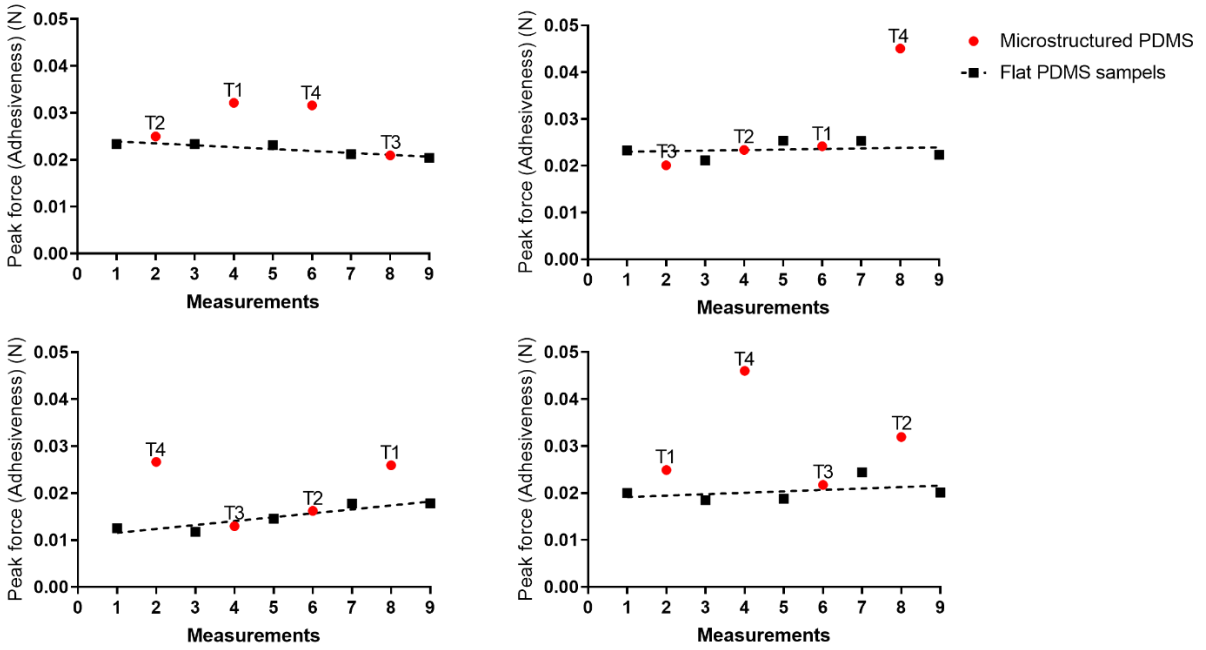

Figure 20: Peak force (N) measurements of different PDMS microstructures (T1, T2, T3 and T4) displayed in a random rang order, illustrated by the red dots. The black squares represents the baseline points, measured with a flat PDMS sample, connected by a dotted line. Each graph represents results from different pieces of porcine intestinal tissue. n = 9.

Statistical evaluation

To illustrate the value of the statistical design, in **Figure 21** is shown the peak forces for the different topographies with and without statistical evaluation. **Figure 21A** shows raw peak force values where tissue and time variations still interfere and affect the estimated peak forces. **Figure 21B** shows the estimated peak forces corrected for tissue and time variations. Applying the statistical design, removed the effect of disturbing factors such as tissue and time variations. As a consequence, the peak forces were about two-fold lower than the raw peak forces, however, T4 was now significantly higher than all the other microstructures. Eliminating the interfering forces of tissue and time resulted in lower values as the forces only represents the topographies peak forces. The statistical design successfully eliminated the interfering effect of tissue and time variations. After applying the statistical evaluation, the confidence interval became closer to 0, indicating that the measured mean is more reliable.

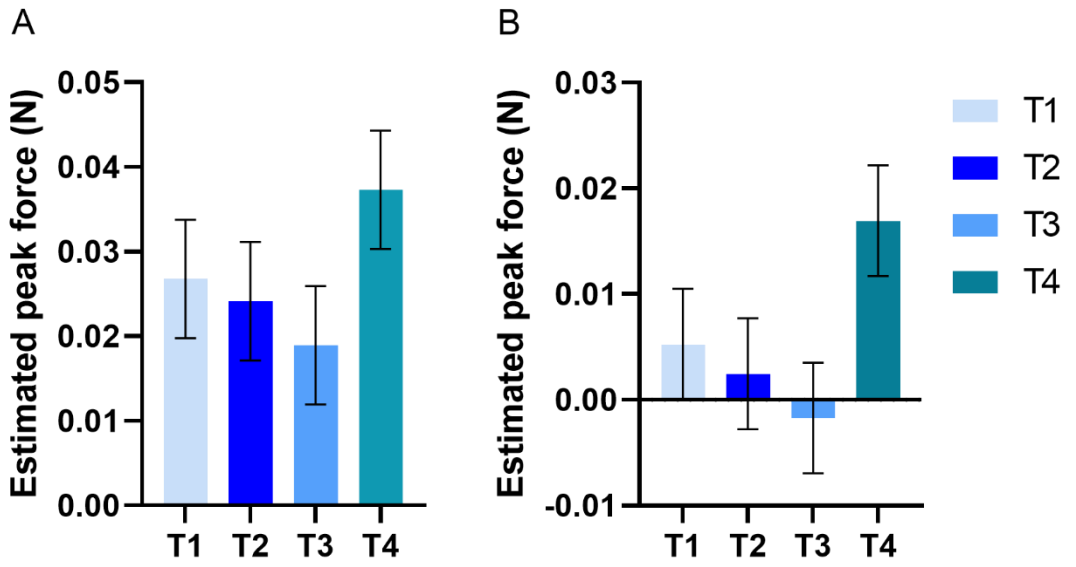

Figure 21: Peak force measurements of the different PDMS microstructures (T1, T2, T3 and T4) conducted on four different pieces of porcine small intestinal tissue. **A)** The plot represents raw peak force estimates and **B)** the graph shows peak force estimates after evaluation with the statistical guidelines presented in this study. All the estimates are shown as estimated peak forces ± confidence intervals (95 %). n = 4.

Surface topography

The results, after the statistical evaluation, clearly demonstrates that micropillars have an enhanced adhesion to mucosa compared to the microcavities. However, this was only the case for one of the micropillars topography, T4, and not for T2. The micropillars of T2 was longer than the T4 and longer pillars have an increased tendency to bend, which makes the surface smoother and less pillar-like. The T4 topography presents pillar-like structures that are placed more closely than for T2. Both micropillars and microcavities processes an increased surface area compared to plane surfaced, pillars are more adhesive, which could be explained by the higher surface roughness and the fact that they get entangled more easily into the mucus network. Applying micropillars on microcontainers would most likely enhance the adhesion and result in a longer retention time at the mucosal surface. Christfort *et al.* have recently demonstrated how to fabricate microcontainers with microstructures and tested them in a closed-loop intestinal perfusion model in anesthetized rats. However, no significant enhancement in mucoadhesion was seen then compared to microcontainers without microstructures (78). This could be explained by the size of the pillars on the microcontainers, which were 41 µm in height and 35 µm in diameter. Fox *et al.* have demonstrated an increased adhesion *in vitro* and *ex vivo* when modifying the microdevice surface with pillars approximately 60-160 nm (75). The studies presented in this thesis demonstrates an improved adhesion *ex vivo* when applying micropillars on PDMS surfaces. Applying micropillars could potentially increase the adhesion of microcontainers to mucosa, however, the size of the pillars

appears to have an important impact on adhesion to mucosa. Further studies have to be conducted to elucidate that statement.

3.3 Optimization of mucoadhesive coatings on microcontainers for oral drug delivery

The following subsection presents results obtained in **Paper III** "Optimization of mucoadhesive coatings on microcontainers for oral drug delivery" (for full paper, see Appendix III).

Purpose:

The aim of this study was to determine the optimal mucoadhesive coating on furosemide-loaded microcontainers to achieve an efficient adhesion to the intestinal lining.

Outcomes:

In previous studies, microcontainers have been coated with different polymeric coatings to achieve specific behaviors in the GI tract (115,116,164). Different polymers have been used, but the impact of the polymer thicknesses on mucoadhesion has not been investigated until now. **Paper III** addresses the question whether the thickness of polymeric coatings has an effect on drug release and the ability to adhere to the mucosal surface in the small intestine (**Figure 22**).

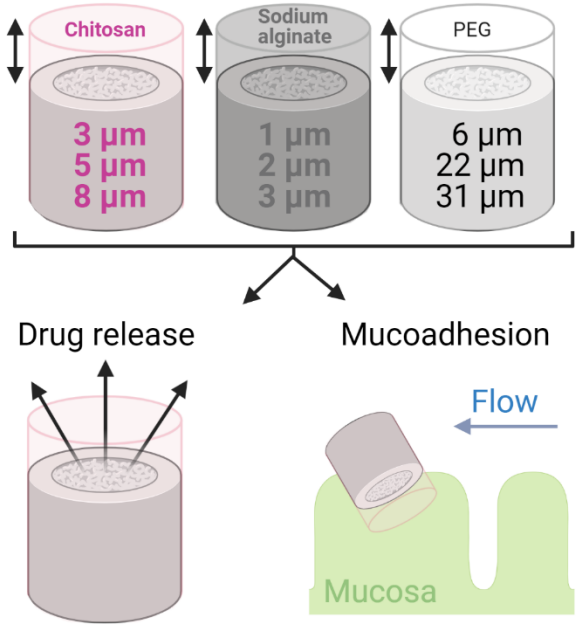

Figure 22: Schematic overview of the conducted experiments aimed to establish the optimal polymeric coating for obtaining mucoadhesive microcontainers without compromising the drug release profile.

Experimental setup and drug loading

The mucoadhesiveness of the polymer-coated microcontainers was first evaluated in the *ex vivo* perfusion model developed in **Paper I**. Evaluating mucoadhesion of the polymer-coated

microcontainers with the perfusion model enabled easier comparison to the results obtained in **Paper I**. This elucidated the two different adhesion strategies, morphology or polymeric coatings and their impact on mucoadhesion. The perfusion model was, however, not suitable for evaluation of polymeric coatings that swells. Chitosan swells when in contact with aqueous solutions above pH 6.2 (126). In the perfusion model, microcontainers were inserted into the small intestine in a capsule that slowly dissolved and allowed slow hydration of the chitosan coating. In this study, the swelling of chitosan showed, to improve its interaction with mucus, but also showed to result in accumulation of microcontainers (they clump together). This resulted in a prolonged release profile as the drug has to diffuse through the chitosan hydrogel. Moreover, the aggregation of the chitosan-coated microcontainer will prevent them from being spread out in the small intestine to target a larger surface area. This behavior can have a major impact on *in vivo* results, and complicate the administration of chitosan-coated microcontainers. For this reason, the flow through model was used for evaluating the microcontainers mucoadhesion when applied polymeric coatings.

Furosemide was utilized as model drug in this study. Furosemide is a weak acid (pK_a 3.5 and 9.9) with poor aqueous solubility of 5–20 µg/mL at pH 7 and has a low intestinal permeability (BCS class IV compound) (169–171). Furosemide is challenged by site-specific absorption, in the stomach, but mainly in the upper part of the small intestine resulting in inter- and intra-individual variation of oral bioavailability (20-60 %) (172,173). Granero *et al.* describe that the dosage form of furosemide and food passage highly influences furosemides intestinal absorption (172). This clearly emphasizes the need for improving the absorption of furosemide and to reduce the varying oral bioavailability. Furosemide as a poorly soluble drug was selected in order to investigate the ability of the microcontainers to release the drug unidirectional. Highly water-soluble drugs will quickly be released from the cavity of the microcontainers and will most likely be more challenging to up-concentrate at the intestinal lining. Evaluating the effect of unidirectional drug release from microcontainers and how they orient themselves can be difficult under *in vivo* conditions if the drug is highly water-soluble.

Polymeric coatings

Chitosan, sodium alginate and PEG are three well-known mucoadhesive polymers that have shown strong adhesion to mucus. They were selected due to their diverse polymeric properties and their different abilities to interact with mucus (see section 2.4.1). Three different thicknesses of each polymer was spray coated on furosemide-loaded microcontainers. The

selected coating thicknesses were based on the coating quality and data obtained from unpublished studies. Chitosan and PEG showed smooth coherent coating layers on the microcontainers. On the other hand, sodium alginate showed less coherent and a rough coating layer on the microcontainers (**Figure 23**).

Drug release through the polymeric coatings

In this study, neither PEG nor sodium alginate affected the release profiles of furosemide compared to non-coated microcontainers. Chitosan-coated microcontainers gave rise to a sustained release of furosemide, and all three chitosan thicknesses showed a significant reduction in the release of furosemide compared to release from non-coated microcontainers. Interestingly, no significant difference was observed between the three chitosan thicknesses after 1 h of release (approximately 40-48 % released). The release of furosemide from chitosan-coated microcontainers was prolonged when compared to non-coated microcontainers and 100 % release was observed after 7 h. The drug in question plays a major role when evaluating the release profile through mucoadhesive coatings. Birk *et al.* observed that the release profile of ciprofloxacin through an 8.9±0.7 µm thick chitosan layer was affected greatly as it took 28 h to release 100 %, whereas ciprofloxacin was released completely from non-coated microcontainers after 7 h (116). The desired release profiles from the microcontainers highly depends on the intended drug response. Often a fast release is desired as transit time of the microcontainers through the small intestine has been shown to range between 0.5 – 4 h (24). However, a sustained release was not a problem for mucoadhesive microcontainers as they can increase the retention time at the mucosal surface to some extend and, thereby, achieve the desired drug response. Mucus is constantly secreted from the epithelial lining, and its turnover time has been estimated to be between 47-270 min (33). The turnover time clearly challenges mucoadhesive formulations with the desire of a slow release profile. The outer mucus layer, where the microcontainers are adhering, will most likely detach itself from the more coherent mucus layer and both mucus and microcontainers will follow the passage of fluid and food down the GI tract. Sodium alginate and PEG are both water soluble and may not be able to maintain the microcontainers at the mucosal surface to ensure complete drug release of a sustained drug release profile.

Mucoadhesion of polymer-coated microcontainers

Only minor differences were observed between the different thicknesses of each polymer when evaluated on the flow through setup. Approximately 80 % of the chitosan-coated

microcontainers adhered to mucosa, whereas 50 % and 60 % of sodium alginate and PEG-coated microcontainers adhered, respectively (**Figure 23**). All three polymer-coated microcontainers showed a significantly higher adhesion to mucosa than non-coated microcontainers. Adhesion has been explained by different theories (see section 2.2.2). Adhesion of the polymers are believed to follow different adhesion theories such as the diffusion theory that explains adhesion due to entanglement between mucus and polymer chains, which all the three polymers are believed to do. The absorption theory describes adhesive attachment through chemical interactions, which is applicable for all three polymers. The electrostatic adhesion theory can be evident for chitosan as it can form electrostatic interactions with mucin.

Testing more newly developed mucoadhesive polymers could be interesting for future studies such as thiolated chitosan. Thiolated mucoadhesive polymers have gained much attention as they have shown to interact strongly with mucus as disulfide bonds can be established (174).

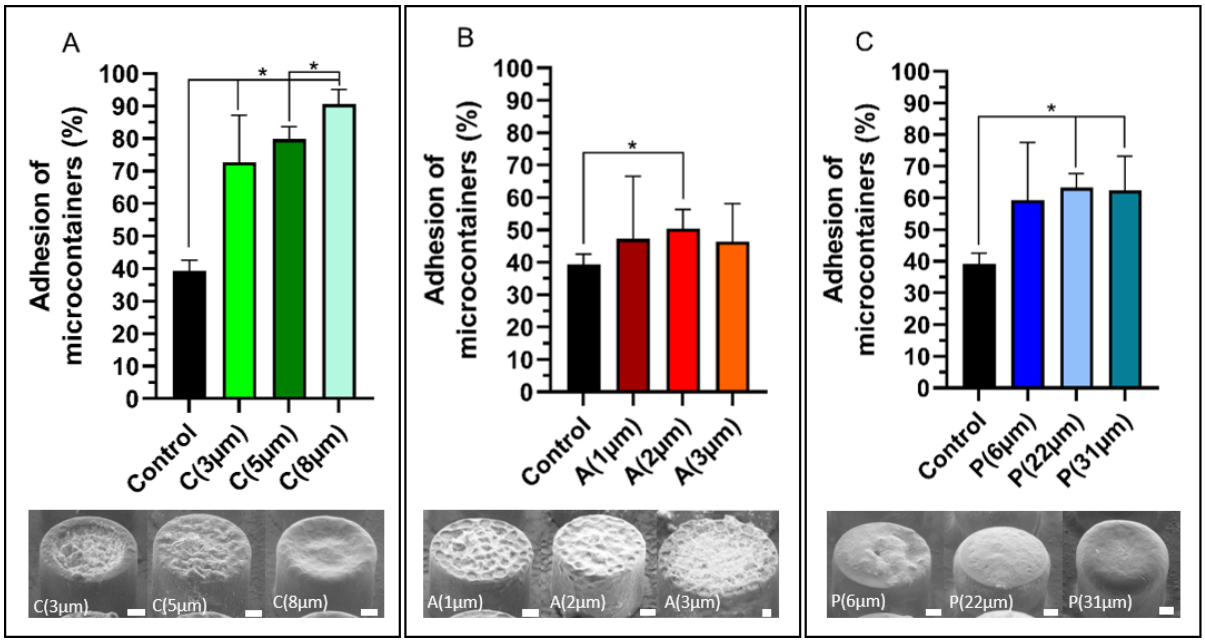

Figure 23: The plots illustrate the ability of polymeric-coated and non-coated microcontainers to adhere to the mucosal lining of the small intestine from a pig. Black bar represents adhesion of non-coated microcontainers. **A)** Adhesion of chitosan-coated microcontainers coated with different thicknesses. SEM images of the three chitosan thicknesses are shown underneath the graph. **B)** Adhesion of sodium alginate-coated microcontainers in different thicknesses. SEM images of the three sodium alginate thicknesses are shown underneath the graph. **C)** Adhesion of PEG-coated microcontainers in different thicknesses. SEM images of the three PEG thicknesses are shown underneath the graph. Black lines with * indicate significant difference in the adhesion of non-coated microcontainers and microcontainers coated with the different mucoadhesive polymers. Data represent mean ± SD, n = 4-5. All scale bars represents 50 µm except for A(3µm) which represents 20 µm.

Tensile forces between mucus and a single microcontainer could give a great insight into the actual mucoadhesive forces of polymeric-coated microcontainers and how the coating layer is behaving when retained. A special load cell was developed for the commercially available

texture analyzer to enable tensile force measurements of single polymer-coated microcontainers. Tests were conducted, but were not reliable due to a lack of sensitivity of the setup, thus, the results were not included in **Paper III**. Further optimization of tensile force measurements of single microcontainers is currently ongoing in the research group. One could upscale the whole microcontainer (make them bigger) to be able to measure tensile forces, but this would still give a false perspective on how the microcontainers would behave in *in vivo* settings.

Targeting specific areas of the GI tract is a major challenge. Addressing mucosal targeting is difficult to control as polymeric coatings can interact and adhere to many surfaces down the GI tract. First and foremost, surfaces coated with a mucoadhesive polymer can interact and adhere to one another, which can prevent them from interacting with the mucosal surface. Secondly, mucoadhesive surfaces can interact with loose mucus as well as food residuals that are present in the intestinal lumen and, thus, prevent drug release close to the epithelium wall.

The microcontainers with polymeric coatings showed stronger adhesion to mucosa than non-coated microcontainers *ex vivo*. This was, however, not evident for Christfort *et al.* when evaluating PEG- and chitosan-coated microcontainers *in vivo* (164). No significant differences were observed for paracetamol absorption when delivered orally in microcontainers coated with either chitosan, PEG or Eudragit® S100. High forces are present *in vivo*, such as peristaltic forces and passage of fluid/food. The force required for retaining a microcontainer to the mucosal surface needs to be very strong to overcome the applied forces under *in vivo* conditions. Addition of peristaltic movement in the flow through setup would clarify the forces needed to enable retainment of the microcontainers at the mucosal surface.

This study highlights an improved adhesion *ex vivo* when applying chitosan-coatings on the cavity of the microcontainers. Whether this is evident *in vivo* needs to be investigated. Numerous research groups have studied polymeric coatings to obtain adhesion to mucosa as well as to enhance the resident time at the mucosal surface (21,56,57,175). Many have demonstrated increased adhesion both *in vitro* and *ex vivo* when functionalizing microdevices with specific polymers, however, only a limited amount of *in vivo* evaluation of microdevices has been reported. Chirra *et al.* demonstrated an increased retention of lectin-conjugated planar microdevices in the proximal part of the small intestine in mice when compared to microdevices without lectin (72).

3.4 Investigation of mucoadhesion and degradation of PCL and PLGA microcontainers for oral drug delivery

This subsection represents results presented in **Paper IV** "Investigation of mucoadhesion and degradation of PCL and PLGA microcontainers for oral drug delivery" (for full paper, see Appendix IV).

Purpose

The aim of this work was to evaluate microcontainers fabricated in different polymeric materials (PLGA 50:50, PLGA 75:25 or PCL) and to compare their biodegradation *in vitro* as well as their ability to adhere to the mucosal surface (**Figure 24**).

Outcomes

Microcontainers have most often been fabricated in SU-8 by photolithography (11,76,78). SU-8 is a great material for establishing proof of concept in regards to microcontainers as a promising drug delivery system. However, SU-8 is not biodegradable and not approved for oral intake by the FDA. Therefore, throughout this PhD project, it has been of major importance that the microcontainers could be fabricated in biocompatible and biodegradable material.

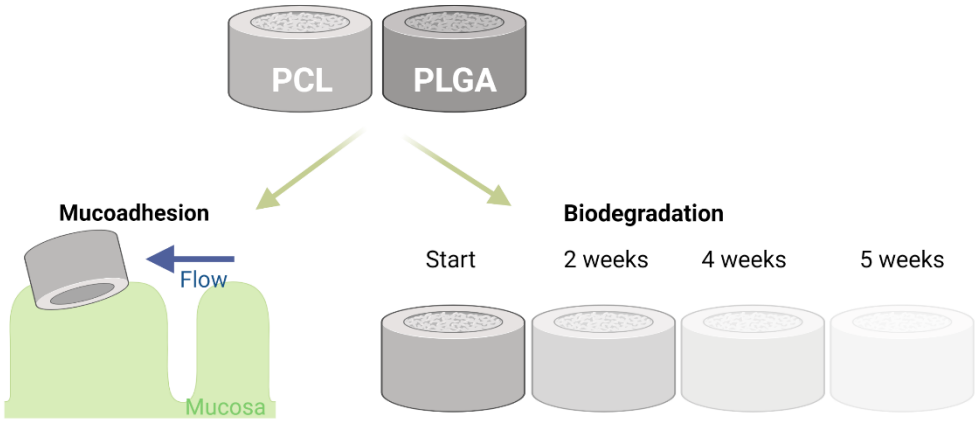

Figure 24: Schematic overview of the conducted experiments aimed to establish the ability of biodegradable microcontainers to adherer to mucosa as well as to establish the duration of degradation.

Fabrication of PLGA microcontainers

To ensure successful fabrication of microcontainers with the hot punching process, the polymers have to fulfill certain criteria such as, the underlying PVA substrate must process a higher T_g than the T_g of the device polymers (PCL and PLGA). This ensures that the PVA substrate was not influenced by the hot punching process. T_g of PVA is 85°C, and the PCL were punched for obtaining the microcontainer structure at 70°C. This punching temperature

allowed the PVA substrate to maintain its elastic-like properties and mechanical stability, which was required for punching. The PLGA microcontainer were punched at 80°C, which still enables the PVA to maintain its desirable properties. The PCL and PLGA microcontainers were punched onto a PVA layer to enable release of individual microcontainers. PVA is highly water soluble and after fabrication of the microcontainers were they harvested by dissolving the underlying PVA layer. The underlying polymer requires high water solubility for obtaining individual microcontainers. The device polymers mechanical properties (e.g. elastic properties) was of great importance in order to be able to peel of the surrounding film layer. The adhesion between the PVA and PCL/PLGA layers has to be sufficient enough for removing the surrounding film without removing the punched microcontainers (100).

PLGA has been widely used in the pharmaceutical field in numerous drug delivery systems such as nanoparticles (176,177). The polymer is approved by FDA for medical applications, such as tissue engineering and drug delivery. This is mainly due to its biodegradability and non-toxicity in humans (178,179). PLGA is a co-polymer consisting of various ratios of lactic and glycolic acid. In this study, PLGA 75:25 and 50:50 was used, as this most likely would affect the adhesion and degradation (180). PLGA 75:25 contains 75 % of lactic acid and 25 % of glycolic acid meaning it is more hydrophobic than PLGA 50:50 and, therefore, it is expected to have a slower degradation than PLGA 50:50 (**Figure 25**).

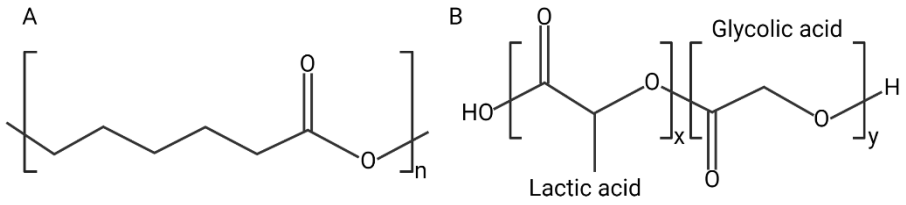

Figure 25: Chemical structure of **A)** poly-ε-caprolactone (PCL) and **B)** poly(lactic-co-glycolic acid) (PLGA).

Fabrication of microcontainers in other polymers such as carbopol or other more mucoadhesive polymers could be of great interest. However, this would challenge the hot punching technique and optimizations would be needed such as the integration of a polytetrafluoroethylene (PTFE) film, which was done in this study for fabricating PLGA microcontainers. The PTFE film prevented the PLGA from adhering to the nickel stamp used for punching the microcontainers.

Generally, increasing the hot punching methods versatility in regards to shape, surface structuring and fabrication material could open for numerous possibilities for improving the behavior of the microcontainers in the GI tract and improve their adhesion to mucosa. The height of the PCL and PLGA were significantly lower (approximately 100 µm) than the

original SU-8 microcontainers (approximately 300 µm). The hot punching technique is challenged in fabricating higher walls of the microcontainer as they will break or collapse. The same could be the case for surface structuring, however, fabrication of various shapes should be possible but further studies are needed to elucidate this statement.

Adhesion of biodegradable microcontainers to mucosa

The adhesion of biodegradable microcontainers was compared to the SU-8-based microcontainers (100 µm high) by using the *ex vivo* perfusion model developed in **Paper I** (**Figure 26A**). No significant differences were observed between the four types of microcontainers and all of them showed great adhesion to mucosa as they primarily were located in the beginning of the intestinal tissue. PCL and PLGA 75:25 showed a slightly lower adhesion in the beginning of the tissue compared to PLGA 50:50 and SU-8. Instead, a large fraction of PLGA 75:25 was found in the middle part as well as the end of the tissue, and many of the PCL microcontainers were found to exit the tissue (found on the filter paper). SU-8 is highly hydrophobic thus, one would expect an improved adhesion to mucosa due to hydrophobic interactions with mucus components. PLGA has a hydrophilic structure compared to PCL and can form hydrogen bonds with mucus, however, PCL can form hydrophobic interactions with mucus. PLGA 50:50 contains more hydrophilic functional groups, such as carboxyl and hydroxyl, which could facilitate hydrogen bonding and thereby promote adhesion to mucosa. Large adhesion differences between the four types of microcontainers were not expected to be explained by their abilities to form chemical interactions with mucus as they are very similar. Other parameters such as weight, height or surface roughness could also influence their adhesion to mucosa.

Orientation of biodegradable microcontainers

In **Paper I,** it was shown that the size of the microcontainers highly influenced their orientation on the intestinal tissue. Results from **Paper IV** support this conclusion. All four types of microcontainers were mainly oriented with the cavity up or down into the mucus layer (**Figure 26B**). Yet, 20.2 ± 5 % of the SU-8 microcontainers and 7.7 ± 3 % of PCL were oriented sideways, whereas only 0.4 ± 0 % of PLGA 75:25 and 1.3 ± 0.4 % of PLGA 50:50 were lying sideways. This corresponds well with their respective heights with SU-8 being 131 ± 0.4 µm, PCL 92 ± 2 µm, PLGA (50:50) 73 ± 6 µm and PLGA (75:25) 56 ± 1 µm. This supports the observation from **Paper I** where microcontainers with a greater height are more likely to be positioned sideways.

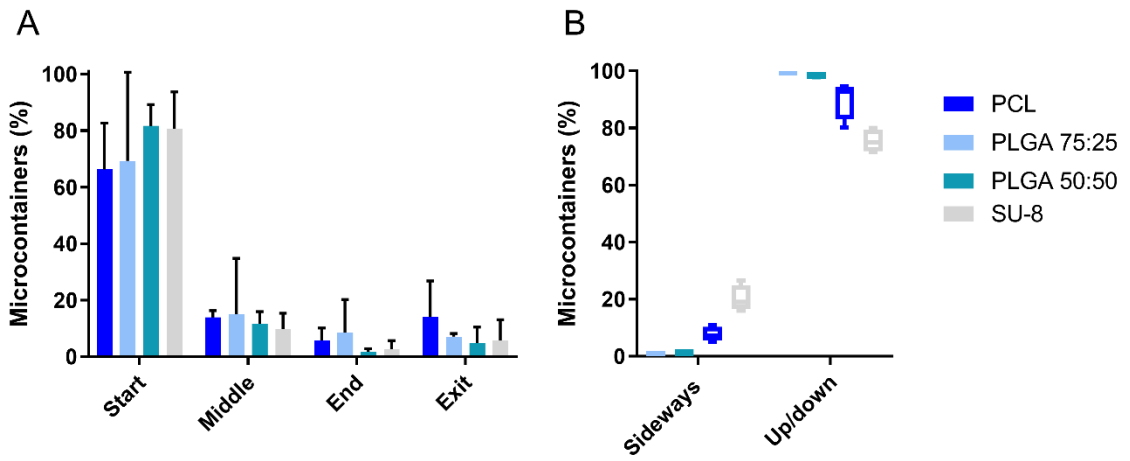

Figure 26: Adhesion and orientation of microcontainers (%) fabricated in either poly-ε-caprolactone (PCL) (blue), poly(lactic-co-glycolic acid (PLGA) 75:25 (light blue), PLGA 50:50 (blue green) or SU-8 (grey). **A)** Percentage of microcontainers placed in the start, middle, end, and exit of a piece of porcine small intestine after an *ex vivo* perfusion study. **B)** Percentage of microcontainers oriented sideways or up/down. Data is presented as mean ± SD with n = 3–4.

Degradation of biodegradable microcontainers

Degradation is of great importance when working with oral devices, both due to a health issue and an environmental concern. Degradation is a key factor to avoid accumulation of microdevices in the body, as well as avoiding accumulation of polymers in the environment.

Previously, the *in vivo* transit time of the SU-8 microcontainers (originally height of 257 ± 4 µm) through the GI tract of rats was investigated (24). They observed that microcontainers started to leave the stomach 0.5-2 h after oral dosing and they entered cecum after 3-4 h. In addition, it was observed that the microcontainers left the cecum and colon after 8-10 h. The study was terminated at 10 h, thus, it is not known when or if all the microcontainers exited the GI tract (24). This is especially important for less degradable materials, such as PCL, as they can up-concentrate in the GI tract and cause harmful side effects. However, it is believed that the constant secretion of mucus and transit of food/fluid through the GI tract can prevent microcontainers from being retained in the system for longer periods.

This degradation study was conducted in biorelevant medium with pancreatic lipase to resemble the intestinal fluid. Preliminary evaluation of degradation of the PCL microcontainers in biorelevant (FaSSIF) medium without enzymes showed that they were completely unaffected for 20 days. Yet, the presence of enzymes, such as lipase, is paramount as they degrade polymers. PLGA 50:50 microcontainers presented signs of degradation after two weeks immersed in the FaSSIF medium with lipase (**Figure 27**). The first signs were loss of structural integrity, which was more and more evident from week to week. After four weeks, all the PLGA 50:50 microcontainers were degraded. In comparison, PCL and PLGA 75:25

microcontainers only showed minor deformation of the walls after two weeks. After four weeks, PCL and PLGA 75:25 microcontainers started to break apart and showed loss of the structural integrity. After five weeks, the shape of the microcontainers had completely changed and only small polymer lumps remained. Finally, none of the three polymers could be detected after six weeks.

The observed degradation of the three polymers was faster compared to what was expected from other degradation studies reported in the literature, however, many of these studies did not add lipase to the medium, which might explain the differences (181,182). The added lipase includes a mixture of enzymes, which can hydrolyzes ester bonds in polyesters (183). PCL is degraded by hydrolytic mechanisms, enzymes and microorganisms under physiological conditions (184,185). PLGA is degraded through hydrolytic degradation and through enzymatic degradation (186,187). Therefore, an increased degradation rate for both PCL and PLGA was expected when adding lipase to the FaSSIF medium. The PCL microcontainers degraded more slowly than the microcontainers fabricated in PLGA, which is in accordance with the degradation rates reported in the literature (187). As expected, PLGA 50:50 degraded faster than the PLGA 75:25 microcontainers, presumably due to the higher amount of hydrophobic groups in PLGA 75:25. An even faster degradation could be expected *in vivo* in the GI tract due to the presence of other enzymes and bacteria.

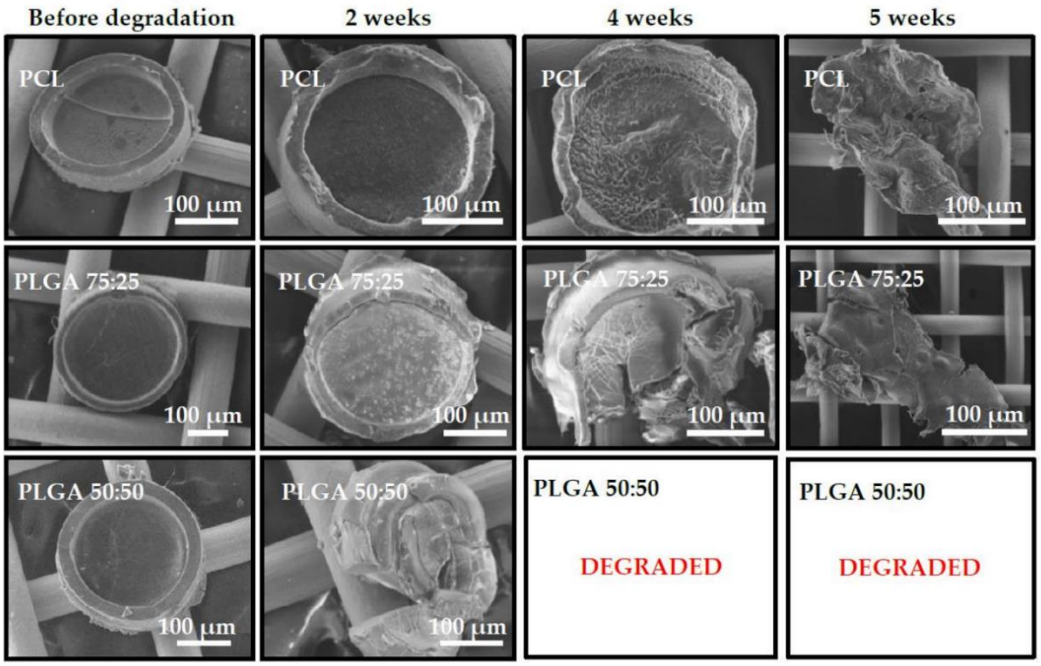

Figure 27: SEM images evaluating the morphology of poly-ε-caprolactone (PCL), poly(lactic-co-glycolic acid) (PLGA) 75:25 and PLGA 50:50 microcontainers before degradation, after two weeks, four weeks, and five weeks, in simulated intestinal media with pancreatic lipase.

The adhesion of the different microcontainers indicated that further optimization of adhesion might not be needed, however, *in vivo* experiments has to support this. Abid *et al.* demonstrated that PCL microcontainers displayed the same promising features in regards to a delayed and sustained *in vivo* absorption as obtained from the original SU-8 microcontainers (10,100). Both these studies explain the sustained absorption by the ability of the microcontainers to adhere to the mucosal surface.

4 Conclusion

Reliable *ex vivo* models are essential in order to estimate the mucoadhesive behavior of microcontainers in the small intestine. In this PhD thesis, a novel porcine *ex vivo* small intestinal perfusion model for evaluation of mucoadhesion and orientation of microcontainers was developed. The perfusion model enabled investigation of how different modifications or functionalization's of microcontainers affected the adhesion to mucosa and their orientation at the intestinal lining (**Paper I**). A texture analyzer was utilized to investigate the adhesion forces of various surface structures to mucosa. Unfortunately, no significant differences in adhesion forces were found between the different surfaces. This was presumably due to the large standard deviations observed caused by large variations in tissue structure and time variations between the sample measurements. To improve this, a statistical guide was developed to be able to eliminate the highly disturbing factors; tissue and time variations. By applying the statistical tool, we succeeded in eliminating noise factors, shown to highly affect the adhesion force measurements (**Paper II**) and more reliable tensile force measurements were obtained. The peak forces were reduced indicating the elimination of noise from the measurements and statistical difference were now observed between the measured samples.

Different adhesion strategies were tested in the PhD project to obtain mucoadhesive microcontainers with drug release into the mucosa. Microcontainers with different shapes and sizes were investigated to elucidate the impact of varying morphology on the behavior of the microcontainers in the intestine (**Paper I**). Neither size nor shape differences appeared to affect the ability of the microcontainers to adhere to mucosa. In general, microcontainers with varying heights (300 µm vs. 100 µm) and shape (cylindrical vs. triangular) showed strong adhesion to mucosa, which minor differences. Different surface topographies were tested and compared in regard to their mucoadhesive strength. Micropillars applied on a PDMS surface showed more than a 2-fold increase in adhesion when compared to microcavities and micropillars with a smoother surface (**Paper II**). Microcontainers were functionalized with well-known mucoadhesive polymers (chitosan, sodium alginate or PEG). All the polymers were applied in three different thicknesses to estimate the impact of thickness on adhesion to mucosa and drug release (**Paper III**). Chitosan-coated microcontainers showed the strongest adhesion to mucosa compared to PEG- and sodium alginate-coated microcontainers. Interestingly, it appeared that the thicker the chitosan coating, the better the adhesion to mucosa. No differences in mucoadhesion were found between the different thicknesses of PEG- and sodium alginate-coated microcontainers. The release profile of furosemide was sustained through the chitosan-

coating, whereas PEG and sodium alginate did not influence the drug release. In general, all polymeric functionalization's resulted in great adhesion to mucosa when evaluated *ex vivo*. Estimating the impact *in vivo* is essential, as the applied forces *in vivo* might dominate the forces between mucosa and the microcontainers modifications.

The majority of published studies has been conducted using SU-8-based microcontainers. However, these prototypes are not suitable for oral intake. To fully realize the microcontainers as drug delivery devices, one needs to fabricate these in biodegradable and biocompatible materials. Thus, microcontainers were fabricated in PCL and PLGA, and evaluated in regards to their mucoadhesion, orientation and degradation (**Paper IV**). Microcontainers fabricated in SU-8 and PLGA 50:50 showed stronger mucosal adhesion than the PCL and PLGA 75:25 microcontainers. PCL, PLGA 75:25 and PLGA 50:50 microcontainers degraded within six weeks in biorelevant fluids with pancreatic lipase added. PLGA 50:50 was the fastest with a complete degradation after only two weeks.

The overall conclusion is that, microcontainers show strong adhesion to mucosa and modifying the microcontainers in terms of functionalized polymeric coatings and varying morphology appears to only show minor improvements of the abilities to adhere to the mucosal surface in the small intestine.

5 Future perspectives

Investigating and evaluating different adhesion strategies *ex vivo* implies the need for *in vivo* evaluation to determine its impact *in vivo* where more advanced forces are applied such as peristaltic movement and passage of food/fluids. This could help establish the need for modifying microcontainers to promote stronger adhesion to the mucosa. Further investigations *in vivo* of the studied adhesion strategies could determine the actual impact on the microcontainers adhesion and drug absorption.

The impact of unidirectional release on drug permeation still needs to be investigated. We believe, the unidirectional drug release promotes drug absorption but further studies investigating the actual release profile of the unidirectional release when ensuring direct delivery into mucus are needed. Development of cell culture models could elucidate the questions in regard to drug permeation when ensuring unidirectional drug release in the mucus layer.

In regards to using polymeric coatings to improve the adhesion to mucus, further studies are needed to emphasize the time of adhesion and the time needed for the mucoadhesive coating to dissolve and loose its mucoadhesive strength. A Caco-2 cell system with flow could help clarifying the impact of the polymeric coatings in relation to adhesion. Peristaltic movement has a major impact on the behavior of the microcontainers but are also lacking in a cell culture systems. Development of a setup simulating more realistically peristaltic movement could help elucidate the microcontainers movement in the GI tract. Scientist become more and more advanced in developing artificial organs and mechanical instruments, which hopefully could result in more realistic *in vitro* or *ex vivo* models to evaluate physiological processes in the human body. Complex digestive models have been developed, such as the TNO gastrointestinal model (TIM), where many of the GI tract physiological properties are simulated, however, simplified. A mucus layer that resembles *in vivo* conditions needs to be added to be able to evaluate mucoadhesion of microdevices.

We have succeeded in developing biodegradable and biocompatible microcontainers, however, so far the versatility of the fabrication process is limited to approximately 100 µm high cylindrical microcontainers. Further development of the fabrication process is needed to enable fabrication of varying shapes and sizes. Applying a mucoadhesive coating underneath an enteric coating can be challenging as the mucoadhesive coatings are exposed to the gastric fluid since the enteric coating cannot cover the mucoadhesive coating completely. This would result

in hydration of the mucoadhesive coating resulting in a swelling or a dissolved coating layer, which would limit the protective function of the enteric coating. Future studies to modify the coating process of the biodegradable and biocompatible microcontainers are needed when applying two coatings.

In order to receive an increased oral bioavailability of challenging drugs one could combine the microcontainers with other drug delivery systems, such as nanoparticles. Nanoparticles loaded into microcontainers could enable mucus penetration, which would ensure drug delivery into the mucus layer and possibly close to the epithelium lining. Fabrication of nanoparticles with high drug loading and low affinity polymers would allow diffusion through the mucus layer. The role of the microcontainers would be to provide protection through the GI tract and target the small intestine where the nanoparticles would be released. However, this would highly complicate the delivery system and numerous fabrication steps would be required. On the other hand, this illustrates the versatility of the microcontainers as a vehicle in oral drug delivery.

This work has emphasized the value of integrating a strong statistical design into the experimental work. This needs to be more common in the experimental research field as this will provide better experimental evaluation and make science more reproducible. For implementing stronger statistical designs the whole research field will have to change its perspective on experiment planning, as external help might be needed. More published research as **Paper II** could help provide statistical designs for others to implement in their research.

6 References

1. Maher S, Brayden DJ. Overcoming poor permeability: translating permeation enhancers for oral peptide delivery. Drug Discov Today Technol [Internet]. 2012 Jun 1 [cited 2019 Apr 29];9(2):e113–9. Available from: https://www.sciencedirect.com/science/article/pii/S1740674911000266

2. Neutel JM, Smith DHG. Improving Patient Compliance: A Major Goal in the Management of Hypertension. J Clin Hypertens [Internet]. 2003 Mar 1 [cited 2021 Apr 30];5(2):127–32. Available from: http://doi.wiley.com/10.1111/j.1524-6175.2003.00495.x

3. Becker MH, Maiman LA. STRATEGIES FOR ENHANCING PATIENT COMPLIANCE. Vol. 6, Journal of Community Health Voh. 1980.

4. Loftsson T, Brewster ME. Pharmaceutical applications of cyclodextrins: basic science and product development. J Pharm Pharmacol [Internet]. 2010 Jul 20 [cited 2021 Mar 12];62(11):1607–21. Available from: https://academic.oup.com/jpp/article/62/11/1607/6135671

5. Taylor LS, Zhang GGZ. Physical chemistry of supersaturated solutions and implications for oral absorption. Vol. 101, Advanced Drug Delivery Reviews. Elsevier B.V.; 2016. p. 122–42.

6. Nielsen LH, Keller SS, Boisen A. Microfabricated devices for oral drug delivery. Lab Chip [Internet]. 2018 Aug 7 [cited 2019 Jul 3];18(16):2348–58. Available from: http://xlink.rsc.org/?DOI=C8LC00408K

7. Homayun B, Lin X, Choi HJ. Challenges and recent progress in oral drug delivery systems for biopharmaceuticals [Internet]. Vol. 11, Pharmaceutics. MDPI AG; 2019 [cited 2021 Apr 30]. p. 129. Available from: www.mdpi.com/journal/pharmaceutics

8. Sinko PJ, Lee YH, Makhey V, Leesman GD, Sutyak JP, Yu H, et al. Biopharmaceutical approaches for developing and assessing oral peptide delivery strategies and systems: In vitro permeability and in vivo oral absorption of salmon calcitonin (sCT). Pharm Res [Internet]. 1999 [cited 2021 Feb 25];16(4):527–33. Available from: https://link.springer.com/article/10.1023/A:1018819012405

9. Colombo P, Sonvico F, Colombo G, Bettini R. Novel platforms for oral drug delivery [Internet]. Vol. 26, Pharmaceutical Research. Springer; 2009 [cited 2021 Apr 30]. p. 601–11. Available from: https://link.springer.com/article/10.1007/s11095-008-9803-0

10. Nielsen LH, Melero A, Keller SS, Jacobsen J, Garrigues T, Rades T, et al. Polymeric microcontainers improve oral bioavailability of furosemide. Int J Pharm [Internet]. 2016 May 17 [cited 2018 Dec 11];504(1–2):98–109. Available from: https://www.sciencedirect.com/science/article/pii/S0378517316302599

11. Mazzoni C, Tentor F, Strindberg SA, Nielsen LH, Keller SS, Alstrøm TS, et al. From concept to in vivo testing: Microcontainers for oral drug delivery. J Control Release [Internet]. 2017 Dec 28 [cited 2018 Apr 30];268:343–51. Available from: https://www.sciencedirect.com/science/article/pii/S0168365917309008

12. Jørgensen JR, Yu F, Venkatasubramanian R, Nielsen LH, Nielsen HM, Boisen A, et al. In Vitro, Ex Vivo and In Vivo Evaluation of Microcontainers for Oral Delivery of Insulin. Pharmaceutics [Internet]. 2020 Jan 7 [cited 2021 Feb 24];12(1):48. Available

from: https://www.mdpi.com/1999-4923/12/1/48

13. Thanki K, Gangwal RP, Sangamwar AT, Jain S. Oral delivery of anticancer drugs: Challenges and opportunities. J Control Release [Internet]. 2013 Aug 28 [cited 2018 Nov 28];170(1):15–40. Available from: https://www.sciencedirect.com/science/article/pii/S0168365913002393

14. Loh CS, MacRobert AJ, Bedwell J, Regula J, Krasner N, Bown SG. Oral versus intravenous administration of 5-aminolaevulinic acid for photodynamic therapy. Br J Cancer [Internet]. 1993 [cited 2021 Mar 8];68(1):41–51. Available from: https://www.nature.com/articles/bjc1993284

15. Man Dell Frcpc LA, Berg Eron Abim Frcpc MG, GRIB BLE ChB ABIM FRCPC MJ, Jew Es Son Fcshp PJ, Ald Low Frcpc DE, Mas Mar Rie Frcpc TJ, et al. Sequential antibiotic therapy: Effective cost management and patient care.

16. Sevinc F, Prins JM, Koopmans RP, Langendijk PNJ, Bossuyt PM, Dankert J, et al. Early switch from intravenous to oral antibiotics: guidelines and implementation in a large teaching hospital. J Antimicrob Chemother [Internet]. 1999 Apr 1 [cited 2021 Mar 8];43(4):601–6. Available from: https://academic.oup.com/jac/article-lookup/doi/10.1093/jac/43.4.601

17. Helander HF, Fändriks L. Surface area of the digestive tract – revisited. Scand J Gastroenterol [Internet]. 2014 Jun 2 [cited 2021 May 3];49(6):681–9. Available from: http://www.tandfonline.com/doi/full/10.3109/00365521.2014.898326

18. Sjögren E, Abrahamsson B, Augustijns P, Becker D, Bolger MB, Brewster M, et al. In vivo methods for drug absorption â€“ Comparative physiologies, model selection, correlations with in vitro methods (IVIVC), and applications for formulation/API/excipient characterization including food effects. Eur J Pharm Sci [Internet]. 2014 [cited 2016 Oct 10];57:99–151. Available from: http://dx.doi.org/10.1016/j.ejps.2014.02.010

19. Ensign LM, Cone R, Hanes J. Oral drug delivery with polymeric nanoparticles: The gastrointestinal mucus barriers. Adv Drug Deliv Rev [Internet]. 2012 May 1 [cited 2019 Mar 18];64(6):557–70. Available from: https://www.sciencedirect.com/science/article/pii/S0169409X11003036

20. Zhou XH. Overcoming enzymatic and absorption barriers to non-parenterally administered protein and peptide drugs. J Control Release [Internet]. 1994 Mar 1 [cited 2019 Jan 18];29(3):239–52. Available from: https://www.sciencedirect.com/science/article/pii/016836599490071X

21. Peppas NA, Buri PA. Surface, interfacial and molecular aspects of polymer bioadhesion on soft tissues. J Control Release. 1985 Nov 1;2(C):257–75.

22. Fallingborg J, Christensen LA, Ingeman-Nielsen M, Jacobsen BA, Abildgaard K, Rasmussen HH. pH-Profile and regional transit times of the normal gut measured by a radiotelemetry device. Aliment Pharmacol Ther. 1989;3(6):605–14.

23. Billat PA, Roger E, Faure S, Lagarce F. Models for drug absorption from the small intestine: where are we and where are we going? Vol. 22, Drug Discovery Today. Elsevier Ltd; 2017. p. 761–75.

24. Kjeldsen RB, Kristensen MN, Gundlach C, Thamdrup LHE, Müllertz A, Rades T, et

al. X-ray Imaging for Gastrointestinal Tracking of Microscale Oral Drug Delivery Devices. ACS Biomater Sci Eng. 2021;

25. Andrews GP, Laverty TP, Jones DS. Mucoadhesive polymeric platforms for controlled drug delivery. Eur J Pharm Biopharm. 2008;71:505–18.

26. Clark MA, Hirst BH, Jepson MA. Lectin-mediated mucosal delivery of drugs and microparticles. Adv Drug Deliv Rev. 2000;43(2):207–23.

27. Khanvilkar K, Donovan MD, Flanagan DR. Drug transfer through mucus. Adv Drug Deliv Rev [Internet]. 2001 Jun 11 [cited 2019 Jun 11];48(2–3):173–93. Available from: https://www.sciencedirect.com/science/article/pii/S0169409X01001156

28. Cone RA. Barrier properties of mucus. Vol. 61, Advanced Drug Delivery Reviews. Elsevier; 2009. p. 75–85.

29. Bansil R, Turner BS. Mucin structure, aggregation, physiological functions and biomedical applications. Vol. 11, Current Opinion in Colloid and Interface Science. Elsevier; 2006. p. 164–70.

30. Rathbone MJ, Hadgraft J. Absorption of drugs from the human oral cavity. Vol. 74, International Journal of Pharmaceutics. Elsevier; 1991. p. 9–24.

31. Bhat PG, Flanagan DR, Donovan MD. intemational journal of pharmaceutics The limiting role of mucus in drug absorption: drug permeation through mucus solution. Int J Pharm. 1995;126:179–87.

32. Shen L. Functional morphology of the gastrointestinal tract [Internet]. Vol. 337, Current Topics in Microbiology and Immunology. Springer Verlag; 2009 [cited 2021 Apr 6]. p. 1–35. Available from: https://link.springer.com/chapter/10.1007/978-3-642-01846-6_1

33. Lehr CM, Poelma FGJ, Junginger HE, Tukker JJ. An estimate of turnover time of intestinal mucus gel layer in the rat in situ loop. Int J Pharm. 1991 Apr 1;70(3):235–40.

34. Atuma C, Strugala V, Allen A, Holm L. The adherent gastrointestinal mucus gel layer: Thickness and physical state in vivo. Am J Physiol - Gastrointest Liver Physiol [Internet]. 2001 [cited 2021 Mar 9];280(5 43-5). Available from: http://www.ajpgi.org

35. Lai SK, Wang YY, Hanes J. Mucus-penetrating nanoparticles for drug and gene delivery to mucosal tissues. Vol. 61, Advanced Drug Delivery Reviews. Elsevier; 2009. p. 158–71.

36. Boegh M, Nielsen HM. Mucus as a Barrier to Drug Delivery - Understanding and Mimicking the Barrier Properties. Basic Clin Pharmacol Toxicol [Internet]. 2015 Mar 1 [cited 2019 Jun 11];116(3):179–86. Available from: http://doi.wiley.com/10.1111/bcpt.12342

37. Harding SE. The Macrostructure of Mucus Glycoproteins in Solution. Adv Carbohydr Chem Biochem. 1989 Jan 1;47(C):345–81.

38. Peppas NA, Huang Y. Nanoscale technology of mucoadhesive interactions. Vol. 56, Advanced Drug Delivery Reviews. Elsevier; 2004. p. 1675–87.

39. Bromberg LE, Barr DP. Self-association of mucin. Biomacromolecules [Internet]. 2000 [cited 2021 Apr 25];1(3):325–34. Available from:

https://pubs.acs.org/sharingguidelines

40. Johnson P, Rainsford KD. The physical properties of mucus: Preliminary observations on the sedimentation behaviour of porcine gastric mucus. BBA - Gen Subj. 1972 Nov 24;286(1):72–8.

41. Sheehan JK, Kirkham S, Howard M, Woodman P, Kutay S, Brazeau C, et al. Identification of Molecular Intermediates in the Assembly Pathway of the MUC5AC Mucin. J Biol Chem. 2004 Apr 9;279(15):15698–705.

42. Johansson ME V, Hansson GC, Johansson ME V, Sjövall H, Hansson GC. The gastrointestinal mucus system in health and disease. Nat Publ Gr [Internet]. 2013 [cited 2021 Apr 25];10:352–61. Available from: www.nature.com/nrgastro

43. Hicks SJ, Corfield AP, Kaswan RL, Hirsh S, Stern M, Bara J, et al. Biochemical analysis of ocular surface mucin abnormalities in dry eye: The canine model. Exp Eye Res. 1998 Dec 1;67(6):709–18.

44. Kesimer M, Ehre C, Burns KA, Davis CW, Sheehan JK, Pickles RJ. Molecular organization of the mucins and glycocalyx underlying mucus transport over mucosal surfaces of the airways. Mucosal Immunol [Internet]. 2013 Mar 29 [cited 2021 Apr 25];6(2):379–92. Available from: www.nature.com/mi

45. Gamazo C, Martín-Arbella N, Brotons A, Camacho AI, Irache JM. Mimicking microbial strategies for the design of mucus-permeating nanoparticles for oral immunization. Eur J Pharm Biopharm. 2015;96:454–63.

46. Johansson ME V, Hansson GC, Johansson ME V, Sjövall H, Hansson GC. The gastrointestinal mucus system in health and disease. Nat Publ Gr [Internet]. 2013 [cited 2021 Mar 9];10:352–61. Available from: www.nature.com/nrgastro

47. Round AN, Berry M, McMaster TJ, Stoll S, Gowers D, Corfield AP, et al. Heterogeneity and persistence length in human ocular mucins. Biophys J. 2002 Sep 1;83(3):1661–70.

48. Tam PY, Verdugo P. Control of mucus hydration as a Donnan equilibrium process. Nature [Internet]. 1981 [cited 2021 Apr 25];292(5821):340–2. Available from: https://www.nature.com/articles/292340a0

49. Wolf DP, Sokoloski J, Khan MA, Litt M. Human cervical mucus. III. Isolation and characterization of rheologically active mucin. Fertil Steril. 1977 Jan 1;28(1):53–8.

50. Ensign LM, Henning A, Schneider CS, Maisel K, Wang Y-Y, Porosoff MD, et al. Ex Vivo Characterization of Particle Transport in Mucus Secretions Coating Freshly Excised Mucosal Tissues. 2013 [cited 2021 Apr 25]; Available from: https://pubs.acs.org/sharingguidelines

51. Turner BS, Bhaskar KR, Hadzopoulou-Cladaras M, Lamont JT. Cysteine-rich regions of pig gastric mucin contain von Willebrand factor and cystine knot domains at the carboxyl terminaL. Biochim Biophys Acta - Gene Struct Expr. 1999 Oct 6;1447(1):77–92.

52. Bernkop-Schnürch A, Schwarz V, Steininger S. Polymers with Thiol Groups: A New Generation of Mucoadhesive Polymers? Pharm Res [Internet]. 1999 [cited 2019 Mar 18];16(6):876–81. Available from: http://link.springer.com/10.1023/A:1018830204170

53. King M, Rubin BK. Pharmacological approaches to discovery and development of new mucolytic agents. Adv Drug Deliv Rev. 2002 Dec 5;54(11):1475–90.

54. Perera G, Zipser M, Bonengel S, Salvenmoser W, Bernkop-Schnürch A. Development of phosphorylated nanoparticles as zeta potential inverting systems. 2015;

55. Pereira De Sousa I, Steiner C, Schmutzler M, Wilcox MD, Veldhuis GJ, Pearson JP, et al. Mucus permeating carriers: formulation and characterization of highly densely charged nanoparticles. 2015;

56. Smart JD. The basics and underlying mechanisms of mucoadhesion. Adv Drug Deliv Rev [Internet]. 2005 Nov 3 [cited 2019 Sep 24];57(11):1556–68. Available from: https://www.sciencedirect.com/science/article/pii/S0169409X05001390

57. FLOREY HW. The secretion and function of intestinal mucus. Gastroenterology. 1962 Sep 1;43(3):326–9.

58. Smart JD. The basics and underlying mechanisms of mucoadhesion. Vol. 57, Advanced Drug Delivery Reviews. Elsevier; 2005. p. 1556–68.

59. Ahuja A, Khar RK, Ali J. Mucoadhesive drug delivery systems [Internet]. Vol. 23, Drug Development and Industrial Pharmacy. Informa Healthcare; 1997 [cited 2021 Apr 26]. p. 489–515. Available from: https://www.tandfonline.com/action/journalInformation?journalCode=iddi20

60. Derjaguin B V., Toporov YP, Muller VM, Aleinikova IN. On the relationship between the electrostatic and the molecular component of the adhesion of elastic particles to a solid surface. J Colloid Interface Sci. 1977 Mar 1;58(3):528–33.

61. Ponchel G, Touchard F, Duchêne D, Peppas NA. Bioadhesive analysis of controlled-release systems. I. Fracture and interpenetration analysis in poly(acrylic acid)-containing systems. J Control Release. 1987 Sep 1;5(2):129–41.

62. Kinloch AJ. Review The science of adhesion Part 1 Surface and interfacia/ aspects. Vol. 15, JOURNAL OF MATERIALS SCIENCE. 1980.

63. Peppas NA, Sahlin JJ. Hydrogels as mucoadhesive and bioadhesive materials: A review. Vol. 17, Biomaterials. Elsevier Science Ltd; 1996. p. 1553–61.

64. Inchaurraga L, Martín-Arbella N, Zabaleta V, Quincoces G, Peñuelas I, Irache JM. In vivo study of the mucus-permeating properties of PEG-coated nanoparticles following oral administration. Eur J Pharm Biopharm. 2015 Nov 1;97:280–9.

65. Gupta V, Hwang BH, Lee J, Anselmo AC, Doshi N, Mitragotri S. Mucoadhesive intestinal devices for oral delivery of salmon calcitonin. J Control Release [Internet]. 2013 [cited 2020 Oct 29];172(3):753–62. Available from: http://dx.doi.org/10.1016/j.jconrel.2013.09.004

66. Behrens I, Vila Pena AI, Alonso MJ, Kissel T. Comparative uptake studies of bioadhesive and non-bioadhesive nanoparticles in human intestinal cell lines and rats: The effect of mucus on particle adsorption and transport. Pharm Res [Internet]. 2002 [cited 2021 Mar 4];19(8):1185–93. Available from: https://link.springer.com/article/10.1023/A:1019854327540

67. Mazzoni C, Jacobsen RD, Mortensen J, Jørgensen JR, Vaut L, Jacobsen J, et al. Polymeric Lids for Microcontainers for Oral Protein Delivery. Macromol Biosci

[Internet]. 2019 May 2 [cited 2020 Aug 27];19(5):1900004. Available from: https://onlinelibrary.wiley.com/doi/abs/10.1002/mabi.201900004

68. Tao SL, Lubeley MW, Desai TA. Bioadhesive poly(methyl methacrylate) microdevices for controlled drug delivery. J Control Release. 2003 Mar 7;88(2):215–28.

69. Nielsen LH, Keller SS, Boisen A, Müllertz A, Rades T. A slow cooling rate of indomethacin melt spatially confined in microcontainers increases the physical stability of the amorphous drug without influencing its biorelevant dissolution behaviour. Drug Deliv Transl Res [Internet]. 2014 Jun 14 [cited 2019 Jul 1];4(3):268–74. Available from: http://link.springer.com/10.1007/s13346-013-0166-7

70. Ainslie KM, Lowe RD, Beaudette TT, Petty L, Bachelder EM, Desai TA. Microfabricated Devices for Enhanced Bioadhesive Drug Delivery: Attachment to and Small-Molecule Release Through a Cell Monolayer Under Flow. Small [Internet]. 2009 Dec 18 [cited 2019 Jan 23];5(24):2857–63. Available from: http://doi.wiley.com/10.1002/smll.200901254

71. Nielsen LH, Nagstrup J, Gordon S, Keller SS, Østergaard J, Rades T, et al. pH-triggered drug release from biodegradable microwells for oral drug delivery. Biomed Microdevices [Internet]. 2015 Jun 22 [cited 2020 Sep 30];17(3):1–7. Available from: https://link.springer.com/article/10.1007/s10544-015-9958-5

72. Chirra HD, Shao L, Ciaccio N, Fox CB, Wade JM, Ma A, et al. Planar Microdevices for Enhanced In Vivo Retention and Oral Bioavailability of Poorly Permeable Drugs. Adv Healthc Mater [Internet]. 2014 Oct 1 [cited 2019 Jan 29];3(10):1648–54. Available from: http://doi.wiley.com/10.1002/adhm.201300676

73. Malik R, Garg T, Goyal AK, Rath G. Polymeric nanofibers: targeted gastro-retentive drug delivery systems. J Drug Target [Internet]. 2015 Feb 7 [cited 2021 Mar 19];23(2):109–24. Available from: http://www.tandfonline.com/doi/full/10.3109/1061186X.2014.965715

74. Ahmed A, Bonner C, Desai TA. Bioadhesive microdevices with multiple reservoirs: a new platform for oral drug delivery. J Control Release [Internet]. 2002 Jun 17 [cited 2018 Nov 29];81(3):291–306. Available from: https://www.sciencedirect.com/science/article/pii/S0168365902000743

75. Fox CB, Cao Y, Nemeth CL, Chirra HD, Chevalier RW, Xu AM, et al. Fabrication of Sealed Nanostraw Microdevices for Oral Drug Delivery. ACS Nano [Internet]. 2016 Jun 28 [cited 2021 Mar 4];10(6):5873–81. Available from: www.acsnano.org

76. Nielsen LH, Keller SS, Gordon KC, Boisen A, Rades T, Müllertz A. Spatial confinement can lead to increased stability of amorphous indomethacin. Eur J Pharm Biopharm. 2012;81:418–25.

77. Mosgaard MD, Strindberg S, Abid Z, Singh Petersen R, Højlund Eklund Thamdrup L, Joukainen Andersen A, et al. Ex vivo intestinal perfusion model for investigating mucoadhesion of microcontainers. Int J Pharm. 2019 Oct 30;570:118658.

78. Christfort JF, Guillot AJ, Melero A, Thamdrup LHE, Garrigues TM, Boisen A, et al. Cubic Microcontainers Improve In Situ Colonic Mucoadhesion and Absorption of Amoxicillin in Rats. Pharmaceutics [Internet]. 2020 Apr 14 [cited 2020 Sep 3];12(4):355. Available from: https://www.mdpi.com/1999-4923/12/4/355

79. De Ávila BEF, Angsantikul P, Li J, Angel Lopez-Ramirez M, Ramírez-Herrera DE, Thamphiwatana S, et al. Micromotor-enabled active drug delivery for in vivo treatment of stomach infection. Nat Commun [Internet]. 2017 Dec 1 [cited 2021 Mar 12];8(1):1–9. Available from: www.nature.com/naturecommunications

80. Kirtane AR, Abouzid O, Minahan D, Bensel T, Hill AL, Selinger C, et al. Development of an oral once-weekly drug delivery system for HIV antiretroviral therapy. Nat Commun [Internet]. 2018 Dec 1 [cited 2021 Mar 12];9(1):1–12. Available from: www.nature.com/naturecommunications

81. Ghosh A, Li L, Xu L, Dash RP, Gupta N, Lam J, et al. Gastrointestinal-resident, shape-changing microdevices extend drug release in vivo. Sci Adv [Internet]. 2020 Oct 28 [cited 2021 Mar 22];6(44):4133–61. Available from: http://advances.sciencemag.org/

82. Ghosh A, Li L, Xu L, Dash RP, Gupta N, Lam J, et al. Gastrointestinal-resident, shape-changing microdevices extend drug release in vivo. Sci Adv [Internet]. 2020 Oct 28 [cited 2021 Mar 12];6(44):4133–61. Available from: http://advances.sciencemag.org/

83. Guan J, He H, Lee LJ, Hansford DJ. Fabrication of Particulate Reservoir-Containing, Capsulelike, and Self-Folding Polymer Microstructures for Drug Delivery. Small [Internet]. 2007 Mar 5 [cited 2018 Nov 30];3(3):412–8. Available from: http://doi.wiley.com/10.1002/smll.200600240

84. McHugh KJ, Nguyen TD, Linehan AR, Yang D, Behrens AM, Rose S, et al. Fabrication of fillable microparticles and other complex 3D microstructures. Science (80-) [Internet]. 2017 Sep 15 [cited 2021 Mar 12];357(6356):1138–42. Available from: http://science.sciencemag.org/

85. Nielsen LH, Melero A, Keller SS, Jacobsen J, Garrigues T, Rades T, et al. Polymeric microcontainers improve oral bioavailability of furosemide. Int J Pharm. 2016;504(1–2):98–109.

86. Tao SL, Popat K, Desai TA. Off-wafer fabrication and surface modification of asymmetric 3D SU-8 microparticles. Nat Protoc [Internet]. 2007 Jan 31 [cited 2019 Jan 22];1(6):3153–8. Available from: http://www.nature.com/doifinder/10.1038/nprot.2006.451

87. Ahmed A, Bonner C, Desai TA. Bioadhesive microdevices for drug delivery: A feasibility study. Biomed Microdevices [Internet]. 2001 [cited 2021 Mar 18];3(2):89–96. Available from: https://link.springer.com/article/10.1023/A:1011489907820

88. Keller S, Haefliger D, Boisen A. Optimized plasma-deposited fluorocarbon coating for dry release and passivation of thin SU-8 cantilevers. Cit J Vac Sci Technol B Microelectron Nanom Struct Process [Internet]. 2007 [cited 2019 May 21];25:1903. Available from: https://doi.org/10.1116/1.2806960

89. Mazzoni C, Tentor F, Antalaki A, Jacobsen RD, Mortensen J, Slipets R, et al. Where Is the Drug? Quantitative 3D Distribution Analyses of Confined Drug-Loaded Polymer Matrices. ACS Biomater Sci Eng [Internet]. 2019 Jun 10 [cited 2020 Aug 14];5(6):2935–41. Available from: https://pubs.acs.org/sharingguidelines

90. Nemani K V., Moodie KL, Brennick JB, Su A, Gimi B. In vitro and in vivo evaluation of SU-8 biocompatibility. Mater Sci Eng C. 2013 Oct 1;33(7):4453–9.

91. Gross RA, Kalra B. Biodegradable polymers for the environment [Internet]. Vol. 297, Science. American Association for the Advancement of Science; 2002 [cited 2021 Mar 27]. p. 803–7. Available from: www.fluorous.com/02primer.html

92. Petersen RS, Keller SS, Boisen A. Hot punching of high-aspect-ratio 3D polymeric microstructures for drug delivery. Lab Chip [Internet]. 2015 Jun 21 [cited 2021 Mar 27];15(12):2576–9. Available from: www.rsc.org/loc

93. Zhang Y, Chan HF, Leong KW. Advanced materials and processing for drug delivery: The past and the future. Vol. 65, Advanced Drug Delivery Reviews. Elsevier; 2013. p. 104–20.

94. DeSimone JM. Co-opting Moore's law: Therapeutics, vaccines and interfacially active particles manufactured via PRINT®. J Control Release. 2016 Oct 28;240:541–3.

95. Petersen RS, Mahshid R, Andersen NK, Keller SS, Hansen HN, Boisen A. Hot embossing and mechanical punching of biodegradable microcontainers for oral drug delivery. Microelectron Eng. 2015 Feb 5;133:104–9.

96. Gratton SEA, Williams SS, Napier ME, Pohlhaus PD, Zhou Z, Wiles KB, et al. The pursuit of a scalable nanofabrication platform for use in material and life science applications. Acc Chem Res [Internet]. 2008 Dec 16 [cited 2021 Mar 27];41(12):1685–95. Available from: https://pubs.acs.org/sharingguidelines

97. Rolland JP, Maynor BW, Euliss LE, Exner AE, Denison GM, DeSimone JM. Direct fabrication and harvesting of monodisperse, shape-specific nanobiomaterials. J Am Chem Soc [Internet]. 2005 Jul 20 [cited 2021 Mar 27];127(28):10096–100. Available from: https://pubs.acs.org/sharingguidelines

98. Tao SL, Desai TA. Microfabrication of Multilayer, Asymmetric, Polymeric Devices for Drug Delivery. Adv Mater [Internet]. 2005 Jul 4 [cited 2021 Mar 11];17(13):1625–30. Available from: http://doi.wiley.com/10.1002/adma.200500017

99. Nagstrup J, Keller S, Almdal K, Boisen A. 3D microstructuring of biodegradable polymers. In: Microelectronic Engineering. Elsevier; 2011. p. 2342–4.

100. Abid Z, Strindberg S, Javed MM, Mazzoni C, Vaut L, Nielsen LH, et al. Biodegradable microcontainers – towards real life applications of microfabricated systems for oral drug delivery. Lab Chip [Internet]. 2019 Aug 20 [cited 2019 Aug 27];19(17):2905–14. Available from: http://xlink.rsc.org/?DOI=C9LC00527G

101. Abid Z, Dalskov Mosgaard M, Manfroni G, Singh Petersen R, Hagner Nielsen L, Müllertz A, et al. Investigation of Mucoadhesion and Degradation of PCL and PLGA Microcontainers for Oral Drug Delivery. Polymers (Basel) [Internet]. 2019 Nov 7 [cited 2020 Aug 6];11(11):1828. Available from: https://www.mdpi.com/2073-4360/11/11/1828

102. Abid Z, Strindberg S, Javed MM, Mazzoni C, Vaut L, Nielsen LH, et al. Biodegradable microcontainers-towards real life applications of microfabricated systems for oral drug delivery. Lab Chip [Internet]. 2019 Sep 7 [cited 2021 Mar 14];19(17):2905–14. Available from: https://pubs.rsc.org/en/content/articlehtml/2019/lc/c9lc00527g

103. Marizza P, Keller SS, Müllertz A, Boisen A. Polymer-filled microcontainers for oral delivery loaded using supercritical impregnation. J Control Release. 2014;173:1–9.

104. Grohganz H, Priemel PA, Löbmann K, Nielsen LH, Laitinen R, Mullertz A, et al. Refining stability and dissolution rate of amorphous drug formulations. Expert Opin Drug Deliv [Internet]. 2014 Jun 23 [cited 2021 Mar 22];11(6):977–89. Available from: http://www.tandfonline.com/doi/full/10.1517/17425247.2014.911728

105. Marizza P, Pontoni L, Rindzevicius T, Alopaeus JF, Su K, Zeitler JA, et al. Supercritical impregnation of polymer matrices spatially confined in microcontainers for oral drug delivery: Effect of temperature, pressure and time. J Supercrit Fluids. 2016 Jan 1;107:145–52.

106. Fox CB, Nemeth CL, Chevalier RW, Cantlon J, Bogdanoff DB, Hsiao JC, et al. Picoliter-volume inkjet printing into planar microdevice reservoirs for low-waste, high-capacity drug loading. Bioeng Transl Med [Internet]. 2017 Mar 1 [cited 2021 Mar 22];2(1):9–16. Available from: http://doi.wiley.com/10.1002/btm2.10053

107. Marizza P, Keller SS, Boisen A. Inkjet printing as a technique for filling of micro-wells with biocompatible polymers. Microelectron Eng. 2013 Nov 1;111:391–5.

108. Ainslie KM, Kraning CM, Desai TA. Microfabrication of an asymmetric, multi-layered microdevice for controlled release of orally delivered therapeutics. Lab Chip [Internet]. 2008 Jun 27 [cited 2021 Mar 22];8(7):1042–7. Available from: www.rsc.org/loc

109. Chirra HD, Desai TA. Multi-Reservoir Bioadhesive Microdevices for Independent Rate-Controlled Delivery of Multiple Drugs. Small [Internet]. 2012 Dec 21 [cited 2019 Feb 19];8(24):3839–46. Available from: http://doi.wiley.com/10.1002/smll.201201367

110. Petersen RS, Keller SS, Boisen A. Loading of Drug-Polymer Matrices in Microreservoirs for Oral Drug Delivery. Macromol Mater Eng [Internet]. 2017 Mar 1 [cited 2021 Mar 22];302(3):1600366. Available from: http://doi.wiley.com/10.1002/mame.201600366

111. Abid Z, Gundlach C, Durucan O, von Halling Laier C, Nielsen LH, Boisen A, et al. Powder embossing method for selective loading of polymeric microcontainers with drug formulation. Microelectron Eng [Internet]. 2017 Mar 5 [cited 2018 Apr 30];171:20–4. Available from: https://www.sciencedirect.com/science/article/pii/S0167931717300278

112. Jørgensen JR, Jepsen ML, Nielsen LH, Dufva M, Nielsen HM, Rades T, et al. Microcontainers for oral insulin delivery – In vitro studies of permeation enhancement. Eur J Pharm Biopharm. 2019 Oct 1;143:98–105.

113. Birk SE, Haagensen JAJ, Johansen HK, Molin S, Nielsen LH, Boisen A. Microcontainer Delivery of Antibiotic Improves Treatment of Pseudomonas aeruginosa Biofilms. Adv Healthc Mater. 2020 May 1;9(10).

114. Bose S, Keller SS, Alstrøm TS, Boisen A, Almdal K. Process optimization of ultrasonic spray coating of polymer films. Langmuir [Internet]. 2013 Jun 11 [cited 2021 Mar 4];29(23):6911–9. Available from: https://pubs.acs.org/sharingguidelines

115. Mazzoni C, Jacobsen RD, Mortensen J, Jørgensen JR, Vaut L, Jacobsen J, et al. Polymeric Lids for Microcontainers for Oral Protein Delivery. Macromol Biosci [Internet]. 2019 May 2 [cited 2020 Aug 14];19(5):1900004. Available from: https://onlinelibrary.wiley.com/doi/abs/10.1002/mabi.201900004

116. Birk SE, Haagensen JAJ, Johansen HK, Molin S, Nielsen LH, Boisen A. Microcontainer Delivery of Antibiotic Improves Treatment of *Pseudomonas aeruginosa* Biofilms. Adv Healthc Mater [Internet]. 2020 May 22 [cited 2021 Mar 17];9(10):1901779. Available from: https://onlinelibrary.wiley.com/doi/abs/10.1002/adhm.201901779

117. Grabovac V, Guggi D, Bernkop-Schnürch A. Comparison of the mucoadhesive properties of various polymers. Adv Drug Deliv Rev [Internet]. 2005 Nov 3 [cited 2018 Oct 15];57(11):1713–23. Available from: https://www.sciencedirect.com/science/article/pii/S0169409X05001468

118. Prego C, Torres D, Alonso MJ. Expert Opinion on Drug Delivery The potential of chitosan for the oral administration of peptides The potential of chitosan for the oral administration of peptides. 2005 [cited 2020 Sep 22]; Available from: https://www.tandfonline.com/action/journalInformation?journalCode=iedd20

119. Lehr CM, Bouwstra JA, Schacht EH, Junginger HE. In vitro evaluation of mucoadhesive properties of chitosan and some other natural polymers. Int J Pharm. 1992 Jan 1;78(1–3):43–8.

120. Sogias IA, Williams AC, Khutoryanskiy V V. Why is chitosan mucoadhesive? Biomacromolecules [Internet]. 2008 Jul [cited 2021 Feb 18];9(7):1837–42. Available from: https://pubs.acs.org/sharingguidelines

121. Vila A, Sánchez A, Janes K, Behrens I, Kissel T, Jato JLV, et al. Low molecular weight chitosan nanoparticles as new carriers for nasal vaccine delivery in mice. Eur J Pharm Biopharm. 2004 Jan 1;57(1):123–31.

122. Mohammed M, Syeda J, Wasan K, Wasan E. An Overview of Chitosan Nanoparticles and Its Application in Non-Parenteral Drug Delivery. Pharmaceutics [Internet]. 2017 Nov 20 [cited 2021 Mar 31];9(4):53. Available from: http://www.mdpi.com/1999-4923/9/4/53

123. Ways TMM, Lau WM, Khutoryanskiy V V. Chitosan and its derivatives for application in mucoadhesive drug delivery systems [Internet]. Vol. 10, Polymers. MDPI AG; 2018 [cited 2021 Mar 3]. p. 267. Available from: www.mdpi.com/journal/polymers

124. M. Ways T, Lau W, Khutoryanskiy V. Chitosan and Its Derivatives for Application in Mucoadhesive Drug Delivery Systems. Polymers (Basel) [Internet]. 2018 Mar 5 [cited 2021 Mar 31];10(3):267. Available from: https://www.mdpi.com/2073-4360/10/3/267

125. Hejazi R, Amiji M. Chitosan-based gastrointestinal delivery systems. Vol. 89, Journal of Controlled Release. Elsevier; 2003. p. 151–65.

126. Gupta S. Carbopol/Chitosan Based pH Triggered In Situ Gelling System for Ocular Delivery of Timolol Maleate. Sci Pharm [Internet]. 2010 Oct 5 [cited 2021 Mar 31];78(4):959–76. Available from: http://www.mdpi.com/2218-0532/78/4/959

127. Inchaurraga L, Martín-Arbella N, Zabaleta V, Quincoces G, Peñuelas I, Irache JM. In vivo study of the mucus-permeating properties of PEG-coated nanoparticles following oral administration. 2015;

128. Liu M, Zhang J, Shan W, Huang Y. Developments of mucus penetrating nanoparticles. Vol. 10, Asian Journal of Pharmaceutical Sciences. Shenyang Pharmaceutical

University; 2014. p. 275–82.

129. Wang Y-Y, Lai SK, Suk JS, Pace A, Cone R, Hanes J. Addressing the PEG Mucoadhesivity Paradox to Engineer Nanoparticles that “Slip” through the Human Mucus Barrier. Angew Chemie [Internet]. 2008 Dec 1 [cited 2021 Mar 31];120(50):9872–5. Available from: http://doi.wiley.com/10.1002/ange.200803526

130. Sahlin JJ, Peppas NA. Enhanced hydrogel adhesion by polymer interdiffusion: Use of linear poly(ethylene glycol) as an adhesion promoter. J Biomater Sci Polym Ed [Internet]. 1997 Jan 1 [cited 2021 Feb 15];8(6):421–36. Available from: https://www.tandfonline.com/action/journalInformation?journalCode=tbsp20

131. Serra L, Doménech J, Peppas NA. Design of poly(ethylene glycol)-tethered copolymers as novel mucoadhesive drug delivery systems. Eur J Pharm Biopharm. 2006 May 1;63(1):11–8.

132. Mallikarjuna Setty C, Sahoo SS, Sa B. Alginate-Coated Alginate-Polyethyleneimine Beads for Prolonged Release of Furosemide in Simulated Intestinal Fluid. Drug Dev Ind Pharm [Internet]. 2005 Jan 26 [cited 2021 Mar 17];31(4–5):435–46. Available from: http://www.tandfonline.com/doi/full/10.1080/03639040500214647

133. Hjorth Tønnesen H, Karlsen J. Drug Development and Industrial Pharmacy Alginate in Drug Delivery Systems Alginate in Drug Delivery Systems. 2002 [cited 2021 Mar 4]; Available from: https://www.tandfonline.com/action/journalInformation?journalCode=iddi20

134. George M, Abraham TE. Polyionic hydrocolloids for the intestinal delivery of protein drugs: Alginate and chitosan-a review. 2006 [cited 2020 Sep 22]; Available from: www.elsevier.com/locate/jconrel

135. Cho WJ, Oh SH, Lee JH. Alginate film as a novel post-surgical tissue adhesion barrier. J Biomater Sci Polym Ed [Internet]. 2010 Apr 1 [cited 2021 Mar 3];21(6–7):701–13. Available from: https://www.tandfonline.com/action/journalInformation?journalCode=tbsp20

136. Déat-Lainé E, Hoffart V, Garrait G, Jarrige JF, Cardot JM, Subirade M, et al. Efficacy of mucoadhesive hydrogel microparticles of whey protein and alginate for oral insulin delivery. Pharm Res [Internet]. 2013 Mar 24 [cited 2021 Mar 3];30(3):721–34. Available from: https://link.springer.com/article/10.1007/s11095-012-0913-3

137. Champion JA, Katare YK, Mitragotri S. Particle shape: A new design parameter for micro- and nanoscale drug delivery carriers. J Control Release [Internet]. 2007 Aug 16 [cited 2019 Jan 17];121(1–2):3–9. Available from: https://www.sciencedirect.com/science/article/pii/S0168365907001769

138. Pereira de Sousa I, Steiner C, Schmutzler M, Wilcox MD, Veldhuis GJ, Pearson JP, et al. Mucus permeating carriers: formulation and characterization of highly densely charged nanoparticles. Eur J Pharm Biopharm [Internet]. 2015 Nov 1 [cited 2019 Jan 18];97:273–9. Available from: https://www.sciencedirect.com/science/article/pii/S0939641114003798

139. Dunne M, Corrigan OI, Ramtoola Z. Influence of particle size and dissolution conditions on the degradation properties of polylactide-co-glycolide particles. Biomaterials [Internet]. 2000 Aug 1 [cited 2019 Jan 18];21(16):1659–68. Available from: https://www.sciencedirect.com/science/article/pii/S0142961200000405

140. Patil VRS, Campbell CJ, Yun YH, Slack SM, Goetz DJ. Particle Diameter Influences Adhesion under Flow. Biophys J [Internet]. 2001 Apr 1 [cited 2019 Jan 18];80(4):1733–43. Available from: https://www.sciencedirect.com/science/article/pii/S0006349501761449

141. Chirra HD, Shao L, Ciaccio N, Fox CB, Wade JM, Ma A, et al. Planar Microdevices for Enhanced In Vivo Retention and Oral Bioavailability of Poorly Permeable Drugs. Adv Healthc Mater [Internet]. 2014 Oct [cited 2018 Nov 28];3(10):1648–54. Available from: http://doi.wiley.com/10.1002/adhm.201300676

142. Chirra HD, Desai TA. Multi-Reservoir Bioadhesive Microdevices for Independent Rate-Controlled Delivery of Multiple Drugs. Small [Internet]. 2012 Dec 21 [cited 2019 Jan 11];8(24):3839–46. Available from: http://doi.wiley.com/10.1002/smll.201201367

143. Autumn K, Liang YA, Hsieh ST, Zesch W, Chan WP, Kenny TW, et al. Adhesive force of a single gecko foot-hair. Nature [Internet]. 2000 Jun 8 [cited 2021 Mar 11];405(6787):681–5. Available from: www.nature.com

144. Fischer KE, Jayagopal A, Nagaraj G, Daniels RH, Li EM, Silvestrini MT, et al. Nanoengineered surfaces enhance drug loading and adhesion. Nano Lett [Internet]. 2011 Mar 9 [cited 2021 Mar 11];11(3):1076–81. Available from: https://pubs.acs.org/sharingguidelines

145. Mody R, Joshi SH antara., Chaney W. Use of lectins as diagnostic and therapeutic tools for cancer. Vol. 33, Journal of Pharmacological and Toxicological Methods. Elsevier; 1995. p. 1–10.

146. Fischer KE, Nagaraj G, Hugh Daniels R, Li E, Cowles VE, Miller JL, et al. Hierarchical nanoengineered surfaces for enhanced cytoadhesion and drug delivery. Biomaterials. 2011 May 1;32(13):3499–506.

147. Fischer KE, Alemán BJ, Tao SL, Hugh Daniels R, Li EM, Bü nger MD, et al. Biomimetic Nanowire Coatings for Next Generation Adhesive Drug Delivery Systems. Nano Lett [Internet]. 2009 [cited 2021 Mar 11];9(2):716–20. Available from: https://pubs.acs.org/sharingguidelines

148. Vaut L, Juszczyk JJ, Kamguyan K, Jensen KE, Tosello G, Boisen A. 3D Printing of Reservoir Devices for Oral Drug Delivery: From Concept to Functionality through Design Improvement for Enhanced Mucoadhesion. 2020 [cited 2021 Apr 1]; Available from: https://dx.doi.org/10.1021/acsbiomaterials.9b01760

149. Rao KVR, Buri P. A novel in situ method to test polymers and coated microparticles for bioadhesion. Int J Pharm [Internet]. 1989 Jun 15 [cited 2018 May 15];52(3):265–70. Available from: https://www.sciencedirect.com/science/article/pii/0378517389902299

150. Madsen KD, Sander C, Baldursdottir S, Pedersen AML, Jacobsen J. Development of an ex vivo retention model simulating bioadhesion in the oral cavity using human saliva and physiologically relevant irrigation media. Int J Pharm [Internet]. 2013 May 20 [cited 2018 May 15];448(2):373–81. Available from: https://www.sciencedirect.com/science/article/pii/S0378517313002500

151. Lee Y-AL, Zhang S, Lin J, Langer R, Traverso G. A Janus Mucoadhesive and Omniphobic Device for Gastrointestinal Retention. Adv Healthc Mater [Internet]. 2016 May 1 [cited 2018 Nov 30];5(10):1141–6. Available from:

http://doi.wiley.com/10.1002/adhm.201501036

152. Madsen KD, Sander C, Baldursdottir S, Marie A, Pedersen L, Jacobsen J. Development of an ex vivo retention model simulating bioadhesion in the oral cavity using human saliva and physiologically relevant irrigation media. Int J Pharm. 2013;448:373–81.

153. Sotres J, Jankovskaja S, Wannerberger K, Arnebrant T. Ex-Vivo Force Spectroscopy of Intestinal Mucosa Reveals the Mechanical Properties of Mucus Blankets. Sci Rep [Internet]. 2017 Dec 4 [cited 2019 Mar 18];7(1):7270. Available from: http://www.nature.com/articles/s41598-017-07552-7

154. Thirawong N, Nunthanid J, Puttipipatkhachorn S, Sriamornsak P. Mucoadhesive properties of various pectins on gastrointestinal mucosa: An in vitro evaluation using texture analyzer. [cited 2020 Nov 5]; Available from: www.elsevier.com/locate/ejpb

155. das Neves J, Amaral MH, Bahia MF. Performance of an in vitro mucoadhesion testing method for vaginal semisolids: Influence of different testing conditions and instrumental parameters. Eur J Pharm Biopharm [Internet]. 2008 Jun 1 [cited 2019 Jun 13];69(2):622–32. Available from: https://www.sciencedirect.com/science/article/pii/S0939641107004110

156. Estrellas KM, Fiecas M, Azagury A, Laulicht B, Cho DY, Mancini A, et al. Time-dependent mucoadhesion of conjugated bioadhesive polymers. Colloids Surfaces B Biointerfaces [Internet]. 2019 Jan 1 [cited 2019 Mar 18];173:454–69. Available from: https://www.sciencedirect.com/science/article/pii/S0927776518307045

157. Moreno JAS, Mendes AC, Stephansen K, Engwer C, Goycoolea FM, Boisen A, et al. Development of electrosprayed mucoadhesive chitosan microparticles. Carbohydr Polym [Internet]. 2018 Jun 15 [cited 2019 Jun 13];190:240–7. Available from: https://www.sciencedirect.com/science/article/pii/S0144861718302200

158. Boegh M, Baldursdóttir SG, Müllertz A, Nielsen HM. Property profiling of biosimilar mucus in a novel mucus-containing in vitro model for assessment of intestinal drug absorption. Eur J Pharm Biopharm. 2014;87(2):227–35.

159. Al Naib A, Ward F, Kelly AK, Wade M, Marti JI, Lonergan P. Effect of duration of storage at ambient temperature on fertilizing ability and mucus penetration ability of fresh bovine sperm. Theriogenology. 2011 Oct 1;76(6):1070–5.

160. Donnelly RF, McCarron PA, Cassidy CM, Elborn JS, Tunney MM. Delivery of photosensitisers and light through mucus: Investigations into the potential use of photodynamic therapy for treatment of Pseudomonas aeruginosa cystic fibrosis pulmonary infection. J Control Release. 2007 Feb 12;117(2):217–26.

161. Baker M. 1,500 scientists lift the lid on reproducibility. Nature [Internet]. 2016 May 25 [cited 2019 Oct 8];533(7604):452–4. Available from: http://www.nature.com/articles/533452a

162. Ioannidis JPA, Greenland S, Hlatky MA, Khoury MJ, Macleod MR, Moher D, et al. Increasing value and reducing waste in research design, conduct, and analysis. Lancet [Internet]. 2014 Jan 11 [cited 2019 Oct 8];383(9912):166–75. Available from: https://www.sciencedirect.com/science/article/pii/S0140673613622278

163. Shaw LR, Irwin WJ, Grattan TJ, Conway BR. Drug Development and Industrial

Pharmacy The Effect of Selected Water-Soluble Excipients on the Dissolution of Paracetamol and Ibuprofen The Effect of Selected Water-Soluble Excipients on the Dissolution of Paracetamol and Ibuprofen. 2008 [cited 2019 Feb 18]; Available from: https://www.tandfonline.com/action/journalInformation?journalCode=iddi20

164. Christfort JF, Strindberg S, Al-khalili S, Bar-Shalom D, Boisen A, Nielsen LH, et al. In vitro and in vivo comparison of microcontainers and microspheres for oral drug delivery. Int J Pharm [Internet]. 2021 May 1 [cited 2021 Apr 12];600:378–5173. Available from: https://doi.org/10.1016/j.ijpharm.2021.120516

165. Chen XM, Elisia I, Kitts DD. Defining conditions for the co-culture of Caco-2 and HT29-MTX cells using Taguchi design. J Pharmacol Toxicol Methods. 2010 May 1;61(3):334–42.

166. Fabiano A, Zambito Y, Bernkop-Schnürch A. About the impact of water movement on the permeation behaviour of nanoparticles in mucus. Int J Pharm. 2017;517:279–85.

167. das Neves J, Bahia MF, Amiji MM, Sarmento B. Mucoadhesive nanomedicines: characterization and modulation of mucoadhesion at the nanoscale. Expert Opin Drug Deliv [Internet]. 2011 Aug 21 [cited 2021 Mar 3];8(8):1085–104. Available from: http://www.tandfonline.com/doi/full/10.1517/17425247.2011.586334

168. Walsh LA, Allen JL, Desai TA. Nanotopography applications in drug delivery. Expert Opin Drug Deliv [Internet]. 2015 Dec 2 [cited 2021 Apr 2];12(12):1823–7. Available from: http://www.tandfonline.com/doi/full/10.1517/17425247.2015.1103734

169. Perioli L, D'Alba G, Pagano C. New oral solid dosage form for furosemide oral administration. Eur J Pharm Biopharm. 2012 Apr 1;80(3):621–9.

170. Nielsen LH, Gordon S, Holm R, Selen A, Rades T, Müllertz A. Preparation of an amorphous sodium furosemide salt improves solubility and dissolution rate and leads to a faster Tmax after oral dosing to rats. Eur J Pharm Biopharm. 2013;85(3):942–51.

171. Matsuda Y, Tatsumi E. Physicochemical characterization of furosemide modifications. Int J Pharm. 1990 Apr 20;60(1):11–26.

172. Granero GE, Longhi MR, Mora MJ, Junginger HE, Midha KK, Shah VP, et al. Biowaiver monographs for immediate release solid oral dosage forms: Furosemide. Vol. 99, Journal of Pharmaceutical Sciences. John Wiley and Sons Inc.; 2010. p. 2544–56.

173. Iannuccelli V, Coppi G, Leo E, Fontana F, Bernabei MT. PVP Solid Dispersions for the Controlled Release of Furosemide from a Floating Multiple-Unit System. Drug Dev Ind Pharm [Internet]. 2000 Jan 24 [cited 2021 Mar 30];26(6):595–603. Available from: http://www.tandfonline.com/doi/full/10.1081/DDC-100101274

174. Bernkop-Schnürch A, Guggi D, Pinter Y. Thiolated chitosans: development and in vitro evaluation of a mucoadhesive, permeation enhancing oral drug delivery system. J Control Release [Internet]. 2004 Jan 8 [cited 2019 Mar 18];94(1):177–86. Available from: https://www.sciencedirect.com/science/article/pii/S0168365903004747

175. Park K, Robinson JR. Bioadhesive polymers as platforms for oral-controlled drug delivery: method to study bioadhesion. Int J Pharm. 1984 Apr 1;19(2):107–27.

176. Charles Griffiths P, Cattoz B, Shafik Ibrahim M, Chibuzor Anuonye J. Probing the interaction of nanoparticles with mucin for drug delivery applications using dynamic

light scattering. 2015;

177. Wilcox MD, Rooij LK Van, Chater PI, Pereira De Sousa I, Pearson JP. The effect of nanoparticle permeation on the bulk rheological properties of mucus from the small intestine. Eur J Pharm Biopharm. 2015;96:484–7.

178. Gentile P, Chiono V, Carmagnola I, Hatton P. An Overview of Poly(lactic-co-glycolic) Acid (PLGA)-Based Biomaterials for Bone Tissue Engineering. Int J Mol Sci [Internet]. 2014 Feb 28 [cited 2021 Apr 16];15(3):3640–59. Available from: http://www.mdpi.com/1422-0067/15/3/3640

179. Makadia HK, Siegel SJ. Poly Lactic-co-Glycolic Acid (PLGA) as Biodegradable Controlled Drug Delivery Carrier. Polymers (Basel) [Internet]. 2011 Aug 26 [cited 2021 Apr 16];3(3):1377–97. Available from: http://www.mdpi.com/2073-4360/3/3/1377

180. Eliaz RE, Kost J. Characterization of a polymeric PLGA-injectable implant delivery system for the controlled release of proteins. J Biomed Mater Res. 2000;50(3):388–96.

181. Abedalwafa M, Wang F, Wang L, Li C. BIODEGRADABLE POLY-EPSILON-CAPROLACTONE (PCL) FOR TISSUE ENGINEERING APPLICATIONS : A REVIEW. 2013;34:123–40.

182. Heimowska A, Morawska M, Bocho-janiszewska A. Biodegradation of poly (ε -caprolactone) in natural water environments. 2017;120–6.

183. Whitcomb DC, Lowe ME. Human Pancreatic Digestive Enzymes. Dig Dis Sci [Internet]. 2007 Jan 11 [cited 2019 Sep 10];52(1):1–17. Available from: http://link.springer.com/10.1007/s10620-006-9589-z

184. Armani DK, Liu C. Microfabrication Technology for Polycaprolactone, A Biodegradable Polymer. :294–9.

185. Gan Z, Liang Q, Zhang J, Jing X. Enzymatic degradation of poly(ε-caprolactone) film in phosphate buffer solution containing lipases. Polym Degrad Stab. 1997 May 1;56(2):209–13.

186. Park TG. Degradation of poly(d,l-lactic acid) microspheres: effect of molecular weight. J Control Release. 1994;30(2):161–73.

187. Schliecker G, Schmidt C, Fuchs S, Wombacher R, Kissel T. Hydrolytic degradation of poly(lactide-co-glycolide) films: Effect of oligomers on degradation rate and crystallinity. Int J Pharm. 2003;266(1–2):39–49.

Appendix I

Paper I

***Ex vivo* intestinal perfusion model for investigating mucoadhesion of microcontainers**

Mette Dalskov Mosgaard, Sophie Strindberg, Zarmeena Abid, Ritika Singh Petersen, Lasse Højlund Eklund Thamdrup, Alina Joukainen Andersen, Stephan Sylvest Keller, Anette Müllertz, Line Hagner Nielsen, Anja Boisen

International Journal of Pharmaceutics 570 (2019) 118658

International Journal of Pharmaceutics 570 (2019) 118658

Contents lists available at ScienceDirect

International Journal of Pharmaceutics

journal homepage: www.elsevier.com/locate/ijpharm

Ex vivo intestinal perfusion model for investigating mucoadhesion of microcontainers

Mette Dalskov Mosgaard[a,*], Sophie Strindberg[b], Zarmeena Abid[c], Ritika Singh Petersen[c], Lasse Højlund Eklund Thamdrup[a], Alina Joukainen Andersen[a], Stephan Sylvest Keller[c], Anette Müllertz[b], Line Hagner Nielsen[a], Anja Boisen[a]

[a] Department of Health Technology, Technical University of Denmark, Ørsteds Plads 345C, 2800 Kgs. Lyngby, Denmark
[b] Department of Pharmacy, Faculty of Health and Medical Sciences, University of Copenhagen, Universitetsparken 2, 2100 Copenhagen, Denmark
[c] National Center of Nano Fabrication and Characterization, DTU Nanolab, Technical University of Denmark, Ørsteds Plads 345C, 2800 Kgs. Lyngby, Denmark

ARTICLE INFO

Keywords:
Microdevices
Microcontainers
Oral drug delivery
Ex vivo intestinal perfusion
Mucoadhesion

ABSTRACT

Micro fabricated delivery systems have shown promise in increasing oral bioavailability of drugs. Micrometer-sized polymeric devices (microcontainers) have the potential to facilitate unidirectional drug release directly into the intestinal mucosa whereby, drug absorption can be enhanced. The aim of this study was to develop an *ex vivo* model to investigate mucosal adhesion and orientation of microcontainers. Furthermore, to investigate how microcontainers with varying height, shape and material behave in regards to mucoadhesion and orientation. Microcontainers were placed at the top of an inclined piece of porcine small intestine. The tissue was perfused with biorelevant medium followed by microscopic examination to observe the orientation and amount of microcontainers on the tissue. The mucoadhesion of the microcontainers were evaluated based on the observed position on the tissue after being exposed to flow. When comparing the varying types of microcontainers, good adhesion was in general observed since most of the microcontainers were located in the beginning of the intestine. Microcontainers fabricated from the epoxy-based photoresist SU-8 had a slightly better adherence than those fabricated from poly-ε-caprolactone (PCL). The orientation of the microcontainers appeare to be dictated mainly by the height. In general, the model showed promising results in evaluating mucoadhesion and orientation.

1. Introduction

Oral administration is the preferred route for drugs, as it offers low production costs and high patient compliance due to self-administration (Liu, 1997; Thanki et al., 2013). However, oral administration has various limitations and challenges. Numerous physiological parameters in the gastrointestinal tract such as a harsh acidic gastric environment in the fasted state, digestive enzymes and a highly viscous mucus layer have shown to compromise the oral bioavailability of many drugs (Sjögren et al., 2014; Zhou, 1994). One strategy to overcome some of these challenges is to use microdevices as oral drug delivery systems (Nielsen et al., 2018). Several studies have shown an increased oral bioavailability of pharmaceuticals when using these platforms (Chirra et al., 2014; Mazzoni et al., 2017; Nielsen et al., 2016). Microcontainers are one type of such microdevices. These are micrometer-sized hollow shapes, fabricated in polymeric materials with an inner cavity for drug storage (Nielsen et al., 2014, 2012). Only one side of the microcontainer is open, allowing unidirectional drug release. Coating of the open cavity with an enteric polymer can provide protection against the acidic environment as well as enzymatic degradation in the stomach and allow for release in the small intestine (Nielsen et al., 2016). Unidirectional release is believed to result in an increased local drug concentration at the intestinal wall (Ainslie et al., 2009; Nielsen et al., 2018). This is, however, only possible if the unidirectional release is occurring directly into the mucus layer. Another advantage of using microcontainers as an oral drug delivery system is that polydispersity can be avoided. The fabrication technique allows for very precise sizes and shapes of the microcontainers enabling uniform drug loading.

There are many possibilities for changing and optimising microcontainers to achieve a direct drug release into the mucus layer. The

Abbreviations: PCL, poly-ε-caprolactone; FaSSIF, Fasted State Simulated Intestinal Fluid; Si, silicon; PVA, Poly(vinyl alcohol); LYD, Landrace x Yorkshire x Duroc; SEM, Scanning electron microscope; HPLC, High performance liquid chromatography

* Corresponding author.
E-mail address: medmo@dtu.dk (M. Dalskov Mosgaard).

https://doi.org/10.1016/j.ijpharm.2019.118658
Received 8 July 2019; Received in revised form 29 August 2019; Accepted 31 August 2019
Available online 03 September 2019
0378-5173/

fabrication technique of the microcontainers make them a very flexible and versatile drug delivery system (Ahmed et al., 2002; Chirra and Desai, 2012; Tao et al., 2007). Previous studies have shown that e.g. size, shape and material of polymeric carriers affect their behaviour and performance in *in vivo* settings (Champion et al., 2007; Pereira de Sousa et al., 2015). The surface chemistry of polymeric drug carriers for oral delivery has been extensively studied, as it has been demonstrated to influence the interaction between the polymeric carrier and the mucosal surface, hence drug absorption (Champion et al., 2007; Pereira de Sousa et al., 2015). Furthermore, the size of the polymeric carriers influences flow properties, clearance and degradation in the mucus layer in the small intestine (Dunne et al., 2000; Patil et al., 2001). Few studies have investigated nanosized polymeric carriers with different shapes, and it is believed that shape differences will affect the movement of these carriers when exposed to a flow (Champion and Mitragotri, 2009). The above mentioned studies have been conducted on nanoparticles. However, the same parameters can be important for microcontainers and their behaviour in the small intestine (Chirra et al., 2014).

Previously, it has been reported from *in situ* and *in vivo* studies in rats that the microcontainers embed deeply into the intestinal mucus layer, resulting in increased absorption and thereby, enhanced oral bioavailability of ketoprofen and of an amorphous sodium salt of furosemide when compared to controls using the free drug (Mazzoni et al., 2017; Nielsen et al., 2016). These results have shown that dosing of a drug in microcontainers can indeed increase oral bioavailability. This is believed to be associated with an enhanced mucoadhesion of the microcontainers.

In rats, the size ratio (small intestinal diameter in rats 0.3–0.5 cm and in human 5 cm) between the intestinal lumen and the microcontainers is significantly smaller than in humans (Kararli, 1995). To provide a better *in vitro/in vivo* correlation of how the microcontainers are interacting and orientating themselves in the intestinal mucus layer in humans, the size ratio should be larger (Swindle et al., 2012). Using intestinal tissue from pigs (small intestinal diameter 2.5–3.5 cm) is one way to achieve this, as the size ratio is more similar to human intestine (Kararli, 1995). Furthermore, humans and pigs have comparable digestive processes as well as similar viscoelastic properties of their mucus layer (Lai et al., 2009).

Many well documented methods have investigated *ex vivo* mucoadhesion. One of these has been developed by Rao and Buri, who used an open piece of small intestine from a rat to measure bioadhesiveness of coated particles (Rao and Buri, 1989). This method has been modified by others to test e.g. mucoadhesion of a dual-sided planar macro device, spray dried chitosan particles and nanoparticles (Lee et al., 2016; Madsen et al., 2013; Nielsen et al., 1998). Many of the studies use the same setup but the experimental parameters such as the angle of the tissue, flow rate, tissue size and duration of the experiments are varying and depends on the formulations being investigated. The drawback of this approach is that the tissue is cut open, and the mucus layer is thereby exposed to stress and the realistic *in vivo* setting of the intestine is lost. When opening the intestinal tissue the mucus layer will be affected by hydration which will change the viscoelastic properties and ionic strength of the mucus (Lieleg and Ribbeck, 2011). The parameters used in this study has been inspired by perfusion studies conducted *in situ* on rat intestine and in general from physiological conditions in pigs. The flow rate was e.g. calculated in relation to the size ratio between a rat and pig intestine (Sinko et al., 1995). Fabiano et al. have developed another simple setup for testing mucoadhesion of nanoparticles with an applied water flow through a mucus layer (Fabiano et al., 2017). However, this setup is limited by the size of the drug delivery systems as larger microdevices, such as microcontainers, are less affected by the water flow through the mucus layer compared to nanoparticles. The developed models lack the information on how microcontainers will orient themselves in the intestine and how they perform when exposed to a flow in the lumen.

Another very important aspect of testing microcontainers and their behaviour *ex vivo* is to evaluate drug release profiles. Methods to improve mucoadhesion of microcontainers, such as using mucoadhesive surfaces, must not compromise the release profile. Therefore, evaluation of the drug release profile from microcontainers is a desirable feature in a new model.

The aim of this study was to develop and evaluate a novel *ex vivo* porcine intestinal perfusion model to test mucoadhesion and orientation of microcontainers. Four types of microcontainers were tested and compared with respect to height, shape and material. Also, drug concentration was measured over time in the perfused fluid, and a drug release profile from the microcontainers was recorded. These investigations served two purposes: evaluation of (1) the porcine *ex vivo* small intestinal perfusion model and (2) microcontainer behaviour when exposed to the porcine *ex vivo* small intestinal perfusion model.

2. Materials and methods

2.1. Materials

Fasted State Simulated Intestinal Fluid (FaSSIF) powder was purchased from Biorelevant.com, (London, UK). Monobasic sodium phosphate dehydrate, sodium chloride, acetonitrile anhydrous 99.8%, trichloroacetic acid 99.0%, poly-ε-caprolactone (PCL) (Mn = 80,000 g/mol) and paracetamol were all acquired from Sigma-Aldrich (St. Louis, USA). Trifluoroacetic acid ≥99.9% was obtained from Carl Roth® (Karlsruhe, Germany) and gelatine capsules size 9 were purchased from Torpac® (Fairfield, USA). Stainless steel Spectra/Mesh® woven filters with a mesh opening of 213 µm and a thickness of 178 µm were from Spectrum®Labs.com (CA, USA). Poly(vinyl alcohol) (PVA) Mowiflex C17 was kindly provided by Kuraray (Tokyo, Japan). Silicon (Si) wafers 4-inch (1 0 0) single-side polished were obtained from Topsil (Frederikssund, Denmark), whereas SU-8 2035, 2075 and SU-8 developer were purchased from Microresist Technology GmbH (Berlin, Germany). The 3D printed components used in the custom-made setup were made from polylactic acid (PLA) and polyethylene terephthalate glycol (PETG), which were obtained from Devil Design (Ryszka Mateja Sp. J., Poland).

2.2. Fabrication of SU-8 and PCL microcontainers

Microcontainers with different heights and shapes were fabricated in two different materials (Table 1). SU-8 cylindrical microcontainers were fabricated as previously described with two steps of conventional mask-based photolithography on a silicon (Si) wafer with a fluorocarbon coating deposited by plasma polymerisation (Keller et al., 2007; Nielsen et al., 2016). This allowed for dry release of individual microcontainers from the support substrate (Keller et al., 2007). The triangular microcontainers were fabricated in a similar fashion but the UV exposure was conducted with a maskless aligner. The dimensions of the various microcontainers are shown in Table 1 and were characterized using an optical profiler (PLu Neox 3D Optical Profiler from Sensofar, Spain) as well as optical microscopy (Nikon Eclipse L200, NY USA). After fabrication, the wafer was cut into squared chips using a dicing saw (DISCO, automatic dicing saw, DAD 321, Japan). Each chip of cylindrical microcontainers contained 625 microcontainers and had a size of 12.8 × 12.8 mm. Chips of triangular microcontainers contained 625 microcontainers and had a size of 25 × 25 mm.

Microcontainers in the biodegradable polymer PCL were fabricated by a hot punching process as previously described (Abid et al., 2019; Petersen et al., 2015). These microcontainers were fabricated on a water soluble PVA substrate containing 1600 microcontainers. To obtain individual microcontainers, the whole substrate was soaked into water and stirred at 1200 rpm for 35 min to dissolve the PVA, leaving only the free floating PCL microcontainers. The microcontainers were then filtered with a woven stainless steel filter and dried at 37 °C before

Table 1
Design parameters of the microcontainers used in this study.

Name	Shape	Illustration	Material	Weight (μg)	Outer diameter (μm)	Total height (μm)
High	Cylindrical		SU-8	21.1 ± 1.4	326 ± 1	257 ± 4
Low	Cylindrical		SU-8	7.5 ± 0.1*	316 ± 5	108 ± 11
Tri	Triangular		SU-8	7.0 ± 0.6*	368 ± 4	131 ± 0.4
PCL	Cylindrical		PCL	3.7 ± 0.4	304 ± 3	92.0 ± 2

* No significant difference between the weights. P-values below 5% ($p < 0.05$) were considered statistically significant.

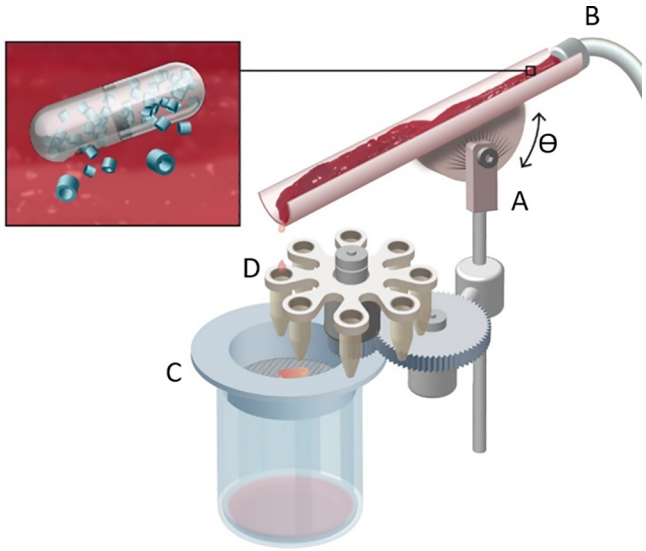

Fig. 1. Schematic of the *ex vivo* intestinal perfusion model. A piece of intestinal tissue is placed on an angle adjustable tissue holder (A), which is connected to a tube (B). A gelatine capsule loaded with microcontainers was placed at the top part of the tissue (the inserted box). A filter was placed below the tissue holder (C). An auto sampler with test tubes facilitates sampling of the perfused fluid over time (D).

further use.

2.3. Drug loading and capsule filling

Only the *high* SU-8 microcontainers were loaded with paracetamol as model drug and compared with empty *high* microcontainers. The drug loading procedure was performed as described previously by Abid et al. (2017). A silicon chip with 625 microcontainers was gently placed in a holder and a shadow mask was aligned to the cavities of the microcontainers. Paracetamol powder was distributed with a brush across the shadow mask thereby, loading the cavities of the microcontainers. Afterwards, the mask was gently removed and excess drug in between the microcontainers was removed with pressurised air. The chip was weighed before and after loading to determine the amount of drug loaded into the microcontainers.

The four microcontainer types (both with and without paracetamol) were filled into gelatine capsules. The capsules were weighed before and after filling to determine the amount of microcontainers in one capsule.

2.4. Visualisation of microcontainers

The height, shape and dimensions of the different microcontainers and the loading quality of the *high* microcontainers were investigated using scanning electron microscope (SEM) (TM3030Plus Tabletop Microscope, Hitachi®, Tokyo, Japan). The inspection was done using the SE detector and an acceleration voltage of 15 kV to obtain high quality images.

2.5. Porcine small intestinal ex vivo perfusion model

The *ex vivo* study was conducted at the Department of Health Technology at the Technical University of Denmark under the license number DK-10-13-oth-736416. The Department of Experimental Medicine, University of Copenhagen, kindly donated the small intestine from Landrace × Yorkshire × Duroc (LYD) pigs. The pigs were 15–16 weeks of age and the weight was 50–55 kg. The small intestine was cut into pieces with a length of approximately 18 cm and stored at −20 °C until further use.

A specially designed setup, including a humidity chamber and tissue holder, was developed and fabricated for these experiments (Fig. 1) (Vaut et al., 2019). A heating lamp was placed inside the sealed chamber and was programmed to maintain a temperature of 37 ± 1.1 °C. A humidifier was also located inside the chamber to keep the humidity high and stable. The tissue holder was fabricated in glycol-modified polyethylene and was 19.5 cm long and 3.3 cm in width. In one end of the tissue holder, a small connector was attached to a tube, which was connected to a peristaltic pump (Watson Marlow 120S/DV, Falmouth, UK). From the connector, the holder was

narrowed (11.8 mm) to be able to fasten a piece of porcine small intestine. The tissue holder can be set at different angles to change the position of the tissue. A self-constructed filter holder with a woven stainless steel filter with a pore size of 213 µm was placed underneath the exit of the intestine. A custom-made auto sampler was also developed for sampling the perfused fluid over time.

2.6. Perfusion experiments

Perfusion experiments were conducted in the designed setup. Two hours prior to an experiment, FaSSIF was prepared at pH 6.5 and kept at 37 °C until further use. An 18 cm long piece of small intestine from a pig was thawed for 30–50 min at room temperature followed by immediately placing and fastening it to the tissue holder. Then, the tissue was placed at an angle of 20° in the pre-heated chamber with an average humidity during the experiment of 60.9 ± 11.5% (Nielsen et al., 1998). Next, the intestine was flushed with FaSSIF for 15 min (4.1 mL/min) to remove all residues. After the washing procedure, the tissue holder was placed at an angle of 10° and flushed for 5 min (1.55 mL/min) to obtain a water rich environment for dissolving the microcontainer-filled capsule. A capsule filled with microcontainers was then placed approximately 2 cm from the start of the intestine. After 15 min, the tissue holder was placed back at an angle of 20° and a flow of FaSSIF 1.55 mL/min was initiated (Sinko et al., 1995). After 30 min of perfusion, the tissue holder was gently removed and the tissue was detached from the holder. The piece of tissue was then cut into pieces with a length of approximately 2 cm, opened and divided into sections named start, middle, end and exit (each section consists of three pieces except for the exit part which is the microcontainers found on the filter). The tissue was placed onto microscope glass slides and dried in air for approximately 1 h before visualisation on a microscope (see Section 2.7). The number of microcontainers in each piece was counted and their orientation was noted. The orientation of the microcontainers was classified as: (I) sideways, (II/III) with bottom up/down or (IV) deeply embedded into the mucus layer (Fig. 2). A microcontainer was defined as lying 'sideways' when the open side of container was placed facing horizontally into the mucus layer, partly or fully embedded in the mucus layer. The orientation 'bottom up/down' was used when the open cavity of a container was facing towards the mucus or out towards the lumen of the intestine.

For the paracetamol-loaded microcontainers, samples were taken at different time intervals from the perfused fluid to investigate the drug concentration over time. Samples were taken after 1, 5, 10, 15, 20, 25 and 29 min and the samples were collected for 1 min to receive approximately 1.55 mL. The first sample was collected from flow initiation to 1 min after initiation.

2.7. Fluorescence and light microscopy of the microcontainers on the intestinal tissue

Fluorescence microscopy was used to locate and visualise the microcontainers fabricated in SU-8. A U-RFL-T mercury/xenon burner was utilised with a U-LH100HG microscope (Olympus®, Tokyo, Japan), and CellSens Entry software (version 1.12, Olympus®, Tokyo, Japan) was used to take images of the microcontainers. A DAPI filter was employed to identify the SU-8 microcontainers in the mucus layer as well as clarifying the orientation of them.

A light microscope (Zeiss Axio Scope.A1, Carl Zeiss, Göttingen, Germany) with a C-DIC filter and AxioVision SE64 software (version 4.9.1 SP1) was used for visualising the PCL microcontainers on the intestine.

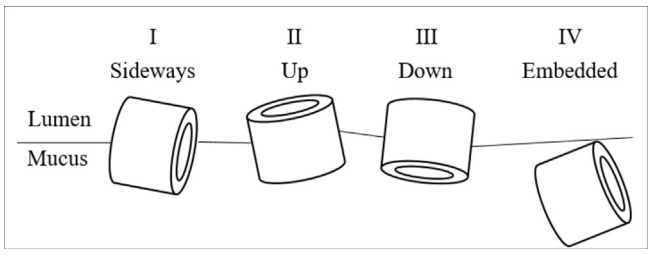

Fig. 2. Schematic of the microcontainer orientation on the porcine intestinal tissue. (I) sideways, (II) with bottom down, (III) with bottom up and (IV) deeply embedded in the mucus layer.

2.8. High performance liquid chromatography (HPLC) for quantification of paracetamol

The amount of paracetamol in the perfused fluid over time was determined by UV-detection on a HPLC (Shimadzu, Kyoto, Japan). Protein precipitation in the samples was conducted with 10% (w/v) trichloroacetic acid in a 1:1 ratio. The samples were centrifuged at 14,000 rpm for 10 min and analysed on the HPLC.

The HPLC system was equipped with a SIL-20AC HT automated sample injector and a SPD-M20A photodiode array detector. LabSolutions Lite (version 5.82) software was employed to analyse the data (shimadzu, Kyoto, Japan), and paracetamol was detected at 250 nm with a reverse-phase Kinetix® C18 column with the dimensions of 100 × 4.6 mm (Phenomenex®, Torrance, CA, USA). The mobile phase consisted of 95% (v/v) trifluoroacetic acid 0.1% (v/v) and 5% (v/v) acetonitrile with isocratic elution. The flow rate was 0.5 mL/min with an injection volume of 20 µL. The retention time was 6.6 min and paracetamol was quantified using a standard calibration curve in the linear range of 0.5–75 µg/mL.

2.9. Statistics

All data presented in this study are expressed as mean ± standard deviation (SD). Statistical analysis was carried out using Student t-tests in GraphPad Prism version 7.04 (CA, USA). P-values below 5% ($p < 0.05$) were considered statistically significant.

3. Results and discussion

The developed porcine *ex vivo* small intestinal model can provide information on mucoadhesion, orientation of microcontainers and drug release profiles.

3.1. Microcontainer characterization

SEM images show the design of the four types of microcontainers (Fig. 3). The different design parameters are listed in Table 1.

The differences in shapes, heights and material resulted in different weights of the microcontainers (Table 1). The shape, height, material and thereby also weight of the microcontainers are believed to play a role in how the microcontainers are behaving in the small intestine, and this could influence the mucoadhesion.

3.2. Mucoadhesion of microcontainers

The mucoadhesion of the microcontainers was evaluated based on the observed position of the microcontainers on the intestinal tissue (Fig. 4). The movement of the microcontainers is an estimate of how mucoadhesive the microcontainers are. The longer they move in the intestine the less adhesive they are. The *high* and *low* microcontainers were in general behaving very similar (Fig. 4A), and significantly more were found in the start of the intestine (77.6 ± 25.1% and 80.8 ± 12.9%, respectively) compared to the other sections. However, there was a tendency that more *high* microcontainers were found in the middle (19.5 ± 22.6%) of the intestine when compared to the *low* microcontainers (9.7 ± 5.6%). More of the *low* microcontainers were

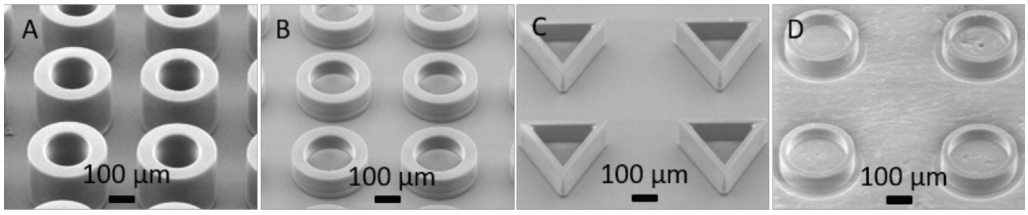

Fig. 3. SEM images of the four types of microcontainers. A) 257 ± 4 µm in height SU-8 microcontainers. B) 108 ± 11 µm high SU-8 microcontainers. C) 131 ± 0.4 µm high triangular SU-8 microcontainers. D) 92 ± 2 µm high microcontainers fabricated in PCL.

observed to exit (5.8 ± 7.3%) the intestine than the *high* microcontainers (1.8 ± 2.0%). When comparing the adhesion abilities of the *tri* and *low* microcontainers (Fig. 4B), there were again significantly more microcontainers found in the start of the intestine (67.1 ± 13.8% and 80.8 ± 12.9%, respectively) compared to the other sections. Significantly, more of the *tri* microcontainers were observed in the middle section compared to the *low* microcontainers (P = 0.049). Only small amounts of the *tri* and *low* microcontainers were observed in the end and exit section. The data indicates that the *tri* microcontainers adhered less in the start of the intestine as more of the microcontainers had moved to the middle section. When comparing the adhesion abilities of PCL and SU-8 microcontainers with the same height (Fig. 4C), the SU-8 microcontainers seem more adhesive. A larger number of PCL microcontainers were observed in the sections further down the intestine, whereas the *low* SU-8 microcontainers were more abundant in the start of the intestine. Significantly more of the PCL and *low* microcontainers were found in the start of the intestine (65.0 ± 14.2% and 80.8 ± 12.9%, respectively) compared to the other sections.

In general, all the different types of microcontainers showed good adhesion properties. Between 65 and 81 % of the microcontainers were located in the start of the intestine. However, the graphs indicate variations between the microcontainers' ability to adhere to the mucosal surface. The *high* microcontainers seemed to adhere more to the intestinal surface as their movement practically stopped after reaching the middle part of the intestine. In contrast, more of the *low* microcontainers, that were not adhering in the beginning, moved all the way through the intestine and were found to exit the intestine. The *high* microcontainers have a larger surface that can adhere to mucus and, in addition, they are heavier than the *low* microcontainers, which could result in increased adhesion. The height of microcontainers is believed to influence how they adhere to the mucosal surface. Thick microdevices have been reported to increase the shear forces, per mass, and to be more likely to dislodge themselves from a mucosal surface when exposed to flow conditions (Chirra and Desai, 2012). However, this effect was not observed in our model for the *high* microcontainers. When comparing the *tri* and *low* microcontainers, it was expected that the triangular shaped microcontainers would adhere more to the mucosal surface than the cylindrical shaped due to the sharp edges. These two types of microcontainers had similar weight but significantly different shapes. The data suggest that the *tri* microcontainers adhere less in the start section and adhere more in the middle section as compared to the *low* microcontainers. This suggests that *tri* microcontainers moved easier with the flow at the beginning, but the sharp edges also made it more likely for them to adhere to the surface in the middle.

There was a tendency that the PCL microcontainers were adhering less to the mucosal surface than the SU-8 microcontainers of similar height. The chemical structure of the two polymers can affect the microcontainers' ability to adhere to the mucus layer. SU-8 is a very hydrophobic polymer and can create numerous hydrophobic interactions with mucus (Abgrall et al., 2007). PCL is believed to interact less with mucus as it is less hydrophobic, thus, SU-8 might be more mucoadhesive when compared to PCL (Norris and Sinko, 1997; Sigurdsson et al., 2013).

Another factor that can influence the tendency of the PCL microcontainers to adhere less to the mucosal surface than the SU-8 microcontainers is there weight difference. The PCL microcontainers had a weight of 3.7 ± 0.4 µg which make them significantly lighter than the *low* SU-8 microcontainers with a weight of 7.5 ± 0.1 µg. This might make the PCL microcontainers more prone to move with a continuous flow. This aspect was difficult to circumvent since the weight will be affected when changing either the height, shape or material.

One possible explanation for the lack of significant difference between the ability of the different microcontainers to adhere to the mucosal surface could be physiological variations of the tissue. The model has been simplified to limit the amount of affecting parameters meaning that the intestinal segment in this model is lacking motility and presence of food. Moreover, the amount of fluid is constant, and all the parameters are rarely the case *in vivo*. Further studies are needed to clarify the effect of such parameters.

One challenge, with this setup and when working with microcontainers, is to achieve an acceptable recovery. The recovery is an estimate of the amount of microcontainers added to an experiment and how many of the microcontainers that can be found again. However, this experimental setup enabled good results in this regard, as the average recovery for all the experiments was above 75%. Table 2 states the recovery of the different microcontainers which indicates the capability of the model.

3.3. Orientation of microcontainers

Several studies have emphasized the importance of controlling the direction of drug release from microdevices (Ahmed et al., 2002; Ainslie et al., 2009; Chirra et al., 2014). Most drug delivery systems have omnidirectional drug release which results in a loss of drug into the lumen. This will reduce the drug absorption into the systemic circulation and thereby, the oral bioavailability. By achieving a unidirectional release

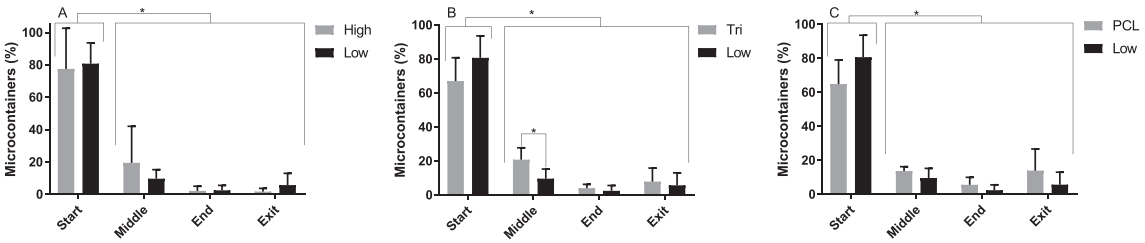

Fig. 4. Percentage of microcontainers located in the start, middle, end and exit of the porcine small intestine after perfusion studies. A) Comparison of microcontainers with a height of 257 ± 4 µm (high) and 108 ± 11 µm (low). B) Triangular (tri) and cylindrical (low) shaped microcontainers with similar heights. C) Microcontainers with similar heights fabricated from PCL and SU-8 (low). Data is represented as mean ± SD with n = 4.* indicates significant difference.

Table 2
The average recovery ± SD of the various types of microcontainers (n = 4).

	High	Low	Tri	PCL
Recovery (%)	90.6 ± 7.4	84.6 ± 5.2	83.2 ± 12.1	86.9 ± 5.3

from microcontainers directly into the mucus layer, one would expect an increased drug absorption (Chirra et al., 2014; Chirra and Desai, 2012). Microcontainers oriented sideways (I) or with the open cavity up (II) or down (III) are illustrated in Fig. 5. It was uncertain to distinguish between cavity facing up or down, and these microcontainers were therefore grouped together.

The orientation of all the microcontainers found in the different sections of the intestine on the mucosal surface is shown in Fig. 6. The *high* microcontainers were mainly lying sideways (I) (P = 0.0006) and showed a significant difference compared to the *low* microcontainers that were primarily oriented with the cavity up or down (II)/(III) (P = 0.001). No significant difference was observed when looking at the amount of *high* and *low* microcontainers found deeply embedded (IV) into the mucus layer (Fig. 6A). When comparing the orientation of the *tri* and *low* microcontainers, no significant differences were observed (Fig. 6B), and both *tri* and *low* microcontainers were primarily lying with the cavity up or down (II)/(III). Significantly more of the SU-8 microcontainers (*low*) were oriented sideways (I) when compared to the PCL microcontainers (P = 0.03). However, significantly more of the PCL microcontainers were oriented with the cavity up or down (II)/(III) (P = 0.003). PCL microcontainers could not be seen as clearly as SU-8 microcontainers when embedded deeply in mucus. SU-8 is autoflorescent, and this is not the case for PCL. Therefore, microcontainers located deep in the mucus layer was not included in Fig. 6C.

The data indicated that the height of the microcontainers was a dominant factor in determining the orientation of the microcontainers, compared to shape and material. From the results obtained, it is clear that the microcontainers with *low* height were more prone to adhere with the cavity up or down (II)/(III), while the *high* microcontainers were lying sideways (I).

The data for the *high* microcontainers showed that 60 ± 12% of the microcontainers were lying sideways (I) (partly embedded) and 13 ± 6% were deeply embedded (IV) into mucus. This means that approximately 73% of the microcontainers were orientated with the open cavity very close to the mucus layer and could deliver drug directly into the mucus layer. The amount could most likely be even higher, as 26 ± 8% of the microcontainers are lying with the cavity up or down (II)/(III). If it is assumed that half of these were oriented with the cavity down, it resulted in approximately 86% of the *high* microcontainers releasing the drug into the mucus layer. If the same assumption is done with the *low* microcontainers then 66% of the microcontainers would be oriented with the open cavity very close to the mucus layer and could deliver drug directly into the layer. These indications state how important it is to evaluate the orientation of the microcontainers as further optimization might not be needed to increase the oral bioavailability. These results correlated well with the results obtained in previous *in vivo* studies with the microcontainers, where an increased oral bioavailability was obtained when using *high* microcontainers (Nielsen et al., 2016). Another advantage of the *high* microcontainers is that they have a high loading capacity compared to more planar microdevices (Chirra et al., 2014; Nielsen et al., 2018).

3.4. Drug loaded microcontainers

The model developed in this study can provide information about the drug release profile from the microcontainers. The *high* microcontainers were loaded with paracetamol to investigate the effect of loading the microcontainers with a drug. The average paracetamol loading capacity for each microcontainer was 3.1 ± 1.1 µg (n = 3000) and paracetamol-loaded microcontainers are shown in Fig. 7A. The loaded microcontainers were compared to empty *high* microcontainers to investigate how these microcontainers moved in the intestine when exposed to a constant flow (Fig. 7B). As can be seen in Fig. 7B was their ability to adhere to the intestinal surface similar. The orientation of the drug-loaded microcontainers was also similar to the empty ones (Fig. 7C). The drug-loaded microcontainers were mainly oriented sideways. It was possible to measure the concentration of paracetamol in the perfused fluid over time. The highest drug concentration was measured as soon as the flow was initiated, followed by decreasing drug

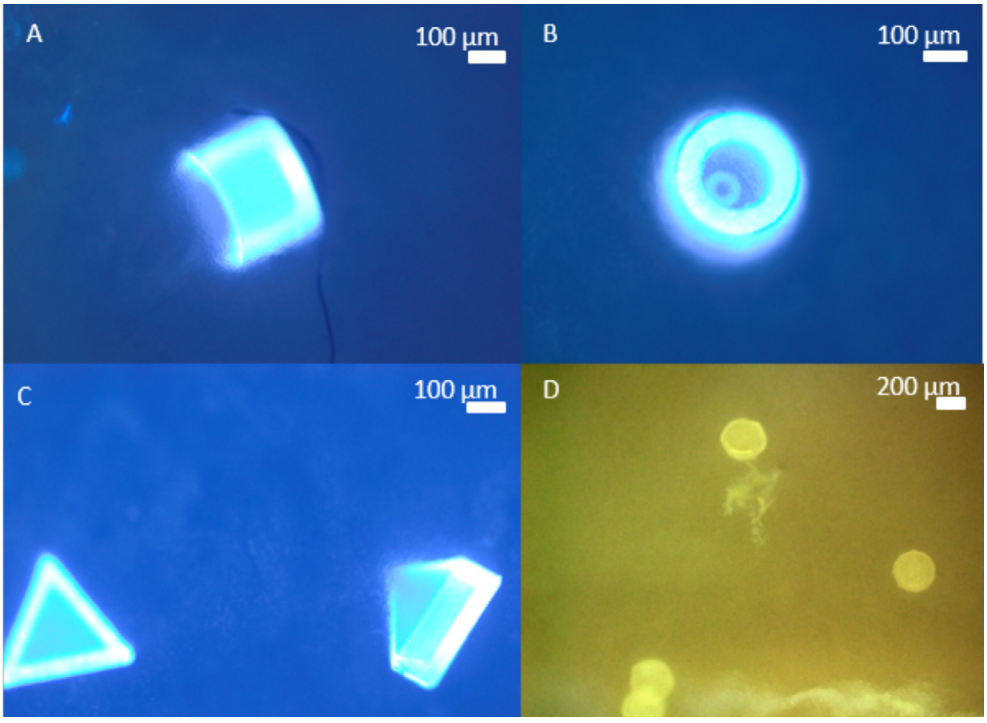

Fig. 5. Microscopy images of microcontainers located in the intestinal tissue. A) Image of 257 ± 4 µm high microcontainer with a cylindrical shape lying sideways (I). B) 257 ± 4 µm high microcontainer lying up or down (II)/(III). C) Image of microcontainers with a triangular shape with one lying sideways (I) and one lying with the cavity up or down (II)/(III). D) Four PCL microcontainers lying up or down (II)/(III). A), B), C) Show SU-8 microcontainers investigated with fluorescence microscopy with a DAPI filter and 5× in magnification. D) Show PCL microcontainers with a light microscope with a C-DIC filter.

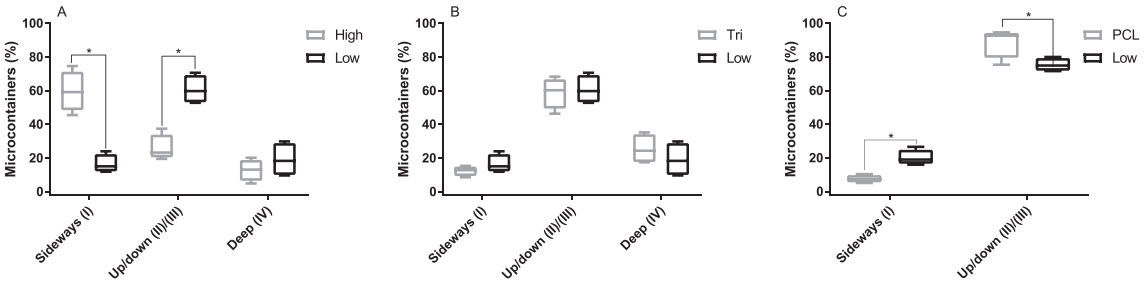

Fig. 6. Percentage of microcontainers that were oriented sideways (I), up/down (II)/(III) or deep (IV) in the surface of the porcine small intestine after the perfusion experiment. A) Comparison between 257 ± 4 μm (high) and 108 ± 11 μm (low) high microcontainers. B) Triangular (tri) and cylindrical microcontainers (low). C) PCL and SU-8 (low) microcontainers. Data is represented as mean ± SD with n = 4.* indicates significant difference.

concentrations over time, and after 21 min there was no drug present in the samples (Fig. 7D). This was expected since paracetamol is highly water soluble and is easily released from the microcontainers in an aqueous environment (Shaw et al., 2005; Szałek et al., 2011).

4. Conclusion

In this work, a porcine *ex vivo* small intestinal perfusion model for evaluation of mucoadhesion and orientation of microcontainers was developed. The model is a promising alternative to well-established mucoadhesion models and is suitable for investigating microdevices. The model showed promising results in evaluating mucoadhesion, orientation and the drug release profile of microcontainers. Comparisons of microcontainers with different height, shape and material properties were carried out both to evaluate the porcine *ex vivo* small intestinal perfusion model and to identify parameters affecting mucoadhesion and orientation of the microcontainers. In general, all the different types of microcontainers showed good adhesion properties, as they were mainly located in the start of the intestine. The orientation of the microcontainers was mainly controlled by the height of the microcontainers and was less affected by shape and material. Loading the microcontainers with paracetamol did not affect the orientation nor the mucoadhesion. These results indicate that the microcontainers fabricated from SU-8 are mucoadhesive, which is in line with the *in vivo* results obtained in previous studies. However, when changing the material of the microcontainers to a more biodegradable polymer, such as PCL, one might need to improve the mucoadhesion with surface modifications to control the orientation of the microcontainers.

Declaration of Competing Interest

The authors declare that they have no known competing financial interests or personal relationships that could have appeared to influence the work reported in this paper.

Acknowledgments

The authors would like to acknowledge the Danish National Research Foundation, Denmark (DNRF122) and Villum Fonden, Denmark (Grant No. 9301) for Intelligent Drug Delivery and Sensing Using Microcontainers and Nanomechanics (IDUN). The authors would also like to acknowledge Nanna Bild, Department of Health

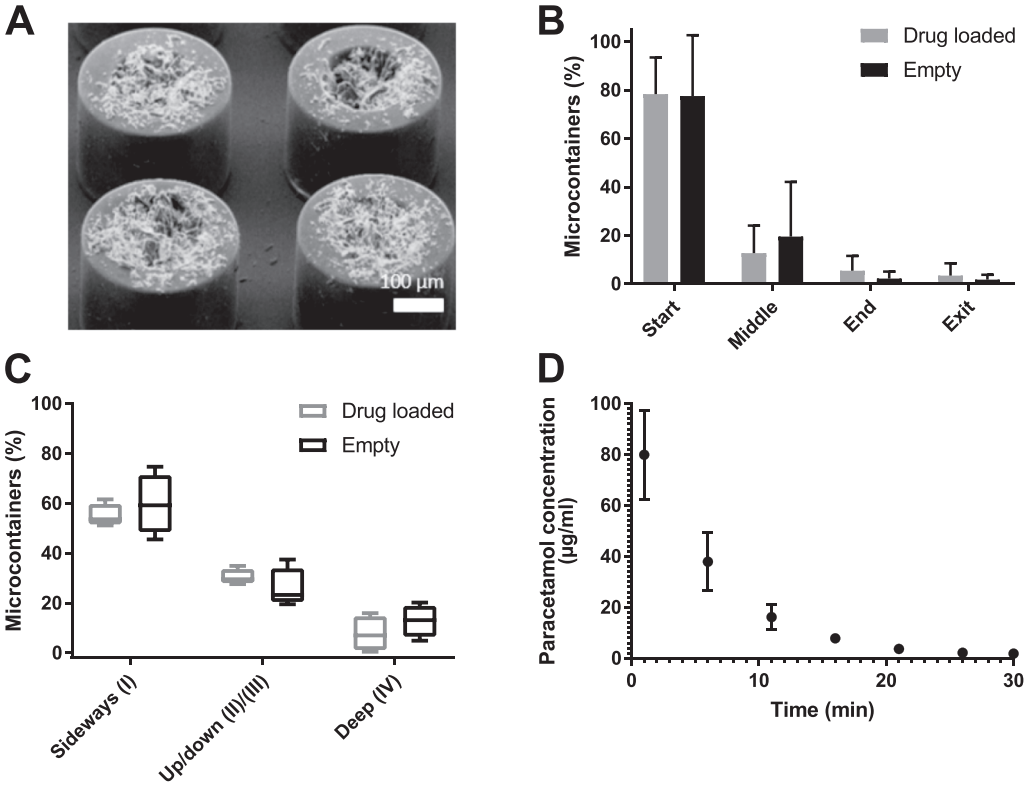

Fig. 7. A) SEM image of paracetamol-loaded 257 ± 4 μm high SU-8 microcontainers. B) The amount of microcontainers in percent located in the start, middle, end and exit of the porcine small intestine after being exposed to a perfusion experiment. Data is represented as mean ± SD, n = 4. C) The amount of microcontainers in percent that were oriented sideways (I), up/down (II)/(III) and deep (IV) in the surface of the porcine small intestine. Data is represented as mean ± SD, n = 4. D) Graph of the paracetamol concentration as a function of time. Data is represented as mean ± SD, n = 4.

Technology, Technical University of Denmark, for the illustrations. The authors would also like to acknowledge Lukas Vaut, Department of Health Technology, Technical University of Denmark for designing, developing and constructing the partly 3D printed *ex vivo* retention model setup featuring a tissue holder, a temperature and humidity-controlled chamber and a remotely controlled rotary sampler.

References

Abgrall, P., Conedera, V., Camon, H., Gue, A.-M., Nguyen, N.-T., 2007. SU-8 as a structural material for labs-on-chips and microelectromechanical systems. Electrophoresis 28, 4539–4551. https://doi.org/10.1002/elps.200700333.

Abid, Z., Gundlach, C., Durucan, O., von Halling Laier, C., Nielsen, L.H., Boisen, A., Keller, S.S., 2017. Powder embossing method for selective loading of polymeric microcontainers with drug formulation. Microelectron. Eng. 171, 20–24. https://doi.org/10.1016/J.MEE.2017.01.018.

Abid, Z., Strindberg, S., Javed, M.M., Mazzoni, C., Vaut, L., Nielsen, L.H., Gundlach, C., Petersen, R.S., Müllertz, A., Boisen, A., Keller, S.S., 2019. Biodegradable microcontainers – towards real life applications of microfabricated systems for oral drug delivery. Lab Chip 19, 2905–2914. https://doi.org/10.1039/C9LC00527G.

Ahmed, A., Bonner, C., Desai, T.A., 2002. Bioadhesive microdevices with multiple reservoirs: a new platform for oral drug delivery. J. Control. Release 81, 291–306. https://doi.org/10.1016/S0168-3659(02)00074-3.

Ainslie, K.M., Lowe, R.D., Beaudette, T.T., Petty, L., Bachelder, E.M., Desai, T.A., 2009. Microfabricated devices for enhanced bioadhesive drug delivery: attachment to and small-molecule release through a cell monolayer under flow. Small 5, 2857–2863. https://doi.org/10.1002/smll.200901254.

Champion, J.A., Katare, Y.K., Mitragotri, S., 2007. Particle shape: a new design parameter for micro- and nanoscale drug delivery carriers. J. Control. Release 121, 3–9. https://doi.org/10.1016/J.JCONREL.2007.03.022.

Champion, J.A., Mitragotri, S., 2009. Shape induced inhibition of phagocytosis of polymer particles. Pharm. Res. 26, 244–249. https://doi.org/10.1007/s11095-008-9626-z.

Chirra, H.D., Desai, T.A., 2012. Multi-reservoir bioadhesive microdevices for independent rate-controlled delivery of multiple drugs. Small 8, 3839–3846. https://doi.org/10.1002/smll.201201367.

Chirra, H.D., Shao, L., Ciaccio, N., Fox, C.B., Wade, J.M., Ma, A., Desai, T.A., 2014. Planar microdevices for enhanced in vivo retention and oral bioavailability of poorly permeable drugs. Adv. Healthc. Mater. 3, 1648–1654. https://doi.org/10.1002/adhm.201300676.

Dunne, M., Corrigan, O.I., Ramtoola, Z., 2000. Influence of particle size and dissolution conditions on the degradation properties of polylactide-co-glycolide particles. Biomaterials 21, 1659–1668. https://doi.org/10.1016/S0142-9612(00)00040-5.

Fabiano, A., Zambito, Y., Bernkop-Schnürch, A., 2017. About the impact of water movement on the permeation behaviour of nanoparticles in mucus. Int. J. Pharm. 517, 279–285. https://doi.org/10.1016/j.ijpharm.2016.12.024.

Kararli, T.T., 1995. Comparison of the gastrointestinal anatomy, physiology, and biochemistry of humans and commonly used laboratory animals. Biopharm. Drug Dispos. 16, 351–380. https://doi.org/10.1002/bdd.2510160502.

Keller, Stephan, Haefliger, Daniel, Boisen, Anja, 2007. Optimized plasma-deposited fluorocarbon coating for dry release and passivation of thin SU-8 cantilevers. J. Vac. Sci. Technol. B 25 (6), 1903. https://doi.org/10.1116/1.2806960.

Lai, S.K., Wang, Y.-Y., Wirtz, D., Hanes, J., 2009. Micro- and macrorheology of mucus. Adv. Drug Deliv. Rev. 61, 86–100. https://doi.org/10.1016/J.ADDR.2008.09.012.

Lee, Y.-A.L., Zhang, S., Lin, J., Langer, R., Traverso, G., 2016. A janus mucoadhesive and omniphobic device for gastrointestinal retention. Adv. Healthc. Mater. 5, 1141–1146. https://doi.org/10.1002/adhm.201501036.

Lieleg, O., Ribbeck, K., 2011. Biological hydrogels as selective diffusion barriers. Trends Cell Biol. 21, 543–551. https://doi.org/10.1016/j.tcb.2011.06.002.

Liu, G., 1997. Patient preferences for oral versus intravenous palliative chemotherapy. J. Clin. Oncol. 15.

Madsen, K.D., Sander, C., Baldursdottir, S., Pedersen, A.M.L., Jacobsen, J., 2013. Development of an ex vivo retention model simulating bioadhesion in the oral cavity using human saliva and physiologically relevant irrigation media. Int. J. Pharm. 448, 373–381. https://doi.org/10.1016/J.IJPHARM.2013.03.031.

Mazzoni, C., Tentor, F., Strindberg, S.A., Nielsen, L.H., Keller, S.S., Alstrøm, T.S., Gundlach, C., Müllertz, A., Marizza, P., Boisen, A., 2017. From concept to in vivo testing: microcontainers for oral drug delivery. J. Control. Release 268, 343–351. https://doi.org/10.1016/J.JCONREL.2017.10.013.

Nielsen, L.H., Keller, S.S., Boisen, A., 2018. Microfabricated devices for oral drug delivery. Lab Chip 18, 2348–2358. https://doi.org/10.1039/c8lc00408k.

Nielsen, L.H., Keller, S.S., Boisen, A., Müllertz, A., Rades, T., 2014. A slow cooling rate of indomethacin melt spatially confined in microcontainers increases the physical stability of the amorphous drug without influencing its biorelevant dissolution behaviour. Drug Deliv. Transl. Res. 4, 268–274. https://doi.org/10.1007/s13346-013-0166-7.

Nielsen, L.H., Keller, S.S., Gordon, K.C., Boisen, A., Rades, T., Müllertz, A., 2012. Spatial confinement can lead to increased stability of amorphous indomethacin. Eur. J. Pharm. Biopharm. 81, 418–425. https://doi.org/10.1016/j.ejpb.2012.03.017.

Nielsen, L.H., Melero, A., Keller, S.S., Jacobsen, J., Garrigues, T., Rades, T., Müllertz, A., Boisen, A., 2016. Polymeric microcontainers improve oral bioavailability of furosemide. Int. J. Pharm. 504, 98–109. https://doi.org/10.1016/j.ijpharm.2016.03.050.

Nielsen, L.S., Schubert, L., Hansen, J., 1998. Bioadhesive drug delivery systems: I. Characterisation of mucoadhesive properties of systems based on glyceryl monooleate and glyceryl monolinoleate. Eur. J. Pharm. Sci. 6, 231–239. https://doi.org/10.1016/S0928-0987(97)10004-5.

Norris, D.A., Sinko, P.J., 1997. Effect of size, surface charge, and hydrophobicity on the translocation of polystyrene microspheres through gastrointestinal mucin. J. Appl. Polym. Sci. 63, 1481–1492. https://doi.org/10.1002/(SICI)1097-4628(19970314)63:11<1481::AID-APP10>3.0.CO;2-5.

Patil, V.R.S., Campbell, C.J., Yun, Y.H., Slack, S.M., Goetz, D.J., 2001. Particle diameter influences adhesion under flow. Biophys. J. 80, 1733–1743. https://doi.org/10.1016/S0006-3495(01)76144-9.

Pereira de Sousa, I., Steiner, C., Schmutzler, M., Wilcox, M.D., Veldhuis, G.J., Pearson, J.P., Huck, C.W., Salvenmoser, W., Bernkop-Schnürch, A., 2015. Mucus permeating carriers: formulation and characterization of highly densely charged nanoparticles. Eur. J. Pharm. Biopharm. 97, 273–279. https://doi.org/10.1016/J.EJPB.2014.12.024.

Petersen, R.S., Keller, S.S., Boisen, A., 2015. Hot punching of high-aspect-ratio 3D polymeric microstructures for drug delivery. Lab Chip 15, 2576–2579. https://doi.org/10.1039/C5LC00372E.

Rao, K.V.R., Buri, P., 1989. A novel in situ method to test polymers and coated microparticles for bioadhesion. Int. J. Pharm. 52, 265–270. https://doi.org/10.1016/0378-5173(89)90229-9.

Shaw, L.R., Irwin, W.J., Grattan, T.J., Conway, B.R., 2005. The effect of selected water-soluble excipients on the dissolution of paracetamol and ibuprofen. Drug Dev. Ind. Pharm. 31, 515–525. https://doi.org/10.1080/03639040500215784.

Sigurdsson, H.H., Kirch, J., Lehr, C.-M., 2013. Mucus as a barrier to lipophilic drugs. Int. J. Pharm. 453, 56–64. https://doi.org/10.1016/j.ijpharm.2013.05.040.

Sinko, P.J., Hu, P., Waclawski, A.P., Patel, N.R., 1995. Oral absorption of anti-aids nucleoside analogues. 1. Intestinal transport of didanosine in rat and rabbit preparations. J. Pharm. Sci. 84, 959–965. https://doi.org/10.1002/jps.2600840811.

Sjögren, E., Abrahamsson, B., Augustijns, P., Becker, D., Bolger, M.B., Brewster, M., Brouwers, J., Flanagan, T., Harwood, M., Heinen, C., Holm, R., Juretschke, H.-P., Kubbinga, M., Lindahl, A., Lukacova, V., Münster, U., Neuhoff, S., Nguyen, M.A., van Peer, A., Reppas, C., Hodjegan, A.R., Tannergren, C., Weitschies, W., Wilson, C., Zane, P., Lennernäs, H., Langguth, P., 2014. In vivo methods for drug absorption – Comparative physiologies, model selection, correlations with in vitro methods (IVIVC), and applications for formulation/API/excipient characterization including food effects. Eur. J. Pharm. Sci. 57, 99–151. https://doi.org/10.1016/J.EJPS.2014.02.010.

Swindle, M.M., Makin, A., Herron, A.J., Clubb, F.J., Frazier, K.S., 2012. Swine as models in biomedical research and toxicology testing. Vet. Pathol. 49, 344–356. https://doi.org/10.1177/0300985811402846.

Szałek, E., Kamińska, A., Murawa, D., Połom, K., Urbaniak, B., Sobiech, M., Grześkowiak, E., Grabowski, T., Wolc, A., Kokot, Z.J., Murawa, P., 2011. Comparison of the pharmacokinetics of paracetamol from two generic products in patients after total gastric resection. Pharmacol. Reports 63, 1518–1525. https://doi.org/10.1016/S1734-1140(11)70715-0.

Tao, S.L., Popat, K., Desai, T.A., 2007. Off-wafer fabrication and surface modification of asymmetric 3D SU-8 microparticles. Nat. Protoc. 1, 3153–3158. https://doi.org/10.1038/nprot.2006.451.

Thanki, K., Gangwal, R.P., Sangamwar, A.T., Jain, S., 2013. Oral delivery of anticancer drugs: challenges and opportunities. J. Control. Release 170, 15–40. https://doi.org/10.1016/J.JCONREL.2013.04.020.

Vaut, L., Scarano, E., Tosello, G., Boisen, A., 2019. Fully replicable and automated retention measurement setup for characterization of bio-adhesion. HardwareX 6, e00071. https://doi.org/10.1016/J.OHX.2019.E00071.

Zhou, X.H., 1994. Overcoming enzymatic and absorption barriers to non-parenterally administered protein and peptide drugs. J. Control. Release 29, 239–252. https://doi.org/10.1016/0168-3659(94)90071-X.

Appendix II

Paper II

General experimental design for testing adhesion to mucosal tissue

M. D. Mosgaard, A. J. Andersen, E. Ingallinera, M. Viehrig, L. H. Nielsen, T. S. Alstrøm and A. Boisen

In preparation

General experimental design for testing adhesion to mucosal tissue

Mette Dalskov Mosgaard[a*], *Alina Joukainen Andersen*[a], *Eugenia Ingallinera*[a], *Marlitt Viehrig*[a], *Line Hagner Nielsen*[a], *Tommy Sonne Alstrøm*[b] *and Anja Boisen*[a]

[a]The Danish National Research Foundation and Villum Foundation's Center for Intelligent Drug Delivery and Sensing Using Microcontainers and Nanomechanics (IDUN), Department of Health Technology, Technical University of Denmark, Ørsteds Plads 345C, 2800 Kgs. Lyngby, Denmark

[b]Department of Applied Mathematics and Computer Science, Technical University of Denmark, Richard Petersens Plads 321, 2800 Kgs. Lyngby, Denmark

[*]**Corresponding author:** Mette Dalskov Mosgaard, e-mail: medmo@dtu.dk

Abstract

The awareness of poor reproducibility in some experimental setups has gained much attention during the past years and novel guidelines are needed to improve experimental reproducibility. Especially, when working with animals or animal tissue a poor reproducibility is often observed. The aim of this study is to develop statistical guidelines for designing, investigating and assessing *ex vivo* tensile adhesion force studies to gain reproducible outcomes. The presented statistical design is validated by tensile force measurements of various surface topographies conducted with a texture analyzer, as a case study. The interfering factors on tensile forces measurements are observed after repeating measurements of polydimethylsiloxane (PDMS) microstructures on four different pieces of porcine intestinal tissue. Measurement results highlight that tissue variations as well as the time point of the measurements are affecting the adhesion. In order to eliminate these two factors from the measurements a statistical model is developed and made available as an R-script. Flat PDMS surface structures are measured before and after measuring the PDMS microstructures to establish a baseline. Correcting the peak force measurements of the PDMS microstructures with the statistical model makes the measurements more sensitive and enhances the results reliability and eliminate tissue and time variations. The developed statistical guidelines facilitates a precise and more reproducible evaluation of surface topographies as varying factors are eliminated during analysis. In conclusion, the topographies has a real effect on tissue adhesion, which is not evident without the statistical model and pillar-like topographies presents stronger adhesion forces to mucosa compared to both flat and cavity-liked structures.

Keywords
mucoadhesion, Design of experiment, guidelines, texture analyzer, polydimethylsiloxane (PDMS), nanostructures, Latin square design.

1. Introduction

Measurements of tensile adhesion forces between pharmaceutical dosage forms/drug delivery devices and animal mucosa, have been widely conducted since the 1990's for determining *ex vivo* mucoadhesion[1]. The assessment of mucoadhesive properties is an important aspect when developing advanced drug delivery systems for mucosal delivery[2]. The advantages of implementing mucoadhesion in drug delivery systems is the increased residence time at the mucosal surface at the desired target site, improved bioavailability and the possibility of targeting particular body sites and tissues. All this can result in better treatments for the patients with less side effects and reduced drug administration frequency[3].

Several methods have been developed to evaluate the adhesion properties between a drug delivery systems and a mucosal surface. Mucoadhesion of both semi-solid and solid formulations has been investigated extensively in pharmaceutical field with a commercialized method called the texture analyzer. Other methods for measuring adhesion have been used over the years, and includes the rotating dice method, flow through method and rheology[4–7]. Both the rotating dice and the flow through techniques vary from lab to lab as they are not commercially available. This imposes a challenge on data reproducibility and comparing results with other research groups is unreliable. The rotating dice method estimates the ability of drug delivery devices to adhere to a surface e.g. tissue, however, the method is far from *in vivo* conditions. The rotating dice consists of a rotating sample holder that is rotated at 125 rpm in simulated fluid[8]. The rotation disc method can, evaluate mucoadhesive properties of different drug delivery systems. Previous studies have seen correlating ranking orders of mucoadhesive polymers from both the rotating dice method and tensile force studies, which demonstrates the methods potential[4]. The flow through method simulates *in vivo* settings to estimate the behavior of drug delivery devices at the mucosal surface. The drawback with this method is the lack of peristaltic movement, which is needed to apply the needed force to simulate *in vivo* conditions. The rheology approach evaluates the strength of interactions between mucus and polymers[5]. A mucoadhesive polymer is believed to be more viscous when mixed with mucus compared to the viscosity of the individual polymer and mucus. This synergism is used to evaluate the properties of the mucoadhesive polymers. This evaluation strategy is far from *in vivo* conditions as drug delivery systems not always will be mixed with

mucus but only show slight attachment at the surface, however, this depends on the drug delivery system. Overall, the texture analyzer is often the method used to evaluate tensile adhesion forces, as higher reproducibility should be expected as it is a commercialized method and the texture analyzer can measure precise tensile forces[9].

Despite the simplicity of the texture analyzer for the tensile force measurements, many factors needs to be considered before conducting the experiments. Each test sample requires individually optimized test settings making the comparison between samples less reliable. The settings include contact time and contact force, which play an important role in the adhesion force abilities[10–12]. The test environment, including pH and ionic strength are also important factors and has to be optimized for each experiment as well[10]. In addition, the biological variation of the animal tissue needs to be considered as well. Although, tissue heterogeneity is often mentioned in published adhesion studies using tensile strength measurements, measures are generally not accounting for this effect, nor is the extent of this effect demonstrated[12]. There are examples of studies, where potential differences between mucosa of individual animals have been taken into account[13] and site-to-site differences on mucosa of the same animal are known[14]. In addition, hydration or dehydration of tissue can damage the structure and thereby, affect the adhesion measurements. Furthermore, the aspect of time when working with tissue is of great importance as studies have shown variation in the structure of the tissue over time[15]. In general, tissue is highly sensitive to outer forces, which can compromise its properties.

The above-mentioned factors are just some that can potentially affect the tensile adhesion forces and give unreliable results. Awareness must be drawn to the experimental designs when working with the texture analyzer to improve the reproducibility. Poor experimental design is a common problem across all scientific fields and not just seen in regard to the texture analyzer[16]. The awareness of poor reproducibility in research has gained much attention during the past five years. A multitude of factors are believed to contribute to irreproducible research results but most researchers believe that “more robust experimental design” and “better statistics” will improve reproducibility[17]. In general, it is a problem that laboratory scientists have insufficient training in statistical methods and study design[18]. Therefore, it is suggested that a statistician and/or methodologist should be involved in all stages of a research project[18]. Not only are many experiments poorly designed and insufficiently evaluated in regard to statistics, but many experiments are also challenged due to ethical aspects. Many studies conducted on or with animals are limited in sample sizes and biological variations, which challenges the reproducibility of *ex vivo* experiments. Good experimental designs and better

statistical methods are, therefore, highly needed to improve the reproducibility and validity of *ex vivo* data.

The aim of this study is to improve reproducibility for standardized tensile forces measurements with a texture analyzer by applying new experimental and statistical guidelines. These guidelines are applicable for most experimental instruments/methods involving tensile forces to biological tissue. This study provides tools for designing, analyzing and evaluating *ex vivo* experiments by using statistical tools to get reproducible results with less standard variations. Mucoadhesion of different polydimethylsiloxane (PDMS) samples with microstructures is measured and compared, as a case study, to emphasize the effect of our guidelines.

2. Results

2.1 Characterization of PDMS microstructures

Rapid prototyping using PDMS-based soft lithography is a popular tool, as it allows for fast and cheap manufacturing of micropatterned surfaces using simple processes[19]. In this study, four microstructures; T1 microcavities, T2 micropillars, T3 microcavities and T4 micropillars are manufactured in PDMS (Figure 1A-D). Each structure of cavities and pillars consist of different dimensions as seen in Figure 1. The fabrication of the microcavities, possesses some limitations in regard to demolding of the polymer resulting in a poor structural yield. This is shown for structure T3. The T3 surface has microcavities of approximately 10 µm in cavity width, whereas T1 microcavities are approximately 5 µm in cavity width. Demolding seems to affect T3 more than T1, which might be explained by the difference in the width of the cavities. Both T2 and T4 have micropillars on the PDMS surface and are illustrated in Figure 1B and 1D, respectively. T2 micropillars are bending, which results in a smoother surface. T2 micropillars are 60 µm long, which is much more than T4 micropillars that are 15 µm long and, therefore, not bending.

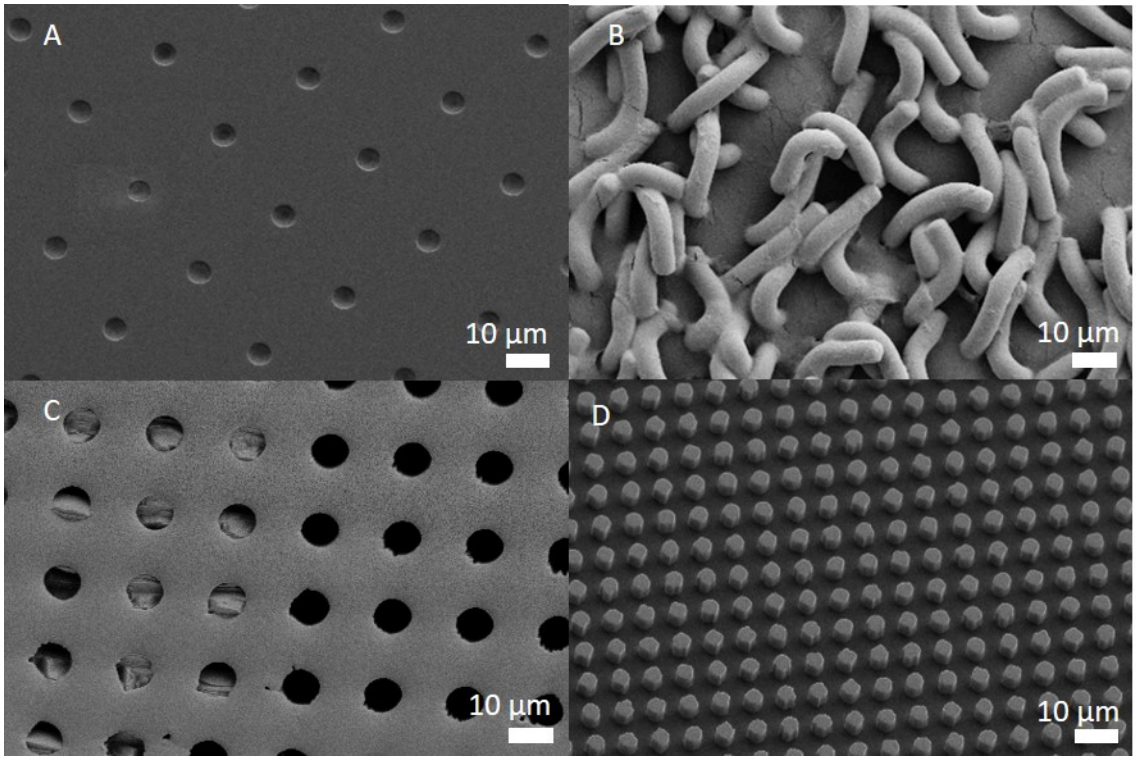

Figure 1: SEM images of the PDMS microstructures: A) T1 shows microcavities of 5 µm in width, B) T2 has long micropillars on the surface (60 µm), C) T3 presents microcavities of 10 µm in width and D) T4 has short micropillars (15 µm).

2.2 Tensile force measurements

The tensile adhesion forces of all four microstructures to porcine small intestinal mucosa are investigated in this study. For obtaining the right experimental settings, optimization tests are performed for determining the contact force and contact time.

2.2.1 Optimization test

Three different contact forces are tested to find the most optimal one for the PDMS samples. The average peak forces measured at the three different contact forces are shown in supplementary material, Figure S1. The highest peak force is measured at a contact force of 0.10 N where lower standard deviations are observed. After selecting, the most optimal contact force at 0.10 N, three following contact times are tested; 60 sec, 180 sec and 300 sec. Contact time is defined as the time the PDMS sample and the tissue are in contact with each other before the sample is withdrawn from the tissue. The average peak force measured at the three contact times is shown in supplementary material in Figure S2. The highest peak force is measured with a contact time of 180 sec. The measured peak forces after 60 and 300 sec of contact time show lower forces. It appears from the results that 60 sec of contact time is too little time for the PDMS samples and the mucus layer to interact sufficiently. A contact time of 300 sec does not improve the peak force between the PDMS sample and the mucosal surface.

Therefore, a contact time of 180 sec is selected for future studies. All the optimization measurements show large standard deviations, which is expected when combining measurements from four different pieces of tissue.

Stability tests are performed to establish the effects of repeated measurements on a single piece of tissue. Four pieces of tissue are exposed to ten adhesion measurements of the PDMS sample T1. The data indicates that ten measurements on one piece of tissue is acceptable as the measured forces follow a linear trend over time. Additionally, a high variance of the adhesion on the four pieces of tissue are observed with the strongest being ~0.025N and the weakest being ~0.006N. Curiously, we also observe both an increase as well as decrease in peak force as the number of measurements increases. This indicates that both tissue and time variations affect the measurements of a structured sample (Figure 2). The following two terms refers to the same; repeating measurement effect and time effect.

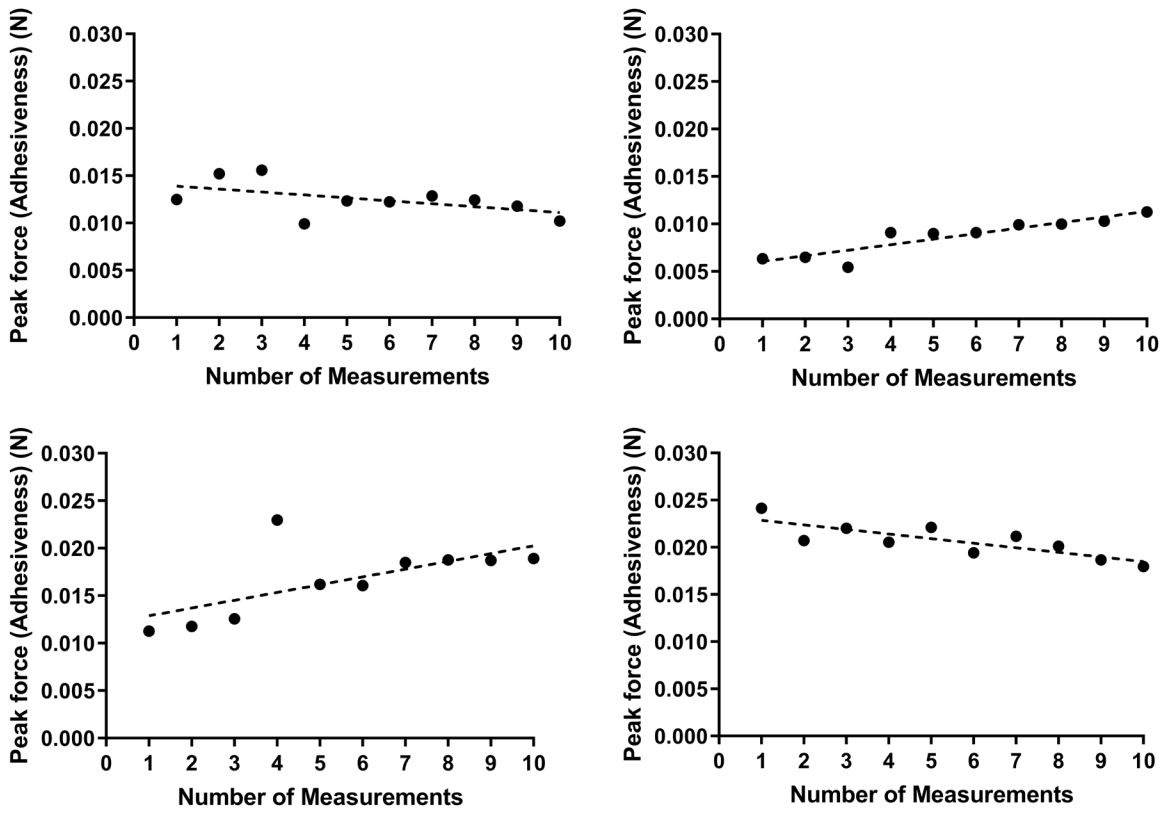

Figure 2: Graphs illustrating repeating measurements of PDMS microstructures (T1) on four different pieces of porcine intestinal mucosa. The peak force is measured for each repetition and each graph show measurements on a new intestinal tissue piece.

Table 1 reports the intercept and slope of the linear fits, where the intercept indicates the basic adhesiveness of the piece of tissue, and the slope indicates the effect repeated measurements

have on the peak force. The intercepts of the repeating measurements show that the basic adhesion varies to a large degree between the different pieces of tissues. The lowest observed intercept is $0.55 \cdot 10^{-2}$ (tissue piece 2) and the largest $2.34 \cdot 10^{-2}$ (tissue piece 4), hence, almost five times higher. There is no clear tendency in the time evolution. For three pieces of tissues (2 - 4), the 95% confidence interval excludes zero meaning that a significant change in adhesion is observed with repeated measurements. This is not observed for tissue piece 1. A negative slope is obtained on one tissue piece (4) and two positive slopes on two other pieces of tissue (2 and 3), meaning that repeated measurements both increase and decrease the adhesion depending on the tissue. The evidence here simply suggests that there is a large variability of tissue and when using tissue for statistical analysis, there is a need to minimize the impact this natural variability will have on the statistical analysis.

Table 1: Statistical values for tissue pieces. The intervals on intercept and slope are the 95% confidence intervals. All numbers reported have been calculated using an R-script, version 4.0.2 and fitted with a linear model using ordinary least squares.

	Tissue piece 1	**Tissue piece 2**	**Tissue piece 3**	**Tissue piece 4**
R^2	0.27	0.83	0.43	0.66
F-stat	2.94	39.65	6.14	15.62
Intercept (10^{-2})	1.42 ± 0.26	0.55 ± 0.13	1.21 ± 0.47	2.34 ± 0.18
Slope (10^{-4})	-3.10 ± 4.17	5.84 ± 2.14	8.19 ± 7.82	-4.86 ± 2.84

2.2.2 Adhesion measurements of PDMS microstructures

The stability test (Figure 2) indicates the troublesome variations of both tissue and time. To enable further establishment of the adhesion forces of the microstructure surfaces, a statistical design that reduces the variability of the factors is needed. Large standard deviations are common when conducting tensile adhesion forces *ex vivo* and significant evidence is rarely observed[12,20]. This could most likely be coursed by disturbing factors that affect the adhesion force of the samples. In this study, two factors, the tissue (or location on the tissue) and the number of times each tissue is exposed to a sample are shown to affect the force measurements of the microstructures.

2.2.3 Statistical evaluation of adhesion measurements

A type of baseline of the tissue could help determine the tissues adhesiveness. In order to "calibrate" the tissue, flat PDMS surfaces are measured before and after each actual sample measurement. These flat PDMS surfaces create a baseline that can estimate the state of the

tissues at the time where the actual sample is conducted. Time variation can be eliminated by measuring all the repetitions in a random order (available in an R-script), which allows all the samples to be measured at different time points. All the adhesion force measurements of the PDMS microstructures have been following this design. The flat PDMS measurements (calibration samples) and the peak force measurements of the PDMS samples are shown in Figure 3. The adhesion force values of the flat PDMS samples are displayed in a linear regression model. The baseline of tissue 1, 2 and 4 are very similar and has a peak force of approximately 0.02 and 0.03 N. The baseline of tissue 3 is lower and observed around 0.01 and 0.02 N. However, all the measurements of the microstructures are also low on tissue piece 3 compared to the other pieces of tissue. This could indicate that tissue 3 is less adhesive than the other three pieces of tissues.

Microstructure T4 shows the longest distance from the baseline when compared to the other microstructures suggesting that T4 has the strongest adhesion forces to the mucosa compared to the other microstructures. T3 shows weakest adhesion forces to the mucosa on all four pieces of tissue. Microstructure T1 demonstrates strong adhesion on tissue 1 and 3, which is less evident on tissue 2 and 4. T2 displays strong adhesion on tissue piece 4, but has low adhesion to tissue pieces 1, 2 and 3.

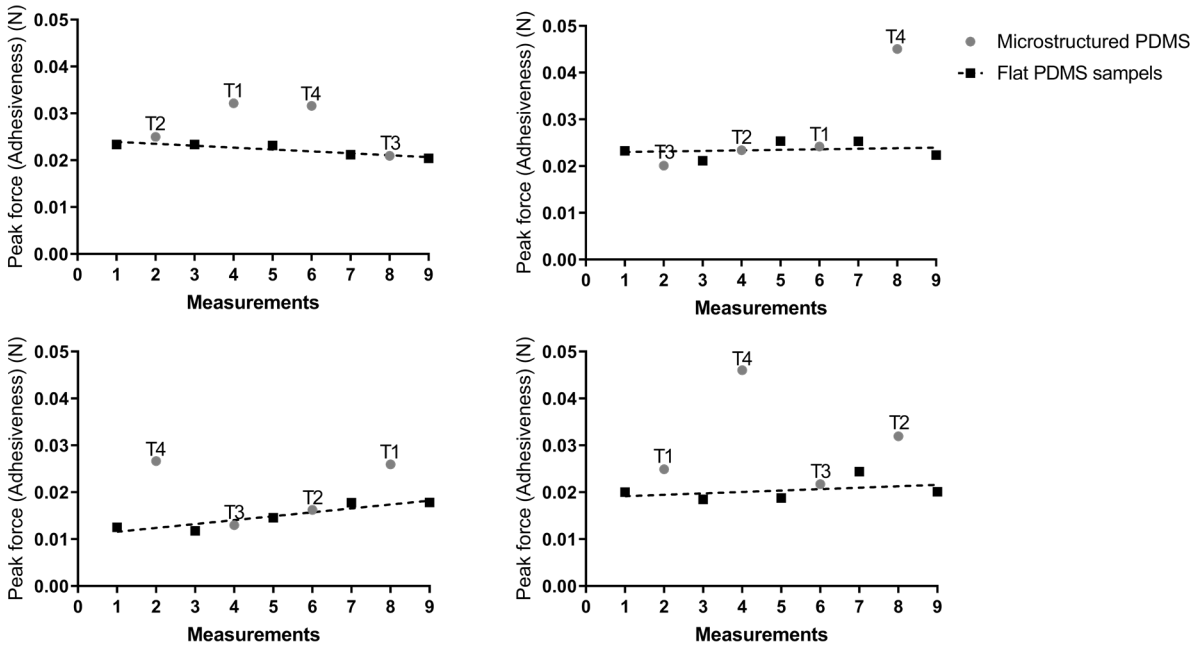

Figure 3: Peak force (N) measurements of the four different PDMS microstructures (T1, T2, T3 and T4) in a random order and they are displayed as grey dots. Each graph shows results from one piece of porcine intestinal tissue. The black squares connected by a dotted line represent the baseline points. The baseline points are made using flat PDMS samples to "calibrate" the tissues and points are connected by a dotted line made with linear regression. n = 9.

The experiment is analyzed using analysis of variance fitted with ordinary least squares[21,22]. Three different analysis models that have access to experimental data in varying degree are examined:

- One-way Analysis of variance (ANOVA), where the peak force is estimated using the topography of the microstructures alone.
- Latin square ANOVA, where the peak force is additionally explained using the tissue and repeated measurement, where both are modeled as categorical factors.
- Latin square ANOVA, where the peak force is additionally adjusted using a linear model fitted to the flat microstructures. For example (Figure 3), for tissue piece 1, the peak force for T2 and T3 would be adjusted to roughly zero, whereas both T1 and T4 would be adjusted to roughly 0.01.

The statistical estimates are reported in Table 2. The R-scripts used to compute the different models can be found in the supplementary material. From simple to complex models, it is observed that the mean squares of the residuals are being reduced for each piece of information the model has access to.

The linear correction additionally reduces the amount of variance explained by the time and tissue, from $5.21 \cdot 10^{-5}$ to $4.37 \cdot 10^{-5}$ for time, and from $8.20 \cdot 10^{-5}$ to $3.05 \cdot 10^{-5}$ for tissue, where the largest reduction is seen for tissue. This is expected behavior as, observed on the stability test (Figure 2), the tissue variation is stronger than the time effect. It is also noticed that the Prob>F values are, as expected, (marginally) higher when the linear correction is conduced compared to the uncorrected design.

Table 2: Test of effect using ANOVA on the three models. The label 'Prob>F' indicates the p-value for the established test: small values are considered evidence that there is significant effect(s) in the model, in this case, topography ($p < 0.05$).

Effect	**One-way ANOVA**		**Latin square, no correction**		**Latin square, linear correction**	
	MS	Prob>F	MS	Prob>F	MS	Prob>F
Topography	$2.38 \cdot 10^{-4}$	0.011	$2.39 \cdot 10^{-4}$	0.003	$2.56 \cdot 10^{-5}$	<0.001
Time			$5.21 \cdot 10^{-5}$	0.097	$4.37 \cdot 10^{-5}$	0.065

Tissue		$8.20 \cdot 10^{-5}$	0.041	$3.05 \cdot 10^{-5}$	0.124
Residuals	$4.13 \cdot 10^{-5}$	$1.56 \cdot 10^{-5}$		$1.05 \cdot 10^{-5}$	

Multiple comparison tests are performed to obtain confidence levels that compare means of the model effects. The goal of these tests is to determine whether group means differ and to identify the topography with the highest mean peak force. A Tukeys multiple comparisons test is used on the topographies, where we report the comparisons with p-values lower than 0.05(Table 3)[23]. The one-way ANOVA model is only able to detect one difference (T4 is different than T3), whereas both Latin Square models are able to identify significant difference between T4 and the other microstructures. Additionally, the linear corrected model observes lower values for all comparisons, implying that the linear correction has reduced the variance of the model and increased the detection capability. Thereby, this can identify smaller differences in topography compared to the model where no corrections are made.

Table 3: P-values using Tukeys multiple comparison test for the differences in topography.

	One way ANOVA	**Latin square, no correction**	**Latin square, linear correction**
T4 vs T1	0.147	0.035	0.009
T4 vs T2	0.056	0.013	0.003
T4 vs T3	0.008	0.002	<0.001

Figure 4 shows topography estimates using the linear corrected ANOVA model with no intercept that estimates topographies effects relative to the flat PDMS samples. The estimate represents the estimate of the peak force of the microstructures with the 95% confidence interval stated. Here, it is observed that only T4 has a significant elevated peak force compared to the other microstructures.

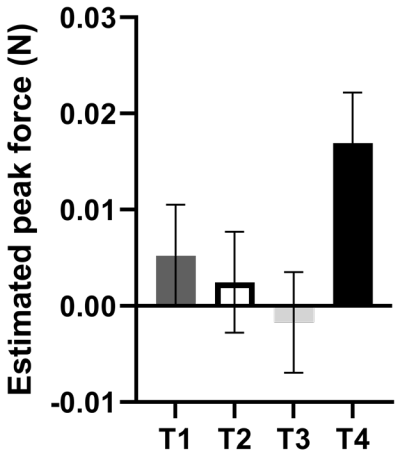

Topography	Estimate	Lower	Upper
T1	0.00522	-0.0000232	0.0105
T2	0.00246	-0.00771	0.00771
T3	-0.00171	-0.00696	0.00353
T4	0.0169	0.0117	0.0222

Figure 4: The graph illustrates the peak forces measured of the four different PDMS microstructures (T1, T2, T3 and T4) conducted on four different pieces of porcine small intestinal tissue. The table shows the mean of the estimates of last squares, which also has been illustrated in the graph. Lower and upper values are also shown in the table.

Noise caused by tissue and time effects are eliminated from the data shown in Figure 4. Microstructure T4 shows the significantly strongest adhesion forces to the intestinal tissue, compared to T1, T2 and T3. Surface microstructure T1, T2 and T3 show no significant difference to the adhesion forces measured with the flat PDMS samples. Before applying the statistical correction of the data, only T3 and T4 are significantly different. Elimination of the noise made it easier to evaluate the mucoadhesion of the microstructures.

3. Discussion

Tensile force measurements between pharmaceutical dosage forms and mucosa have been extensively studied and many face the same limitations as reported here, when conducting the experiments with a texture analyzer. The importance of optimizing instrumental parameters such as contact force and contact time is clearly stated[12,24,25]. A major challenge is that different research groups use different instrumental parameters and experimental designs, which makes comparisons unreliable[25,26]. Lastly, large variations are seen when applying biological tissue[14]. There is awareness of these major challenges, however studies mainly focus on the instrumental parameters and how that influences the tensile forces[12,25]. The experimental design presented in this study enables easy removal of different disturbing factors. Eliminating tissue and time variations would improve the reproducibility of the peak force measurements and give a better evaluation of the different dosage forms.

The statistical design presented in this study is developed with the purpose of being applicable for others in the research field. The design is user-friendly, also for non-experts in statistical

evaluation. For this reason, the statistical design is coded into R-scripts to make the process more user friendly. The statistical correction of the data enables detection of weaker forces as the actual force between two surfaces are not hidden in noise. One could imagine a statistical model where the linear correction and test for topography is carried out jointly. However, this would assume that the noise for each tissue is roughly the same, which is highly unlikely. It should be mentioned that the presented model requires more measurements compared to standard Latin square. Both flat and microstructured surfaces need to be measured, and the design require n(2n+1) (n begin the number of tested topographies) measurements. As an example, if a new topography is added to the experimental setup, then the number of measurements increases from 36 (n=4) to 55 (n=5), whereas a standard Latin square model would require 16 (n=4) and 25 (n=5), respectively.

There are many approaches to increase and improve the adhesion of a material such as changing the surface chemistry as well as changing the surface topography[27,28]. Topography-based adhesion is widely studied especially in regards to implants and drug delivery microdevices[28]. Improving the roughness or creating micro/nano topographies on microdevices seems to enhance the adhesion to the mucus layer and other biological surfaces. Nanowire-based bioadhesives show great potential in oral drug delivery, because they provide strong adhesion of the system to the mucosal surface[29]. Many of these topographic structures are inspired by nature, e.g. the ability of a gecko to adhere to surfaces[28]. Polydimethylsiloxane (PDMS) is widely used for fabricating implants and microdevices, as it is a biocompatible and non-toxic polymer. It is used as an elastomer and is known for being non-adhesive with makes it a perfect material for determining mucoadhesion of different topographies[30].

To address the outcome of the case studies, an enhancement in mucoadhesion is expected for both cavity-like structures and pillar-like structures since the surface area of both surfaces are increased[31,32]. Pillar-like structures are, however, believed to have the strongest adhesion as they enable penetration into the mucus layer, which is not the case for the cavities[32].

4. Conclusion

This study demonstrates guidelines of how to evaluate adhesion measurements to mucosal tissue. The guidelines show the importance of knowing the weaknesses of the method/instruments being used and, thereby, making it possible to circumvent them in the measurements. Furthermore, the study present how to statistically evaluate the data to receive results that are less affected by noise and interfering parameters such as time and tissue

variations. The use of design of experiment (DoE) shows that topography has a real effect on tissue adhesion and that issues such as biological tissue variations and time variations are possible to eliminate. The case study of the PDMS microstructures demonstrates how pillar-like topography enhances adhesion of PDMS compared to both flat and cavity-like structures. The purpose of these guidelines is to improve the validity of adhesion to mucosal tissue measurements and to make them more reproducible.

5. Materials and Methods

5.1 Mold fabrication used for fabrication of PDMS microstructures

For the PDMS microstructures, silicon (Si) and nickel (Ni) based molds are fabricated to obtain four distinct microstructures (T1 – T4, see section 2.1) as illustrated in Figure 5.

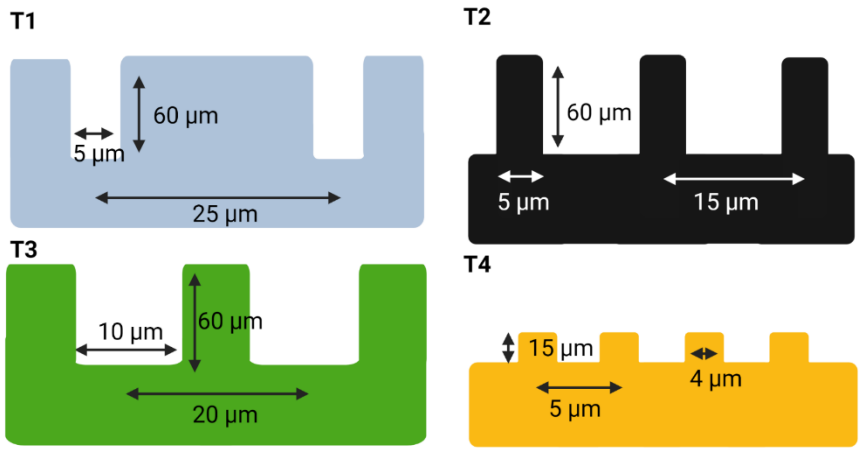

Figure 5: Schematic of the four different PDMS microstructures and their pattern. T1, T2 and T4 have been fabricated with a negative photoresist, whereasT3 has been fabricated with a positive photoresist.

The Si mold is fabricated using a photolithographic mask followed by defining pattern geometry followed by a reactive ion dry etching process (DRIE Pegasus, SPTS Technologies Ltd.) and subsequent, photoresist strip (Plasma Asher, Diener electronic GmbH & Co KG).

A lithographic pattern (t = 2 µm) is defined on a Si substrate utilizing a positive (AZ MiR 701, MicroChemicals GmbH, Germany) or a negative (AZ nLOF 2020, MicroChemicals GmbH, Germany) photoresist, allowing for a wide variety of micropatterns being obtained from the same chromium mask. Three different Si molds are prepared in order to manufacture PDMS topographies T1–T3. The first topography (T1) has cavity-like structures (negative photoresist), the second topography (T2) consists of pillar-like structures (negative photoresist) and the third topography (T3) has cavity-like structures (positive photoresist). The patterned Si

substrate is etched using a dry etching process, resulting in 50 µm (T1–T3) high three-dimensional microstructures. Dry etching of the silicon substrate is performed at 0°C for 8 min (T1, T2) and 5 min (T3). The chamber is cleaned before and after each silicon etching process. The photoresist mask is subsequently removed from the obtained Si mold using a plasma Asher for 40 min at 1000 W, 400 mL/min oxygen and 70 mL/min nitrogen flow.

The fourth topography (T4) is manufactured utilizing a nickel (Ni) mold. The Ni mold is fabricated from a Si mold in identical fashion as T1–T3. T4 uses a positive photoresist and the surface is subsequently dry etched for 1 min to obtain 10 µm high structures. In order to transfer the micropattern into Ni, first nickel vanadium (NiV, t = 100 nm) is sputtered (Wordentec) on the patterned Si wafer as a seed layer. Subsequently, 340 µm of Ni are electroplated (Electroplater Techno Trans) and, finally, the Si masters are etched away using a standard potassium hydroxide (KOH) wet etching process leaving a Ni mold with a tight array of micropillars (T4). In order to prevent adhesion between PDMS and the Ni mold, a Teflon monolayer (1H,1H,2H,2H-perfluorodecyltrichlorosilane (FDTS)) is added as an anti-stiction layer through molecular vapor deposition.

5.2 Fabrication of PDMS microstructures

Polydimethylsiloxane (PDMS) (Sylgard 184, Dow Corning Corporation, Michigan, United State) pre-polymer (monomer base) is mixed with a cross-linker (curing agent) in a ratio of 10:1. Bubbles introduced during mixing are subsequently removed through a degassing process in a vacuum chamber before pouring the mixture into the molds.

In order to obtain a leveled PDMS surface as well as simplify mold handling and demolding, a custom made mold housing is manufactured from poly(methyl methacrylate) (PMMA) utilizing a CO_2 laser. The mold housing is composed of a circular base (d = 6.5 cm) connected to a circular edge (h = 4 mm) fastened with screws.

The Si and Ni molds containing the microstructures are placed on the bottom of the mold housing with the structured side facing up. The degassed PDMS mixture is subsequently poured on top of the mold followed by a second degassing step. Finally, the PDMS is cured for 10 h at 70°C.

The cured PDMS slab is removed from the mold and structured areas (PDMS samples) are cut out using a circular surgical punch (d = 6 mm). The final circular PDMS samples utilized for testing have a diameter of 6 mm and height of 4 mm.

5.3 Characterization of PDMS microstructures

PDMS microstructures are characterized using a Scanning Electron Microscope (SEM) (SEM Supra from Carl Zeiss, Germany). Prior to imaging, gold was sputtered for 30 sec on the PDMS sample.

5.4 Tensile force measurements

Mucoadhesion measurements are evaluated by tensile tests with a TA.XT plus texture analyzer (Stable Micro Systems, Surry, United Kingdom). The maximum force (adhesiveness, detachment force (N)) and the work (work of adhesion) required to detach a piece of porcine intestinal mucosa from a PDMS sample are measured. All the adhesion measurements of the PDMS microstructures are conducted on porcine small intestinal tissue kindly donated from the Department of Experimental Medicine, University of Copenhagen, Denmark. The fresh tissue is cut into pieces of 4-5 cm and frozen at -20°C until further use. Before each experiment, the tissue is thawed at room temperature for 40-45 min. The tissue is then longitudinally cut and the outer muscular layer is peeled off. The intestine is then placed on a custom made tissue holder (obtained from the workshop of DTU Health Tech, Kgs. Lyngby, Denmark) with the mucus layer upwards and held in place. The entire platform as well as the tissue is then covered with Dulbecco's Phosphate Buffered Saline (PBS), pH 7.4 (Sigma-Aldrich, St. Louis, Missouri, United States). The tissue is stabilized in the buffer for approximately 15 min before testing. All the PDMS samples are cut into circular samples of 8 mm in diameter and connected to a TA probe with carbon pads. All the measurements are performed in the same fashion as explained previous in the literature[11,26,33]. All the adhesion tests are conducted with a 500 g load cell to increase the sensitivity of the instrument and the compression tests are conducted with a 5 kg load cell (both purchased from Stable Micro Systems, Surry, United Kingdom).

5.4.1 Adhesion measurements of PDMS microstructures

Adhesion tests are performed to measure mucoadhesion between PDMS microstructures and porcine small intestinal tissue. Adhesion tests are completed on both plain and structured PDMS surfaces using a texture analyzer. The parameters used in these tests are listed in Table 4.

Table 4: Instrumental parameters for a texture analyzer used for conducting the adhesion measurements of the PDMS microstructures.

Caption	Value
Pre-test speed (mm/sec)	0.50
Test speed (mm/sec)	0.10
Post-test speed (mm/sec)	0.10
Applied Force (N)	0.10
Contact time (sec)	180
Trigger force (N)	0.1

5.4.2 Optimization tests

Previous studies have shown how important, it is to adjust all the parameters for tensile force measurements to each sample or material [11,12,25]. Accordingly, optimization tests for the PDMS microstructures are carried out. The elastic modulus of PDMS differs with varying ratios of PDMS and cross-linker. The studied mixture of PDMS and cross-linker is exposed to a compression test to clarify how the PDMS specimen behaves under compression. This can give a statement of how affected the samples are when exposed to forces. Compression tests of plain PDMS surfaces are performed directly on the tissue holder without tissue (data shown in supplementary material, Table S1).

The most affecting parameters are the contact force and the contact time. Three values for each parameter have been selected from the literature and are tested to establish the optimal values[11]. For the contact force, 0.05 N, 0.1 N and 0.2 N are tested with a contact time of 180 sec. After selecting the contact force, the contact times of 60, 180 and 300 sec are tested and the most optimal are selected. All the optimization test are conducted on T2 microstructures and the rest of the parameters used to conduct these measurements are listed in Table 2.

Stability tests are also carried out on T1 PDMS microstructures, in order to establish the number of measurements that can be performed on a single piece of tissue (on the same spot) and still obtain acceptable results. Four different pieces of tissue are tested and ten measurements per tissue are conducted, using the same parameters. The PDMS surfaces are

looked at after each measurement to see if residuals from the mucosal surface where adhering to the surface.

5.5 Design of Experiments and statistical analysis

DoE is a systematic, standardized procedure to ensure solid and supportable conclusions. The purpose of this approach is to minimize consumption of runs, time and expenses. Using a consistent DoE provides important information about the effect on a response variable due to other factors. In all experiments, interfering factors can affect the results, originating some unwanted variabilities. To make the experimental error as small as possible and control or compensate for the interfering factors, the randomized complete block design (RCBD) is used. In this sort of design, each block (i.e. the intestinal tissue, in this case) contains all the treatments (i.e. PDMS microstructures with different topographies), see Table 5. In this way, the accuracy of comparisons between the different treatments selected is improved, by eliminating the variability among different blocks. For each block (i.e. tissue), the order in which the different treatments are tested is randomly determined, so that a time factor can be eliminated. The design chosen for these experiments are called Latin Square Designs. It is testing each structure exactly once, in each block. For example, considering four different treatments A, B, C, D, the software randomizes the order in which they should be tested, and an output table with the Latin square order is generated (Table 5).

Table 5: A schematic overview of the randomized order of the samples. All the four PDMS microstructures are tested in a random order on a single piece of tissue.

Tissue 1	T2	T1	T4	T3
Tissue 2	T3	T2	T1	T4
Tissue 3	T4	T3	T2	T1
Tissue 4	T1	T4	T3	T2

All statistical analysis have been performed on 64-bit Windows 10 using R, version 4.0.2. The R scripts and data can be found at https://data.dtu.dk

6. References

1. BOTTENBERG, P. *et al.* Development and Testing of Bioadhesive, Fluoride-containing Slow-release Tablets for Oral Use. *J. Pharm. Pharmacol.* **43**, 457–464 (1991).

2. Smart, J. D. The basics and underlying mechanisms of mucoadhesion. *Adv. Drug Deliv. Rev.* **57**, 1556–1568 (2005).

3. Bassi da Silva, J., Ferreira, S. B. de S., de Freitas, O. & Bruschi, M. L. A critical review about methodologies for the analysis of mucoadhesive properties of drug delivery systems. *Drug Dev. Ind. Pharm.* **43**, 1053–1070 (2017).

4. Grabovac, V., Guggi, D. & Bernkop-Schnürch, A. Comparison of the mucoadhesive properties of various polymers. *Adv. Drug Deliv. Rev.* **57**, 1713–1723 (2005).

5. Rao, K. V. R. & Buri, P. A novel in situ method to test polymers and coated microparticles for bioadhesion. *Int. J. Pharm.* **52**, 265–270 (1989).

6. Mosgaard, M. D. *et al.* Ex vivo intestinal perfusion model for investigating mucoadhesion of microcontainers. *Int. J. Pharm.* **570**, 118658 (2019).

7. Hassan, E. E. & Gallo, J. M. A Simple Rheological Method for the in Vitro Assessment of Mucin-Polymer Bioadhesive Bond Strength. *Pharm. Res. An Off. J. Am. Assoc. Pharm. Sci.* **7**, 491–495 (1990).

8. Grabovac, V., Guggi, D. & Bernkop-Schnürch, A. Comparison of the mucoadhesive properties of various polymers. *Advanced Drug Delivery Reviews* vol. 57 1713–1723 (2005).

9. Khutoryanskiy, V. V. Advances in Mucoadhesion and Mucoadhesive Polymers. *Macromol. Biosci.* **11**, 748–764 (2011).

10. Thirawong, N., Nunthanid, J., Puttipipatkhachorn, S. & Sriamornsak, P. Mucoadhesive properties of various pectins on gastrointestinal mucosa: An in vitro evaluation using texture analyzer. *Eur. J. Pharm. Biopharm.* **67**, 132–140 (2007).

11. das Neves, J., Amaral, M. H. & Bahia, M. F. Performance of an in vitro mucoadhesion testing method for vaginal semisolids: Influence of different testing conditions and instrumental parameters. *Eur. J. Pharm. Biopharm.* **69**, 622–632 (2008).

12. Wong, C. F., Yuen, K. H. & Peh, K. K. An in-vitro method for buccal adhesion studies: Importance of instrument variables. *Int. J. Pharm.* **180**, 47–57 (1999).

13. Hägerström, H. & Edsman, K. Interpretation of mucoadhesive properties of polymer gel preparations using a tensile strength method. *J. Pharm. Pharmacol.* **53**, 1589–1599 (2001).

14. TOBYN, M. J., JOHNSON, J. R. & DETTMAR, P. W. Factors affecting in vitro gastric mucoadhesion. I: Test conditions and instrumental parameters. *Eur. J. Pharm. Biopharm.* **41**, (1995).

15. Tam, P. Y. & Verdugo, P. Control of mucus hydration as a Donnan equilibrium process. *Nature* **292**, 340–342 (1981).

16. Chalmers, I. *et al.* How to increase value and reduce waste when research priorities are set. *Lancet* **383**, 156–165 (2014).

17. Baker, M. 1,500 scientists lift the lid on reproducibility. *Nature* **533**, 452–454 (2016).

18. Ioannidis, J. P. A. *et al.* Increasing value and reducing waste in research design, conduct, and analysis. *Lancet* **383**, 166–175 (2014).

19. Duffy, D. C., McDonald, J. C., Schueller, O. J. A. & Whitesides, G. M. Rapid prototyping of microfluidic systems in poly(dimethylsiloxane). *Anal. Chem.* **70**, 4974–4984 (1998).

20. Bassi da Silva, J., Ferreira, S., Reis, A., Cook, M. & Bruschi, M. Assessing Mucoadhesion in Polymer Gels: The Effect of Method Type and Instrument Variables. *Polymers (Basel).* **10**, 254 (2018).

21. Fisher, R. A. *The American Statistician*. (Taylor & Francis, Ltd, 1980).

22. Montgomery, D. C. *Design and Analysis of Experiments*. (John-Wiley & Sons Inc., 2012).

23. Tukey, J. W. Comparing Individual Means in the Analysis of Variance. *Biometrics* **5**, 99 (1949).

24. Vetchý, D. *et al.* Determination of dependencies among in vitro and in vivo properties of prepared mucoadhesive buccal films using multivariate data analysis. *Eur. J. Pharm.*

Biopharm. **86**, 498–506 (2014).

25. Bassi da Silva, J., Ferreira, S., Reis, A., Cook, M. & Bruschi, M. Assessing Mucoadhesion in Polymer Gels: The Effect of Method Type and Instrument Variables. *Polymers (Basel).* **10**, 254 (2018).

26. Tamburic, S. & Craig, D. Q. M. A comparison of different in vitro methods for measuring mucoadhesive performance. *Eur. J. Pharm. Biopharm.* **44**, 159–167 (1997).

27. Leh, C.-M. The second generation of bioadhesives. *J. Control. Release* **65**, 19–29 (2000).

28. Fischer, K. E. *et al.* Biomimetic Nanowire Coatings for Next Generation Adhesive Drug Delivery Systems. *Nano Lett.* **9**, 716–720 (2009).

29. Fox, C. B. *et al.* Fabrication of Sealed Nanostraw Microdevices for Oral Drug Delivery. *ACS Nano* **10**, 5873–5881 (2016).

30. Mata, A., Fleischman, A. J. & Roy, S. Characterization of Polydimethylsiloxane (PDMS) Properties for Biomedical Micro/Nanosystems. *Biomed. Microdevices* **7**, 281–293 (2005).

31. Fischer, K. E. *et al.* Biomimetic Nanowire Coatings for Next Generation Adhesive Drug Delivery Systems. *Nano Lett.* **9**, 716–720 (2009).

32. Fox, C. B. *et al.* Fabrication of Sealed Nanostraw Microdevices for Oral Drug Delivery. *ACS Nano* **10**, 5873–5881 (2016).

33. Jones, D. S. *et al.* Design, characterisation and preliminary clinical evaluation of a novel mucoadhesive topical formulation containing tetracycline for the treatment of periodontal disease. *J. Control. Release* **67**, 357–368 (2000).

Supplementary materials

General experimental design for testing adhesion to mucosal tissue

Mette Dalskov Mosgaard, Alina Joukainen Andersen, Eugenia Ingallinera, Marlitt Viehrig, Line Hagner Nielsen, Tommy Sonne Alstrøm and Anja Boisen

Optimization test of the measurements

The goal of the compression tests are to calculate Young Modulus (E) of the PDMS surface. The surface area of each specimen is A = 28.27 mm^2 (diameter = 6 mm, circular area) and the average height is 4 mm. The parameters used for the compression tests are listed in table 1.

Table S1 displays the instrumental parameters used for conducting the compression test of PDMS.

Caption	Value
Pre-test speed (mm/sec)	0.50
Test speed (mm/sec)	0.10
Post-test speed (mm/sec)	0.10
Trigger force (g)	3.0

Stress and strain is determined through the measurements and young modulus are calculated in accordance with previous studies [33].

The calculated elastic modulus of PDMS is estimated to be 2.241 ± 0.097 (n=4) MPa which matches the literature[33]. This indicates the homogeneity of the PDMS structures and the compression test indicates that the adhesion test will not have any influence on the PDMS samples.

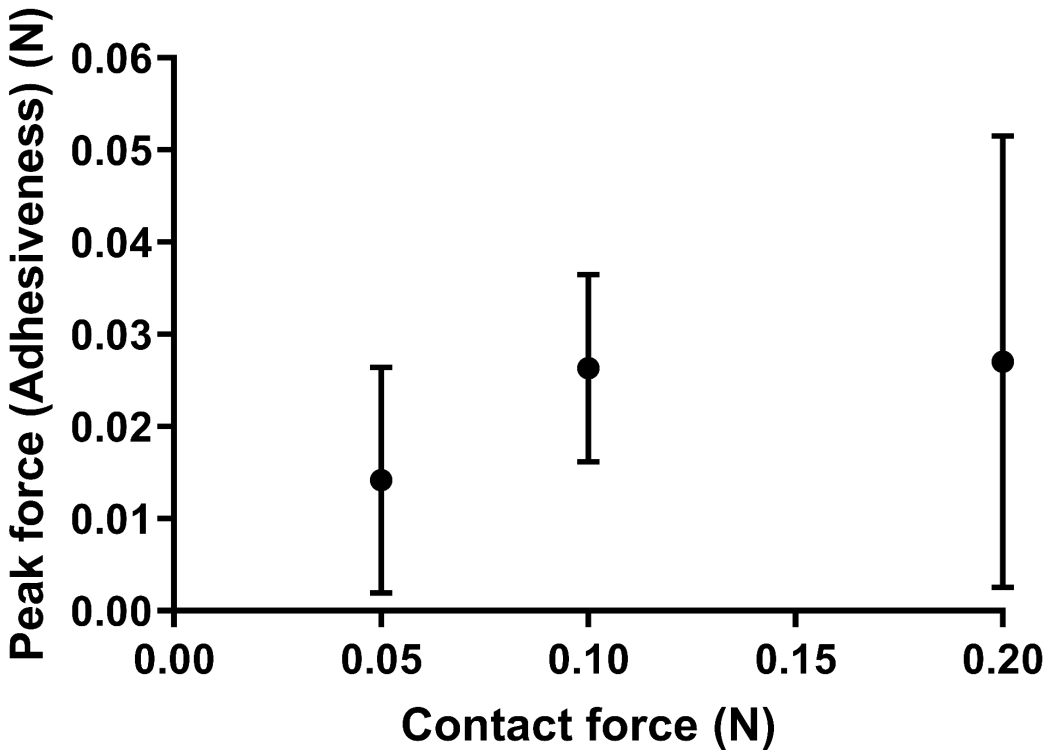

Figure: S1. Peak force measurements with contact forces of 0.05 N, 0.10 N and 0.20 N. n = 24

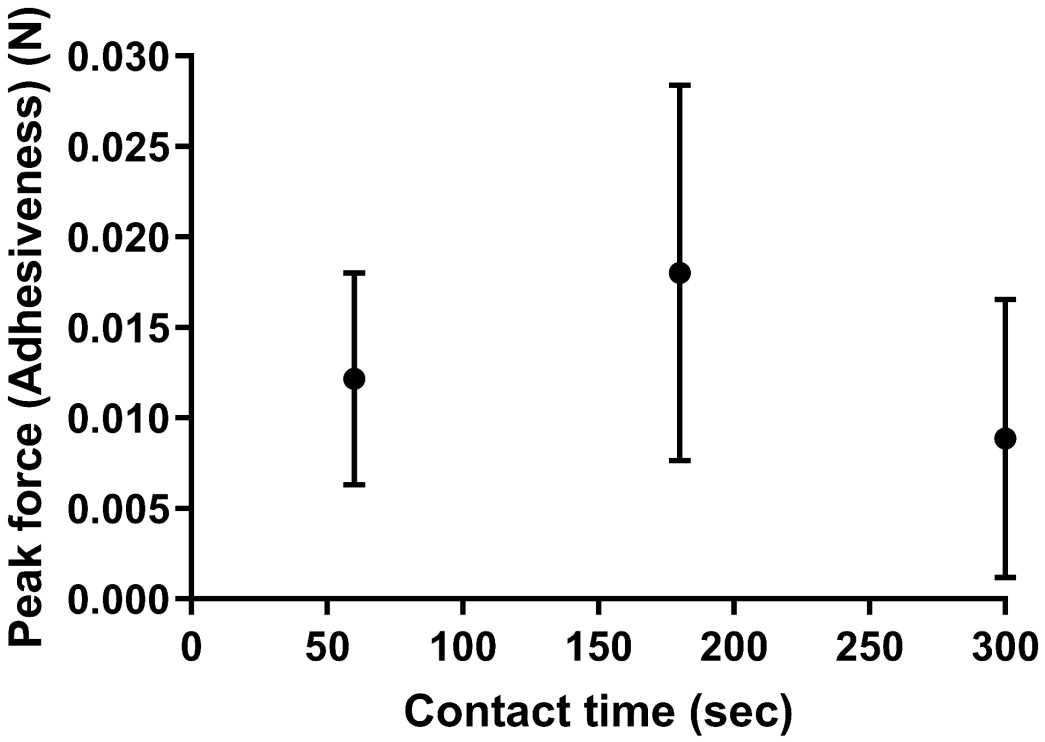

Figure S2. Peak force measurements after 60 sec, 180 sec and 300 sec of contact time. n = 24.

Appendix III

Paper III

Optimization of mucoadhesive coatings on microcontainers for oral drug delivery

M. D. Mosgaard, M. C. Johannesen, A. Müllertz, A. Boisen and L. H. Nielsen

In preparation

Optimization of mucoadhesive coatings on microcontainers for oral drug delivery

Mette D. Mosgaard[a*], *Mia Chen Johannesen*[a], *Anette Müllertz*[b], *Anja Boisen*[a] *and Line Hagner Nielsen*[a]

[a]Center for Intelligent Drug Delivery and Sensing Using Microcontainers and Nanomechanics (IDUN), Department of Health Technology, Technical University of Denmark, Denmark, Ørsteds Plads 345C, 2800 Kgs. Lyngby, Denmark

[b] Department of Pharmacy, Faculty of Health and Medical Sciences, University of Copenhagen, Universitetsparken 2, 2100 Copenhagen, Denmark

[*]**Corresponding author:** Mette D. Mosgaard, e-mail medmo@dtu.dk

Graphical abstract

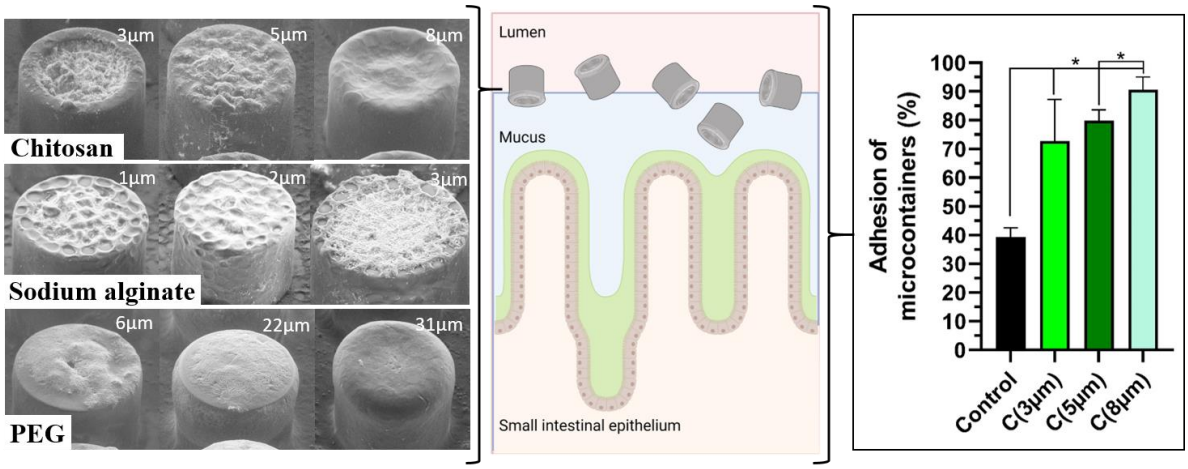

Abstract

Microcontainers facilitate unidirectional drug release and enable enhancement in oral bioavailability. Promoting the mucoadhesive abilities of microcontainers will most likely result in a higher drug release into the mucus layer leading to an increased drug absorption. The aim of this study was to optimize the mucoadhesive properties of microcontainers by coating them with one of the following polymers; chitosan, sodium alginate or PEG. The polymers were spray coated in three different thicknesses on furosemide-loaded microcontainers. The microcontainers were investigated with respect to mucoadhesion, using an *ex vivo* flow retention model, and drug release. Chitosan-coated microcontainers showed stronger mucoadhesion (between 72.8-90.6 % of the chitosan-coated microcontainers adhered) to intestinal tissue compared to PEG, sodium alginate and non-coated microcontainers (39.3 % adhered), and showed a prolonged release of furosemide for up to 7 h. For PEG-coated microcontainers, 59.4-62.4 % were adhering to the mucosa, whereas for sodium alginate-coated microcontainers 43.2-47.3 % adhered. For PEG and sodium alginate, the release of furosemide from the microcontainers were not affected, as they showed similar release as non-coated microcontainers. The coating thicknesses of chitosan, PEG and sodium alginate appear to have a minor effect on mucoadhesion and only chitosan-coated microcontainers showed adhesion differences between the thicknesses.

Keywords; mucoadhesion, poly(ethylene glycol), chitosan, sodium alginate, microdevices, furosemide.

Introduction

Microdevices have over the past decade attracted more and more attention as advanced oral drug delivery systems (Chirra et al., 2014a; Mazzoni et al., 2017; Nielsen et al., 2016; Sarah L Tao et al., 2003). Microcontainers are one type of such devices. They are cylindrical hollow shapes in micrometer size, fabricated in polymeric material. The inner cavity, used for drug storage, has a single open side for unidirectional drug release facilitating a high drug concentration close to a desired target site (often the small intestine) enabling an increased drug absorption (Chirra and Desai, 2012a; Eleftheriadis et al., 2019; Nielsen et al., 2014, 2012). Ideally, the unidirectional drug release should be directly into or close to the intestinal mucus layer. This emphasizes the need for having mucoadhesive microcontainers that promote adhesion of the open cavity to the mucosal surface and enhance the resident time at the mucosal surface (Ahmed et al., 2002; Leh, 2000).

Since the discovery of mucoadhesion, researchers have tried to understand and enhance the ability of materials to adhere to the mucus layers (Florey, 1962; Park and Robinson, 1984). Numerous polymers have shown to retain formulations at the mucosal surfaces and improve drug absorption (Peppas and Buri, 1985; Smart, 2005). Selecting the right mucoadhesive polymer for a specific drug delivery system requires several considerations such as adhesion strength, low toxicity, physiological settings, mechanical forces and physical/chemical properties of the polymer. The mucoadhesive properties of a polymer are important for retaining the drug formulation at a desired target, but have shown to hamper drug release, which can compromise the desired drug effect.

Mucoadhesive polymers can make numerous interactions with the mucus layer depending on the polymer in focus (Sigurdsson et al., 2013). The most promoted strategy is the use of cationic material for electrostatic interaction with the anionic regions in the mucus (Lehr et al., 1992; Sogias et al., 2008). Chitosan is the most studied cationic polymer due to its strong adhesion to the mucosal lining, and its ability to enhance and prolong intestinal absorption of various drug delivery formulations, such as nanoparticles and chitosan-coated liposomes (Behrens et al., 2002; Prego et al., 2006, 2005; Thongborisute et al., 2006). Sharma et al. demonstrated an improved oral relative bioavailability of carvedilol where a 9.76 fold increase was observed after oral administration of carvedilol-loaded chitosan nanoparticles when compared to marked carvedilol tables (Sharma et al., 2019).

The mucoadhesive properties of polymers containing anionic carboxyl groups are related to their ability to form hydrogen bonds to the mucins side chains. Sodium alginate is such a polymer. Alginate is a linear polysaccharide facilitating entanglement of the polymeric chains into the mucus layer where hydrogen bonding can occur. Furthermore, it is a viscous slippery gel-like solution, which also promotes adhesion (Cho et al., 2010). Previously, sodium alginate microspheres loaded with insulin showed a potential improvement in the relative bioavailability of 8.8 % after oral dosing when compared to the typical oral bioavailability of proteins (1-2 %) (Déat-Lainé et al., 2013). The blood glucose levels were significantly lower after oral dosing of sodium alginate microspheres when compared to insulin in free solution.
Poly(ethylene glycol) (PEG) has also gained a lot of attention in relation to mucus penetration and mucoadhesion. PEG is a hydrophilic neutral polymer allowing for very few possibilities of interactions with other molecules. However, studies have shown that some PEG surfaces facilitate adhesion to the mucosal surface, which is believed to be related to penetration of long PEG chains into the mucus mesh where hydrogen bonds can occur. The penetrating PEG chains can also facilitate adhesion due to entanglement in the mucus mesh (Sahlin and Peppas, 1997; Serra et al., 2006). The molecular weight of PEG play an important role in the adhesion process since the chain length of PEG affects adhesion. Studies have shown that PEG with low molecular weight of approximately 2 kDa penetrates into mucus, whereas larger molecular weight of PEG (~10 kDa) promotes mucoadhesion (Bourganis et al., 2015; Netsomboon and Bernkop-Schnürch, 2016).

The aim of this study was to establish the most optimal mucoadhesive coating on the cavity of furosemide-loaded microcontainers to achieve good adhesive properties to intestinal tissue. Either chitosan, sodium alginate or PEG were spray coated onto furosemide-microcontainers in three different thicknesses. For evaluating the optimal polymer for coating and the ideal thickness, the coated microcontainers were tested with respect to i) mucoadhesion, using an *ex vivo* retention model and ii) drug release.

2. Material and Method

2.1 Materials

Furosemide was obtained from Fagron Nordic (Copenhagen, Denmark), and poly(ethylene glycol) (PEG) 12,000 Da was purchased from FLUKA of Fischer (Hampton, NH, USA). Sodium chloride, acetic acid, sodium phosphate monobasic dehydrate, chitosan (deacetylated

75-85 %, low molecular weight) and sodium alginate were all from Sigma-Aldrich (St. Louis, Mo, USA). Fasted state simulated intestinal fluid (FaSSIF) was acquired from biorelevant.com (London, UK). SU-8 2035, 2075 and SU-8 developer were purchased from Microresist Technology GmbH (Berlin, Germany) and the silicon (Si) wafers 4-inch (1 0 0) single-side polished were obtained from Topsil (Frederikssund, Denmark).

2.2 Fabrication of SU-8 microcontainers and drug loading

Microcontainers were fabricated on silicon wafers with the epoxy-based photoresist SU-8 in a similar fashion as previously described (Nielsen et al., 2014, 2012; Tao and Desai, 2007). Briefly, to fabricate the bottom and the walls of the microcontainers two steps of photolithography was conducted. The silicon wafers were pretreated with a titanium/gold (Ti/Au) coating to enable dry removal of the SU-8 microcontainers (Christfort et al., 2020). After fabrication, the wafers were cut into squared chips (12.8 x 12.8 mm^2) each containing 625 microcontainers.

For loading the microcontainers with furosemide, a shadow mask was aligned onto the microcontainer chip. This was applied to prevent drug powder from being deposited between the microcontainers and only allow it to be in the cavity of the microcontainers. After aligning the shadow mask, furosemide powder was then manually loaded into the cavity of the microcontainers using a brush. Afterwards, the shadow mask was removed and air pressure was applied on the chip to remove excess drug not loaded into the cavity (Abid et al., 2017).

2.3 Mucoadhesive coatings onto furosemide-loaded microcontainers

Either chitosan, sodium alginate or PEG were spray coated on the cavity of furosemide-loaded microcontainers using a spray coater system (ExactaCoat, Sono Tek, USA) equipped with an ultrasonic nozzle actuated at 120 kHz (Keller et al., 2013). The three polymeric solutions were either chitosan 0.5 % w/v in 0.1 M acetic acid, sodium alginate 0.5 % w/v in water or PEG 2.66 % w/v in water (Cui et al., 2006; Mazzoni et al., 2019; Salamat-Miller et al., 2005; Solomonidou et al., 2001). All the polymers were spray coated with a flow rate of 0.1 mL/min and a generator power at 1.3 W. A wavy line spray path was used for each microcontainer chip having an offset of 2 mm to allow for an even coating layer on the chip with the microcontainers. A shaping air of 0.02 bar was applied for all the polymers. Table 1 list the instrument settings.

Table 1: The experimental settings for spray coating the three mucoadhesive polymers of either chitosan, sodium alginate or PEG onto furosemide-loaded microcontainers. Three different thicknesses of each polymer was utilized, which is indicated by the different numbers of used loops.

Parameters	**Chitosan**	**Sodium alginate**	**PEG**
Nozzle speed (mm/s)	25	25	20
Distance between nozzle	25	25	20
Temperature (◦C)	50	50	40
Loops	60/120/180	75/125/175	35/70/109
Concentration of polymer (% w/v)	0.5	0.5	2.66

A scanning electron microscope (SEM) (TM3030Plus Tabletop Microscope, Hitachi®, Tokyo, Japan) was utilized to investigate the quality and appearance of the coating layers. All inspections used SE detector and an acceleration voltage of 15 kV. The thickness and roughness of the different polymeric coatings were measured by a surface profilometer (KLA-Tencor Alpha-Step IQ, CA, USA).

2.4 *In vitro* drug release from the coated microcontainers

The release of furosemide from the differently coated microcontainers was measured using a µDiss profiler™ (pION Inc., Woburn, MA). 2 h prior to the experiments, FaSSIF was prepared at pH 6.5 and kept at 37 °C until further use.

First, a stock solution of 10 mg/mL furosemide in water adjusted to pH 10 was prepared. Then, calibration curves were constructed by adding accurate volumes of the stock solution to 10 mL of FaSSIF followed by UV absorbance measurements within the range of 300-350 nm.

For the release study, a microcontainer chip was attached to a cylindrical magnetic stirrer using doubled-sided carbon tape, and transferred to a glass vial. Here, 10 mL of FaSSIF was added at the same time as the experiment was initiated. The studies were carried out with a stirring rate of 100 rpm at 37°C and a path length of the *in situ* UV probe of 1 mm. Spectra were collected over 7.5 h and in four replicates.

2.5 *Ex vivo* retention model for evaluation of mucoadhesive coatings

Small intestines from Landrace×Yorkshire×Duroc (LYD) pigs were kindly donated from the Department of Experimental Medicine, University of Copenhagen, Denmark. On arrival, the small intestine was cut into pieces with a length of approximately 10 cm and stored at −20°C until further use.

An *ex vivo* retention model similar to the one described in the literature was used to evaluate mucoadhesion of microcontainers with polymeric coatings (Madsen et al., 2013; Mazzoni et al., 2019; Rao and Buri, 1989). FaSSIF was prepared 2 h prior to the experiments and kept at 37°C until further use. A 10 cm piece of porcine small intestine was thawed for 30–50 min at room temperature before longitudinally cutting it open and placing it on a supporting slide with the mucosal surface upwards. The slide was placed in a humidity chamber fabricated and designed by Vaut et al. (Mosgaard et al., 2019; Vaut et al., 2019). The chamber facilitated a constant humidity of approximately 80 % and a temperature of 37°C. A peristaltic pump was connected to the supporting slide to facilitate a constant flow across the surface of the tissue. After placing the tissue slide in the chamber and adjusting its angle to 20°, a washing step with FaSSIF was initiated for 1-5 min with a flow rate of 10 mL/min. Underneath the tissue, a filter paper was placed to collect non-adhering microcontainers. The microcontainers with or without polymeric coatings were manually scraped off the silicon chip and applied onto a spatula where they were counted. 183 ± 8 microcontainers were placed in the top part of the tissue. After placing the microcontainers on the tissue, their location was noted and a flow of 10 mL/min of FaSSIF was initiated and continued for 5 min. Immediately after, the movement of the microcontainers down the mucosal surface was investigated using a light microscope (Zeiss Axio Scope.A1, Carl Zeiss, Göttingen, Germany) with a C-DIC filter and AxioVision SE64 software (version 4.9.1 SP1). The amount of microcontainers adhering to the tissue and the amount of microcontainers being on the filter was counted after the 5 min of flow. The amount of microcontainers remaining on the tissue gave an estimate of the ability of the microcontainers to adhere to the mucosal surface. The orientation and location of the microcontainers were investigated and categorized into laying sideways, up/down or deeply covered into mucus as described previously (Mosgaard et al., 2019).

2.6 Statistics

All data were shown as mean ± standard deviation (SD). Statistical analysis were carried out using Student t-tests or one-way ANOVA using GraphPad Prism, version 7.04 (CA, USA) and p-values below 5% ($p < 0.05$) were statistically significant.

3. Results and discussion

Addition of mucoadhesive polymers to the cavity of microcontainers is believed to promote unidirectional drug release directly into the mucus layer as well as to retain the microcontainers at the absorption site. This will result in an enhanced drug absorption that can improve oral bioavailability. Previously, it was shown, lectin-conjugated microdevices targeting the epithelium significantly enhanced *in vitro* bioadhesion to Caco-2 cells compared to microparticles with the same surface area. Lectin is binding specifically to N-acetylglucosamine groups that are located on the intestinal epithelial lining, which thereby increases bioadhesion and their retention (Chirra et al., 2014b; Chirra and Desai, 2012b; Sarah L. Tao et al., 2003). Lectin binds to the intestinal epithelium lining whereas in this study the polymers were targeting the mucus layer at the intestinal lining.

3.1 Drug loading and mucoadhesive coating of microcontainers

The microcontainers were successfully fabricated with dimensions of an individual microcontainer being an average cavity diameter of 234.3±2.2 µm, outer diameter of 324.7±2.2 µm and total height of 252.0±1.7 µm (Fig. 1A). Each chip was loaded with 3.71 ± 0.55 mg (n= 40 chips) of furosemide corresponding to 5.9 µg/microcontainer and the loading quality is shown in Fig. 1B. Furosemide is a weak acid (pKa 9.9 and 3.5) and classified as a class IV compound in the biopharmaceutical classification system, meaning it has low permeability and poor aqueous solubility (Matsuda and Tatsumi, 1990). Furosemide is a challenging drug to deliver orally and by prolonging the residence time at the mucosal surface an increased absorption might occur.

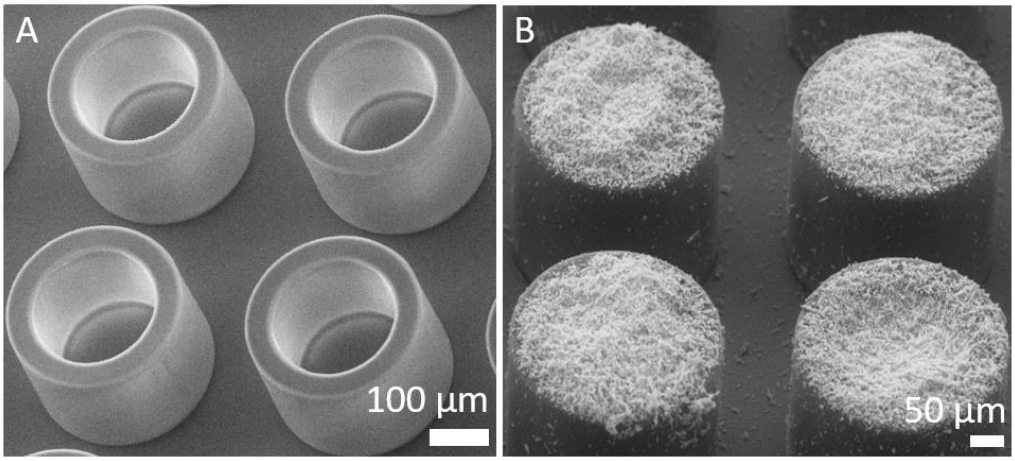

Figure 1: SEM images of A) empty microcontainers sitting on a silicon chip and B) microcontainers loaded with furosemide (in average 5.9 µg furosemide/microcontainer).

Chitosan, sodium alginate and PEG are polymers which possess low toxicity, are biocompatible and biodegradable hence, suitable for oral delivery (Cho et al., 2010; Sharma et al., 2003; Vila et al., 2004). Following drug loading with furosemide, the microcontainers were coated on the cavity with three different thicknesses of either chitosan, sodium alginate or PEG. The resulting coatings are shown in Fig. 2 and the thicknesses are listed in Table 2.

The polymer concentration of chitosan and sodium alginate was lower than the PEG concentration as both chitosan and sodium alginates produces viscous solutions, which can compromise the spray coating process. The chitosan concentration contributes to the coating thickness of chitosan on the microcontainers. The chitosan thicknesses coated on the microcontainers were between 3-8 µm (Table 2). Previously, it was shown that coating microcontainers with a chitosan thickness of 6.9 ± 1.1 µm led to a two-fold increase in mucoadhesion when compared to microcontainers without chitosan (Mazzoni et al., 2019). In another study, an enhanced adhesion of microcontainers was observed when they were coated with chitosan (8.9±0.7 µm thickness) (Birk et al., 2020). Both studies showed a sustained drug release profile with the use of chitosan.

Chitosan is hygroscopic and swells when in contact with water above pH 6.2 and thereby, forms a hydrogel on the cavity of the microcontainers (Gupta, 2010). The coating layers of 3 µm and 5 µm chitosan resulted in smooth thin coatings where furosemide crystals were visible below (Fig. 2). The chitosan coating layer of 8 µm covered the cavity of the microcontainers with an almost coherent film. The coating roughness was studied for all three thicknesses by profilometry, which revealed a low surface roughness. Chitosan's low surface roughness may be explained by chitosan droplets ability to be able to mobilize for a long time, which allow

the droplets to coalesce and form a dense smooth layer before drying on the microcontainer surface (Bose et al., 2013).

Table 2: The thicknesses of the polymeric coatings of chitosan, sodium alginate or PEG. Each polymer were coated in three different thicknesses, which are seen in the names of the different coatings. Data represent mean ± SD and n=3.

Name	Polymer	Coating thickness (µm)
C(3µm)	Chitosan	2.96 ± 0.19
C(5µm)	Chitosan	5.27 ± 0.86
C(8µm)	Chitosan	7.82 ± 0.48
A(1µm)	Sodium alginate	1.07 ± 0.14
A(2µm)	Sodium alginate	1.97 ± 0.12
A(3µm)	Sodium alginate	2.87 ± 0.24
P(6µm)	PEG	5.76 ± 0.44
P(22µm)	PEG	22.17 ± 1.98
P(31µm)	PEG	30.57 ± 3.45

Sodium alginate showed less ability to form a film than chitosan and PEG, and this resulted in an uneven coating layer on the microcontainers. This was substantiated by profiolmetry measurements showing high surface roughness of the sodium alginate coating layer (Fig. 2). The surface tension of a polymeric solution can affect the coating coalescence, which makes the coating surface less coherent and smooth. McGrath et al. tested the film forming properties of carboxymethylcellulose sodium salt (CMC) on a plain silicon surface. Here, the CMC solution gave large uncoated areas where some droplets had dried in solution as well as larger areas where droplets had coalesced well and formed a coherent coating surface. Furthermore, the edges of the coated areas were jagged, indicating that the coating layer had retracted from the silicon during drying (McGrath et al., 2011). The same was evident for the sodium alginate coating solution investigated in this study. McGrath et al. explains this behavior by the CMC solutions high surface tension. This was believed to promote cohesion of the coated droplets and prevent an even spread of the droplets across the silicon surface (McGrath et al., 2011).

Another study showed that CMC and sodium alginate have similar surface tension, which supports the similar coating behavior of CMC and sodium alginate (Lee et al., 2012). Both sodium alginate and CMC are salts, which could also explain the uneven coating. Salts can be difficult to spray coat to a coherent film due to crystallization during film formation. In this study, we made the following observations; a thickness of 1 µm resulted in an irregular coating but seemed to cover the open cavity, a thickness of 2 µm appeared smoother than the other two thicknesses and the furosemide crystals were covered, a thickness of 3 µm gave the roughest surface and furosemide crystals seemed uncoated. The smooth appearance of the 2 µm thick coating layer of sodium alginate could be explained from the amount of salt present. A 1 µm thick layer of sodium alginate might be too thin to observe a salt effect in the film and for the 3 µm thick layer, the amount of salt present on the surface was enough for creating cracks.

Microcontainers were spray coated with PEG in the thicknesses: 6, 22 and 31 µm (Table 2). Christfort et al. have previously used a thick PEG coating of 73±14 µm on drug-loaded microcontainers, however no significant difference in mucoadhesion was observed *in vivo* when comparing to microcontainers without PEG (Christfort et al., 2021). A thinner PEG coating of 17.0±5.6 µm has earlier let to a two-fold increase in *ex vivo* mucoadhesion when compared to microcontainers without PEG. This thickness was obtained with a PEG concentration of 0.7 % w/v in dichloromethane, where the current study used 2.66 % w/v in water (Mazzoni et al., 2019). It was expected that more PEG chains were present at the coating surface with higher concentrations; therefore, a high PEG concentration was chosen here. In this study, a PEG thickness of 6 µm resulted in a thin uniform layer where furosemide crystals were still visible, whereas for a thickness of 22 µm the cavity of the microcontainers was covered with a thin layer and the furosemide crystals were less visible (Fig. 2). A PEG coating thickness of 31 µm covered the entire microcontainer with an even layer. The surface roughness was low for PEG when compared to sodium alginate coatings.

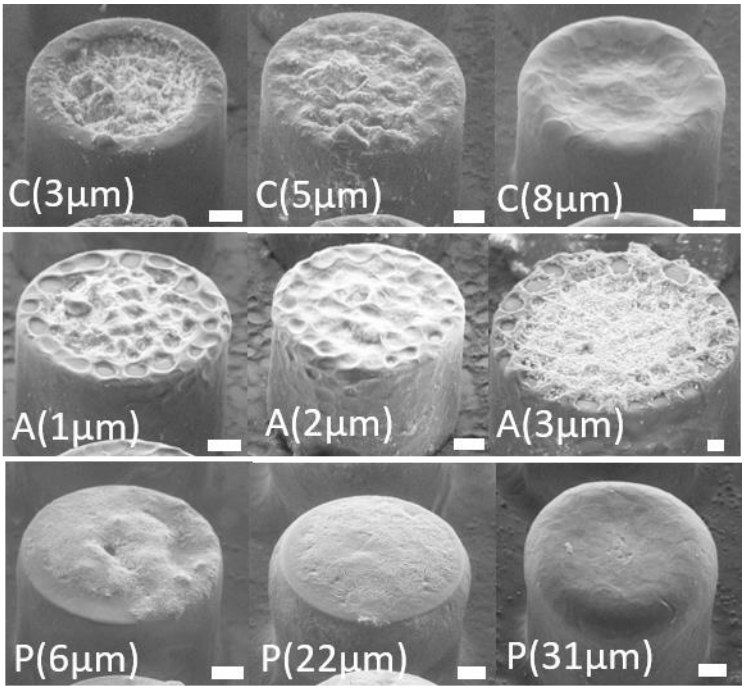

Figure 2: SEM images of the different polymeric coatings for different thicknesses. The first row of images shows chitosan-coated microcontainers with C(3µm), C(5µm) and C(8µm). Second row of images shows microcontainers coated with sodium alginate, A(1µm), A(2µm) and A(3µm). The third row of images displays the PEG-coated microcontainers with P(6µm), P(22µm) and P(31µm). The chitosan and PEG coatings showed low surface roughness compared to sodium alginate. All scale bars represent 50 µm except for A(3µm) which represents 20 µm.

3.3 *In vitro* drug release from the coated microcontainers

Drug release profiles are of great importance when evaluating mucoadhesive coatings and their thicknesses. The release profile can give an idea of whether the coating layer is too thick to obtain a sufficient drug release.

Chitosan-coated microcontainers gave an initial release within the first hour of 42.9±5.1 % for C(3µm), 48.8±3.1 % for C(6µm) and 39.5±5.1 % for C(8µm) (Fig. 3A). However, no significant difference between the three chitosan thicknesses were observed within this time frame. Furosemide was sustained released for all three thicknesses and after 7 h, 85.4±8.7 % for C(3µm) was released, whereas 95.0±0.3 % and 91.1±9.5 % was released from C(6µm) and C(8µm), respectively. No significant difference was observed between the chitosan-coated microcontainers after 7.5 h. For the non-coated microcontainers 92.1±1.2 % of furosemide was released within the first hour. The release profile of the chitosan-coated microcontainers showed that all three thicknesses were significantly different from the microcontainers without coating after 1 h ($P = <0.0001$ for all three thicknesses). The ability of chitosan to swell when in contact with water has shown to affect its adhesiveness and drug release profile (Gombotz and Wee, 1998; Lehr et al., 1992). In accordance, it has previously been shown that chitosan

induces sustained release of both ciprofloxacin (25.9±5.6 % after 90 min) and lysozyme (70.6±6.6 % after 2 hours) (Birk et al., 2020; Mazzoni et al., 2019). With ciprofloxacin loaded into the microcontainers and coated with chitosan, a complete release of ciprofloxacin was observed after 28 h (99.5±9.1%), whereas for non-coated ciprofloxacin-loaded microcontainers, a complete release took 7 h (Birk et al., 2020). The sustained release profile through a chitosan layer is greatly dependent on the drug and its physical and chemical properties.

Sodium alginate-coated microcontainers resulted in a fast release of furosemide and within the first hour 90.0±6.9 % was released through A(1µm), and 99.6±1.6 % and 99.2±6.5 % were released through A(2µm) and A(3µm), respectively. No significant difference was observed between the three coating thicknesses (Fig. 3B), nor when compared to the non-coated microcontainers. This was expected as sodium alginate is water soluble, which allows for unaffected release rates.

The release profiles of furosemide from PEG-coated microcontainers are shown in Fig. 3C. A fast release of furosemide was observed within the first hour and 99.4±19.6 %, 114.1±8.9 % and 91.8±2.2 % were released from P(6µm), P(22µm) and P(31µm), respectively. No significant difference was observed between P(6µm) and the other two thicknesses. However, P(22µm) showed significantly higher release than P(31µm) and from non-coated microcontainers after 1 h of release ($P = 0.0028$ and $P = 0.0027$). No significant difference was observed between microcontainers without coating and P(6µm) and P(31µm). An unaffected release profile of furosemide from PEG-coated microcontainers was expected as PEG is water soluble, and therefore, solubilizes fast in the aqueous medium (Efremova et al., 2002).

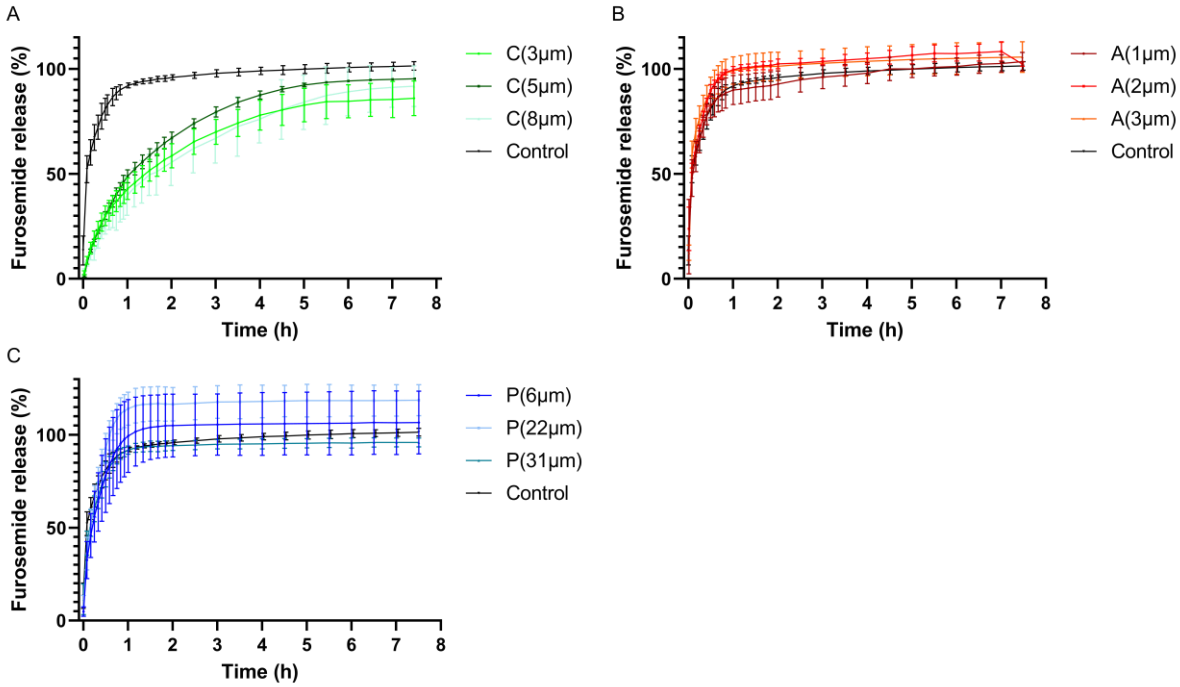

Figure 3: *In vitro* release of furosemide from microcontainers as a function of time. The microcontainer were either without coating or coated with either chitosan, sodium alginate or PEG. Furosemide release from microcontainers coated with A) three different thicknesses of chitosan, B) three different thicknesses of sodium alginate and C) three different thicknesses of PEG. Black curve in all three graphs represents the control release profile (microcontainers without coating). Data represent mean ± SD, n = 4.

3.4 Mucoadhesion of microcontainers using *ex vivo* retention model

Several studies have stated the importance of being able to control the direction of drug release from microdevices (Ahmed et al., 2002; Ainslie et al., 2009; Chirra and Desai, 2012c). By controlling a direct drug release into the mucus layer, one could expect an increased absorption and thereby, an increased oral bioavailability (Chirra et al., 2014a; Chirra and Desai, 2012c). Coating the cavity of the microcontainers with a mucoadhesive polymer will not just result in an increased residence time but will also secure attachment between the cavity of the microcontainers and the mucosal surface. A flow retention model using porcine small intestinal tissue was used to evaluate the ability of the coated microcontainers to adhere. Mucoadhesion was determined from the amount of microcontainers adhering to the mucosal surface after exposure to a continuous flow.

Fig. 4 shows the ability of the different polymers to adhere to the tissue and the dependency of thicknesses. 72.8 ± 14.4 % of the C(3µm) microcontainers adhered to the tissue after 5 min of flow, but here, a large standard variation was observed. C(5µm) and C(8µm) showed similar strength of adhesion where 90.6 ± 4.4 % and 79.9 ± 3.4 % were adhering, respectively. The

high variability between the same samples can be explained by varying mucus thicknesses on the tissue, which can lead to different adhesion of the microcontainers. All three thicknesses of chitosan were significantly different from the microcontainers without coating where only 39.3 ± 3.3 % were adhering (C(3µm) P=0.0027, C(5µm) and C(8µm) P=<0.0001). The microcontainers coated with the thickest layer C(8µm) adhered better than C(3µm) and C(5µm). The ability of chitosan to adhere to mucosal surfaces is well-known and therefore, strong adhesion was expected from the chitosan coatings. Sogias et al. showed that chitosan, was not only adhering from electrostatic interactions, but the adhesion was also strengthened by hydrogen bonding and hydrophobic interactions (Sogias et al., 2008). The ability of chitosan to swell and interact with mucus improves the adhesion but the question is if it is always in its favor. Preliminary studies (not included) have shown that a thick layer of chitosan can result in accumulation of microcontainers (as they clump together), which thereby, can prolong the release profile and prevent efficient delivery to a large surface area in the small intestine. This is especially important when administering the microcontainers in a capsule where chitosan slowly will hydrate and stick together. This limits the use of chitosan as a mucoadhesive polymer on microcontainers.

It can be observed that 50.3 ± 6.0 % A(2µm)-coated microcontainers adhered to the mucus on the small intestine (Fig. 4). There was no significant difference between the three coating thicknesses of sodium alginate, but there was a significant difference between the non-coated microcontainers and the A(2µm)-coated microcontainers (P=0.018). In general, sodium alginate was not expected to show stronger adhesion than chitosan and PEG due to a poor coating layer and low thickness when compared to the chitosan- and PEG-coated microcontainers. Sodium alginate will dissolve when exposed to the intestinal fluid, which limits the duration of adhesion (Cho et al., 2010). It is clear from the results that not only the ability of the polymer to adhere but also the coating quality of the polymers is important. This can explain the low adhesion and the large standard deviations observed for microcontainers coated with sodium alginate.

All three coating thicknesses of PEG resulted in similar adhesion strengths (Fig. 4). For P(6µm) microcontainers, 59.4 ± 18.1 % was adhering, however, no significant difference were observed when comparing to the non-coated microcontainers. Both P(22µm) with 63.3 ± 4.5 % and P(31µm) with 62.4 ± 10.7 % of adhering microcontainers showed significant difference to the non-coated ones (P=0.0001 and P=0.0062). The data suggest that P(22µm) and P(31µm) have similar adhesion to mucosa. In general, the thickness of PEG did not affect the adhesion

to mucosa, and therefore, it can be concluded that the thinnest layer of PEG would be the most optimal as the production time and use of excipients can be reduced. Previously, adhesion of microcontainers coated with either PLGA+PEG or PLGA+chitosan has been compared and they showed similar adhesion strength of the two polymer combinations, however, only approximately 35-40 % of the microcontainers were adhering to the mucosal surface (Mazzoni et al., 2019). In this study, 60 % of the PEG-coated microcontainers were adhering and 80 % of chitosan-coated microcontainers were adhering. Indicating a stronger adhesion shown in this study compared to the previous studies. This could either indicate that the different coating thicknesses affected the mucoadhesion or simply be due to biological variations. Minor variations in the setup and interpretation of the results could also explain the variations in adhesion.

Coating the microcontainers with chitosan gave the strongest adhesion to the mucosal surface in general. However, no significant difference was observed between chitosan-coated microcontainers and P(22µm) and P(31µm). C(5µm) and C(8µm) gave significantly higher adhesion then all the sodium alginate-coated microcontainers. Furthermore, C(8µm) showed significantly higher adhesion then P(6µm) (P=0.0135). The most preferred chitosan thickness is C(8µm), since it showed the best adhesion abilities compared to C(3µm) and C(5µm). Nevertheless, from C(8µm), there was a sustained release profile of furosemide which might limit its usability as a drug delivery system. No significant differences were observed between the sodium alginate- and PEG-coated microcontainers.

The polymeric thickness deposited onto microcontainers has shown minor effect on the mucoadhesion. Significant difference in mucoadhesion of the different thicknesses was observed for chitosan but not for PEG and alginate. This could be explained by the investigated thickness or that the adhesion was not affected much by the polymer thickness. Further studies could establish whether the mucoadhesion could be improved by increasing the polymer concentration or the molecular weight of the polymer.

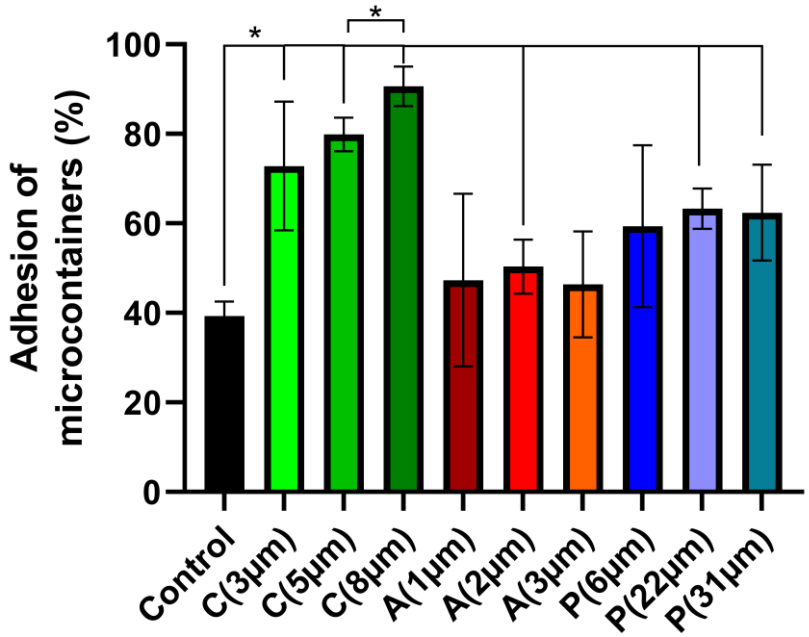

Figure 4: The ability of coated and non-coated microcontainers to adhere to the mucosal surface of the small intestine from a pig. Black bar show results of non-coated microcontainers. Green bars are chitosan-coated microcontainers where each green colure represents different chitosan thicknesses. Red bars are sodium alginate-coated microcontainers and each red colure represents different sodium alginate coating thicknesses, and blue bars are PEG-coated microcontainers, where each blue colure represents a different PEG coating thickness. Black * shows significant difference between the groups. Data represent mean ± SD, n = 4-5.

3.4.1 Distribution of microcontainers and their orientation

The flow retention model gives a clear indication of the adhesion of the microcontainers to the mucosal surface. Furthermore, it provides an indication of how the microcontainers are distributed on the tissue after being exposed to a continuous flow. The orientation of the microcontainers, after adhering to the mucosal surface, contributes to the idea of unidirectional release and whether the cavity is facing the mucus layer (Mosgaard et al., 2019). The distribution and orientation of the different polymeric coated microcontainers are shown in Fig. 5.

The majority (30-80 % compared to 5-13 % found distributed on the tissue) of the microcontainers were located where they initially were placed after being exposed to a continuously flow. This was observed for all three polymeric coatings as well as for the non-coated microcontainers. The amount of microcontainers found in the first part of the tissue is shown in Fig. 5A where their orientation is also shown. The orientation being sideways or up/down of the microcontainers in the first part of the tissue was biased by how they were initially placed. However, microcontainers deeply covered in mucus can give an idea of the ability of the polymers to penetrate into the mucus. The amount of microcontainers distributed down the tissue surface is shown in Fig. 5B as well as their orientation. A high amount of 68-

82 % (68±12 % C(3µm), 74±4 % C(6µm) and 82±4 % C(8µm)) of the chitosan-coated microcontainers were found in the first part of the tissue, indicating their strong adhesion to the mucosal surface. Their orientation was well distributed in the three orientations and 52±6 % of C(8µm) were found deeply in the mucus layer. Chitosan-coated microcontainers were distributed along the tissue supporting their strong ability to adhere to mucosa. C(3µm) were mainly found lying sideways where C(5µm) and C(8µm) were found lying up/down, which could be explained by the thicker chitosan layer on the cavity promoting up/down orientation.

Only 41-47 % of sodium alginate-coated microcontainers were located in the beginning of the tissue (Fig. 5A) (41±20 % A(1µm), 47±10 % A(2µm) and 45±13 % A(3µm)). This support the lower adhesion forces of sodium alginate when compared to chitosan- and PEG-coated microcontainers. The orientation of the microcontainers was similar for the three sodium alginate thicknesses and they were mainly oriented up/down or deep in the mucus (Fig. 5B). Moreover, the sodium alginate-coated microcontainers were distributed along the tissue. A(1µm) and A(2µm) showed that 9±4 % and 5±2 % of the microcontainers were adhering, whereas 3±1 % of A(3µm) microcontainers were adhering to the intestinal tissue. This could be explained by the coating of sodium alginate where A(3µm) showed a less coherent coating compared to the other two thicknesses.

55-62 % of PEG-coated microcontainers were located in the beginning of the tissue (Fig. 5A) which fits with the observation that PEG showed second strongest adhesion to mucosa when compared to chitosan and sodium alginate (55±9 % P(6µm), 60±4 % P(22µm) and 56±9 % P(31µm)). 22-35 % of them were found deeply covered in mucus (31±6 % P(6µm), 35±1 % P(22µm) and 22±9 % P(31µm)) (Fig. 5B). PEG is known for having mucopentrating abilities and PEG-coated microcontainers were expected to be embedded into mucus (Sahlin and Peppas, 1997). However, the large size of the microcontainers will prevent them from penetrating completely into the mucus layer but the PEG chains will be able to drag the microcontainers closer to the mucus. This could explain the large amount of PEG-coated microcontainers covered in mucus. Only 2±1 % for P(6µm) and P(22µm)-coated microcontainers were seen distributed down the tissue surface which could be explained by PEG being highly water soluble. The PEG coating will dissolve in the aqueous medium and when they detach from the mucosal surface, PEG will no longer be present to reattach the microcontainers to mucosa. 11±2 % of P(31µm) microcontainers were found along the tissue lying sideways, however, this was only seen for one repetition and could therefore be coursed by tissue differences.

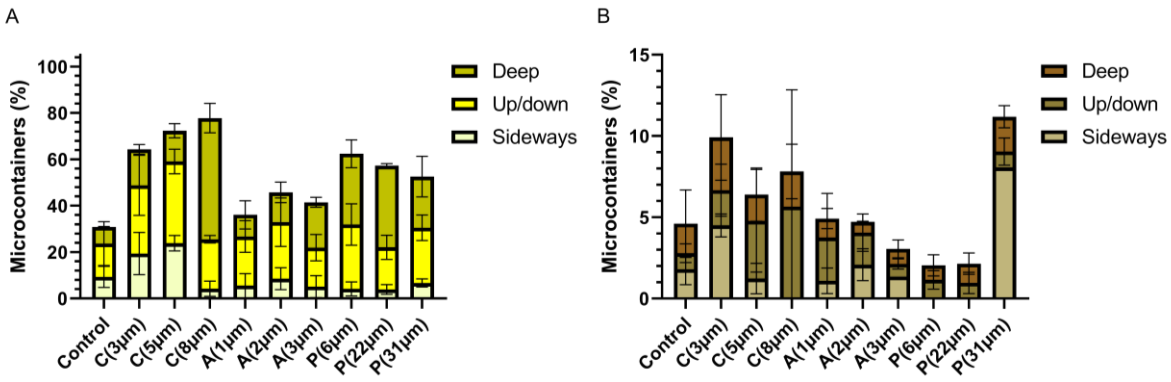

Figure 5: Percentage of polymeric-coated microcontainers orientated sideways, up/down or deeply covered in mucus. A) The orientation of the microcontainers at the start of the tissue after being exposed to a continuous flow (where the microcontainers were initially placed on the tissue). B) Orientation of the microcontainers distributed on the tissue after being exposed to a continuous flow for 5 min. Data represent mean ± SD, n = 4-5.

All the polymeric coated microcontainers seemed to be adhering better than non-coated microcontainers in the first part of the tissue. However, the non-coated microcontainers seemed to be better at adhering further down the tissue when compared to PEG-coated microcontainers. Previously, we have demonstrated that microcontainers prefer to orient themselves sideways with approximately 60 ± 12 % of the microcontainers lying sideways (Mosgaard et al., 2019). Therefore, this was expected but was not the case in this study since the non-coated microcontainers were oriented in all three orientations. This could most likely be explained by the variations in the methods used, as Mosgaard et al. used an *ex vivo* perfusion setup for evaluating the microcontainers behavior, which uses an intact small intestinal tissue piece.

4. Conclusion

In this work, three well-known polymers of chitosan, sodium alginate and PEG were investigated as mucoadhesive coatings on microcontainers for oral drug delivery. The three polymers were successfully coated on the cavity of the microcontainers. However, sodium alginate showed less promising coating abilities than chitosan and PEG. The three coating thicknesses of both PEG and sodium alginate did not compromise the *in vitro* release of furosemide, whereas chitosan did delay the release of furosemide for up to 7 h. By the use of an *ex vivo* retention model, it was observed that chitosan-coated microcontainers were adhering better than PEG- and sodium alginate-coated microcontainers. The 8 µm thick chitosan coating resulted in the strongest adhesion. This study provides valuable knowledge in how polymeric coatings on microdevices can improve their mucoadhesion. Testing different thicknesses of mucoadhesive polymers can help clarifying what effect this has on the microdevices in terms of drug release and their ability to adhere to mucosa.

5. Acknowledgments

The authors would like to acknowledge the Danish National Research Foundation, Denmark (DNRF122) and Villum Fonden, Denmark (Grant No. 9301) for Intelligent Drug Delivery and Sensing Using Microcontainers and Nanomechanics (IDUN). Graphical abstract was created with BioRender.com.

6. References

Abid, Z., Gundlach, C., Durucan, O., von Halling Laier, C., Nielsen, L.H., Boisen, A., Keller, S.S., 2017. Powder embossing method for selective loading of polymeric microcontainers with drug formulation. Microelectron. Eng. 171, 20–24. https://doi.org/10.1016/J.MEE.2017.01.018

Ahmed, A., Bonner, C., Desai, T.A., 2002. Bioadhesive microdevices with multiple reservoirs: a new platform for oral drug delivery. J. Control. Release 81, 291–306. https://doi.org/10.1016/S0168-3659(02)00074-3

Ainslie, K.M., Lowe, R.D., Beaudette, T.T., Petty, L., Bachelder, E.M., Desai, T.A., 2009. Microfabricated Devices for Enhanced Bioadhesive Drug Delivery: Attachment to and Small-Molecule Release Through a Cell Monolayer Under Flow. Small 5, 2857–2863. https://doi.org/10.1002/smll.200901254

Behrens, I., Vila Pena, A.I., Alonso, M.J., Kissel, T., 2002. Comparative uptake studies of bioadhesive and non-bioadhesive nanoparticles in human intestinal cell lines and rats: The effect of mucus on particle adsorption and transport. Pharm. Res. 19, 1185–1193. https://doi.org/10.1023/A:1019854327540

Birk, S.E., Haagensen, J.A.J., Johansen, H.K., Molin, S., Nielsen, L.H., Boisen, A., 2020. Microcontainer Delivery of Antibiotic Improves Treatment of *Pseudomonas aeruginosa* Biofilms. Adv. Healthc. Mater. 9, 1901779. https://doi.org/10.1002/adhm.201901779

Bose, S., Keller, S.S., Alstrøm, T.S., Boisen, A., Almdal, K., 2013. Process optimization of ultrasonic spray coating of polymer films. Langmuir 29, 6911–6919. https://doi.org/10.1021/la4010246

Bourganis, V., Karamanidou, T., Samaridou, E., Karidi, K., Kammona, O., Kiparissides, C., 2015. On the synthesis of mucus permeating nanocarriers. Eur. J. Pharm. Biopharm. 97, 239–249. https://doi.org/10.1016/j.ejpb.2015.01.021

Chirra, H.D., Desai, T.A., 2012a. Multi-Reservoir Bioadhesive Microdevices for Independent Rate-Controlled Delivery of Multiple Drugs. Small 8, 3839–3846. https://doi.org/10.1002/smll.201201367

Chirra, H.D., Desai, T.A., 2012b. Multi-Reservoir Bioadhesive Microdevices for Independent Rate-Controlled Delivery of Multiple Drugs. Small 8, 3839–3846. https://doi.org/10.1002/smll.201201367

Chirra, H.D., Desai, T.A., 2012c. Emerging microtechnologies for the development of oral drug delivery devices. Adv. Drug Deliv. Rev. 64, 1569–1578. https://doi.org/10.1016/J.ADDR.2012.08.013

Chirra, H.D., Shao, L., Ciaccio, N., Fox, C.B., Wade, J.M., Ma, A., Desai, T.A., 2014a. Planar Microdevices for Enhanced In Vivo Retention and Oral Bioavailability of Poorly Permeable Drugs. Adv. Healthc. Mater. 3, 1648–1654. https://doi.org/10.1002/adhm.201300676

Chirra, H.D., Shao, L., Ciaccio, N., Fox, C.B., Wade, J.M., Ma, A., Desai, T.A., 2014b. Planar Microdevices for Enhanced In Vivo Retention and Oral Bioavailability of Poorly Permeable Drugs. Adv. Healthc. Mater. 3, 1648–1654. https://doi.org/10.1002/adhm.201300676

Cho, W.J., Oh, S.H., Lee, J.H., 2010. Alginate film as a novel post-surgical tissue adhesion barrier. J. Biomater. Sci. Polym. Ed. 21, 701–713. https://doi.org/10.1163/156856209X435835

Christfort, J.F., Guillot, A.J., Melero, A., Thamdrup, L.H.E., Garrigues, T.M., Boisen, A., Zór, K., Nielsen, L.H., 2020. Cubic Microcontainers Improve In Situ Colonic Mucoadhesion and Absorption of Amoxicillin in Rats. Pharmaceutics 12, 355. https://doi.org/10.3390/pharmaceutics12040355

Christfort, J.F., Strindberg, S., Al-khalili, S., Bar-Shalom, D., Boisen, A., Nielsen, L.H., Müllertz, A., 2021. In vitro and in vivo comparison of microcontainers and microspheres for oral drug delivery. Int. J. Pharm. 600, 378–5173. https://doi.org/10.1016/j.ijpharm.2021.120516

Cui, F., Qian, F., Yin, C., 2006. Preparation and characterization of mucoadhesive polymer-coated nanoparticles. Int. J. Pharm. 316, 154–161. https://doi.org/10.1016/j.ijpharm.2006.02.031

Déat-Lainé, E., Hoffart, V., Garrait, G., Jarrige, J.F., Cardot, J.M., Subirade, M., Beyssac, E., 2013. Efficacy of mucoadhesive hydrogel microparticles of whey protein and alginate for oral insulin delivery. Pharm. Res. 30, 721–734. https://doi.org/10.1007/s11095-012-0913-3

Efremova, N. V., Huang, Y., Peppas, N.A., Leckband, D.E., 2002. Direct measurement of interactions between tethered poly(ethylene glycol) chains and adsorbed mucin layers. Langmuir 18, 836–845. https://doi.org/10.1021/la011303p

Eleftheriadis, G.K., Ritzoulis, C., Bouropoulos, N., Tzetzis, D., Andreadis, D.A., Boetker, J., Rantanen, J., Fatouros, D.G., 2019. Unidirectional drug release from 3D printed mucoadhesive buccal films using FDM technology: In vitro and ex vivo evaluation. Eur. J. Pharm. Biopharm. 144, 180–192. https://doi.org/10.1016/j.ejpb.2019.09.018

FLOREY, H.W., 1962. The secretion and function of intestinal mucus. Gastroenterology 43, 326–329. https://doi.org/10.1016/s0016-5085(19)35011-5

Gombotz, W.R., Wee, S.F., 1998. Protein release from alginate matrices. Adv. Drug Deliv. Rev. https://doi.org/10.1016/S0169-409X(97)00124-5

Gupta, S., 2010. Carbopol/Chitosan Based pH Triggered In Situ Gelling System for Ocular Delivery of Timolol Maleate. Sci. Pharm. 78, 959–976. https://doi.org/10.3797/scipharm.1001-06

Keller, S.S., Bosco, F.G., Boisen, A., 2013. Ferromagnetic shadow mask for spray coating of

polymer patterns. Microelectron. Eng. 110, 427–431. https://doi.org/10.1016/j.mee.2013.03.029

Lee, Boon-Beng, Chan, • Eng-Seng, Ravindra, Pogaku, Tanveer, •, Khan, A., Lee, B.-B, Chan, E.-S., Ravindra, P, Khan, T.A., 2012. Surface tension of viscous biopolymer solutions measured using the du Nouy ring method and the drop weight methods. Polym. Bull 69, 471–489. https://doi.org/10.1007/s00289-012-0782-2

Leh, C.-M., 2000. The second generation of bioadhesives. J. Control. Release 65, 19–29.

Lehr, C.M., Bouwstra, J.A., Schacht, E.H., Junginger, H.E., 1992. In vitro evaluation of mucoadhesive properties of chitosan and some other natural polymers. Int. J. Pharm. 78, 43–48. https://doi.org/10.1016/0378-5173(92)90353-4

Madsen, K.D., Sander, C., Baldursdottir, S., Marie, A., Pedersen, L., Jacobsen, J., 2013. Development of an ex vivo retention model simulating bioadhesion in the oral cavity using human saliva and physiologically relevant irrigation media. Int. J. Pharm. 448, 373–381. https://doi.org/10.1016/j.ijpharm.2013.03.031

Matsuda, Y., Tatsumi, E., 1990. Physicochemical characterization of furosemide modifications. Int. J. Pharm. 60, 11–26. https://doi.org/10.1016/0378-5173(90)90185-7

Mazzoni, C., Jacobsen, R.D., Mortensen, J., Jørgensen, J.R., Vaut, L., Jacobsen, J., Gundlach, C., Müllertz, A., Nielsen, L.H., Boisen, A., 2019. Polymeric Lids for Microcontainers for Oral Protein Delivery. Macromol. Biosci. 19, 1900004. https://doi.org/10.1002/mabi.201900004

Mazzoni, C., Tentor, F., Strindberg, S.A., Nielsen, L.H., Keller, S.S., Alstrøm, T.S., Gundlach, C., Müllertz, A., Marizza, P., Boisen, A., 2017. From concept to in vivo testing: Microcontainers for oral drug delivery. J. Control. Release 268, 343–351. https://doi.org/10.1016/J.JCONREL.2017.10.013

McGrath, M.G., Vrdoljak, A., O'Mahony, C., Oliveira, J.C., Moore, A.C., Crean, A.M., 2011. Determination of parameters for successful spray coating of silicon microneedle arrays. Int. J. Pharm. 415, 140–149. https://doi.org/10.1016/j.ijpharm.2011.05.064

Mosgaard, M.D., Strindberg, S., Abid, Z., Singh Petersen, R., Højlund Eklund Thamdrup, L., Joukainen Andersen, A., Sylvest Keller, S., Müllertz, A., Hagner Nielsen, L., Boisen, A., 2019. Ex vivo intestinal perfusion model for investigating mucoadhesion of microcontainers. Int. J. Pharm. 570, 118658. https://doi.org/10.1016/j.ijpharm.2019.118658

Netsomboon, K., Bernkop-Schnürch, A., 2016. Mucoadhesive vs. mucopenetrating particulate drug delivery. Eur. J. Pharm. Biopharm. https://doi.org/10.1016/j.ejpb.2015.11.003

Nielsen, L.H., Keller, S.S., Boisen, A., Müllertz, A., Rades, T., 2014. A slow cooling rate of indomethacin melt spatially confined in microcontainers increases the physical stability of the amorphous drug without influencing its biorelevant dissolution behaviour. Drug Deliv. Transl. Res. 4, 268–274. https://doi.org/10.1007/s13346-013-0166-7

Nielsen, L.H., Keller, S.S., Gordon, K.C., Boisen, A., Rades, T., Müllertz, A., 2012. Spatial confinement can lead to increased stability of amorphous indomethacin. Eur. J. Pharm. Biopharm. 81, 418–425. https://doi.org/10.1016/j.ejpb.2012.03.017

Nielsen, L.H., Melero, A., Keller, S.S., Jacobsen, J., Garrigues, T., Rades, T., Müllertz, A., Boisen, A., 2016. Polymeric microcontainers improve oral bioavailability of furosemide. Int. J. Pharm. 504, 98–109. https://doi.org/10.1016/J.IJPHARM.2016.03.050

Park, K., Robinson, J.R., 1984. Bioadhesive polymers as platforms for oral-controlled drug delivery: method to study bioadhesion. Int. J. Pharm. 19, 107–127. https://doi.org/10.1016/0378-5173(84)90154-6

Peppas, N.A., Buri, P.A., 1985. Surface, interfacial and molecular aspects of polymer bioadhesion on soft tissues. J. Control. Release 2, 257–275. https://doi.org/10.1016/0168-3659(85)90050-1

Prego, C., Fabre, M., Torres, D., Alonso, M.J., 2006. Efficacy and mechanism of action of chitosan nanocapsules for oral peptide delivery. Pharm. Res. 23, 549–556. https://doi.org/10.1007/s11095-006-9570-8

Prego, C., Torres, D., Alonso, M.J., 2005. Expert Opinion on Drug Delivery The potential of chitosan for the oral administration of peptides The potential of chitosan for the oral administration of peptides. https://doi.org/10.1517/17425247.2.5.843

Rao, K.V.R., Buri, P., 1989. A novel in situ method to test polymers and coated microparticles for bioadhesion. Int. J. Pharm. 52, 265–270. https://doi.org/10.1016/0378-5173(89)90229-9

Sahlin, J.J., Peppas, N.A., 1997. Enhanced hydrogel adhesion by polymer interdiffusion: Use of linear poly(ethylene glycol) as an adhesion promoter. J. Biomater. Sci. Polym. Ed. 8, 421–436. https://doi.org/10.1163/156856297X00362

Salamat-Miller, N., Chittchang, M., Johnston, T.P., 2005. The use of mucoadhesive polymers in buccal drug delivery. Adv. Drug Deliv. Rev. https://doi.org/10.1016/j.addr.2005.07.003

Serra, L., Doménech, J., Peppas, N.A., 2006. Design of poly(ethylene glycol)-tethered copolymers as novel mucoadhesive drug delivery systems. Eur. J. Pharm. Biopharm. 63, 11–18. https://doi.org/10.1016/j.ejpb.2005.10.011

Sharma, M., Sharma, R., Jain, D.K., Saraf, A., 2019. Enhancement of oral bioavailability of poorly water soluble carvedilol by chitosan nanoparticles: Optimization and pharmacokinetic study. Int. J. Biol. Macromol. 135, 246–260. https://doi.org/10.1016/j.ijbiomac.2019.05.162

Sharma, S., Johnson, R.W., Desai, T.A., 2003. Ultrathin poly(ethylene glycol) films for silicon-based microdevices. Appl. Surf. Sci. 206, 218–229. https://doi.org/10.1016/S0169-4332(02)01220-5

Sigurdsson, H.H., Kirch, J., Lehr, C.-M., 2013. Mucus as a barrier to lipophilic drugs. Int. J. Pharm. 453, 56–64. https://doi.org/10.1016/j.ijpharm.2013.05.040

Smart, J.D., 2005. The basics and underlying mechanisms of mucoadhesion. Adv. Drug Deliv. Rev. 57, 1556–1568. https://doi.org/10.1016/J.ADDR.2005.07.001

Sogias, I.A., Williams, A.C., Khutoryanskiy, V. V., 2008. Why is chitosan mucoadhesive? Biomacromolecules 9, 1837–1842. https://doi.org/10.1021/bm800276d

Solomonidou, D., Cremer, K., Krumme, M., Kreuter, J., 2001. Effect of carbomer

concentration and degree of neutralization on the mucoadhesive properties of polymer films. J. Biomater. Sci. Polym. Ed. 12, 1191–1205. https://doi.org/10.1163/156856201753395743

Tao, S.L., Desai, T.A., 2007. Aligned Arrays of Biodegradable Poly(ε-caprolactone) Nanowires and Nanofibers by Template Synthesis. Nano Lett. 7, 1463–1468. https://doi.org/10.1021/nl0700346

Tao, Sarah L, Lubeley, M.W., Desai, T.A., 2003. Bioadhesive poly(methyl methacrylate) microdevices for controlled drug delivery. J. Control. Release 88, 215–228. https://doi.org/10.1016/S0168-3659(03)00005-1

Tao, Sarah L., Lubeley, M.W., Desai, T.A., 2003. Bioadhesive poly(methyl methacrylate) microdevices for controlled drug delivery. J. Control. Release 88, 215–228. https://doi.org/10.1016/S0168-3659(03)00005-1

Thongborisute, J., Takeuchi, H., Yamamoto, H., Kawashima, Y., 2006. Visualization of the Penetrative and Mucoadhesive Properties of Chitosan and Chitosan-Coated Liposomes Through the Rat Intestine. J. Liposome Res. 16, 127–141. https://doi.org/10.1080/08982100600680816

Vaut, L., Scarano, E., Tosello, G., Boisen, A., 2019. Fully replicable and automated retention measurement setup for characterization of bio-adhesion. HardwareX 6, e00071. https://doi.org/10.1016/J.OHX.2019.E00071

Vila, A., Sánchez, A., Janes, K., Behrens, I., Kissel, T., Jato, J.L.V., Alonso, M.J., 2004. Low molecular weight chitosan nanoparticles as new carriers for nasal vaccine delivery in mice. Eur. J. Pharm. Biopharm. 57, 123–131. https://doi.org/10.1016/j.ejpb.2003.09.006

Appendix IV

Paper IV

Investigation of mucoadhesion and degradation of PCL and PLGA microcontainers for oral drug delivery

Z. Abid, M. D. Mosgaard, G. Manfroni, R. S. Petersen, L. H. Nielsen, A. Müllertz, A. Boisen and S. S. Keller

Polymers 2019, 11,1828

polymers

MDPI

Article

Investigation of Mucoadhesion and Degradation of PCL and PLGA Microcontainers for Oral Drug Delivery

Zarmeena Abid [1,2,*], Mette Dalskov Mosgaard [1,3], Giorgio Manfroni [1,2], Ritika Singh Petersen [1,2], Line Hagner Nielsen [1,3], Anette Müllertz [1,4], Anja Boisen [1,3] and Stephan Sylvest Keller [1,2]

1 The Danish National Research Foundation and Villum Foundation's Center for Intelligent Drug Delivery and Sensing Using Microcontainers and Nanomechanics (IDUN), Technical University of Denmark, 2800 Kgs. Lyngby, Denmark; medmo@dtu.dk (M.D.M.); giomanfro94@gmail.com (G.M.); Risi@dtu.dk (R.S.P.); lihan@dtu.dk (L.H.N.); anette.mullertz@sund.ku.dk (A.M.); aboi@dtu.dk (A.B.); Suke@dtu.dk (S.S.K.)

2 National Centre for Nano Fabrication and Characterization, DTU Nanolab, Technical University of Denmark, 2800 Kgs. Lyngby, Denmark

3 Department of Health Technology, DTU Health Tech, Technical University of Denmark, 2800 Kgs. Lyngby, Denmark

4 Department of Pharmacy, Faculty of Health and Medical Sciences, University of Copenhagen, 2100 Copenhagen, Denmark

* Correspondence: zarab@dtu.dk

Received: 2 October 2019; Accepted: 5 November 2019; Published: 7 November 2019

Abstract: Microfabricated devices have been introduced as a promising approach to overcome some of the challenges related to oral administration of drugs and, thereby, improve their oral bioavailability. In this study, we fabricate biodegradable microcontainers with different polymers, namely poly-ε-caprolactone (PCL), poly(lactic-co-glycolic acid) (PLGA) 50:50 and PLGA 75:25 by hot punching. The mucoadhesion of the microcontainers is assessed with an *ex vivo* retention model on porcine intestinal tissue. Finally, *in vitro* degradation studies of the biodegradable microcontainers are completed for six weeks in simulated intestinal medium with the addition of pancreatic enzymes. Through SEM inspection, the PLGA 50:50 microcontainers show the first signs of degradation already after two weeks and complete degradation within four weeks, while the other polymers slowly degrade in the medium over several weeks.

Keywords: hot punching; embossing; drug delivery; biodegradable polymers; thin films; microdevices; mucoadhesion; biodegradation

1. Introduction

Oral drug delivery is the most preferred administration route due to its minimally invasive nature and high patient compliance. Moreover, it provides flexibility to accommodate various types of drug candidates, as oral dosage forms do not require sterile manufacturing conditions and are therefore less expensive to manufacture. However, oral drug delivery faces several challenges, such as pre-systemic intestinal degradation, hepatic first pass elimination, as well as low solubility of some drugs in the fluids of the gastrointestinal (GI) tract, leading to reduced oral bioavailability of the drug [1,2]. One goal in the development of oral drug delivery systems is to reduce the dosage and thereby minimize the adverse effects of the drug, which can be achieved by increasing the amount of drug specifically released and absorbed at the targeted site in the GI tract. In the last decades,

mucoadhesion has been shown increased interest in oral drug delivery as it potentially enhances the bioavailability due to longer retention times of drug at the intended sites of absorption [3,4]. In particular, mucoadhesive drug delivery systems could be of value in delivering the growing number of sensitive high molecular-weight compounds, such as peptides and proteins [5]. Numerous methods have been proposed to assess the mucoadhesive properties of drug formulations *in vitro* and *ex vivo*. These methods can be based on mechanical force determination or on particle interactions [6].

Recently, microfabricated drug delivery systems have been proposed to overcome some of the major challenges in oral drug delivery [7]. For this purpose, microcontainer devices with precisely controlled dimensions and shapes have been introduced [8,9]. Microcontainers are reservoir-based devices, providing a large surface area. After the fabrication of microcontainers, active pharmaceutical ingredients (APIs) in various forms can be loaded into the cavities. This is convenient and avoids potential harm to the drug during the microcontainer processing steps. To control the release kinetics, functional coatings can then be applied on the loaded microcontainers. Due to the design of the devices, they can potentially provide unidirectional release at the intestinal mucosa, control of drug release kinetics, and facilitate targeted delivery of pharmaceuticals in the GI tract [10–12].

Based on the demand of fabricating microdevices in biocompatible and biodegradable materials, we recently demonstrated the successful fabrication of biodegradable microcontainers using hot punching, which is a modified hot embossing method [12]. The novel process is based on the assembly of compression molded polymer films, after which a single processing step produces simultaneous patterning of the device film and thermal bonding to an underlying water soluble poly(vinyl alcohol) (PVA) substrate. This results in replication of large arrays of microcontainers on a sacrificial film, which afterwards can be dissolved in an aqueous solution for harvesting of the devices. Thus far, this method has been applied for the fabrication of microcontainers with poly-ε-caprolactone (PCL).

Recently, an *ex vivo* method was presented for characterization of the mucoadhesive properties of microcontainers and other microfabricated devices intended for oral drug delivery [13]. It is a simple, yet efficient method, where a capsule containing the devices is placed at the top end of an untreated and inclined piece of porcine small intestine. The tissue is perfused with a simulated intestinal medium followed by microscope examination. Using this method, a study was completed evaluating mucoadhesion of the PCL microcontainers fabricated by hot punching. The results showed good adhesion to the intestine with over 60% of the devices residing in the first few cm of intestine [13]. While this is promising for sustained drug delivery, it raises the concern that the microcontainers might accumulate in the GI tract upon repeated administrations. This illustrates that the degradation of the polymeric materials used for oral drug delivery applications is another critical factor to consider. PCL is a polyester with a relatively low degradation rate in physiological conditions [14,15]. By adjusting the fabrication process of biodegradable microcontainers, it could be possible to change the material to a biodegradable polymer with faster degradation and similar, or even better, mucoadhesive properties. A polymer that has attracted considerable interest as a base material in biomedical applications, due to its biocompatibility and tailorable biodegradation rate, is poly(lactic-co-glycolic acid) (PLGA) [16–18]. It is a co-polymer approved by the U.S. Food and Drug Administration (FDA) for several medical applications, such as drug delivery and tissue engineering, due to its non-toxicity in humans [16,18]. In the presence of an aqueous environment, PLGA undergoes hydrolytic degradation to produce lactic and glycolic acid, which are products of normal metabolic pathways in the human body. Based on the percentage of glycolic acid and lactic acid in PLGA, the physical properties, such as the hydration and hydrolysis rate, are different [18].

The aim of this work is to evaluate the suitability of different polymeric materials for microfabricated drug delivery devices where mucoadhesive properties and biodegradability are important. For this purpose, we fabricate microcontainers in PLGA 50:50, PLGA 75:25, and PCL with the hot punching process. Furthermore, we assess and compare the biodegradation *in vitro* and investigate the mucoadhesion of these microcontainers *ex vivo*. The degradation studies are completed in a simulated intestinal medium to evaluate the structural integrity of the microcontainers upon prolonged exposure.

2. Materials and Methods

2.1. Microcontainer Fabrication

PVA (Mowiflex C17) was provided by Kuraray (Vantaa Finland) and PCL (M_n = 80,000 g mol^{-1}) was purchased from Sigma Aldrich (Schnelldorf, Germany) . Circular polymer films with a diameter of approximately 100 mm were prepared by compression molding with a hot embosser (Collin®Press, 300 SV, Ebersberg, Germany) as described earlier [12].

A series of optimization steps were carried out in order to achieve uniform PLGA 50:50 (acid end cap, M_n 85,000–100,000 g/mol, Akina, IN, US) and PLGA 75:25 (acid end cap, M_n 75,000–85,000 g/mol, Akina, IN, US) films with thicknesses corresponding to the height of the desired microcontainer structures. For PLGA 50:50, compression molding temperature was varied between 70 and 90 °C and a film thickness of 83 ± 7 µm was achieved with the optimized parameters, as shown in Table 1. For PLGA 75:25, similar experiments were conducted where the temperature was varied between 90 and 110 °C, while the pressure and holding time were kept the same as for PLGA 50:50. The process was stopped at room temperature and a thickness of 86 ± 10 µm was achieved at a temperature of 105 °C.

Table 1. Parameters for compression molding of poly(lactic-co-glycolic acid) (PLGA) 50:50 and 75:25 films.

Material	Amount [mg]	Compression Time [min]	Holding Temperature [°C]	Cooling Ramp [K/min]	Platen Pressure [bar]
PLGA 50:50	250 ± 20	30	90	20	20
PLGA 75:25	400 ± 200	30	105	20	20

Nickel stamps with the microcontainer patterns were fabricated using dry etching and electroplating in a similar manner as described by Petersen et al. [19]. PLGA 50:50 and PLGA 75:25 microcontainers were fabricated using a similar process flow as for PCL microcontainers presented earlier [12]. A simple assembly of the compression molded polymer films was performed prior to a single step of simultaneous thermal bonding and patterning based on hot punching, as shown in Figure 1. A 28 × 28 mm^2 PVA substrate was used as the sacrificial substrate and the PLGA device film with the same dimensions was assembled on top of it. Due to the high adhesion forces between PLGA and the Ni stamp, a polytetrafluoroethylene (PTFE) film (thickness 0.01 mm, Sigma Aldrich, Schnelldorf, Germany) was added. It was also cut in 28 × 28 mm^2 to fit 4 × 400 microcontainers. The PLGA device film was molded and punched by the Ni stamp (80°C, 600 s, and platen pressure at 12 bars). After the punching process was finished, the temperature was decreased to 50°C with a cooling ramp of 20 °C min^{-1}. Then, the stamp and the un-punched PTFE film were demolded from the polymer by mechanical peeling of the surrounding film, as shown in Figure 1D.

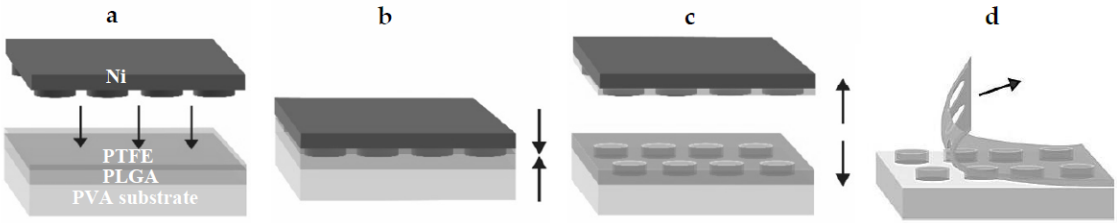

Figure 1. Schematic illustration of: (**a**) the assembly of poly(vinyl alcohol) (PVA) substrate film, a biodegradable PLGA device film, and a polytetrafluoroethylene (PTFE) film prior to the fabrication process; (**b**) hot punching is performed by applying pressure and heat; (**c**) a demolding step of the Ni stamp is completed, leading to separation of PLGA microcontainers from the surrounding film; (**d**) mechanical peeling of the surrounding PLGA film.

Optical profiler measurements were performed with a PLu neox 3D optical profilometer (Sensofar, Barcelona, Spain). Vertical scanning interferometry (VSI) measurements (20×) were conducted on five locations on the samples by attaching it to a silicon carrier wafer using Kapton tape in order to ensure a relatively planar surface prior to optical profiler measurements. Stylus profiler (Dektak XTA, Bruker, Karlsruhe, Germany) measurements were performed to ensure correct height determination by VSI. The data was analyzed using the free SPM data analysis software Gwyddion (version 2.52), and the data was levelled with respect to the indentations. Heights were determined based on profiles extracted across the center of the microcontainers. VSI scans were performed near the center and in each of the four corners of the samples. More detailed scans were also made for use in 3D rendering.

2.2. Harvesting of Biodegradable Microcontainers

For harvesting of the PCL and PLGA microcontainers, the PVA substrate was dissolved. The dissolution of the sacrificial PVA was achieved by immersion in aqueous medium [12]. A sample containing 400 microcontainers was dissolved within 30 min. Subsequently, the free-floating microcontainers were harvested using a stainless steel filter with a mesh opening of 213 µm and thickness of 178 µm (Spectra/Mesh®Woven Filters, Fisher Scientific, Roskilde, Denmark). The microcontainers were dried at 37 °C for 1 h. For further investigation, the filter containing the harvested microcontainers was mounted on aluminum stubs with double-sided carbon adhesive dots. Scanning electron microscopy (SEM) was performed to study the surface and morphology of the microcontainers. All SEM micrographs were acquired by a TM3030Plus Tabletop Microscope (Hitachi, Krefeld, Germany) with a voltage of 15 keV using the SE detector.

2.3. Ex Vivo Mucoadhesion Studies with Biodegradable Microcontainers

The *ex vivo* mucoadhesion studies were conducted as described by Mosgaard et al. [13] and conducted under the license number DK-10-13-oth-736416. An 18 cm piece of small intact intestinal porcine tissue was placed on an angled tissue holder at 20° inside a humidity and heat controlled chamber. The intestine was flushed with fasted state simulated intestinal fluid (FaSSIF, pH 6.5, 37 °C, Biorelevant®, London, UK) for 15 min with a flow rate of 4.1 mL/min using a peristaltic pump. Then, the angle was set to 10° and the tissue was flushed for 5 min at a flow rate of 1.55 mL/min. Gelatin capsules loaded with a known amount of microcontainers were placed at the top of the intestine and were allowed to dissolve for 15 min. The tissue holder was placed back at an angle of 20° and the intestine was perfused for 30 min at a flow rate of 1.55 mL/min. This flow rate was calculated based on earlier studies by Sinko et. al, reporting flow rates for rats of 0.2 mL/min and assuming a size ratio of 7.5 between a pig and rat intestine [20–22]. At the end of the study, the tissue was cut open and divided into 3 sections named “start”, “middle”, and “end”; each having a length of approximately 6 cm. The microcontainers found on the filter paper were referred to as “exit”. The tissue was transferred onto microscope slides and dried overnight at room temperature before visualization under a light microscope. The amount of microcontainers on each intestinal piece and the amount of microcontainers exiting the tissue were assessed.

2.4. Degradation Study in Intestinal Medium

Degradation studies were performed in FaSSIF medium with added pancreatin enzymes, as they play a vital role in protein digestion in the small intestine and are the main enzymes used when simulating digestion [23]. Pancreatin from porcine pancreas (≥3 × USP specifications, Sigma Aldrich, St. Louis, MO, USA, 11.92 USPU/mg activity) was added to yield a lipase activity of 600 USPU/mL. The pancreatic extract was prepared by adding pancreatin to FaSSIF and vortexing until homogeneity was achieved. Afterwards, the mixture was centrifuged for 7 min at 4000 rpm and the supernatant was collected. The pH was adjusted to 6.5. The microcontainers were placed in 3 mL FaSSIF–pancreatin medium and the vials were kept in a 37°C waterbath with constant stirring (100 rpm). The medium was changed three times a week by filtering the microcontainers from the old medium. Once per week, the microcontainers were dried and investigated by SEM. The investigated samples were placed back in the vial before adding freshly prepared medium, and this was continued until no microcontainers could be found in the medium.

3. Results and Discussion

3.1. Fabrication of PLGA Microcontainers

First, the fabrication of PLGA microcontainers by hot punching had to be optimized. The PLGA film was molded and finally punched due to shear stress at the highest protrusion of the stamp, which exceeded the ultimate tensile strength of the material, as shown in Figure 2a. By the addition of the PTFE film between the stamp and the PLGA device film, it was possible to avoid adhesion between the stamp and the PLGA device film upon demolding. After the hot punching process, the sacrificial PTFE film could easily be peeled off. The microcontainers were physically separated from the surrounding PLGA and remained on the underlying PVA substrate, as shown in Figure 2b–d. Microcontainers were successfully fabricated with PLGA 50:50 and 75:25 in arrays of 20 × 20 devices in a single-step hot punching process. The PVA substrate was dissolved in aqueous medium and the microcontainers were harvested on a grid, showing good structural definition and integrity, as shown in Figure 2e. SEM images revealed an excellent replication fidelity. The inner and outer diameter were 240 ± 2 µm and 275 ± 0.5 µm, respectively, the height was 73 ± 6 µm, and the reservoir depth was 56 ± 1 µm as investigated through optical profilometry and shown in Figure 2f,g. Compared to the PCL microcontainers fabricated with the identical Ni stamp [12], it was observed that the PLGA microcontainers were slightly lower. This was attributed to the PTFE film added during the hot punching step, which was not required for PCL. The inner diameter was 10 µm larger for PLGA microcontainers compared to PCL, which was expected as the PFTE had enlarged the stamp features. This led to different volumes of the PLGA and PCL microcontainers of 1.8 and 3.8 nL, respectively. The weight of a single microcontainer was determined experimentally by weighing a defined amount of devices. For PCL, the weight was 3.7 ± 0.4 µg, PLGA 50:50 had a weight of 2.7 ± 0.4 µg, and PLGA 75:25 weighed 3.6 ± 0.04 µg. This was in good agreement with the values estimated based on the measured dimensions and the polymer density.

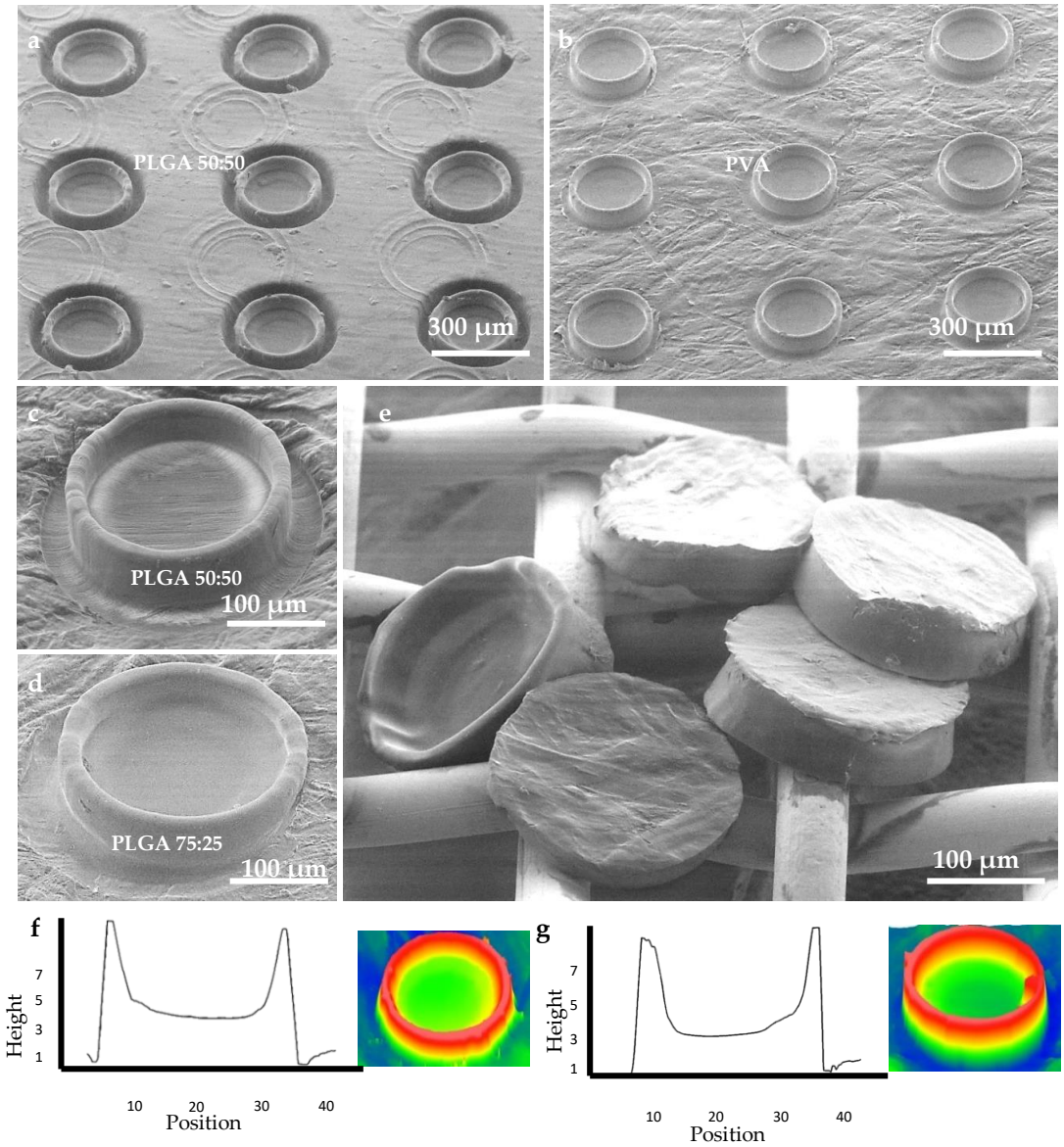

Figure 2. (**a**) SEM micrograph of microcontainer arrays before removal of the surrounding film; (**b**) microcontainer arrays after removal of the surrounding film; (**c**) close-up of a single PLGA 50:50 microcontainer; (**d**) close-up of a single PLGA 75:25 microcontainer; (**e**) harvested PLGA 50:50 microcontainers; (**f**) optical profile curve and 3D rendering of a single PLGA 50:50 microcontainer; (**g**) optical profile curve and 3D rendering of a single PLGA 75:25 microcontainer.

3.2. Ex Vivo Mucoadhesion Study

After harvesting the microcontainers from the PVA substrate, *ex vivo* mucoadhesion tests on porcine small intestinal tissue were performed. The *ex vivo* retention test was used to evaluate the behavior of the microcontainers in the small intestine when exposed to a constant flow. The observation of the movement of the microcontainers down the small intestine, as shown in Supplementary Materials S2, indicates their interaction with the mucus layer. Prolonged movement of the microcontainers down the small intestine can be related to lower mucoadhesion. The recovery rate, which is the percentage of microcontainers that could be identified during the experiments, was 82 ± 6% for PLGA 50:50, 69 ± 10% for PLGA 75:25, and 88 ± 4% for PCL. It is assumed that the missing microcontainers were lost in a distributed manner through all intestinal sections and at the exit. A comparison of the relative percentages of PLGA 50:50, PLGA 75:25, and PCL microcontainers that could be identified

in the respective sections is shown in Figure 3. It was observed that most of the microcontainers (between 66 and 82%) were located in the first part of the intestinal tissue, which indicates their ability to adhere well to the mucosal surface. The microcontainers were then more or less equally distributed throughout the rest of the intestinal sections. A slight tendency of PLGA microcontainers adhering better in the beginning of the tissue was observed compared to PCL microcontainers. A variety of factors could affect mucoadhesion, including the chemical structure which would lead to different interactions on the mucosal surface [24]. PLGA has a more hydrophilic structure than PCL, which can result in numerous hydrogen bonds with the mucus layer. PCL could, on the other hand, present hydrophobic interactions with mucus which explains the good ability to adhere in the beginning of the intestine [20,24]. Also, the size of the microcontainers could have an influence on the mucoadhesion. As the PLGA microcontainers had a slightly smaller diameter, they might have been less affected by the constant flow after adhering to the mucosal surface.

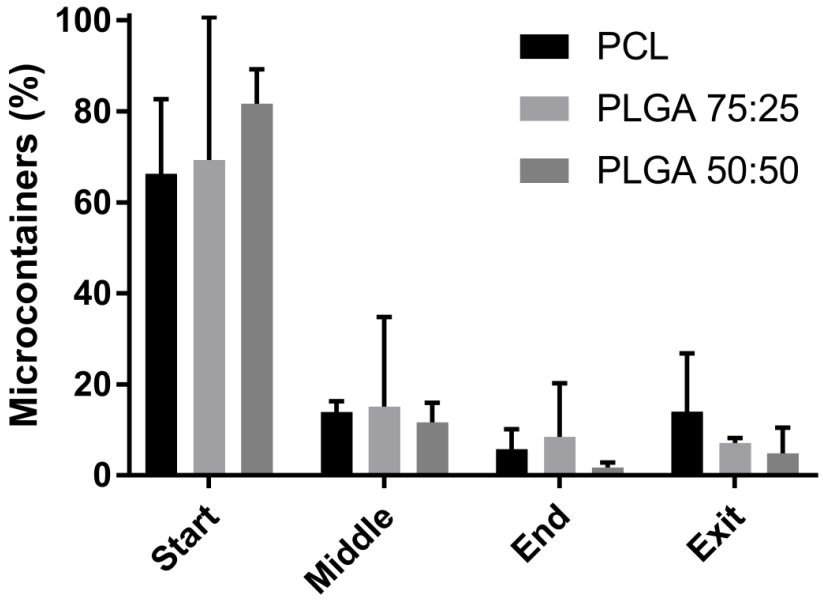

Figure 3. Percentage of microcontainers located in the start, middle, end, and exit of the small intestine of a pig after an *ex vivo* perfusion study. Comparison of poly-ε-caprolactone (PCL) (black) microcontainers, PLGA 75:25 (dark grey), and PLGA 50:50 (light grey). Data is presented as mean ± SD with n = 3–4.

Minor variations between the two PLGA polymers were also observed. PLGA 50:50 microcontainers seemed slightly more prone to adhere to the mucus compared to PLGA 75:25. PLGA 50:50 has more hydrophilic functional groups, such as hydroxyl and carboxyl, which could again allow for better hydrogen bonding, thereby promoting maximal exposure of potential anchor sites.

3.3. In Vitro Degradation Study in Intestinal Medium

The morphology of the microcontainers was analyzed by SEM before and during degradation in FaSSIF with pancreatin, as seen in Figure 4. PLGA 50:50 microcontainers already showed signs of degradation and loss of structural integrity in the first SEM analysis after two weeks. In comparison, PLGA 75:25 and PCL microcontainers only had minor deformation of the microcontainer walls in both cases. After four weeks, PLGA 50:50 microcontainers were completely degraded and thus, could not be detected anymore via SEM inspection. At the same time, PLGA 75:25 and PCL devices showed clear signs of degradation by changing structural integrity and even breaking apart. After five weeks, the morphology of those microcontainers had completely changed and only small polymer lumps remained. Finally, after six weeks, none of the three polymers could be detected through SEM. The

observed degradation for all three polymers was faster compared to what would be expected from typical degradation studies reported in the literature. For PCL in an aqueous environment without any enzymes, degradation is typically slow, which would not allow complete degradation of the microcontainers within six weeks [14,15]. This is also supported by the fact that PCL microcontainers immersed in FaSSIF medium without enzymes were completely unaffected after 20 d, as shown in Supplementary Materials S1. The porcine pancreatin added in the FaSSIF medium contains a mixture of enzymes, including lipase, which readily hydrolyzes ester bonds in polyesters [23]. Furthermore, PCL is generally known to be degraded by microorganisms, as well as by hydrolytic mechanisms, under physiological conditions [25]. PLGA has been proposed to degrade primarily through hydrolytic degradation, but it has also been suggested that enzymatic degradation may play a role in the process [26,27]. Among all the tested polymers, PCL seemed to have the slowest biodegradation rate and literature also evidences that it is a slower degrading polymer in comparison to PLGA [26]. Regarding the difference between PLGA 50:50 and 75:25, it was expected that the degradation time would vary as different ratios of the monomers have a significant influence on hydrolysis and enzymatic degradation. PLGA 50:50 is expected to have the highest degradation rate compared to PLGA 75:25, which typically is approximately twice as slow due to the higher content of hydrophobic groups [27]. This corresponds well to what was observed during the degradation study. It should be noted, that *in vivo* degradation would be expected to occur even faster due to presence of bacteria and other enzymes in the GI tract.

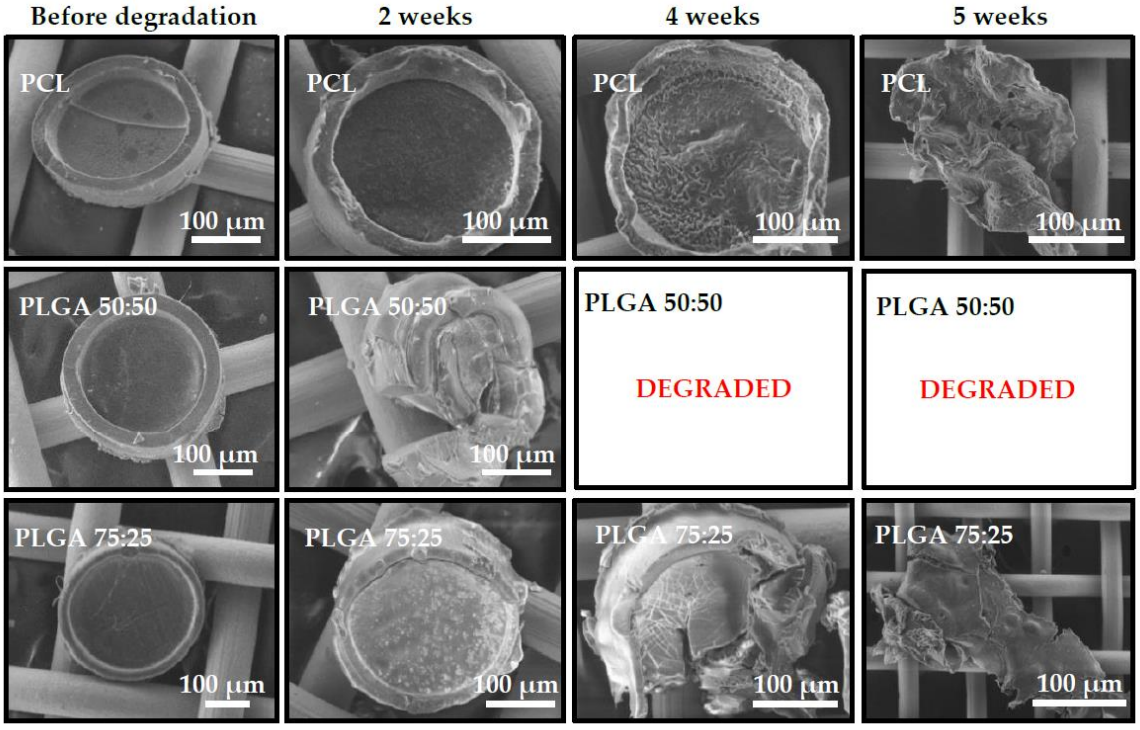

Figure 4. SEM micrographs of the morphology of microcontainers before degradation, after two weeks, four weeks, and six weeks, in simulated intestinal media, containing pancreatic enzymes.

4. Conclusions

In this study, mucoadhesion and degradation of polymeric microcontainers for oral drug delivery were investigated. For this purpose, the hot punching process for the fabrication of PLGA microcontainers had to be optimized. Due to high adhesion forces of PLGA polymer to the Ni stamp, an additional PTFE film was added between the stamp and the PLGA device film. This eased the demolding process and thus PLGA microcontainers in two different compositions, namely PLGA 50:50 and 75:25, were successfully fabricated. This demonstrates the versatility of the recently developed

single-step hot punching method. The fabricated microcontainers were assessed in an *ex vivo* retention model for their mucoadhesion properties. It was found that PLGA 50:50 microcontainers showed the best mucoadhesion characteristics compared to PCL and PLGA 75:25 microcontainers. The degradation properties of the three types of biodegradable microcontainers were also evaluated in an *in vitro* study for six weeks using simulated intestinal medium with the addition of enzymes. Through SEM inspection, it was found that PLGA 50:50 degraded the fastest and no microcontainers could be detected already after four weeks. PCL and PLGA 75:25 microcontainers were completely degraded after six weeks. The results indicate that the fabrication method can indeed be used for various purposes of oral drug delivery and that PLGA 50:50 has the best mucoadhesion and the fastest biodegradation.

Supplementary Materials: The following are available online at http://www.mdpi.com/2073-4360/11/11/1828/s1, Figure S1: Degradation study of PCL microcontainers in PBS, PaSSGF and FaSSIG media for up to 20 days; Figure S2: Microcontainers inside the porcine intestine visualized with an optical microscope.

Author Contributions: Conceptualization, Z.A., M.D.M., S.S.K.; Methodology, Z.A., M.D.M., L.H.N., S.S.K.; Validation, Z.A., G.M., M.D.M.; Formal analysis, Z.A., M.D.M., G.M., S.S.K.; Investigation, Z.A., M.D.M., G.M.; Resources, A.B., S.S.K.; Data curation, Z.A., M.D.M., G.M.; Writing – original draft preparation, Z.A., M.D.M.; Writing – review and editing, Z.A., M.D.M., R.S.P., L.H.N., A.M., A.B., S.S.K.; Visualization, Z.A., M.D.M.; Supervision, R.S.P., L.H.N., A.M., A.B., S.S.K.; Project administration, A.B., S.S.K.; Funding acquisition, A.B.

Funding: This research was funded by The Danish National Research Foundation (Project DNRF122) and Villum Foundation's Center (Grant No. 9301) for Intelligent Drug Delivery and Sensing Using Microcontainers and Nanomechanics (IDUN).

Acknowledgments: The foundations are acknowledged for financial support. Fabrication specialist Lasse Thamdrup is acknowledged for the thorough optical and stylus measurements.

Conflicts of Interest: The authors declare no conflict of interest.

References

1. Taylor, L.S.; Zhang, G.G.Z. Physical chemistry of supersaturated solutions and implications for oral absorption. *Adv. Drug Deliv. Rev.* **2016**, *101*, 122–142. [CrossRef]
2. Agrawal, U.; Sharma, R.; Gupta, M.; Vyas, S.P. Is nanotechnology a boon for oral drug delivery? *Drug Discov. Today.* **2014**, *19*, 1530–1546. [CrossRef]
3. Pereira De Sousa, I.; Steiner, C.; Schmutzler, M.; Wilcox, M.D.; Veldhuis, G.J.; Pearson, J.P.; Huck, C.W.; Salvenmoser, W.; Bernkop-Schnürch, A. Mucus permeating carriers: Formulation and characterization of highly densely charged nanoparticles. *Eur. J. Pharm. Biopharm.* **2015**, *97*, 273–279. [CrossRef]
4. Champion, J.A.; Katare, Y.K.; Mitragotri, S. Particle shape: A new design parameter for micro- and nanoscale drug delivery carriers. *J. Control. Release* **2007**, *121*, 3–9. [CrossRef] [PubMed]
5. Shaikh, R.; Raj Singh, T.R.; Garland, M.J.; Woolfson, A.D.; Donnelly, R.F. Mucoadhesive drug delivery systems. *J. Pharm Bioallied Sci.* **2011**, *3*, 89–100. [PubMed]
6. Mackie, A.R.; Goycoolea, F.M.; Menchicchi, B.; Caramella, C.M.; Saporito, F.; Lee, S.; Stephansen, K.; Chronakis, I.S.; Hiorth, M.; Adamczak, M.; et al. Innovative Methods and Applications in Mucoadhesion Research. *Macromol. Biosci.* **2017**, *17*, 1–32. [CrossRef] [PubMed]
7. Nielsen, L.H.; Keller, S.S.; Boisen, A. Microfabricated devices for oral drug delivery. *Lab Chip* **2018**, *18*, 2348–2358. [CrossRef] [PubMed]
8. Tao, S.L.; Lubeley, M.W.; Desai, T.A. Bioadhesive poly(methyl methacrylate) microdevices for controlled drug delivery. *J. Control. Release* **2003**, *88*, 215–228. [CrossRef]
9. Ainslie, K.M.; Lowe, R.D.; Beaudette, T.T.; Petty, L.; Bachelder, E.M.; Desai, T.A. Microfabricated devices for enhanced bioadhesive drug delivery: Attachment to and small-molecule release through a cell monolayer under flow. *Small* **2009**, *5*, 2857–2863. [CrossRef] [PubMed]
10. Mazzoni, C.; Tentor, F.; Strindberg, S.A.; Nielsen, L.H.; Keller, S.S.; Alstrøm, T.S.; Gundlach, C.; Müllertz, A.; Marizza, P.; Boisen, A. From concept to in vivo testing: Microcontainers for oral drug delivery. *J. Control. Release* **2017**, *268*, 343–351. [CrossRef] [PubMed]
11. Nielsen, L.H.; Melero, A.; Keller, S.S.; Jacobsen, J.; Garrigues, T.; Rades, T.; Müllertz, A.; Boisen, A. Polymeric microcontainers improve oral bioavailability of furosemide. *Int. J. Pharm.* **2016**, *504*, 98–109. [CrossRef] [PubMed]

12. Abid, Z.; Strindberg, S.; Javed, M.M.; Mazzoni, C.; Vaut, L.; Nielsen, L.H.; Gundlach, C.; Petersen, R.S.; Müllertz, A.; Boisen, A.; et al. Biodegradable microcontainers—Towards real life applications for oral drug delivery. *Lab Chip* **2019**, *19*, 2905–2914. [CrossRef] [PubMed]
13. Mosgaard, D.M.; Strindberg, S.; Abid, Z.; Petersen, R.S.; Thamdrup, L.; Keller, S.S.; Müllertz, A.; Nielsen, L.H. Ex vivo intestinal perfusion model for investigating mucoadhesion of microcontainers. *Int. J. Pharm.* **2019**, *570*, 18658.
14. Heimowska, A.; Morawska, M.; Bocho-janiszewska, A. Biodegradation of poly(ε-caprolactone) in natural water environments. *Pol. J. Chem. Technol.* **2017**, *1*, 120–126. [CrossRef]
15. Abedalwafa, M.; Wang, F.; Wang, L.; Li, C. Biodegradable poly-epsilon-caprolactone (pcl) for tissue engineering applications: A review. *Rev. Adv. Mater. Sci.* **2013**, *34*, 123–140.
16. Gentile, P.; Chiono, V.; Carmagnola, I.; Hatton, P.V. An Overview of Poly(lactic-co-glycolic) Acid (PLGA)-Based Biomaterials for Bone Tissue Engineering. *Int. J. Mol. Sci.* **2014**, *15*, 3640–3659. [CrossRef]
17. Ding, D.; Kundukad, B.; Somasundar, A.; Vijayan, S.; Khan, S.A.; Doyle, P.S. Design of Mucoadhesive PLGA Microparticles for Ocular Drug Delivery. *ACS Appl. Bio Mater.* **2018**, *1*, 561–571. [CrossRef]
18. Makadia, H.K.; Siegel, S.J. Poly Lactic-co-Glycolic Acid (PLGA) as Biodegradable Controlled Drug Delivery Carrier. *Polymers* **2011**, *3*, 1–19. [CrossRef]
19. Petersen, R.S.; Keller, S.S.; Hansen, O.; Boisen, A. Fabrication of Ni stamp with high aspect ratio, two-leveled, cylindrical microstructures using dry etching and electroplating. *J. Micromech. Microeng.* **2015**, *25*, 055021. [CrossRef]
20. Sinko, P.J.; Hu, P.; Waclawski, A.P.; Patel, N.R. Oral absorption of anti-aids nucleoside analogues. 1. Intestinal transport of didanosine in rat and rabbit preparations. *J. Pharm. Sci.* **1995**, *84*, 959–965. [CrossRef]
21. Kararli, T.T. Comparison of the gastrointestinal anatomy, physiology, and biochemistry of humans and commonly used laboratory animals. *Biopharm. Drug Dispos.* **1995**, *16*, 351–380. [CrossRef] [PubMed]
22. Sjögren, E.; Abrahamsson, B.; Augustijns, P.; Becker, D.; Bolger, M.B.; Brewster, M.; Brouwers, J.; Flanagan, T.; Harwood, M.; Heinen, C.; et al. In vivo methods for drug absorption—comparative physiologies, model selection, correlations with in vitro methods (IVIVC), and applications for formulation/API/excipient characterization including food effects. *Eur. J. Pharm. Sci.* **2014**, *57*, 99–151. [CrossRef] [PubMed]
23. Whitcomb, D.C.; Lowe, M.E. Human pancreatic digestive enzymes. *Dig. Dis. Sci.* **2007**, *52*, 1–17. [CrossRef]
24. Sigurdsson, H.H.; Kirch, J.; Lehr, C.-M. Mucus as a barrier to lipophilic drugs. *Int. J. Pharm.* **2013**, *453*, 56–64. [CrossRef] [PubMed]
25. Armani, D.K.; Liu, C. Microfabrication Technology for Polycaprolactone, A Biodegradable Polymer. *J. Micromech. Microeng.* **2000**, *10*, 80. [CrossRef]
26. Schliecker, G.; Schmidt, C.; Fuchs, S.; Wombacher, R.; Kissel, T. Hydrolytic degradation of poly(lactide-co-glycolide) films: Effect of oligomers on degradation rate and crystallinity. *Int. J. Pharm.* **2003**, *266*, 39–49. [CrossRef]
27. Park, T.G. Degradation of poly(d,l-lactic acid) microspheres: Effect of molecular weight. *J. Control. Release* **1994**, *30*, 161–173. [CrossRef]